NON-LINEAR OIL FILM FORCE COEFFICIENTS FOR A JOURNAL BEARING OPERATING UNDER ALIGNED AND MISALIGNED CONDITIONS

BY

ROY HENRY BANNISTER, M.Sc., C.Eng., M.I.Mech.E.

Submitted in fulfilment of the Degree of

Doctor of Philosophy

of

The University of Aston in Birmingham

DECEMBER 1972

FACULTY OF ENGINEERING

DEPARTMENT OF MECHANICAL ENGINEERING

HEAD OF DEPARTMENT:-

PROFESSOR A. J. EDE.

SUPERVISOR:-

PROFESSOR E. DOWNHAM.

I N D E X

Page

ACKNOWLEDGEMENTS

ABSTRACT

CHAPTER ONE - INTRODUCTION 1

CHAPTER TWO - HISTORICAL SURVEY

2.1 Instability. 6

2.2 Papers published listing the oil force coefficients. 25

2.3 Papers published after 1970. 33

CHAPTER THREE - ANALYTICAL TREATMENT

3.1 Reynolds equation. 36

3.2 Axes and velocities of the vibrating journal. 38

3.3 Reynolds equation in non-dimensional form. 41

3.4 Fluid film forces. 42

3.5 Force coefficients. 46.

CHAPTER FOUR - NUMERICAL ANALYSIS

4.1 Introduction. 54

4.2 Equations for film thickness. 54

4.3 Solution to Reynolds equation. 56

4.4 Boundary conditions. 59

4.5 Procedure for the finite difference equations. 61

4.6 Procedure for solving the first order coefficients. 65

4.7 Procedure for solving the second order coefficients. 67

4.8 Layout of computer program. 69

Page

CHAPTER FIVE - SOLUTION TO LINEAR EQUATIONS

5.1 General equations of motion. 70

5.2 Determination of the journal whirl trajectory using eight oil film coefficients. 73

5.3 Experimental methods for the determination of the eight oil film force coefficients. 75

5.4 The determination of Hagg and Sankey type of coefficients from synchronous whirl vibrations. 80

CHAPTER SIX - SOLUTION TO NON-LINEAR EQUATIONS OF MOTION

6.1 General equations of motion. 85

6.2 The determination of the non-linear whirl trajectory using an "Analogue Simulator". 86

6.3 Solution to the non-linear equations of motion using a modified Newton-Raphson method. 90

CHAPTER SEVEN - THEORETICAL RESULTS FOR THE OIL FILM PRESSURE DISTRIBUTION

7.1 Oil film pressure distribution, aligned conditions. 100

7.2 Pressure distribution for misaligned conditions. 101

7.3 Comparison with other published work. 103

CHAPTER EIGHT - EXPERIMENTAL TEST EQUIPMENT

8.1 Design considerations. 106

8.2 Test journal and bearing bush. 107

8.3 Lubricating system. 110

Page

8.4 Measurement of shaft displacements. 110

8.5 Shaft speed control and counter. 112

8.6 Shaft position indicator. 113

8.7 Measurement of the oil film temperature. 113

8.8 Calibration of displacement transducers. 114

8.9 Balancing the test journal. 115

CHAPTER NINE - EXPERIMENTAL RESULTS FOR THE STEADY STATE RUNNING CONDITIONS

9.1 Locus of shaft centre-aligned conditions. 116

9.2 Locus of shaft centre under misaligned conditions. 117

CHAPTER TEN - THEORETICAL - EXPERIMENTAL FORCE COEFFICIENTS

10.1 Hagg and Sankey type of coefficient. (i.e. four coefficients) 120

10.2 Consideration to equations of motion having eight force coefficients. 125

10.3 Considerations to equations of motion having twentyeight force coefficients. 127

10.4 Further experimental evidence. 135

10.5 Effects of journal misalignment upon the dynamic characteristics. 136

10.6 Oil film temperature distribution. 138

10.7 Journal response about the steady running position i.e. about ε_o and ϕ_o. 140

10.8 Further visual evidence of the effects of misalignment upon the orbital response. 141

Page

CHAPTER ELEVEN - ACCURACY OF EXPERIMENTAL RESULTS

11.1 Change in the Sommerfeld duty parameter. 143

11.1(i) Viscosity μ. 143

11.1(ii) Journal speed. 145

11.1(iii) Specific Pressure 'P'. 145

11.1(iv) Journal radius (R) and radial clearance (C). 146

11.2 The effects of turbulence. 147

11.3 Sensitivity of the transducers measuring journal movements. 148

11.4 Locus of shaft centre - aligned conditions. 150

11.5 Locus of shaft centre - misaligned conditions 150

CHAPTER TWELVE - DISCUSSION OF THEORETICAL AND EXPERIMENTAL RESULTS

12.1 Oil film pressure distribution. 152

12.2 The effects of the oil pressure distribution upon the critical speed of the shaft system (due to the movement of the centre of pressure). 154

12.3 Locus of the shaft centre for aligned conditions. 155

12.4 Locus of shaft centre for misaligned conditions. 156

12.5 Hagg and Sankey coefficients. 159

12.6 The use of eight force coefficients for predicting the journal whirl trajectory. 161

12.7 The effect of using the second order terms for predicting the journal whirl trajectory - aligned conditions. 163

Page

12.8 The effect of using the second order terms when predicting the journal whirl trajectory, with the bearing operating under misaligned conditions. 171

CHAPTER THIRTEEN - CONCLUSIONS

13.1 Distribution of the hydrodynamic oil film pressures. 175

13.2 Journal locus aligned and misaligned conditions. 176

13.3 Hagg and Sankey force coefficients. 177

13.4 Eight force coefficients. 179

13.5 Twentyeight coefficients aligned conditions. 181

13.6 Twentyeight coefficients misaligned conditions. 183

CHAPTER FOURTEEN - RECOMMENDATIONS

14.1 Recommendations for future investigations. 185

APPENDIX A - THEORETICAL ANALYSIS OF THE OIL FILM FORCES 188

APPENDIX B - JOURNAL BEARING DESIGN AND PERFORMANCE TOGETHER WITH SAMPLE CALCULATION

(I) Selection of journal diameter based on torque requirement. 211

(II) Selection of the journal, based upon reactive loading. 215

(III) Bearing performance calculations. 216

(IV) Minimum oil film thickness. 216

(V) Operating temperatures. 217

(VI) Heat Dissipation. 217

(VII) Graphical representation of the heating thermal balance. 219

Page

(VIII) Method of determining the oil. film force coefficients. 220

(IX) Worked example. 221

APPENDIX C - BIBLIOGRAPHY 222

NOTATION 235.

ACKNOWLEDGEMENTS

The writer wishes to express his gratitude to:-

Professor A. J. Ede, for permission to pursue the research work reported in this thesis.

Professor E. Downham, for his valuable guidance in planning the instrumentation of the test rig, and for the many encouraging discussions on this topic.

Mr. G. Campbell, Company Director of Parsons Peebles Ltd. for providing the test journal and for the computer facilities placed at the writers' disposal, under the direction of Mr. H. Wildey.

Mr. R. Wee, Computer Centre, of the University of Aston, for the entire work done on SLANG.

The many members of the technical and workshop staff who gave their help, in particular Mr. P. Pizer, for manufacturing part of the test equipment and for his assistance in assembling and commissioning of the rig.

ABSTRACT

It is well established that hydrodynamic journal bearings are responsible for self-excited vibrations and have the effect of lowering the critical speeds of rotor systems. The forces within the oil film wedge, generated by the vibrating journal, may be represented by displacement and velocity coefficients thus allowing the dynamical behaviour of the rotor to be analysed both for stability purposes and for anticipating the response to unbalance. However, information describing these coefficients is sparse, misleading, and very often not applicable to industrial type bearings.

Results of a combined analytical and experimental investigation into the hydrodynamic oil film coefficients operating in the laminar region are therefore presented, the analysis being applied to a 120 degree partial journal bearing having a 5.0 in diameter journal and a L/D ratio of 1.0.

The theoretical analysis shows that for this type of popular bearing, the eight linearized coefficients do not accurately describe the behaviour of the vibrating journal based on the theory of small perturbations, due to them being masked by the presence of non-linearity. A method is developed using the second order terms of Taylor expansion whereby design charts are provided which predict the twentyeight force coefficients for both aligned, and for varying amounts of journal misalignment. The resulting non-linear equations of motion are solved using a modified Newton-Raphson method whereby the whirl trajectories are obtained, thus providing a physical appreciation of the bearing characteristics under dynamically loaded conditions.

CHAPTER ONE

CHAPTER ONE

INTRODUCTION

The power to weight ratio of electrical rotating machines has increased enormously over the past decade. This improvement in output is mainly due to the machine working at much higher flux densities and by introducing better methods of cooling, both of these improvements have necessitated in keeping the shaft diameters to a minimum thus introducing greater flexibility into the shaft system. With additional shaft flexibility, together with increased flux density, a third factor is introduced which also effects the resulting critical speed namely the increased value of unbalanced magnetic pull. This magnetic pull is created when the rotor is not running concentrically within the stator, therefore due to the presence of flexibility causing the rotor to run either eccentrically or to whirl, the unbalanced magnetic pull has the effect of lowering the critical speeds. For todays generation of machines the magnetic pull could be approximately equal to half the rotor weight.

Improvements made to the performance of electrical machines has therefore, in the majority of cases, had the accumulative effect of lowering the critical speeds making it increasingly important to assess with greater accuracy the oil-film criticals (the Stodola effect) which are dependant upon the spring constants of the hydrodynamic oil film. Also in recent years the problem of self excited rotor vibrations has been of growing importance owing to their increasing occurrence on high speed machines, which may be partly attributed to the lowering of the rotor criticals.

One of the most ponderous factors affecting the determination of the critical speeds, or the onset of instability whilst still at the design stage, is the insufficient knowledge of the journal bearing characteristics, both for synchronous and nonsynchronous vibrations. Particular instances of observed changes in the critical speed or the onset of instability have been reported and attributed to misaligning couples imposed onto the bearing, caused either by thermal expansions of the bearing supporting structure, or by foundation movement. It is therefore of equal importance to the designer to know to what extent the bearing force coefficients change due to the possibility of misalignment, thus eliminating the serious doubts most design engineers have when working to a discrete line on a design chart. However, most experienced designers are aware that whilst published theoretical dynamic coefficients are perfectly sound from a mathematical viewpoint and in certain cases justified by exhaustive testing under controlled conditions, these coefficients may change because the dynamic system may be subjected to non-linearity due to the presence of large amplitudes of vibration within the oil film, possibly caused by the deterioration in the state of balance or operating within the proximity of a critical speed.

For those not familiar with journal bearings normally used on turbines and electrical machines etc., figure (1-1) shows an exploded view of a bearing bush together with its packing plates used for locating bush within the bearing pedestal. Oil entry to the working face of the bearing is via ports machined along the horizontal split, and the jacking oil supply nozzle is fitted on the B.D.C. which is only used for initial starting thus avoiding boundary lubrication conditions, and is also used when slowly rotating the hot rotor in

to allow it to cool down before a complete shutdown. The end scraper rings are used to scrape the oil off the shaft and avoid leakage from the bearing pedestal, as these bearings require several hundred gallons of cooling oil per hour.

A view looking down into a similar bearing is shown in figure (1-3), this photograph shows the rotor being assembled down an over-speed test pit with the top half of the bearing bush removed exposing the 12.0 in diameter journal, the complete rotor is shown in figure (1-2) the design procedure for this bearing is given in Appendix B. It is of interest to note that this complete rotor, which is for a 33 M.W. turbo-generator weighs in the order of 38,000 lbf (169000 Newtons) and has its first critical in the region of 1070 R.P.M. and its second critical at 3350 R.P.M., if however, the support flexibility had been neglected the calculated criticals would have been 1510 R.P.M. and 4228 R.P.M. for the first and second criticals respectively. Clearly this rotor is sensitive to the bearing support stiffness and if allowed to become too flexible the second critical would be dangerously close to the normal running speed of 3,000 R.P.M. The slope of the bearing for this rotor is in the order of 0.0004 radians which gives an approximate tilt ratio of 0.3, which of course could be increased by pedestal growth or foundation movement. However, during installation every effort is made to obtain parallelism between the journal and bearing bush, by spherical seatings machined onto the bush locating pads which are just noticeable in figure (1-1).

Another flexible rotor but employing a different construction technique is shown in figure (1-4), (note a flexible rotor is one that has its first critical below the normal running speed), this is a high speed rotor capable of operating at speed in excess of 3,800 R.P.M.

having an output of 12,000 H.P. This rotor passes through two critical speeds, the first at 1326 R.P.M. and the second at 2090, if however, the supports were considered to be infinitely rigid the critical speed would have incorrectly been 1388 R.P.M. and 2670 R.P.M. giving a difference of 600 R.P.M. based upon the second critical. Therefore it is essential to be in a position to accurately predict the critical speeds at the design stage, if it is hoped to optimise on the rotor-bearing system. A large 20 in diameter bearing may be seen in the background of this photograph, this size of bearing is one of the largest of its type and is used on 500 M.W. turbo-generators operating at maximum test speeds of 3,600 R.P.M. Figure (1-5) shows a similar size bearing bush resting in its pedestal with the top cap removed exposing the bush. This size of bearing is designed to support rotors weighing up to 85 tons (0.847 MN) and capable of operating at 3,600 R.P.M., the oil film wedge at these speeds would be well within the turbulent region.

A machine having a rigid motor is shown in figure (1-6). For this type of construction it is extremely undesirable to run through a critical speed, usually with this type of rotor the oil film flexibility dominates the critical speed for the complete rotor-bearing system, also it is most susceptible to thermal instability. Therefore it is important not to run above its first critical, or even close to it, as the vibration amplitude would not only depend upon the dynamic magnifier, but also on the load current passing through the pole windings. This particular rotor had a critical speed of 1990 R.P.M. and an overspeed of 1720 R.P.M. therefore an accurate assessment of the oil film flexibility is again most important if the maximum running speed is not to be too near to the critical speed.

For example, if the critical speed for this machine had been calculated using rigid supports a critical of 3420 R.P.M. would have been obtained. The size of bearing used on this machine was 300 M/M diameter and capable of transmitting 20,000 H.P.

Figure (1-7) illustrates another type of rotor construction where it is better not to run through a critical speed if at all possible, the bearing shown is 280 M/M diameter and supports a rotor weighing 23,000 lbf (102,200 N) and capable of an output of 12000 H.P. Again the oil film flexibility plays a dominating role in determining the critical speeds.

Flexible and rigid rotors have been illustrated each having its own particular type of problem associated with oil film flexibility, the problems are by no means isolated or infrequent and must be expected in the future due to the ever increasing demand for machines to have increased output, whilst keeping the frame size the same. Values of the oil film stiffness together with the bearing supporting structure have in the past been obtained from previous and successive designs, this somewhat optimistic method of determining the critical speed has its obvious pitfalls, further if expediency and accuracy of calculation are to play their part in arriving at a solution to the problem, the design engineer must be provided with techniques that ensure adequate accuracy of solution without unnecessary computation. The main objective of the theoretical and experimental investigation described in this thesis is for the accurate representation of the oil film force coefficients for a bearing geometry favoured by most engineers because of its simplicity, indeed the designers viewpoint will be considered throughout and design charts together with design procedure are provided in Appendix B.

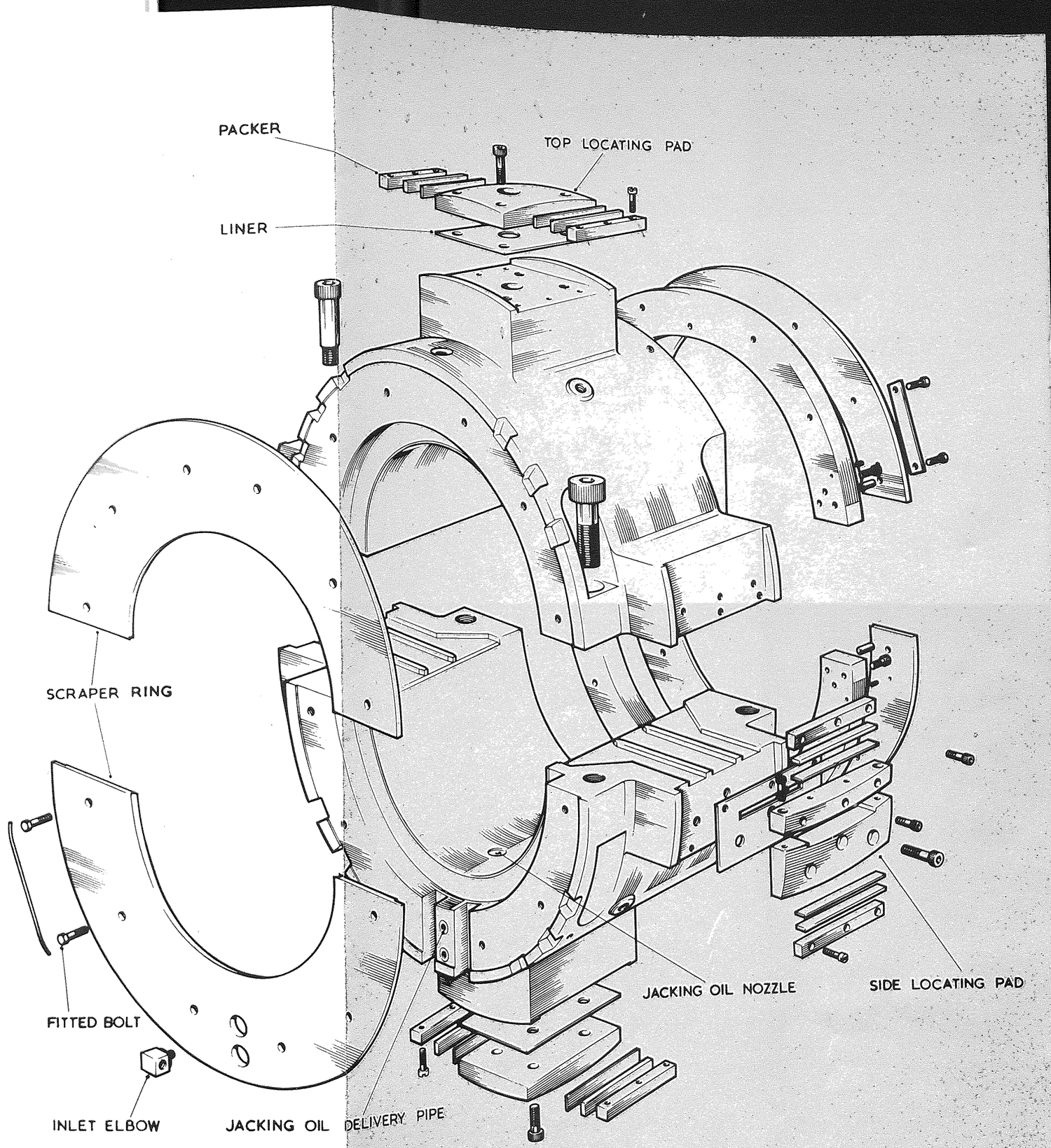

FIG. 1-1 BEARING (TURBINE END)

TMD. 1222

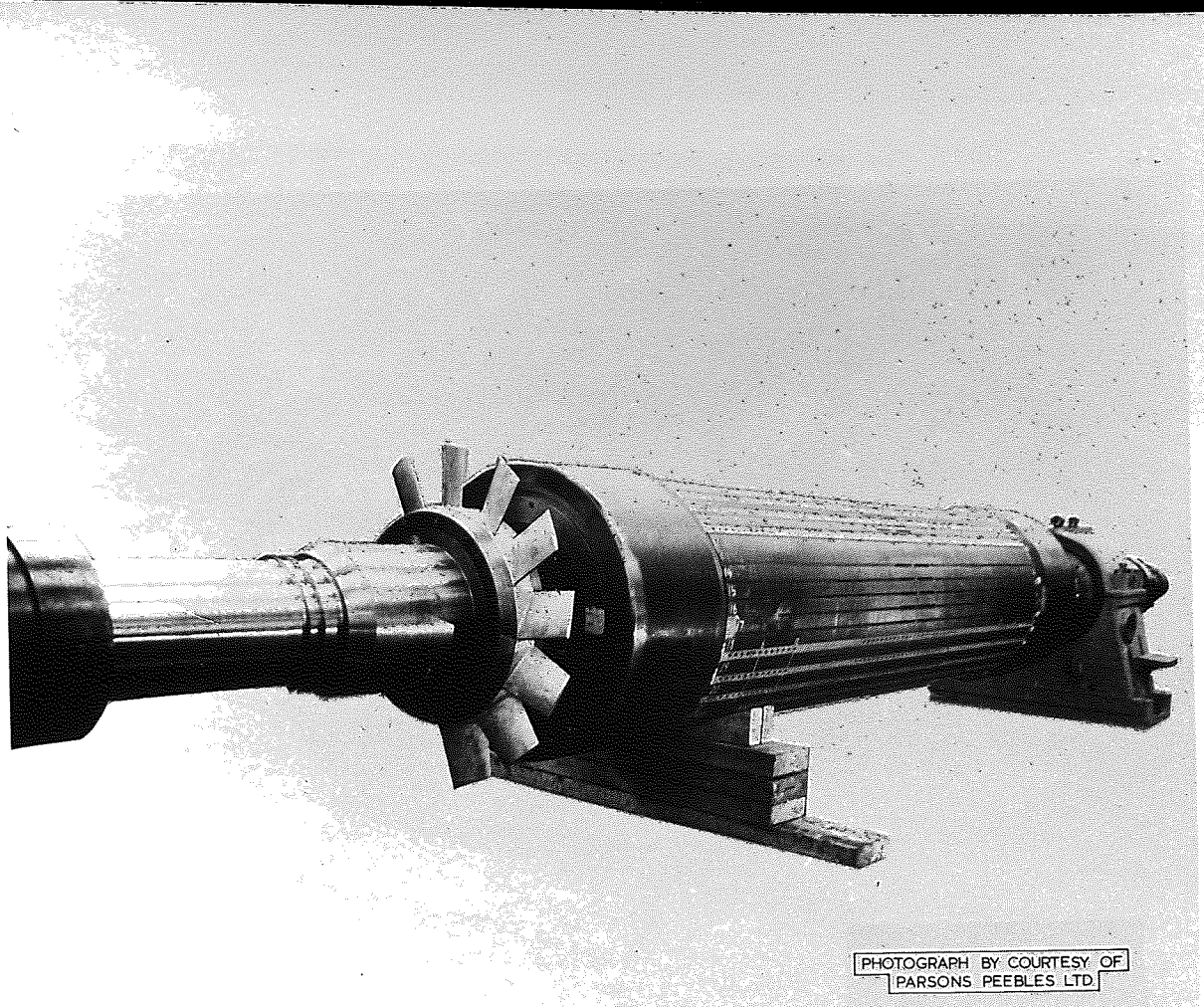

PHOTOGRAPH BY COURTESY OF PARSONS PEEBLES LTD.

FIG 1-2

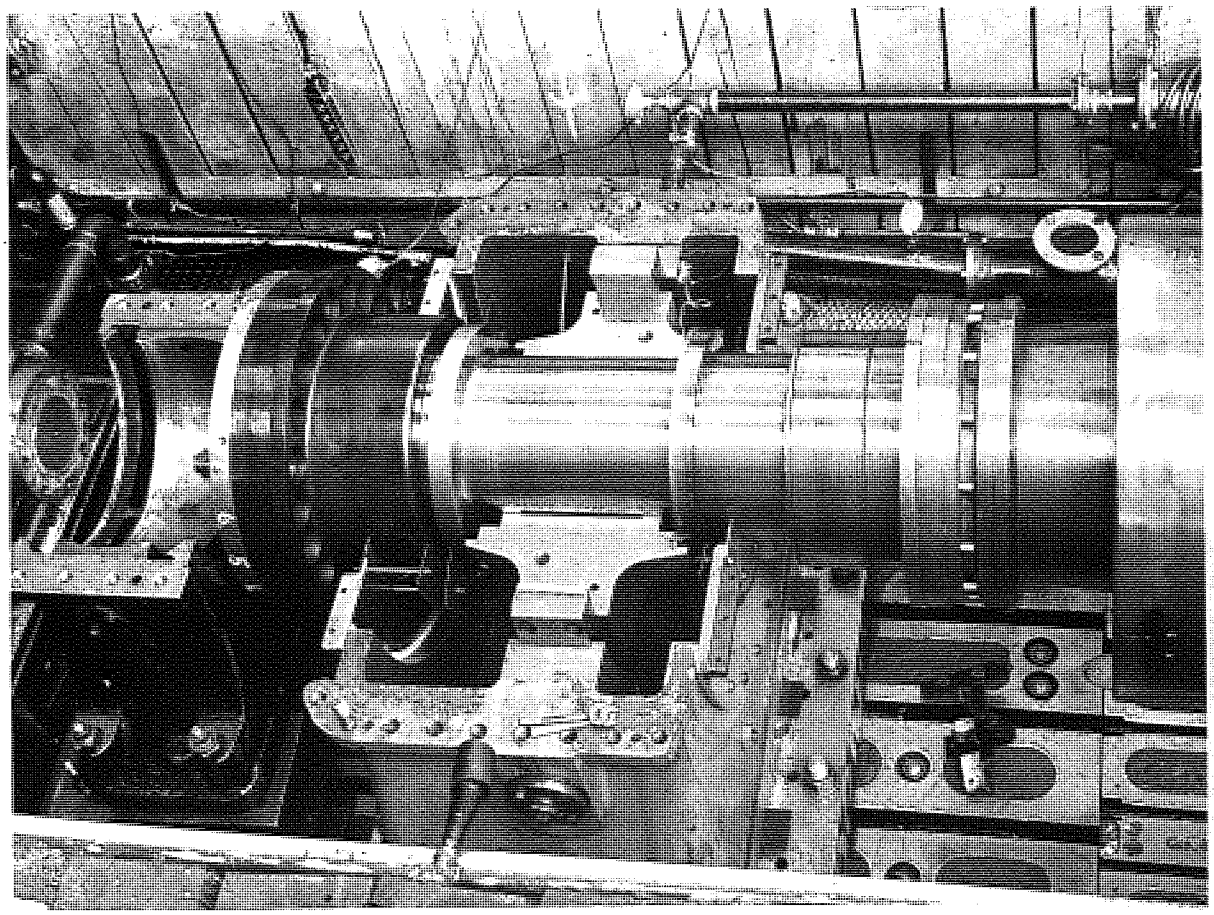

FIG 1-3

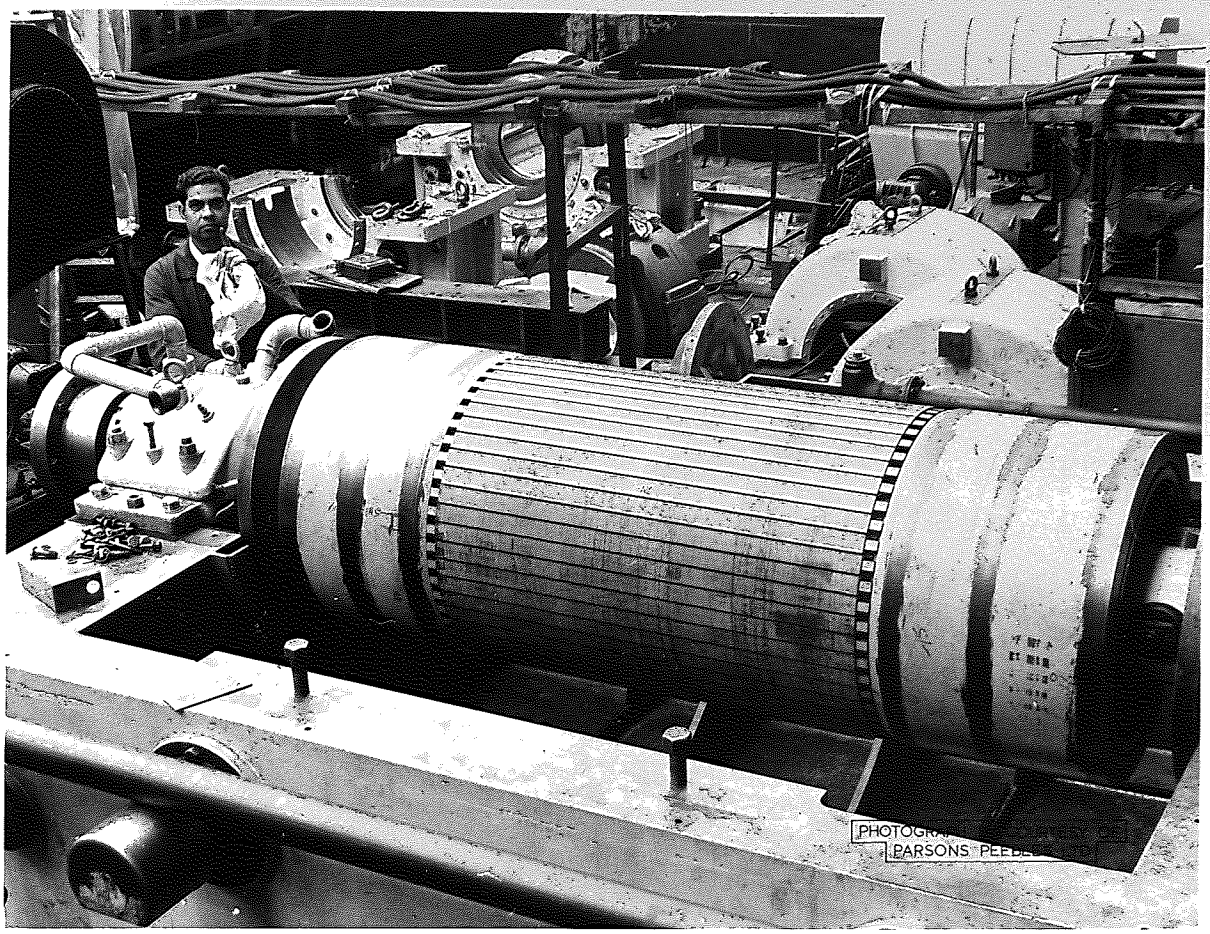
PARSONS PEEBL

FIG 1-4

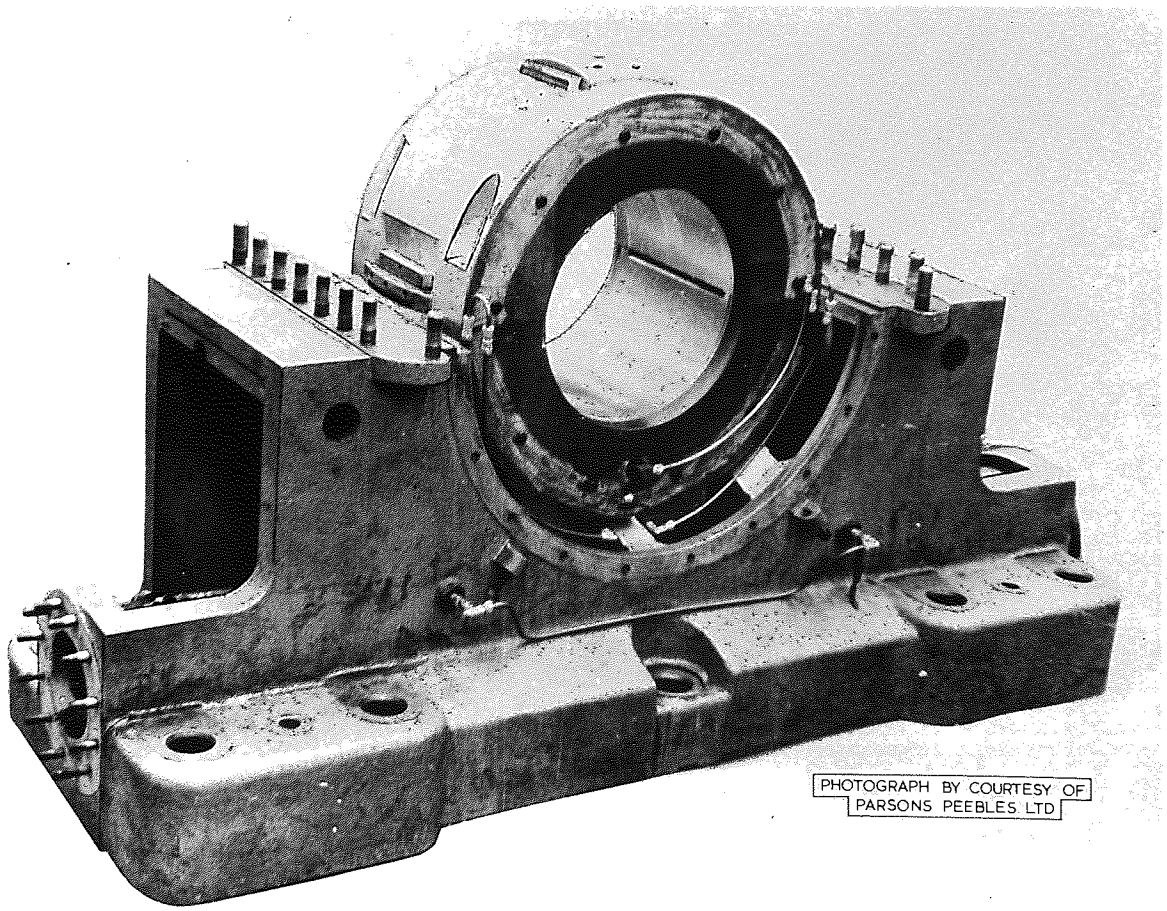
PHOTOGRAPH BY COURTESY OF
PARSONS PEEBLES LTD

FIG 1-5

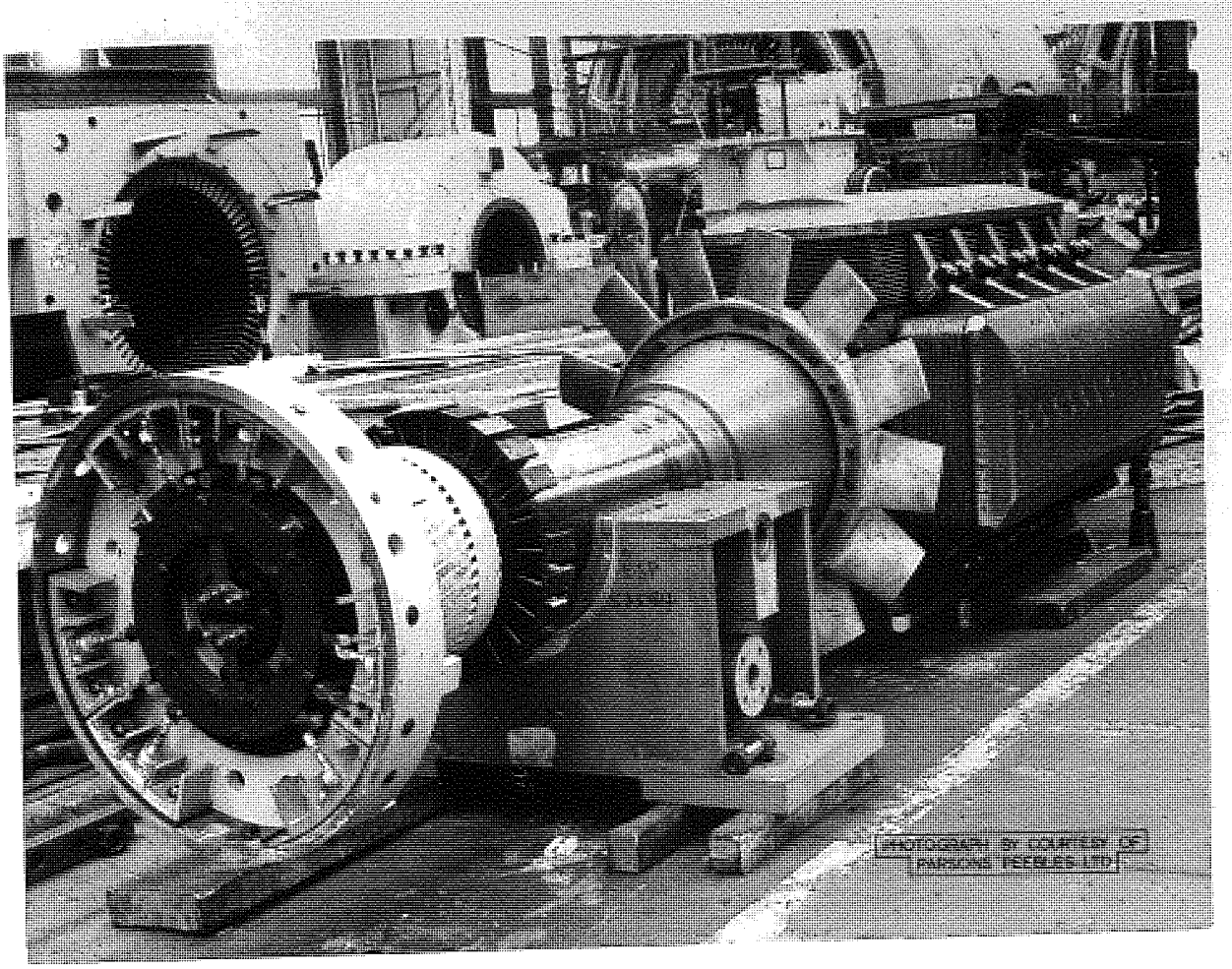

FIG 1-6

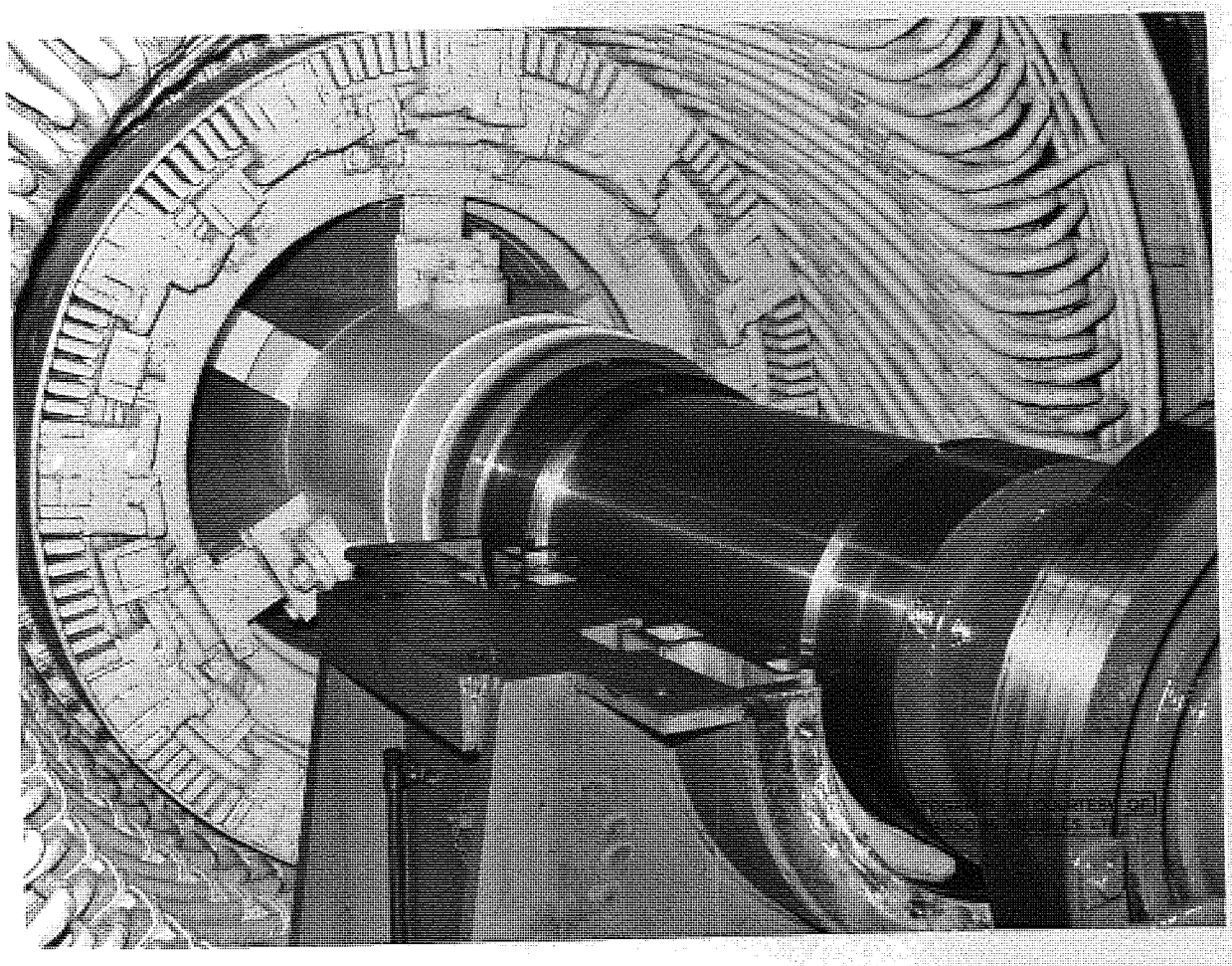

FIG 1 7

CHAPTER TWO

CHAPTER TWO

HISTORICAL SURVEY

The amount of literature grown around the calculation of critical speeds taking into account unequal shaft inertia, gyroscopic couples, support impedance etc. is voluminous and no attempt is made to describe or list the work done up to date. The author believes that those sufficiently interested in obtaining oil film force coefficients will have more than just a working knowledge on the subject of shaft vibrations. However, it is essential to present a survey of both analytical and experimental work allied to the determination of oil film force coefficients.

Investigations into the effects of the hydrodynamic oil film upon rotor speeds and other instabilities have in the past taken two distinct paths, the first and most favoured is the investigation into the complete dynamical system embodying the bearing supporting structure, oil film, and rotor which may be either rigid or flexible; consideration to the entire system is primarily concerned with sub or super harmonics of vibration related to the rotational speed of the shaft, and is usually attributed to the oil film flexibility. The second method of investigation is to separate the rotor dynamics from the oil film characteristics by replacing the two bearings, plus rotor system, with a single bearing supporting a rigid rotor. This latter method has been the subject of research work over the last decade.

2.1 Instability

Harrison(1) was the first pioneer in the study of journal bearing response for a rigid shaft; his paper was presented in 1919 in which he illustrated how the hydrodynamic equation for a cylindrical bearing,

neglecting the reduction in the oil film pressure due to the presence of side leakage, resulted in an orbital motion for a shaft having synchronous disturbing force. However, no consideration was given to the journal inertia forces or the effects of an oil film suppressing the critical speed, further oil film damping was completely neglected when deriving the equations of motion. Indeed it was not until six years later when Stodola(2), who was a notoriously experienced steam turbine design engineer, illustrated that a hydrodynamic oil film acted in the same manner as a non-linear spring, having a different stiffness for each new running position of the journal within the bearing bush. He further demonstrated that the spring like effect of the oil film reduced the critical speed had rigid supports been considered, hence the use of the term "Stodola Effect" which is often used by todays generation of design engineers for describing the suppression in critical speed due to the oil film flexibility. In his first paper of May 1925 Stodola likens the bearing support to a shaft swimming on an oil cushion where secondary disturbing forces are balanced by the counterpressure of the cushion, his analysis assumes that oil side leakage from the bearing does not exist therefore the oil film pressure could be regarded as being directly proportional to the journal eccentricity. A further assumption was the path traced out by the journal centre between extreme running conditions was very nearly a semicircle, hence the eccentricity could be presented as a trigonometric function.

The basic formulation of Stodola's method was to consider a momentory displacement of the journal from its equilibrium position described by the eccentricity ratio ε_o and incidence angle ϕ_o, to some arbitrary position the distance being infinitesimally small but may be described by ε' and ϕ'. The new resulting oil film force P'

was obtained by projecting the displaced system back onto the equilibrium semicircle, and the magnitude P' taken to be the same value had ε' been the original eccentricity ratio. The load angle was also taken to be that angle by which ε' was rotated in order to get back onto the semicircle, hence forces for the displaced journal could be determined along both the horizontal and vertical axes. His analysis concluded with the general equations of motion from which the determinant of the coefficients when equated to zero produced the critical frequencies of the system, his investigations did not however produce the oil film force coefficients.

One year later Stodola(3) extended the above work to include perturbations for an elastic shaft system. His analysis showed that for the region of approximately 1700 to 2500 R.P.M. for the normal critical speed on rigid supports a decrease of 60 per cent could be expected to allow for the oil film flexibility.

In the same year, Hummel(4) demonstrated the practicability of the theory presented by Stodola. Experiments were conducted using a rigid shaft proposed in reference(2) for speeds in excess of 4000 R.P.M. employing bearings having different L/D ratios and radial clearance ratios C/D. Observed values of critical speeds followed the general behaviour suggested by Stodola, however, for eccentricities below 0.6 Hummel found the rotor to be inherently unstable and therefore did not consider journal running positions below this value.

Oil whip was first discovered by Newkirk and Taylor(5) they found under certain conditions the rotor system, supported by journal bearings, whipped when the rotor was made to run at speeds above twice the critical. This whipping originated in the bearings since it could be reduced by operating below twice the shaft first

critical or by increasing the specific pressure of the bearing by applying additional loading or by reducing the bearing length. It was also found that whipping could be reduced by introducing axial misalignment or by starving the bearing of its oil supply. Newkirk gave a quantitative explanation of the phenomenon based on the fact that on average the velocity of the oil film is half the journal rotational velocity, therefore for journal running speeds near double the critical frequency there would be a disturbance force caused by the motion of the oil which would be close to the critical frequency resulting in a whipping of the journal-shaft system.

Whilst the foregoing explanation provides a basic understanding on the phenomenon of oil whip the theory is incomplete as it does not satisfactorily demonstrate why oil whip persists at speeds greater than twice the first critical. However an important observation made by Newkirk and Taylor was that slight misalignment resulted in a remarkable increase in the stabilizing effect of the bearing, a condition which is to be pursued in greater depth in this thesis.

Harrison's(1) theory for the response of a rigid shaft supported by a hydrodynamic oil film was further developed by Robertson(6). In his analysis he discusses how Harrison had unfortunately made an error at the very beginning of his paper by omitting to allow for the movement of the journal centre when estimating the tangential component of the surface velocity. That error by itself invalidates the whole of his subsequent deductions. Also at a later stage he assumes the rotor to be massless which oversimplifies the problem under consideration. An interesting feature of his analysis is that he considers the damping neglected by Stodola but ignored the sub-ambient pressures in the oil film and thus found the journal to be inherently unstable with

with a whirling frequency equal to one-half the speed of rotation, rather than speed exceeding double the critical speed.

Hagg(7) was the first to recognize that most dynamical systems can be idealized as having three springs masses and dampers. The first spring mass and damper representing the bearing supporting structure, the second representing the oil film characteristics and finally the third spring mass and damper to represent the rotating shaft. The oil film forces acting along the 'x' and 'y' axis were obtained in a manner similar to Hummel(4), however, for the first time damping was to be considered in the equations of motion. By obtaining the characteristic equation, and using Routh's criteria, produced conditions of instability which were similar to Stodola provided the damping were made zero. Hagg investigated two journal bearings, the first was a full plain bearing and the other made up of several segmental pivot pads, the latter was found to offer greater stability.

In October 1953 Hagg together with Warner(8) presented a paper which was an extension of Hagg's original work reference(7), this latter paper investigated the stability of flexible rotors. A series of tests were conducted on an industrial size turbine having a single disc testing three types of bearings (a) a full bearing 2.0 in diameter x 2.5 in long; (b) a full bearing having a 0.375 in wide circumferential groove-bearing dimensions as (a); and (c) a 160 degree centrally loaded partial journal bearing. The rotor critical speed on rigid supports was machined to give a critical speed of 5250 R.P.M. and the maximum test speed was up to 12,000 R.P.M. In addition to these tests the authors presented results obtained from an electrical analog computer analysis, obtaining the damping resistance for stability of the analog circuits, results of which checked with theory giving an averaged error of 10 per cent.

The stability criterion for self excited vibrations of the flexible rotor was presented as a series of charts for the various bearings tested, described by the equations given below, further the results demonstrated that rotor flexibility tends to reduce the region of stable operation, but the final question of stability depends upon all of the elements of the dynamical system.

$$\frac{\lambda A^2}{\phi}\left[\left(\frac{R}{C}\right)^2 \frac{\mu N}{p}\right]^2 > \frac{CN^2}{g}$$

where $$\lambda = \left[\frac{K_1}{1 + \frac{K_1}{K_2}} + \frac{4\,K_2}{1 + \frac{K_2}{K_3}}\right] \Big/ K_1 + K_2$$

$$A = \frac{\left(\frac{L}{D}\right)^2}{1 + \left(\frac{L}{D}\right)^2} \times \frac{1}{\left(1 - \frac{\varepsilon}{2C}\right)^3}$$

K_1 and K_2 = force per unit displacement of the journal in the x and y directions respectively.

However, although these equations were presented the oil film stiffness coefficients were still unlisted for the bearings considered, and any coefficient required would have to be approximated according to the theory forwarded by Hummel.

In the same year Poritsky(9) published his work which was of similar context to reference(8). He explained that discrepancies between theoretical reasoning and experimental tests as experienced by reference(8)et.al. were due to the analytical treatment giving no attention to the appearance of negative pressures generated within the oil film wedge, and also the effects of side leakage, if neglected, resulted in film pressures being higher than those experienced in practice. Therefore more realistic results were obtained by using

oil film pressures which had been deduced having allowances made for negative pressures and oil side leakage, his results for predicting stability is now well known and may be found in most text books dealing with rotor-bearing instability.

$$\text{i.e. } M\omega^2 \left(1/_k + 1/_K\right) < 4$$

where k = shaft stiffness

K = stiffness factor of the oil film.

Poritsky suggests that the radial spring constant K of the oil film depends upon the speed of the rotor and not upon the frequency of vibration. However, very little information was given regarding the oil film flexibility.

Investigations into the problems of fluid whirl for a rigid shaft running in the vertical position were made by Boeker and Slernlicht in 1956(10). Use was made of a relative stiff shaft so that the factor $(1/_k + 1/_K)$, used by Poritsky, could be neglected in favour of the term of 1/Ka hence the criterion

$$M\omega^2 \left(1/_k + 1/_K\right) < 4$$

becomes $$\omega_c = 2 \frac{K_a}{M}$$

where ω_c is the frequency at which whirl commences. The authors demonstrated in their analysis, that the threshold whirl frequency for a rigid rotor in a vertical machine was a function of the factor Ka which was the slope of the curve of the radial component of force versus the radial displacement i.e. dFR/de, evaluated at the origin, which of course can be likened to a spring stiffness acting in the radial direction. An experimentally determined curve was presented

allowing Ka to be determined for various running positions of the journal bearing.

Newkirk and Lewis(11) also Newkirk(12) investigated oil film whirl using both flexible rotors together with five different bearings. Reference(11) sets out to define various definitions such as "out of balance", "oil whip" and "oil whirl". These definitions were long overdue as terms describing "whip" and "whirl" were being used indiscriminately, attention was also given to the stabilizing effects caused by the introduction of axial misalignment. Reference(12) demonstrated how the oil film behaviour was affected by the flexibility of the rotor which it supports, flexible shafts produce disturbances which are more dependent upon the shaft flexibility whilst for a rigid shaft the oil film was the influencing factor. In general the authors produced evidence that stable operation could be extended to higher speeds by reducing the axial length of the bearing, indeed this is a modification often made to journal bearings in the event of experiencing a critical speed or instability when commissioning rotating plant. Alternatively, Newkirk suggested dividing the bearing into two short bearings by cutting a central groove completely around the bearing, again this is done when experiencing difficulty which may be controlled by the oil film flexibility.

Experiments were conducted by Downham(13) showing the effects of bearing length, clearance, and lubricant viscosity upon the whirling speed of a single mass system supported by 360 degree plain journal bearings, the bearings tested were 1.2 in diameter by varying length to diameter ratios of 2.71, 1.88 and 1.04. Whilst investigating the effects of rotor unbalance, it was observed that the critical speed of the shaft bearing system increased for a corresponding increase

in unbalance, this was attributed to the change in the equivalent shaft length governed by the slope of the journal within the bearing bush, this phenomenon is discussed in some detail by the author. The effects of bearing clearance was noticed to raise the critical whirling frequency, again due to the slope taken up by the journal.

Changes made to the oil viscosity was also noted to have an appreciable stiffening effect upon the shaft system, for example, an increase in the oil viscosity had the effect of raising the critical together with a corresponding increase in the vibration amplitude, all of these changes being more pronounced for the larger bearing bush. A further observation which is of practical importance was that by reducing the bearing clearance from 0.004 in to 0.001 in a considerable increase in the critical speed was obtained for all bearing lengths to diameter ratios tested, and for all oil viscosities. This experimental observation is contradictory to the theoretical hypothesis put forward by Reddi and Trumpler but indeed substantiates what has long been the practice of engineers associated with the balancing and commissioning of turbo-generators.

Charts illustrating whirl amplitudes against shaft rotational speed presented in this reference clearly demonstrated that because of the elliptic nature of the oil film it was possible to get two first criticals and two second critical speeds, each relating to the major and minor film stiffness. This phenomenon was thought to have little importance for the generation of machine manufactured in 1958 but with todays machine more attention is given to these effects especially when modal balancing.

In 1959 Hori(14) advanced his theories on oil film whip with the intention of offering a plausible explanation for the various discre-

pancies experienced by the proceeding investigators. His work made a comprehensive analysis into inherent rotor instability assuming zero pressure in the divergent region of the oil film wedge, in place of negative pressures as assumed by most of the other papers before him. In order to overcome some of the confusions in the theory of oil whip Hori divided the rotor vibrations into two groups (a) stability for small vibrations and (b) stability for the larger vibration amplitudes. Under group (a) small vibrations were identified as being small compared with the eccentricity of the bearing centre, the equation of motion was linearized by neglecting the shaft deflections and by also neglecting the highest powers of the eccentricity ratio which are normally necessary when determining the radial and tangential oil film pressures. The stability of the rotor was finally determined using "Hurwitz" criteria whereby Hori deduced that $W/mc\omega^2$ must be greater than $W/mc\omega_c^2$ if shaft stability is to be maintained. The exact relationship between the above equations was illustrated by a stability chart, the same chart also demonstrated how the shaft was always stable if the eccentricity ratio of the bearing was always greater than 0.8. For whirl amplitudes greater than the eccentricity i.e. group (b) Hori arrived at the conclusion that all amplitudes of vibration of the rotor can only continue to exist if the speed of shaft rotation was higher than twice the first critical speed, he also provided an equation for the approximate whirling speed which was equal to ω_1 provided the value of $K/2\omega_1$ was equal to zero, and equal to $\omega/2$ provided $K/2\omega_1$ approaches infinity. From these considerations he was able to reproduce the main characteristics of references (5) and (11).

where K = oil film coefficient

ω = angular velocity of shaft rotation

ω_1 = angular velocity of natural vibrations of shaft.

In the early 1960's with the increase in the running speeds of the smaller turbomachines, interest in the theory of oil whip increased. What was an interesting phenomenon was rapidly becoming an important design consideration and information regarding the physical implication was demanding more attention in order to achieve a successful design free from vibrations.

With the design engineers viewpoint in mind Reddi and Trumpler(15) directed their studies towards the stability characteristics of a full journal bearing and a 180 degree partial journal bearing in order to permit a qualitative understanding between two bearing geometries. The authors primarily concerned themselves with the prediction of the whirl trajectories of the journal centre by making use of a digital computer, a solution of the equations of motion was solved using the Runge-Kulta-Gill method for the step by step integration of the differential equations. The dynamical model used throughout their investigations was considered to be infinitely stiff, and the two different films treated, namely, the full 360 degree and the 180 degree partial film allowed for the end leakage assuming it to be the same as the standard leakage factors based on the static equilibrium position.

The results produced some conflicting ideas, for example, the paper suggests that to improve stability it would be better to have a large bearing clearance, when in practice it is found to be the reverse of this, as found by Downham. However, the authors do present a stability chart which goes a long way in providing a general guide

for the full journal bearing, but unfortunately they do not provide a computer solution of the governing equations for the 180 degree bearing, which is the type used in practice.

Later in the same year Jennings and Ocvirk(16) described another method predicting the whirl trajectory, but this time with an analog computer. The assumption of a rigid rotor is used and although this paper did not indicate the stability criteria for the bearings two important observations were made from the growth of the orbits obtained,which have direct significance to the work presented in this thesis, the first observation was that the orbit size became significantly larger as the mass of the journal was increased, and secondly the size of the orbit increased as the speed of the journal increased.

In addition to the forgoing papers Orbeck(17) and Tondl(18) presented their papers in the same year (1962) both investigating self excited vibrations dealing specifically with rotor-bearing systems.

Also in the same year Parszewski and Cameron(19) gave their paper which was one of five presented within the Lubrication and Wear Group of the Institution of Mechanical Engineers. They presented a theoretical investigation which took into account the flexibility of the rotor within the equations of motion. This was basically only an extension of Hummel who originally considered a stiff shaft thus simplifying the problem. By considering Hummel's method the resulting oil film forces acting on the displaced journal was obtained by rotating the whole system of displacements so that the journal bearing was returned back onto the steady state equilibrium semicircle, the resulting oil film forces are then considered to be equal to that force required to displace the journal to this new position on the

equilibrium semicircle. Treating the problem in this manner neglects the effects of the squeeze film velocities which have the effect of increasing the oil film forces. Therefore, results obtained could be expected to be on the low side, indeed what the authors have in fact determined are those forces which would act on the journal had the rotor been made to operate continuously away from its natural running position.

The rotor system under consideration was idealized by considering a central mass having an equal shaft fluxural stiffness either side of it, thus allowing the shaft to be replaced by a spring and mass which when added to the oil film characteristics introduce another degree of freedom; this method was to be used quite extensively by later investigators. Using what the authors describe as a dynamic resilience number, which was a function of the journal eccentricity ratio, the equations of motion were solved and charts provided for determining the whirl frequency of the entire system.

A list of results obtained from a number of interested firms was also presented, showing observed half frequency whirl for full-sized turbines, and a direct comparison made with the calculated result. The majority of results were shown to be low, which may be attributed to the neglect of the squeeze film terms in Reynolds equation and also by making the assumption that displacements are sufficiently small that they may be linearized.

In the same group of papers Morrison(19) demonstrated the effects of a plain 360 degree bearing on the whirling action of an elastic rotor taking into account, for the first time, the effects of both the displacement and velocity components of the hydrodynamic oil film derived from the first order terms of Taylor's series.

The linear coefficients describing the oil film forces were presented as follows:-

$$F_s = a_{ss}s + b_{ss}s' + a_{sr}r + b_{sr}r'$$

$$F_r = a_{rs}s + b_{rs}s' + a_{rr}r + b_{rr}r'$$

where a_{ss} etc. are the displacement force coefficients, and b_{ss} etc. are the velocity force coefficients evaluated from the equations governing the behaviour of the oil film wedge, evoking Ockvirk's short bearing theory whereby the circumferential pressure derivatives in Reynolds equation are neglected. Although the displacement and velocity coefficients were used in their analysis they were described by the authors as being "compounded" with each other making it very difficult in presenting individual values.

The study reported in reference(19) was carried out with reference to a particular problem encountered by Brush Electric, who were experiencing at that time instability problems with a small turbo-generator. Therefore in order to simulate the whirl behaviour of this rotor, investigations were carried out on a model, the results of which produced two distinct modes of vibration, the first being half speed whirl and the second a suppressed first critical.

The authors of this paper highlighted the following two important observations:-

(a) The magnitude of the damping terms are by no means small and will in the majority of cases give rise to forces in the same order as the displacement coefficients.

(b) The displacement coefficients a_{ss} and a_{sr} etc. are not

elastic, therefore $a_{sr} \neq a_{rs}$ due to their non-reciprocal properties and hence stability considerations arise from these terms quite apart from the velocity coefficients, further, they give rise to the well known phenomenon of half speed whirl.

Holmes(21) also investigated oil whip using a rigid rotor, however, in order to provide a qualitative understanding particular attention was given to both very short and very long bearings, his treatment when setting up the equations of motion was to first consider linear motion by assuming small perturbations about the static equilibrium position, and later to analyze larger vibrations using a step by step method of solution with the aid of a digital computer.

By linearizing the equations of motion for small amplitudes of vibration, Holmes deduced four oil film coefficients, compared to eight as used in reference(20) comprising of two displacements and two velocity force coefficients.

Two major disadvantages are to be noted with this paper:-

(a) The bearing used throughout the experimental investigation was 0.76 in diameter by 0.66 in long having a full 360 degree working face, also at the mid-length the bearing had a circumferential groove, further the bush was manufactured from PERSPEX, thus the specific pressure was kept to a deliberately low value of 8.0 lb/in^2 (5.5 N/cm^2) which is far from a realistic value.

(b) A condition under which the operating parameters remained valid, was that the oil film should be free from cavitation. To achieve this condition oil was forced around the central

groove in the bearing, however, in bearings operating under service conditions it is well known that cavitation does exist at the trailing end of the oil film wedge.

The results presented in this paper should therefore be treated with reservation if applied to full size machines.

Later in 1966 Holmes together with Michell and Byrne(22) extended the above experimental analysis by producing an analogue simulation for the solution of the equations of motion, however for the non-linear analysis precise theoretical explanations could not be offered, also the geometry of the central groove was shown to affect the whirl orbit, the authors for the greater majority of cases produced very good traces of the journal centre, both experimentally and with the aid of the analogue computer.

Results obtained in graphical form defining the size and position of the whirl orbit as a function of the bearing duty parameter were published by Lund and Scubel(23). The information in this paper was presented in such a way that either a rigid or flexible rotor resting in plain 360 degree bearings could be investigated.

In solving Reynolds equation an infinitely short bearing theory was evoked whereby the eight oil film force coefficients were determined by expanding the oil film forces into the first order Taylor's series, thus allowing the equations of motion to be written as a function of the journal eccentricity ratio. In the latter part of this paper non-linearities of the oil film force was taken into account by considering the larger amplitudes of vibration, the resulting equations of motion were solved by the method of averaging, whereby the whirl orbit obtained were elliptic and strongly dominated by the fundamental harmonic of motion, higher harmonics could be noticed by displaying

some distortion of the fundamental elliptic shape.

Although eight force coefficients were used in this paper their values were approximated as a function of eccentricity, thus allowing the characteristic equation for stability to be formulated, therefore explicit values were not presented in this reference.

The majority of the preceding papers are restricted to complete 360 degree circular bearings, however bearings of this type are rarely used for industrial applications because it is very much more convenient to split the bearing into at least two parts of 180 degrees or less. Splitting into two parts allows oil ports to be constructed without much difficulty, see drawing of exploded view figure (1-1). For the above reasons few bearings will have a complete oil film extending over more than 180 degrees, usually in practice the bearing arc is 120 degrees to allow reliefs to be machined for the oil inlet wedge to commence forming before entering the working force of the bearing. A further reason for using the small arc's of contact is to help reduce power losses within the bearing.

Glienecke(24) having determined experimental oil film force coefficients, comprising of four stiffners and four clamping provided stability charts for varying amounts of shaft flexibility against a relative Sommerfeld duty parameter. These charts demonstrated that for speeds less than twice the critical speed, self excited vibrations approximately equal to half the rotational frequency may be experienced. Other charts given in this reference are (a) minimum oil film thickness, (b) critical speed and resonance amplitudes, all formulated from experimental observations taken from a 120 M/M diameter pocket type of bearing. Gilienecke tested for different types of bearing geometries:- 360 degree plain bearing, three land bearing, two lobed bearing and a

pocket bearing. Curves presented in this reference demonstrated the three land bearing as offering greater stability, but at the expense of the load carrying capacity, however for good load capacity together with good stabilizing properties the two-lobed and pocket bearing were shown to be the best choice.

A paper dealing with the equations governing the vibrational performance of shaft systems supported by hydrodynamic bearings was presented by Holmes(25) at the I.Mech.E. conference in 1972. In his theoretical treatment, Holmes, considered a bearing which was sufficiently short in the axial length thus allowing the circumferential oil pressure distribution to be neglected and which also allowed Reynolds equation to be greatly simplified. Further the bearing considered was a full 360 degree having the oil film pressures in the cavitation region set to zero.

Solution of the resulting differential equations of motion were solved using Runge Kutta step by step procedure, thus allowing a family of journal whirl orbits to be obtained for different values of u/c, where u is the eccentricity of the rotor mass and c is the radial clearance of the bearing. The results obtained were for fixed values of loading and eccentricity ratio. Holmes also presented the equations of motion using eight oil film coefficients and discussed the beneficial effect of the damping terms in reducing the amplitudes of vibration together with reductions to the vibrational force transmitted to the machine foundations, however the force coefficients used in his paper were taken from experimental results of Woodcock and Holmes(4).

The above survey does not in any way constitute a complete bibliography, the amount of literature grown around this subject is as

numerous as the theories and methods put forward, however, they do provide a quantitative awareness of the oil film characteristics and although reported findings are often at variance with other published results, these papers do nevertheless provide a means of studying trends and relationships which are necessary for complete understanding of instability. Information tends to be spread over many papers therefore the practicing engineer may never find the complete problem solved to its fullest extent, such that a design may be completely finalized, alternatively he may accept a particular conclusion which at some later date be disproved.

The papers used so far help to describe and standardise on ternonology together with related theories for solving the common problem of rotor instability, and have gained the reputation as being classic in their approach, indeed, even as late as 1972, papers discussing machine instability were being published i.e. Kramer(26) and White(27).

When investigating rotor instability the very nature of the problem does not allow the oil film force coefficients to be presented as explicit values, but approximated as to allow their use in the governing equations of motion as a function of eccentricity ratio or Summerfeld number, therefore none of the papers given so far list values for the stiffness and damping coefficients. The purpose therefore of presenting such papers in this historical survey, is to allow the reader to obtain the fullest possible information of the effects of a rotor resting on an oil film cushion, and to provide a quantitative awareness of the behaviour and the formulation of the oil film characteristics even if they are disguised in a mathematical equation not readily recognized as an oil film force describing either a value of stiffness or damping.

2.2 Papers published listing the oil film force coefficients

Hagg and Sankey(28) were the first to publish the elastic and damping properties of a hydrodynamic oil film. Their first paper June 1956 sets out in detail their experimental test rig used to measure the two stiffness and the two damping coefficients necessary to replace the dynamic behaviour of the oil film wedge excited by a synchronous out of balance disturbance force. The authors were not particularly interested in stability such as oil film whip, but in the influence of the oil film in suppressing the critical speed, and the effects of damping which allows a rotor to pass through its critical speed without excessive journal vibration, in contrast to a rolling bearing which would be extremely dangerous. Tests were initially conducted on a 150 degree partial journal bearing having a L/D ratio of 1·0, however in March 1958(29) they extended their work to include a 125 degree partial bearing having a L/D ratio of 1.0 and another having a L/D ratio of 0.4. The above bearing was also tested with a 17.5 degree eccentric load. Dimensionless dynamic properties of the oil film were presented by plotting KC/W and BCω/W against the Sommerfeld duty parameter, here K is the oil film stiffness and B the damping with CW and ω being the bearing radial clearance, loading and rotational speed in rad/sec respectively. These coefficients, were completely separated from the rotor dynamics and it was assumed that the oil film could be expressed by the following equations

$$Pu = K_u u + B_u u$$

$$Pv = K_v v + B_v v$$

The journal motion for a given bearing was found to be elliptic with the major axis of the ellipse inclined to the horizontal, therefore

the maximum and minimum values of elasticity K_v and K_u respectively and similarly for the damping C_v and C_u were also inclined to the horizontal however the value of the inclination was not presented in their design charts. The coefficients recorded may only be applied to rotors having similar operating conditions as those investigated by Hagg and Sankey, for example, synchronous vibration as associated with an unbalanced rotor, further these values must include certain non-linearities together with cross coupling terms which could not be evaluated by the method used in their analysis.

One year later Sternlicht(30) described the equations of motion using four stiffness and four clamping coefficients. His paper sets out an analytical treatment whereby he obtained the eight oil film coefficients by solving Reynolds equation using the method of finite differences employing a 18 x 18 grillage for the finite field. By selecting various values for the radial squeeze film velocity for a given L/D ratio incremental film forces were obtained in the vertical and horizontal directions. However the radial velocity was confined to the vertical axis only, thus eliminating five of the eight coefficients leaving Kyy, Kxy for the stiffness and Byy for the damping, Bxy was not considered as this value was found to be small when compared with Byy. Charts were provided for these remaining coefficients for varying amounts of eccentricity and are listed for three L/D ratios of 0.5, 1.0 and 1.5.

Although this paper is of value from a mathematical point of view, values for the coefficients given in these charts are of little use to the design engineer, as the paper is limited to a full 360 degree bearing bush and by limiting the journal velocity to the radial direction neglects the tangential velocity which must normally be

present in a vibrating rotor. However results presented clearly demonstrated how the oil film pressure is increased when a radial velocity is imparted to the journal, further such velocities are shown to produce an increase in both the radial and tangential oil film pressures.

The author also made the unqualified assumption that for small changes made to the incidence angle, oil film forces do not appreciably change for this type of angular displacement. This assumption is only valid for small values of the eccentricity ratio, but when considering the larger values of eccentricity, the oil film forces have been found to change. For example, a change made to the incidence angle of only 0.8 per cent produces a corresponding rate of change to the radial force in the order of 12.0 and 6.2 for the tangential force, these tangents are by no means small and do in fact present a measurable amount to the tangential velocity, which in reference(30) has been neglected.

Three years later Sternlicht presented another paper as a joint author with Lund(31) this paper also presents a theoretical analysis of the dynamics for a rotor-bearing system by solving the resulting eight force coefficients denoting the spring and damping characteristics of the oil film together with their coupling effects between the bearing and rotor. The authors primarily set out to demonstrate the effect of the oil film as a source of force attenuation by reducing the amount of vibration by absorbing vibrational energy. The hydrodynamic oil film forces were obtained for a full 360 degree bearing and Reynolds equation solved using finite differences, assuming the oil film wedge to operate under constant viscosity conditions. The eight force coefficients were then obtained by

considering changes experienced by the oil film for small displacements and velocities imported to the journal in the radial direction only. As discussed with reference(30) no considerations were given to incremental displacements along the tangential directions.

In order to simplify the equations of motion the resulting coefficients were considered to be linear for small amplitudes of vibration, also the four cross-coupling coefficients were eliminated by assuming a harmonic excitation force having a frequency equal to the rotational frequency of the journal bearing, thus the original eight coefficients were replaced by four equivalent coefficients which would give exactly the same rotor motion for the force considered. The force transmitted to the bearing pedestal was then formulated in terms of only four coefficients which when dimensionalized presented a method for studying the dynamic response of a simplified single mass rotor-bearing system, however the results are limited to a full 360 degree bearing which is not often used on industrial machines.

In 1963 Warner(32) presented an entirely different method for solving Reynolds equation by using the technique of separation of variables. The author simplified the resulting pressure series by using the first characteristic number working on the assumption that second and higher terms rapidly decreased in importance. Also in setting up Reynolds equation Warner neglected the second order partial differential terms describing the pressure along the axial length of the bearing, thus suggesting that the bearing could be infinitely long therefore no oil can leak from the sides of the bearing; however at some later point in his analysis a correction factor was introduced to try and produce more realistic operating conditions.

This same paper also presented the eight analytical force coefficients for a 120 degree partial journal bearing, obtained by considering changes made to the oil film pressure for small displacements in the radial and tangential directions about the steady state running position. The results were non-dimensionalized and charts plotted as a function of the Sommerfeld duty parameter, however the results given in these charts do not behave in a manner described by later research workers in this field. It is interesting to note however, that the cross-coupling damping coefficients were found to be equal to each other, a phenomenon to be found correct during later experimental and theoretical investigations.

A paper which is often referred to is that of Smidth(33) which was presented to the Lubrication and Wear Convention in 1963. This paper presents information on the dynamic characteristics of journal bearings with particular attention given to the problems encountered by turbine design engineers. Here a comprehensive description is given to the behaviour of a rotor when supported by oil film bearings, emphasis being given to the physical aspects of light load instability, half speed whirl, and low frequency whirl. The author assumes that the dynamic characteristics for small amplitudes of vibration can be represented by linear force-displacement-velocity relations similar to Lund and Sternlicht(31) and Morrison(19),

i.e. $$Px = a_{11}x + a_{12}y + b_{11}\dot{x} + b_{12}\dot{y}$$

$$Py = a_{21}x + a_{22}y + b_{21}\dot{x} + b_{22}\dot{y}$$

The displacement coefficient a_{11} etc., and velocity coefficients b_{11} etc. being functions of the bearing geometry which for the bearing investigated was a full 360 degree, having a L/D ratio of 1.0.

The orbital response for a pure out of balance force rotating first in the same direction as the journal rotation and secondly in the reverse direction was given for an unbalance force equal to one-fifth of the steady load. The resulting trajectories demonstrated the consequence of the non-reciprocal properties were $a_{21} \neq a_{12}$ which is quite different to a normal elastic system, thus demonstrating the complexity of the cross-coupling terms. In addition to these whirl trajectories obtained using the eight linear force coefficients, a comparison was made with the Hagg and Sankey results, agreement was shown to be good at the higher eccentricity ratios but poor for the lower values.

In 1965 Michell, Holmes and Ballegooyer(34) measured the four stiffness coefficients using a very narrow test bearing having L/D = 0.33 for a journal diameter of 2.5 in, thus allowing Ocvirk's short bearing theory to be evoked for computing the steady running position and for general comparison purposes. To obtain the stiffness coefficients an incremental load was first applied in the horizontal direction and the resulting journal movement along the x and y axes noted, thus the values of $\Delta Fx/\Delta x$ and $\Delta Fx/\Delta y$ could be computed, similarly the values of $\Delta Fy/\Delta x$ and $\Delta Fy/\Delta y$ were obtained for an incremental load applied along the y axis. Although the coefficients obtained in this manner are correct they are however only "static" values as they do not include the additional contributed by the squeeze film velocity, which of course would normally be present with a vibration shaft-bearing system. The authors demonstrated the closeness of their measured stiffness values with those calculated by Morrison, however, Morrison used the method suggested by Hummel who also neglected the squeeze film velocity. Hence this group of results

only provide the additional oil film force, generated for a bearing when displaced from its normal equilibrium running position.

In the communication section of the paper presented by Morton(35) in 1966 dealing with large turbo-generators, Crook and Grantham forwarded Hagg and Sankey type of force coefficients, measured from a 24.0in diameter journal bearing whilst rotating at 3000 R.P.M. Under these conditions the oil film wedge would most certainly be operating well within the turbulent region, therefore care should be taken when using these values and only like for like conditions will give satisfactory results.

Also in the same year Duffin and Gibson(36) discussed the problems encountered in the design of a test rig for the experimental study of a large turbo-generator bearing, they presented a technique whereby the oil film force coefficients could be measured, however this reference did not in fact publish any measured or analytical values but did provide the power absorbed by the shearing action of the oil film. Later Duffin together with Johnson(37) presented Hagg and Sankey type of coefficients for a large journal bearing but again it is thought that the oil film wedge was operating within the turbulent region.

Riger and Cundiff in the communication section of the paper given by Morton(38) discusses the importance of the cross-coupling terms in suppressing the whirl trajectory and also provided values for the eight force coefficients, obtained experimentally from a full 360 degree journal having a journal diameter of 4.0 in and a bush length of 2.0 in. These results were completely different to those obtained by Warner, and clearly demonstrate the importance of the bearing geometry.

In 1967 Szeri(39) published the eight force coefficients for a 110 degree partial journal bearing, these results were obtained numerically from Reynolds equation with due consideration being given to the squeeze film velocity. However no one has yet verified if these coefficients are correct, indeed it would seem that very few design engineers use these results probably because by now so many results have been published that the engineer who is not fully conversant with the behaviour of journal bearings finds any additional results only serve to confuse. This is not entirely surprising as within the same group of papers Glienecke(24) published his experimental results for a similar type of bearing which in general are contradictory to the results of Szeri.

Also in the same year Orcutt and Arwas(40) investigated the dynamic behaviour of a rigid rotor for various mean values of Reynolds number up to 13,300. In this paper the authors presented values for the dimensionless stiffness and damping coefficients for a 100 degree partial journal bearing, however upon comparing the experimental whirl orbits with those predicted from analytical reasoning, the theoretical whirl trajectories were found in the majority of cases to be greater than those measured experimentally, in some cases they exceeded the experimental results by as much as 100 per cent. The reason for these differences is most certainly due to the presence of non-linearities, indeed the results presented in this thesis will demonstrate exactly the same phenomenon when comparing the whirl orbit using only the eight coefficients with those involving the second order non-linear terms.

2.3 Papers published after 1970

Whilst the research work contained in this thesis was being undertaken, two further papers were published dealing with oil film coefficients. The first was by Woodcock and Holmes in 1970(41) this paper presents a theoretical and experimental assessment of the eight coefficients describing the stiffness and damping properties of the bearing used by reference(34) which has a journal diameter of 2.5 in and a length of 0.825 in. In determining the force coefficient the authors made the unfounded assumption that the stiffness coefficient could be determined statically by applying additional loads to the journal in a similar manner to reference(30) thus allowing the use of synchronous vibrations for determining the damping coefficients when normally such a solution would require two different frequencies of excitation. The physical implication of this assumption is that for the stiffness coefficient obtained the squeeze film effects were completely ignored resulting in values which are low, further the damping coefficients only in part consider the effects of the oil film squeeze velocity.

The experimental bearing bush was manufactured from PERSPEX which in itself could lead to errors because of its low value of Youngs Modulus which would give rise to local distortions for the higher values of loading, this probably accounts for the scatter in the experimental results.

The second paper is by Morton(42) who presented the eight coefficients measured from a 20 in diameter bearing operating at low speeds such that the oil film is laminar, the measured coefficients were found to be low when compared with the computed results using the technique of Sternlicht(30). The method of introducing vibrations to

the oil film was achieved by vibrating the bearing bush, compared to the normal method of vibrating the journal as would be experienced with real rotor bearing system. The bush was forced to vibrate at low frequencies by means of an electrohydraulic vibrator, first acting along the horizontal axis, then quickly dismantling the vibrator it was reassembled so that the bush could be vibrated in the vertical axis. This method is not altogether satisfactory as when the journal is whirling within the bearing bush the oil must be experiencing a pressure wave travelling circumferentially along the active part of the bush, which has the effect of increasing both the oil film stiffness and damping, however, by vibrating along a fixed plane such a travelling pressure wave is not generated. Further, this thesis will demonstrate that for low frequency excitation, the whirl trajectory will be larger than if a synchronous frequency is employed, therefore, it would seem that the oil film coefficients are small, when in fact the non-linearity of the oil film is the influencing factor.

The experimental investigations up to 1970 were not as plentiful as the theoretical studies and frequently inconclusive by over simplifying the problem; certainly the amount of information for design purposes is by no means clear, and final values selected for the dynamical analysis could be challenged by other engineers thus leading to inexhaustible discussions. Although these papers are useful qualitatively most are not sufficiently general in their approach from a design engineers point of view, it is certainly essential to present an adequate theory for the solution of the force coefficients, but it must be emphasized that the adequacy of the analytical work rests on the designers correct idealization of the mechanical system being analyzed, this is particularly so with oil film bearings. Even if

explicit values of the oil film force coefficients could be obtained the enquiring designer would question their accuracy under conditions of misalignment, or if indeed they are even linear as most theorists would suggest.

It is with the problems experienced by design engineers in mind that investigations into the non-linear dynamic characteristics of the oil film was undertaken together with changes experienced resulting from misalignment introduced to the vertical plane. The author is not aware of any other similar results on the uniqueness or otherwise on the solution of Reynolds equation for the determination of the non-linear oil film coefficients for aligned and misaligned operating conditions.

CHAPTER THREE

CHAPTER THREE

ANALYTICAL TREATMENT

3.1 Reynolds Equation

In steady state hydrodynamics a static load yields journal attitudes which are fixed with respect to the bearing bush. However, if a periodic disturbance is introduced to the journal bearing, as is associated with out-of-balance vibration or critical speed phenomena, the resulting motion of the journal would be elliptic. The locus of the vibrating orbit would depend upon the magnitude of the applied out-of-balance force and also upon the steady state running position of the journal before the disturbance force was applied, also it will have as its pole the steady state eccentricity.

In a viscous fluid, across each of the three mutually perpendicular surfaces there are three stresses, giving a total of nine stress components, the magnitude of these stresses depends on the rate at which the fluid is being distorted. From the three resulting equations of equilibrium, plus a fourth equation of continuity, Osborn Reynold derived a single partial differential equation thus:-

$$\frac{\partial}{\partial x'}\left(\frac{\rho' h'^3}{\mu'}\frac{\partial P'}{\partial x'}\right) + \frac{\partial}{\partial z'}\left(\frac{\rho' h'^3}{\mu'}\frac{\partial P'}{\partial z}\right) = 6u'\rho'\frac{\partial h'}{\partial x'} - 12\mu' V' \qquad (3.1)$$

Superscript (-)' denotes dimensional values.

A proof of the above equation is not provided, as it may be obtained from most text books dealing with advanced theories of hydrodynamic lubrication. However, considering equation (3.1) term by term, it can be seen that the first two take into account variations of pressure along the x and z directions respectively. The first of the

two terms on the right-hand side are for steady running conditions i.e. rotation without motion, where $u\partial h/\partial x$ represents the action of the rotating journal with velocity u over a wedge-shaped film given by $h(x)$. The last term is the expression for the velocity of the shaft centre, and is responsible for the squeeze film action. To obtain the above equations Reynolds had to make the following assumptions:-

(I) The thickness of the oil film is small compared to the length x and z. This permitted the curvature of the fluid film to be ignored.

(II) No variation of pressure across the film.

(III) The flow is laminar, no vortex flow and no turbulence may occur anywhere within the film.

(IV) Fluid inertia is small compared to the viscous shear.

(V) Isothermal conditions are assumed, thus averaged viscosity is considered at all positions within the oil film wedge.

(VI) No negative pressures can exist at any point in the film. This assumption is discussed in greater detail in Chapter Four, Section Four.

Reynolds equation holds good for both compressible and incompressible lubricants, however throughout the following work it is assumed that the oil film remain incompressible. This assumption will have negligible effect on the solutions obtained as the maximum specific pressure will not exceed 200 lb/in^2 (138 N/cm^2).

3.2 Axes and velocities of the vibrating journal

In order to obtain a set of co-ordinate axes which describe the vibration velocities, polar axes are chosen such that they are parallel to the steady state journal position shown in figure (3.1). Here the origin is at the position of the minimum film thickness, thus the radial velocity is in the direction of the minimum oil film thickness, and the tangential velocity is normal to the direction of the minimum oil film.

The steady state running position of the journal within the bearing bush may now be completely described by ε, τ, ϕ and ψ where ε and τ are the eccentricity and tilt ratio's respectively, ϕ is the attitude angle and ψ is the angle of tilt.

The minimum oil film thickness may be described by the equation

$$h = c\left[1 + \varepsilon\cos\theta + \frac{2\tau Z}{L}.\ \cos(\theta + \phi - \psi)\right]$$

The above equation is derived in Chapter Two, Section Two.

It can be seen that the radial velocity of the journal centre is simply a derivative of the above equation with respect to time thus:-

$$\frac{dh_o}{dt} = -c\frac{d\varepsilon}{dt}$$

It is more convenient to arrange the radial velocity such that it is positive when moving away from the bush.

To obtain the tangential velocity it is necessary to consider a small displacement of the journal centre O about the bush centre O' with respect to changes in the attitude angle ϕ.

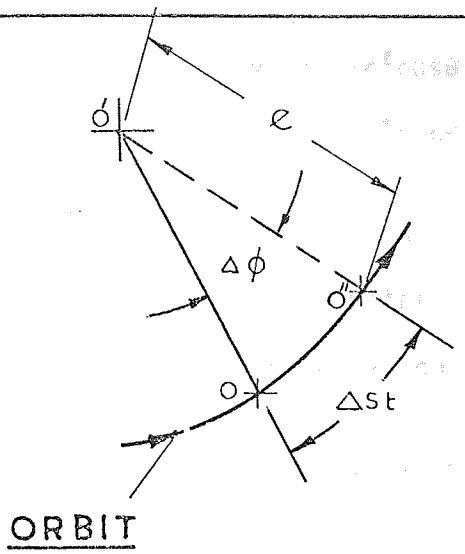

FIG. 3-2 TANGENTIAL DISPLACEMENT OF JOURNAL.

FIG. 3.2 TANGENTIAL DISPLACEMENT OF JOURNAL

$$\Delta St = e\Delta\phi$$

Hence $$\frac{ds}{dt} = e\frac{d\phi}{dt} = c\varepsilon\frac{d\phi}{dt}$$

Therefore the tangential velocity is equal to $c\varepsilon\dot{\phi}$.

Consider now any point P on the surface of the journal, positioned some angular distance θ from the line of centres; the radial velocity v at any circumferential position on the bearing journal may be obtained by adding the components of both the radial and tangential velocities, plus the surface velocity of the shaft rotating about its own centre.

$$v = c\dot{\varepsilon}\cos(\pi - \theta) - c\varepsilon\dot{\phi}\sin(\pi - \theta)$$

and the tangential velocity u is given by:-

$$u = c\dot{\varepsilon}\sin(\pi - \theta) + c\varepsilon\dot{\phi}\cos(\pi - \theta) + \text{Angular Velocity}$$

the above equations may be simplified to give:-

$$v = -c\dot{\varepsilon}\cos\theta - c\varepsilon\dot{\phi}\sin\theta$$
$$u = c\dot{\varepsilon}\sin\theta - c\varepsilon\dot{\phi}\cos\theta + R\omega \qquad (3.2)$$

which describes the radial and tangential velocities in terms of the bearing polar co-ordinates. Substituting equations (3.2) into the right-hand side of equation (3.1) and noting that

$$6u\frac{\partial h}{\partial x} - 12v = 6u\frac{\partial h}{R\partial x} - 12v$$

gives

$$\text{R.H.S.} = \frac{6}{R}\left[c\dot{\varepsilon}\cos\theta + c\varepsilon\dot{\phi}\sin\theta + c\varepsilon\dot{\varepsilon}\cos^2\theta - c\varepsilon\dot{\varepsilon}\sin^2\theta + c\varepsilon^2\dot{\phi}2\sin\theta\cos\theta - R\omega\varepsilon\sin\theta\right] - 12\left[c\dot{\varepsilon}\cos\theta + c\varepsilon\dot{\phi}\sin\theta\right]$$

consider the terms which are not divided by R thus:-

$$\frac{6}{R}u'\frac{\partial h}{\partial x} - 12v' = -6c\omega\varepsilon\sin\theta + 12[c\dot{\varepsilon}\cos\theta + c\varepsilon\dot{\phi}\sin\theta] \qquad (3.3)$$

Although the above equation may look involved it may be seen that the first product term relates to the steady running conditions of the bearing, i.e. rotation without motion, the second product term describes the radial velocity and the final product describes the velocity in the tangential direction.

Midway along the length of the journal, the oil film thickness is given by

$$h = c(1 + \varepsilon\cos\theta)$$
$$\frac{\partial h}{\partial\theta} = -c\,\varepsilon\sin\theta$$
$$\text{also} \quad \frac{\partial h}{\partial x} = \frac{\partial h}{R\partial\theta}$$

thus equation (3.3) becomes:-

$$6u' \frac{\partial h}{\partial x} - 12V' = 6\omega R \left[1 - 2\frac{\dot{\phi}}{\omega}\right] \frac{\partial h}{\partial x} + 12 c\dot{\varepsilon} \cos\theta \qquad (3.4)$$

3.3 Reynolds equation in non-dimensional form

By considering the oil film to be incompressible and also assuming that throughout the entire working face, averaged oil viscosity may be considered, then ρ may be given as averaged value for the entire oil film, equation (3.1) may be written as follows:-

$$\frac{\partial}{\partial x'}\left(\frac{h'^3}{\mu'}\right)\frac{\partial P'}{\partial x'} + \frac{\partial}{\partial z'}\left(\frac{h'^3}{\mu'}\right)\frac{\partial P'}{\partial z'} = 6u' \frac{\partial h}{\partial x'} - 12V' \qquad (3.5)$$

The above equation may be solved for a particular set of operating conditions, however it would be both economical and convenient to arrange the above equation in the form where the quantities appearing are non-dimensional. If this is done over a wide range of non-dimensional values, then the results obtained may be plotted, thus providing a solution to Reynolds equation for the working range of most bearings.

In order to obtain equation (3.5) in dimensionless form the following dimensionless values are defined.

$$x = \frac{x'}{D'} \qquad h = \frac{h'}{c'} \qquad u' = \pi D' N'$$

$$z = \frac{z'}{L'} \qquad \mu = \frac{\mu}{\mu(Ave)} \qquad P = \frac{P'}{\mu(Ave).N'} \left(\frac{c}{R}\right)^2 \qquad (3.6)$$

Substituting equations (3.6), into equation (3.5) gives:-

$$\frac{\partial}{\partial(xD')}\left\{\frac{h^3 c'^3}{\mu\mu(Ave)} \cdot \frac{\partial}{\partial(xD')}\left[P\mu\mu(Ave)N'\left(\frac{R'}{c'}\right)^2\right]\right\}$$

$$+ \frac{\partial}{\partial(zL')}\left\{\frac{h^3 c'^3}{\mu\mu(Ave)} \frac{\partial}{\partial(zL')}\left[P\,\mu\mu(Ave)N'\left(\frac{R'}{c'}\right)^2\right]\right\}$$

$$= 6\pi D'N' \left(1 - 2\frac{\dot{\phi}}{\omega}\right) \frac{\partial(hc')}{\partial(xD')} + 12c'\dot{\varepsilon}\cos\theta$$

giving

$$\frac{\partial}{\partial x}\left[h^3 \frac{\partial P}{\partial x}\right] + \left(\frac{D'}{L'}\right)^2 \left[\frac{\partial}{\partial z}\left(h^3 \frac{\partial P}{\partial z}\right)\right]$$

$$= 24\pi \left[\left(1 - 2\frac{\dot{\phi}}{\omega}\right) \frac{\partial h}{\partial x} + 4\frac{\dot{\varepsilon}}{\omega} \cos\theta\right] \qquad (3.7)$$

Note if $\dot{\varepsilon} = \dot{\phi} = o$ the result is Reynolds equation for a journal rotation zero motion, this condition is used to describe the steady running position of the journal bearing, for both aligned and misaligned operating conditions.

This equation would seemingly appear to be linear in ω, $\dot{\varepsilon}/\omega$ and $\dot{\phi}/\omega$ thus allowing the theory of superposition to be evoked, by integrating separately for stationary centre with $\dot{\phi}/\omega = \dot{\varepsilon}/\omega = 0$, then for the radial velocity with $\dot{\phi}/\omega = \omega = 0$ and finally for the tangential velocity with $\dot{\varepsilon}/\omega = \omega = 0$. However, this is not permissible owing to the non-linear requirements, that the pressure should always be greater than zero, and any negative pressure should be re-assigned to the value of zero, also the fact that cavitation for the higher eccentricity ratio's is dependent on all three parameters, see Chapter Four, Section Four.

In order to solve equation (3.7) it is proposed to use the method of finite differences as described in detail in Chapter Four Section Three.

3.4 Fluid film forces

Consider the case in which a journal is supporting an external load w in some equilibrium position described by ε_o and ϕ_o provided

by the oil film forces FRO and FTO. If the shaft, by some external vibrating force, is momentarily given a secondary displacement to a position ε_1 and ϕ_1 the fluid forces F_{R1} and F_{T1}, corresponding to this new position of the shaft is no longer equal and opposite to w but are changed by some unknown amount, the amount being determined by equation (3.7) yielding the pressure distribution over the oil film for given boundary conditions. Integrating the resulting pressure distribution the forces F_{R1} and F_{R2} are obtained the component of force, generated by finite displacements and velocities about the steady running position, may be expressed by the following functions:-

$$FR' = -\frac{\mu L u}{\pi}\left(\frac{R}{c}\right)^2 f_R \quad (\varepsilon, \phi, \frac{\dot{\varepsilon}}{\omega}, \frac{\dot{\phi}}{\omega})$$

$$FT' = \frac{\mu L u}{\pi}\left(\frac{R}{c}\right)^2 f_T \quad (\varepsilon, \phi, \frac{\dot{\varepsilon}}{\omega}, \frac{\dot{\phi}}{\omega})$$

The negative sign is due to FR' being measured positive in the direction of increasing eccentricity, see equation (3.2).

The first part of the above equations is a dimensionless force obtained from the solution of Reynolds equation, which is a function of the L/D ratio. Rewriting the above equations in terms of the Sommerfeld duty parameter we have

$$FR' = -SF.\ f_R\ (\varepsilon, \phi, \frac{\dot{\varepsilon}}{\omega}, \frac{\dot{\phi}}{\omega})$$

$$FT' = SF.\ f_T\ (\varepsilon, \phi, \frac{\dot{\varepsilon}}{\omega}, \frac{\dot{\phi}}{\omega},) \qquad (3.8$$

where $S = \frac{\mu N}{P}\left(\frac{R}{c}\right)^2$ = Sommerfeld number

If $\frac{\dot{\varepsilon}}{\omega} = \frac{\dot{\phi}}{\omega} = 0$ the resulting components of force would be F_{RO} and F_{TO} as illustrated in figure (3.3) the resultant of these forces would be equal and opposite to the weight of the rotor and its direction would be in line with the y axis. If the rotor journal now experiences a whirling motion about the stable position O' the new hydrodynamic oil film forces would be FR' and FT', it is possible to relate these instantaneous film forces at the disturbed position ε_1, ϕ_1 in terms of the steady state forces at the position ε_o and ϕ_o as shown in figure (3.4).

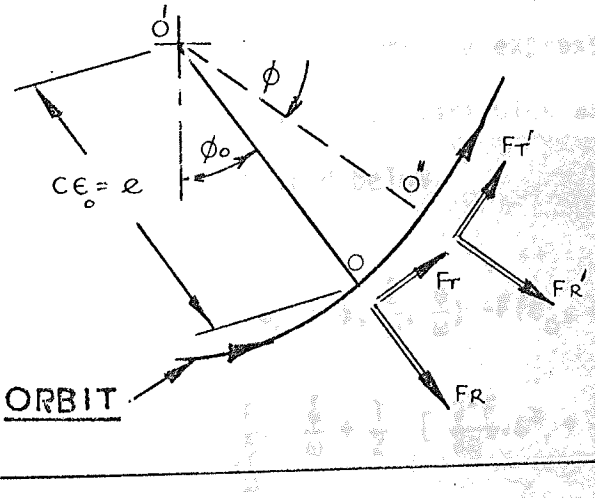

FIG. 3-4

INSTANTANEOUS OIL FILM FORCES

Using figure (3.4) the relationship for the disturbed forces may be written as

$$FR = FR' \cos(\phi - \phi_o) - FT' \sin(\phi - \phi_o)$$

$$FT = FR' \sin(\phi - \phi_o) + FT' \cos(\phi - \phi_o)$$

which may be expressed as follows:-

$$
\begin{aligned}
FR &= -SF\ f_{R'}\ (\varepsilon, \phi, \frac{\dot{\varepsilon}}{\omega}, \frac{\dot{\phi}}{\omega})\ \cos(\phi - \phi_o) \\
&\quad -SF\ f_{T'}\ (\varepsilon, \phi, \frac{\dot{\varepsilon}}{\omega}, \frac{\dot{\phi}}{\omega})\ \sin(\phi - \phi_o) \\
FT &= -SF\ f_{R'}\ (\varepsilon, \phi, \frac{\dot{\varepsilon}}{\omega}, \frac{\dot{\phi}}{\omega})\ \sin(\phi - \phi_o) \\
&\quad +SF\ f_{T'}\ (\varepsilon, \phi, \frac{\dot{\varepsilon}}{\omega}, \frac{\dot{\phi}}{\omega})\ \cos(\phi - \phi_o)
\end{aligned}
\qquad (3.9)
$$

The above dimensionless oil film forces, due to these small perturbations ε_o, ϕ_o, may be expressed in terms of Taylor's series extended to include four variables and to include all second order terms as illustrated below.

$$
\begin{aligned}
&F(\varepsilon_o + \varepsilon, \phi_o + \phi, \frac{\dot{\varepsilon}}{\omega}, \frac{\dot{\phi}}{\omega}) - F(\varepsilon_o, \phi_o, 0, 0,) = \frac{\partial F}{\partial \varepsilon}.\varepsilon + \frac{\partial F}{\partial \phi}.\phi + \\
&+ \frac{\partial F}{\partial \frac{\dot{\varepsilon}}{\omega}}.\frac{\dot{\varepsilon}}{\omega} + \frac{\partial F}{\partial \frac{\dot{\phi}}{\omega}}.\frac{\dot{\phi}}{\omega} + \frac{1}{2}\Big[\frac{\partial^2 F}{\partial \varepsilon^2}.\varepsilon^2 + \frac{\partial^2 F}{\partial \phi^2}.\phi^2 + \frac{\partial^2 F}{\partial \frac{\dot{\varepsilon}}{\omega}^2}\frac{\dot{\varepsilon}}{\omega}^2 \\
&+ \frac{\partial^2 F}{\partial \frac{\dot{\phi}}{\omega}^2}\frac{\dot{\phi}}{\omega}^2 + 2\frac{\partial^2 F}{\partial \phi \partial \varepsilon}.\phi.\varepsilon + 2\frac{\partial^2 F}{\partial \phi \partial \frac{\dot{\varepsilon}}{\omega}}.\phi.\frac{\dot{\varepsilon}}{\omega} + 2\frac{\partial^2 F}{\partial \frac{\dot{\varepsilon}}{\omega} \partial \frac{\dot{\phi}}{\omega}}.\frac{\dot{\varepsilon}}{\omega}.\frac{\dot{\phi}}{\omega}. \\
&+ 2\frac{\partial^2 F}{\partial \frac{\dot{\phi}}{\omega} \partial \varepsilon}.\frac{\dot{\phi}}{\omega}.\varepsilon + 2\frac{\partial^2 F}{\partial \varepsilon \partial \frac{\dot{\varepsilon}}{\omega}}.\varepsilon.\frac{\dot{\varepsilon}}{\omega} + 2\frac{\partial^2 F}{\partial \phi \partial \frac{\dot{\phi}}{\omega}}.\phi.\frac{\dot{\phi}}{\omega}\Big]
\end{aligned}
$$

Applying the above equation to equations (3.9), and taking to the limit for small amplitudes of vibration, provides the radial and tangential oil film forces for a change in journal position and rate of change of position.

3.5 Force coefficients

For design purposes the resulting set of equations are somewhat clumsy, as most computational methods rely on equating forces in the horizontal and vertical axes, and nearly all industrial instrumentation work with the same co-ordinate axes, therefore to use the resulting radial and tangential forces would first neccessitate the user in having to determine the angle of incidence and apply the theory of transformation of axes. It would be convenient therefore, to consider the magnitude of these forms in the horizontal and vertical directions, measured positive as illustrated in figure (3.3) and finally present the force coefficients in the same Cartesian system.

Accomplishing the above in mathematical terms is involved and lengthy therefore it has been set aside in Appendix A and only the first and second order force coefficients are presented in this section, and are as follows:-

The oil film force coefficients acting along the x axis are:-

$$\widehat{Axx} = -\frac{\lambda\omega}{c}\left\{\frac{\partial fR}{\partial\varepsilon}\sin^2\phi + \left(fR - \frac{\partial fT}{\partial\phi}\right)\frac{1}{\varepsilon}\cos^2\phi\right.$$

$$\left. + \left(\frac{1}{\varepsilon}\frac{\partial fR}{\partial\phi} + \frac{fT}{\varepsilon} - \frac{\partial fT}{\partial\varepsilon}\right)\sin\phi\cos\phi\right\}$$

$$\widehat{Axy} = -\frac{\lambda\omega}{c}\left\{-\left(\frac{\partial fR}{\partial\phi} + fT\right)\frac{1}{\varepsilon}\sin^2\phi - \frac{\partial fT}{\partial\varepsilon}\cos^2\phi\right.$$

$$\left. + \left(\frac{1}{\varepsilon}\frac{\partial fT}{\partial\phi} - \frac{fR}{\varepsilon} + \frac{\partial fR}{\partial\varepsilon}\right)\sin\phi\cos\phi\right\}$$

$$\widehat{Axx} = -\frac{\lambda\omega}{c}\left\{\frac{\partial fR}{\partial\varepsilon}\sin^2\phi + \frac{1}{\varepsilon}\frac{\partial fT}{\partial\phi}\cos^2\phi + \left(\frac{1}{\varepsilon}\frac{\partial fR}{\partial\phi} - \frac{\partial fT}{\partial\varepsilon}\right)\sin\phi\cos\phi\right\}$$

$$\widehat{Axy} = -\frac{\lambda\omega}{c}\left\{-\frac{\partial fR}{\partial\phi}\frac{1}{\varepsilon}\sin^2\phi - \frac{\partial fT}{\partial\varepsilon}\cos^2\phi + \left(\frac{\partial fR}{\partial\varepsilon} + \frac{1}{\varepsilon}\frac{\partial fT}{\partial\phi}\right)\sin\phi\cos\phi\right\}$$

$$\widehat{Axx^2} = -\frac{\lambda\omega}{c^2}\left\{\frac{1}{2}\cdot\frac{\partial^2 fR}{\partial\varepsilon^2}\sin^3\phi + \left(\frac{\partial fR}{\partial\phi} - \frac{1}{2}\frac{\partial^2 fT}{\partial\phi^2} + \frac{fT}{2}\right)\frac{1}{\varepsilon^2}\cos^3\phi + \left(\frac{1}{2\varepsilon}\frac{\partial^2 fR}{\partial\phi^2} - \frac{fR}{2\varepsilon} + \frac{\partial fT}{\varepsilon\partial\phi} + \frac{\partial fR}{\partial\varepsilon} - \frac{\partial^2 fT}{\partial\varepsilon\partial\phi}\right)\frac{1}{\varepsilon}\cos^2\phi\sin\phi + \left(\frac{\partial^2 fR}{\partial\varepsilon\partial\phi} + \frac{\partial fT}{\partial\varepsilon} - \frac{\varepsilon}{2}\frac{\partial^2 fT}{\partial\varepsilon^2}\right)\frac{1}{\varepsilon}\sin^2\phi\cos\phi\right.$$

$$\widehat{Axy^2} = -\frac{\lambda\omega}{c^2}\left\{\left(\frac{1}{2}\frac{\partial^2 fR}{\partial\phi^2} - \frac{fR}{2} + \frac{\partial fT}{\partial\phi}\right)\frac{1}{\varepsilon^2}\sin^3\phi - \frac{1}{2}\frac{\partial^2 fT}{\partial\varepsilon^2}\cos^3\phi + \left(-\frac{\partial^2 fR}{\partial\phi\partial\varepsilon} - \frac{\partial fT}{\partial\varepsilon} + \frac{1}{\varepsilon}\frac{\partial fR}{\partial\phi} - \frac{1}{2\varepsilon}\frac{\partial^2 fT}{\partial\phi^2} + \frac{fT}{2\varepsilon}\right)\frac{1}{\varepsilon}\sin^2\phi\cos\phi + \left(\frac{\varepsilon}{2}\frac{\partial^2 fR}{\partial\varepsilon^2} - \frac{\partial fR}{\partial\varepsilon} + \frac{\partial^2 fT}{\partial\varepsilon\partial\phi}\right)\frac{1}{\varepsilon}\cos^2\phi\sin\phi\right.$$

$$\widehat{Axxy} = -\frac{\lambda\omega}{c^2}\{(-\frac{\partial^2 fR}{\partial\phi\partial\varepsilon} - \frac{\partial fT}{\partial\varepsilon})\frac{1}{\varepsilon}\sin^3\phi + (\frac{\partial fR}{\partial\varepsilon} - \frac{\partial^2 fT}{\partial\varepsilon\partial\phi})\frac{1}{\varepsilon}\cos^3\phi$$

$$+ (\varepsilon\frac{\partial^2 fR}{\partial\varepsilon^2} - \frac{1}{\varepsilon}\frac{\partial^2 fR}{\partial\phi^2} + \frac{fR}{\varepsilon} - \frac{2}{\varepsilon}\frac{\partial fT}{\partial\phi} - \frac{\partial fR}{\partial\varepsilon} + \frac{\partial^2 fT}{\partial\varepsilon\partial\phi})\frac{1}{\varepsilon}\sin^2\phi\cos\phi$$

$$\therefore (\frac{\partial^2 fR}{\partial\phi\partial\varepsilon} + \frac{\partial fT}{\partial\varepsilon} - \varepsilon\frac{\partial^2 fT}{\partial\varepsilon^2} - \frac{2}{\varepsilon}\frac{\partial fR}{\partial\phi} + \frac{1}{\varepsilon}\frac{\partial^2 fT}{\partial\phi^2} - \frac{1}{\varepsilon}fT)\frac{1}{\varepsilon}\cos^2\phi\sin\phi\}$$

$$\widehat{Axx^2} = -\frac{\lambda\omega}{c^2\omega^2}\{\frac{1}{2}\frac{\partial^2 fR}{\partial\dot{\varepsilon}^2_{\omega}}\sin^3\phi - \frac{1}{2\varepsilon^2}\frac{\partial^2 fT}{\partial\dot{\phi}^2_{\omega}}\cos^3\phi$$

$$+ (\frac{1}{2\omega}\frac{\partial^2 fR}{\partial\dot{\phi}^2_{\omega}} - \frac{\partial^2 fT}{\partial\dot{\varepsilon}_{\omega}\partial\dot{\phi}_{\omega}})\frac{1}{\varepsilon}\cos^2\phi\sin\phi$$

$$+ (\frac{\partial^2 fR}{\partial\dot{\varepsilon}_{\omega}\partial\dot{\phi}_{\omega}} - \frac{\varepsilon}{2}\frac{\partial^2 fT}{\partial\dot{\varepsilon}^2_{\omega}})\frac{1}{\varepsilon}\sin^2\phi\cos\phi\}$$

$$\widehat{Axy^2} = -\frac{\lambda\omega}{c^2\omega^2}\{\frac{1}{2}\frac{\partial^2 fR}{\partial\dot{\phi}^2_{\omega}}\frac{1}{\varepsilon^2}\sin^3\phi - \frac{1}{2}\frac{\partial^2 fT}{\partial\dot{\varepsilon}^2_{\omega}}\cos^3\phi$$

$$+ (\frac{\varepsilon}{2}\frac{\partial^2 fR}{\partial\dot{\varepsilon}^2_{\omega}} + \frac{\partial^2 fT}{\partial\dot{\varepsilon}_{\omega}\partial\dot{\phi}_{\omega}})\frac{1}{\varepsilon}\cos^2\phi\sin\phi$$

$$+ (-\frac{\partial^2 fR}{\partial\dot{\varepsilon}_{\omega}\partial\dot{\phi}_{\omega}} - \frac{1}{2\varepsilon}\frac{\partial^2 fT}{\partial\dot{\phi}^2_{\omega}})\frac{1}{\varepsilon}\sin^2\phi\cos\phi\}$$

$$\widehat{Axxy} = -\frac{\lambda\omega}{c^2\omega^2}\{-\frac{1}{\varepsilon}\frac{\partial^2 fR}{\partial\dot{\varepsilon}_{\omega}\partial\dot{\phi}_{\omega}}\sin^3\phi - \frac{1}{\varepsilon}\frac{\partial^2 fT}{\partial\dot{\varepsilon}_{\omega}\partial\dot{\phi}_{\omega}}\cos^3\phi$$

$$+ (\frac{\partial^2 fT}{\partial\dot{\varepsilon}_{\omega}\partial\dot{\phi}_{\omega}} + \varepsilon\frac{\partial^2 fR}{\partial\dot{\varepsilon}^2_{\omega}} - \frac{1}{\varepsilon}\frac{\partial^2 fR}{\partial\dot{\phi}^2_{\omega}})\frac{1}{\varepsilon}\sin^2\phi\cos\phi$$

$$+ (\frac{\partial^2 fR}{\partial\dot{\varepsilon}_{\omega}\partial\dot{\phi}_{\omega}} - \varepsilon\frac{\partial^2 fT}{\partial\dot{\varepsilon}^2_{\omega}} + \frac{1}{\varepsilon}\frac{\partial^2 fT}{\partial\dot{\phi}^2_{\omega}})\frac{1}{\varepsilon}\cos^2\phi\sin\phi\}$$

$$\widehat{Axx\hat{x}} = -\frac{\lambda\omega}{c^2\omega}\left\{\frac{\partial^2 fR}{\partial\varepsilon\partial\frac{\hat{\varepsilon}}{\omega}}\sin^3\phi + \left(\frac{\partial fR}{\partial\frac{\hat{\phi}}{\omega}} - \frac{\partial^2 fT}{\partial\phi\partial\frac{\hat{\phi}}{\omega}}\right)\frac{1}{\varepsilon^2}\cos^3\phi\right.$$

$$+ \left(\frac{\partial^2 fR}{\partial\phi\partial\frac{\hat{\varepsilon}}{\omega}} + \frac{\partial fT}{\partial\frac{\hat{\varepsilon}}{\omega}} + \frac{\partial^2 fR}{\partial\varepsilon\partial\frac{\hat{\phi}}{\omega}} - \varepsilon\frac{\partial^2 fT}{\partial\varepsilon\partial\frac{\hat{\varepsilon}}{\omega}}\right)\frac{1}{\varepsilon}\sin^2\phi\cos\phi$$

$$\left. + \left(\frac{1}{\varepsilon}\frac{\partial^2 fR}{\partial\phi\partial\frac{\hat{\phi}}{\omega}} + \frac{1}{\varepsilon}\frac{\partial fT}{\partial\frac{\hat{\phi}}{\omega}} + \frac{\partial fR}{\partial\frac{\hat{\varepsilon}}{\omega}} - \frac{\partial^2 fT}{\partial\phi\partial\frac{\hat{\varepsilon}}{\omega}} - \frac{\partial^2 fT}{\partial\frac{\hat{\phi}}{\omega}\partial\varepsilon}\right)\frac{1}{\varepsilon}\cos^2\phi\sin\phi\right\}$$

$$\widehat{Axx\hat{y}} = -\frac{\lambda\omega}{c^2\omega}\left\{-\frac{1}{\varepsilon}\frac{\partial^2 fR}{\partial\varepsilon\partial\frac{\hat{\phi}}{\omega}}\sin^3\phi + \left(\frac{\partial fR}{\partial\frac{\hat{\varepsilon}}{\omega}} - \frac{\partial^2 fT}{\partial\phi\partial\frac{\hat{\varepsilon}}{\omega}}\right)\frac{1}{\varepsilon}\cos^3\phi\right.$$

$$+ \left(\varepsilon\frac{\partial^2 fR}{\partial\varepsilon\partial\frac{\hat{\varepsilon}}{\omega}} - \frac{1}{\varepsilon}\frac{\partial^2 fR}{\partial\phi\partial\frac{\hat{\phi}}{\omega}} - \frac{1}{\varepsilon}\frac{\partial fT}{\partial\frac{\hat{\phi}}{\omega}} + \frac{\partial^2 fT}{\partial\varepsilon\partial\frac{\hat{\phi}}{\omega}}\right)\frac{1}{\varepsilon}\sin^2\phi\cos\phi$$

$$\left. + \left(\frac{\partial^2 fR}{\partial\phi\partial\frac{\hat{\varepsilon}}{\omega}} + \frac{\partial fT}{\partial\frac{\hat{\varepsilon}}{\omega}} - \varepsilon\frac{\partial^2 fT}{\partial\varepsilon\partial\frac{\hat{\varepsilon}}{\omega}} - \frac{1}{\varepsilon}\frac{\partial fR}{\partial\frac{\hat{\phi}}{\omega}} + \frac{1}{\varepsilon}\frac{\partial^2 fR}{\partial\phi\partial\frac{\hat{\phi}}{\omega}}\right)\frac{1}{\varepsilon}\cos^2\phi\sin\phi\right\}$$

$$\widehat{Axy\hat{y}} = -\frac{\lambda\omega}{c^2\omega}\left\{\left(\frac{\partial^2 fR}{\partial\phi\partial\frac{\hat{\varepsilon}}{\omega}} + \frac{\partial fT}{\partial\frac{\hat{\phi}}{\omega}}\right)\frac{1}{\varepsilon^2}\sin^3\phi - \frac{\partial^2 fT}{\partial\varepsilon\partial\frac{\hat{\varepsilon}}{\omega}}\cos^3\phi\right.$$

$$+ \left(-\frac{\partial^2 fR}{\partial\phi\partial\frac{\hat{\varepsilon}}{\omega}} - \frac{\partial fT}{\partial\frac{\hat{\varepsilon}}{\omega}} - \frac{\partial^2 fR}{\partial\varepsilon\partial\frac{\hat{\phi}}{\omega}} + \frac{1}{\varepsilon}\frac{\partial fR}{\partial\frac{\hat{\phi}}{\omega}} - \frac{1}{\varepsilon}\frac{\partial^2 fT}{\partial\phi\partial\frac{\hat{\phi}}{\omega}}\right)\frac{1}{\varepsilon}\sin^2\phi\cos\phi$$

$$\left. + \left(\varepsilon\frac{\partial^2 fR}{\partial\varepsilon\partial\frac{\hat{\varepsilon}}{\omega}} - \frac{\partial fR}{\partial\frac{\hat{\varepsilon}}{\omega}} + \frac{\partial^2 fT}{\partial\phi\partial\frac{\hat{\varepsilon}}{\omega}} + \frac{\partial^2 fT}{\partial\phi\partial\frac{\hat{\phi}}{\omega}}\right)\frac{1}{\varepsilon}\cos^2\phi\sin\phi\right\}$$

$$\widehat{Axy\hat{x}} = -\frac{\lambda\omega}{c^2\omega}\left\{\left(-\frac{\partial^2 fR}{\partial\phi\partial\frac{\hat{\varepsilon}}{\omega}} - \frac{\partial fT}{\partial\frac{\hat{\varepsilon}}{\omega}}\right)\frac{1}{\varepsilon}\sin^3\phi - \frac{\partial^2 fT}{\partial\varepsilon\partial\frac{\hat{\phi}}{\omega}}\frac{1}{\varepsilon}\cos^3\phi\right.$$

$$+ \left(\varepsilon\frac{\partial^2 fR}{\partial\varepsilon\partial\frac{\hat{\varepsilon}}{\omega}} - \frac{1}{\varepsilon}\frac{\partial^2 fR}{\partial\phi\partial\frac{\hat{\phi}}{\omega}} - \frac{1}{\varepsilon}\frac{\partial fT}{\partial\frac{\hat{\phi}}{\omega}} - \frac{\partial fR}{\partial\frac{\hat{\varepsilon}}{\omega}} + \frac{\partial^2 fT}{\partial\phi\partial\frac{\hat{\varepsilon}}{\omega}}\right)\frac{1}{\varepsilon}\sin^2\phi\cos\phi$$

$$\left. + \left(\frac{\partial^2 fR}{\partial\varepsilon\partial\frac{\hat{\phi}}{\omega}} - \varepsilon\frac{\partial^2 fT}{\partial\varepsilon\partial\frac{\hat{\varepsilon}}{\omega}} - \frac{1}{\varepsilon}\frac{\partial fR}{\partial\frac{\hat{\phi}}{\omega}} + \frac{1}{\varepsilon}\frac{\partial^2 fT}{\partial\phi\partial\frac{\hat{\phi}}{\omega}}\right)\frac{1}{\varepsilon}\cos^2\phi\sin\phi\right\}$$

The oil film force coefficient acting along the y axis are:-

$$\widehat{Ayx} = -\frac{\lambda\omega}{c}\left\{\frac{\partial fT}{\partial\varepsilon}\sin^2\phi + \left(\frac{\partial fR}{\partial\phi} + fT\right)\frac{1}{\varepsilon}\cos^2\phi + \left(\frac{\partial fR}{\partial\varepsilon} - \frac{fR}{\varepsilon} + \frac{1}{\varepsilon}\frac{\partial fT}{\partial\phi}\right)\sin\phi\cos\phi\right\}$$

$$\widehat{Ayy} = -\frac{\lambda\omega}{c}\left\{\left(fR - \frac{\partial fT}{\partial\phi}\right)\frac{1}{\varepsilon}\sin^2\phi + \frac{\partial fR}{\partial\varepsilon}\cos^2\phi + \left(\frac{\partial fT}{\partial\varepsilon} - \frac{1}{\varepsilon}\frac{\partial fR}{\partial\phi} - \frac{fT}{\varepsilon}\right)\cos\phi\sin\phi\right\}$$

$$\widehat{Ay\dot{x}} = -\frac{\lambda\omega}{c}\left\{\frac{\partial fT}{\partial\frac{\dot{\varepsilon}}{\omega}}\sin^2\phi + \frac{1}{\varepsilon}\frac{\partial fR}{\partial\frac{\dot{\phi}}{\omega}}\cos^2\phi + \left(\frac{\partial fR}{\partial\frac{\dot{\varepsilon}}{\omega}} + \frac{1}{\varepsilon}\frac{\partial fT}{\partial\frac{\dot{\phi}}{\omega}}\right)\sin\phi\cos\phi\right\}$$

$$\widehat{Ay\dot{y}} = -\frac{\lambda\omega}{c}\left\{-\frac{1}{\varepsilon}\frac{\partial fT}{\partial\frac{\dot{\phi}}{\omega}}\sin^2\phi + \frac{\partial fR}{\partial\frac{\dot{\varepsilon}}{\omega}}\cos^2\phi + \left(\frac{\partial fT}{\partial\frac{\dot{\varepsilon}}{\omega}} - \frac{1}{\varepsilon}\frac{\partial fR}{\partial\frac{\dot{\phi}}{\omega}}\right)\sin\phi\cos\phi\right\}$$

$$\widehat{Ayx^2} = -\frac{\lambda\omega}{c^2}\left\{\frac{1}{2}\frac{\partial^2 fT}{\partial\varepsilon^2}\sin^3\phi + \left(\frac{1}{2}\frac{\partial^2 fR}{\partial\phi^2} - \frac{fR}{2} + \frac{\partial fT}{\partial\phi}\right)\frac{1}{\varepsilon^2}\cos^3\phi + \left(\frac{\varepsilon}{2}\frac{\partial^2 fR}{\partial\varepsilon^2} - \frac{\partial fR}{\partial\varepsilon} + \frac{\partial^2 fT}{\partial\varepsilon\partial\phi}\right)\frac{1}{\varepsilon}\sin^2\phi\cos\phi + \left(\frac{\partial^2 fR}{\partial\phi\partial\varepsilon} + \frac{\partial fT}{\partial\varepsilon} - \frac{1}{\varepsilon}\frac{\partial fR}{\partial\phi} + \frac{1}{2\varepsilon}\frac{\partial^2 fT}{\partial\phi^2} - \frac{1}{2\varepsilon}fT\right)\frac{1}{\varepsilon}\cos^2\phi\sin\phi\right\}$$

$$\widehat{Ayy^2} = -\frac{\lambda\omega}{c^2}\{(-\frac{\partial fR}{\partial\phi}+\frac{1}{2}\frac{\partial^2 fT}{\partial\phi^2}-\frac{1}{2}fT)\frac{1}{\varepsilon^2}\sin^3\phi+\frac{1}{2}\frac{\partial^2 fR}{\partial\varepsilon^2}\cos^3\phi$$

$$+(\frac{1}{2\varepsilon}\frac{\partial^2 fR}{\partial\phi^2}-\frac{fR}{2\varepsilon}+\frac{1}{\varepsilon}\frac{\partial fT}{\partial\phi}+\frac{\partial fR}{\partial\varepsilon}-\frac{\partial^2 fT}{\partial\varepsilon\partial\phi})\frac{1}{\varepsilon}\sin^2\phi\cos\phi$$

$$+(-\frac{\partial^2 fR}{\partial\phi\partial\varepsilon}-\frac{\partial fT}{\partial\varepsilon}+\frac{\varepsilon}{2}\frac{\partial^2 fT}{\partial\varepsilon^2})\frac{1}{\varepsilon}\cos^2\phi\sin\phi\quad\}$$

$$\widehat{Ayxy} = -\frac{\lambda\omega}{c^2}\{(\frac{\partial fR}{\partial\varepsilon}-\frac{\partial^2 fT}{\partial\varepsilon\partial\phi})\frac{1}{\varepsilon}\sin^3\phi+(\frac{\partial^2 fR}{\partial\phi\partial\varepsilon}+\frac{\partial fT}{\partial\varepsilon})\frac{1}{\varepsilon}\cos^3\phi$$

$$+(-\frac{\partial^2 fR}{\partial\phi\partial\varepsilon}-\frac{\partial fT}{\partial\varepsilon}+\varepsilon\frac{\partial^2 fT}{\partial\varepsilon^2}+\frac{2}{\varepsilon}\frac{\partial fR}{\partial\phi}-\frac{1}{\varepsilon}\frac{\partial^2 fT}{\partial\phi^2}+\frac{fT}{\varepsilon})\frac{1}{\varepsilon}\sin^2\phi\cos\phi$$

$$+(\varepsilon\frac{\partial^2 fR}{\partial\varepsilon^2}-\frac{1}{\varepsilon}\frac{\partial^2 fR}{\partial\phi^2}+\frac{fR}{\varepsilon}-\frac{2}{\varepsilon}\frac{\partial fT}{\partial\phi}-\frac{\partial fR}{\partial\varepsilon}+\frac{\partial^2 fT}{\partial\varepsilon\partial\phi})\frac{1}{\varepsilon}\cos^2\phi\sin\phi\}$$

$$\widehat{Ay\dot{x}^2} = -\frac{\lambda\omega}{c^2\omega^2}\{\frac{1}{2}\frac{\partial^2 fT}{\partial\dot{\varepsilon}_\omega^2}\sin^3\phi+\frac{1}{2}\frac{\partial^2 fR}{\partial\dot{\phi}_\omega^2}\frac{1}{\varepsilon^2}\cos^3\phi$$

$$+(\frac{\varepsilon}{2}\frac{\partial^2 fR}{\partial\dot{\varepsilon}_\omega^2}+\frac{\partial^2 fT}{\partial\dot{\varepsilon}_\omega\partial\dot{\phi}_\omega})\frac{1}{\varepsilon}\sin^2\phi\cos\phi$$

$$+(\frac{\partial^2 fR}{\partial\dot{\varepsilon}_\omega\partial\dot{\phi}_\omega}+\frac{1}{2\varepsilon}\frac{\partial^2 fT}{\partial\dot{\phi}_\omega^2})\frac{1}{\varepsilon}\cos^2\phi\sin\phi\quad\}$$

$$\widehat{Ay\dot{y}^2} = -\frac{\lambda\omega}{c^2\omega^2}\{\frac{1}{2\varepsilon^2}\frac{\partial^2 fT}{\partial\dot{\phi}_\omega^2}\sin^3\phi+\frac{1}{2}\frac{\partial^2 fR}{\partial\dot{\varepsilon}_\omega^2}\cos^2\phi$$

$$+(\frac{1}{2\varepsilon}\frac{\partial^2 fR}{\partial\dot{\phi}_\omega^2}-\frac{\partial^2 fT}{\partial\dot{\varepsilon}_\omega\partial\dot{\phi}_\omega})\frac{1}{\varepsilon}\sin^2\phi\cos\phi$$

$$+(\frac{\varepsilon}{2}\frac{\partial^2 fT}{\partial\dot{\varepsilon}_\omega^2}-\frac{\partial^2 fT}{\partial\dot{\varepsilon}_\omega\partial\dot{\phi}_\omega})\frac{1}{\varepsilon}\cos^2\phi\sin\phi\quad\}$$

$$\widehat{Ayx\hat{y}} = -\frac{\lambda\omega}{c^2\omega^2}\{-\frac{1}{\varepsilon}\frac{\partial^2 fT}{\partial\hat{\varepsilon}_\omega\partial\hat{\phi}_\omega}\sin^3\phi + \frac{1}{\varepsilon}\frac{\partial^2 fR}{\partial\hat{\varepsilon}_\omega\partial\hat{\phi}_\omega}\cos^3\phi$$

$$+ (-\frac{\partial^2 fR}{\partial\hat{\varepsilon}_\omega\partial\hat{\phi}_\omega} + \varepsilon\frac{\partial^2 fT}{\partial\hat{\varepsilon}^2_\omega} - \frac{1}{\varepsilon}\frac{\partial^2 fT}{\partial\hat{\phi}^2_\omega})\frac{1}{\varepsilon}\sin^2\phi\cos\phi$$

$$+ (\varepsilon\frac{\partial^2 fR}{\partial\hat{\varepsilon}^2_\omega} - \frac{1}{\varepsilon}\frac{\partial^2 fR}{\partial\hat{\phi}^2_\omega} + \frac{\partial^2 fT}{\partial\hat{\varepsilon}_\omega\partial\hat{\phi}_\omega})\frac{1}{\varepsilon}\cos^2\phi\sin\phi \}$$

$$\widehat{Ayx\hat{x}} = -\frac{\lambda\omega}{c^2\omega}\{\frac{\partial^2 fT}{\partial\varepsilon\partial\hat{\varepsilon}_\omega}\sin^3\phi + (\frac{\partial^2 fR}{\partial\phi\partial\hat{\phi}_\omega} + \frac{\partial fT}{\partial\hat{\phi}_\omega})\frac{1}{\varepsilon^2}\cos^3\phi$$

$$+ (\frac{\partial^2 fR}{\partial\phi\partial\hat{\varepsilon}_\omega} + \frac{\partial fT}{\partial\hat{\varepsilon}_\omega} + \frac{\partial^2 fR}{\partial\varepsilon\partial\hat{\phi}_\omega} - \frac{1}{\varepsilon}\frac{\partial fR}{\partial\hat{\phi}_\omega} + \frac{1}{\varepsilon}\frac{\partial^2 fT}{\partial\phi\partial\hat{\phi}_\omega})\frac{1}{\varepsilon}\cos^2\phi\sin\phi$$

$$+ (\varepsilon\frac{\partial^2 fR}{\partial\varepsilon\partial\hat{\varepsilon}_\omega} - \frac{\partial fR}{\partial\hat{\varepsilon}_\omega} + \frac{\partial^2 fT}{\partial\phi\partial\hat{\varepsilon}_\omega} + \frac{\partial^2 fT}{\partial\varepsilon\partial\hat{\phi}_\omega})\frac{1}{\varepsilon}\sin^2\phi\cos\phi \}$$

$$\widehat{Ayy\hat{y}} = -\frac{\lambda\omega}{c^2\omega}\{(-\frac{\partial fR}{\partial\hat{\phi}_\omega} + \frac{\partial^2 fT}{\partial\phi\partial\hat{\phi}_\omega})\frac{1}{\varepsilon^2}\sin^3\phi + \frac{\partial^2 fR}{\partial\varepsilon\partial\hat{\varepsilon}_\omega}\cos^3\phi$$

$$+ (\frac{1}{\varepsilon}\frac{\partial^2 fR}{\partial\phi\partial\hat{\phi}_\omega} + \frac{1}{\varepsilon}\frac{\partial fT}{\partial\hat{\phi}_\omega} + \frac{\partial fR}{\partial\hat{\varepsilon}_\omega} - \frac{\partial^2 fT}{\partial\phi\partial\hat{\varepsilon}_\omega} - \frac{\partial^2 fT}{\partial\varepsilon\partial\hat{\phi}_\omega})\frac{1}{\varepsilon}\sin^2\phi\cos\phi$$

$$+ (-\frac{\partial^2 fR}{\partial\phi\partial\hat{\varepsilon}_\omega} - \frac{\partial fT}{\partial\hat{\varepsilon}_\omega} - \frac{\partial^2 fR}{\partial\varepsilon\partial\hat{\phi}_\omega} + \varepsilon\frac{\partial^2 fT}{\partial\varepsilon\partial\hat{\varepsilon}_\omega})\frac{1}{\varepsilon}\cos^2\phi\sin\phi \}$$

$$\widehat{Ayx\hat{y}} = -\frac{\lambda\omega}{c^2\omega}\{-\frac{1}{\varepsilon}\frac{\partial^2 fT}{\partial\varepsilon\partial\hat{\phi}_\omega}\sin^3\phi + (\frac{\partial^2 fR}{\partial\phi\partial\hat{\varepsilon}_\omega} + \frac{\partial fT}{\partial\hat{\varepsilon}_\omega})\frac{1}{\varepsilon}\cos^3\phi$$

$$+ (-\frac{\partial^2 fR}{\partial\varepsilon\partial\hat{\varepsilon}_\omega} + \varepsilon\frac{\partial^2 fT}{\partial\varepsilon\partial\hat{\varepsilon}_\omega} + \frac{1}{\varepsilon}\frac{\partial fR}{\partial\hat{\phi}_\omega} - \frac{1}{\varepsilon}\frac{\partial^2 fT}{\partial\phi\partial\hat{\phi}_\omega})\frac{1}{\varepsilon}\sin^2\phi\cos\phi$$

$$+ (\varepsilon\frac{\partial^2 fR}{\partial\varepsilon\partial\hat{\varepsilon}_\omega} - \frac{1}{\varepsilon}\frac{\partial^2 fR}{\partial\phi\partial\hat{\phi}_\omega} - \frac{1}{\varepsilon}\frac{\partial fT}{\partial\hat{\phi}_\omega} - \frac{\partial fR}{\partial\hat{\varepsilon}_\omega} + \frac{\partial^2 fT}{\partial\phi\partial\hat{\varepsilon}_\omega})\frac{1}{\varepsilon}\cos^2\phi\sin\phi \} \qquad (3.10)$$

$$\widehat{Ayyx} = -\frac{\lambda\omega}{c^2\omega}\Big[\Big(\frac{\partial f_R}{\partial\dot{\varepsilon}}\Big|_{\omega} - \frac{\partial^2 f_T}{\partial\phi\partial\dot{\varepsilon}}\Big|_{\omega}\frac{1}{\varepsilon}\Big)\sin^3\phi$$

$$+ \frac{\partial^2 f_R}{\partial\dot{\phi}\partial\varepsilon}\Big|_{\omega}\frac{1}{\varepsilon}\cos^3\phi$$

$$+ \Big(-\frac{1}{\varepsilon}\frac{\partial^2 f_R}{\partial\phi\partial\dot{\varepsilon}}\Big|_{\omega} - \frac{1}{\varepsilon}\frac{\partial f_T}{\partial\dot{\varepsilon}}\Big|_{\omega} + \frac{\partial^2 f_T}{\partial\varepsilon\partial\dot{\varepsilon}}\Big|_{\omega} + \frac{1}{\varepsilon^2}\frac{\partial f_R}{\partial\dot{\phi}}\Big|_{\omega}$$

$$- \frac{1}{\varepsilon^2}\frac{\partial^2 f_T}{\partial\phi\partial\dot{\phi}}\Big|_{\omega}\Big)\sin^2\phi\cos\phi$$

$$+ \Big(\frac{\partial^2 f_R}{\partial\varepsilon\partial\dot{\varepsilon}}\Big|_{\omega} - \frac{1}{\varepsilon^2}\frac{\partial^2 f_R}{\partial\phi\partial\dot{\phi}}\Big|_{\omega} - \frac{1}{\varepsilon^2}\frac{\partial f_T}{\partial\dot{\phi}}\Big|_{\omega}$$

$$+ \frac{1}{\varepsilon}\frac{\partial^2 f_T}{\partial\varepsilon\partial\dot{\phi}}\Big|_{\omega}\Big)\cos^2\phi\sin\phi\Big]$$

The above force coefficients have explicit values for each running position of the journal relative to the bearing bush, if therefore, the journal could take up an infinite number of steady state running positions, one could also expect the same number of group coefficients. Fortunately when the journal does not experience a misaligning couple and is thus parallel with the bearing bush, the journal centre follows a fixed locus making it possible to present the above twentyeight coefficients for given values of the Sommerfeld duty parameter. However the situation is somewhat different when considering misalignment because of the possibility of any number of running positions the journal may take, the coefficients not only become a function of ε but also of ψ and τ. To provide force coefficients for any combination of ε, ψ and τ would be a most formidable test, hence only the principle directions of misalignment have been considered.

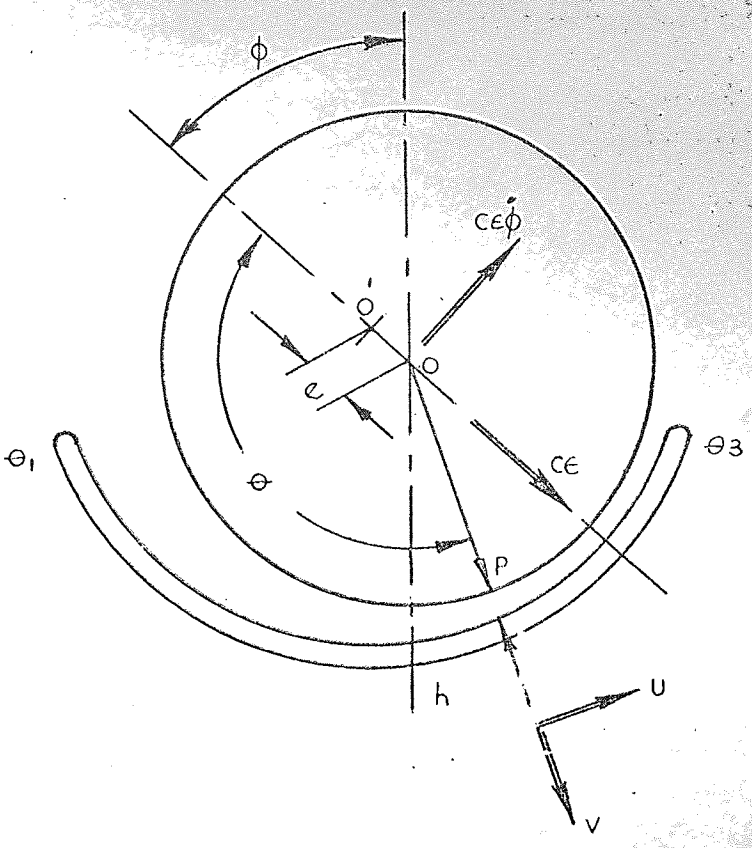

FIG 3-1 POLAR DIAGRAM OF VELOCITIES.

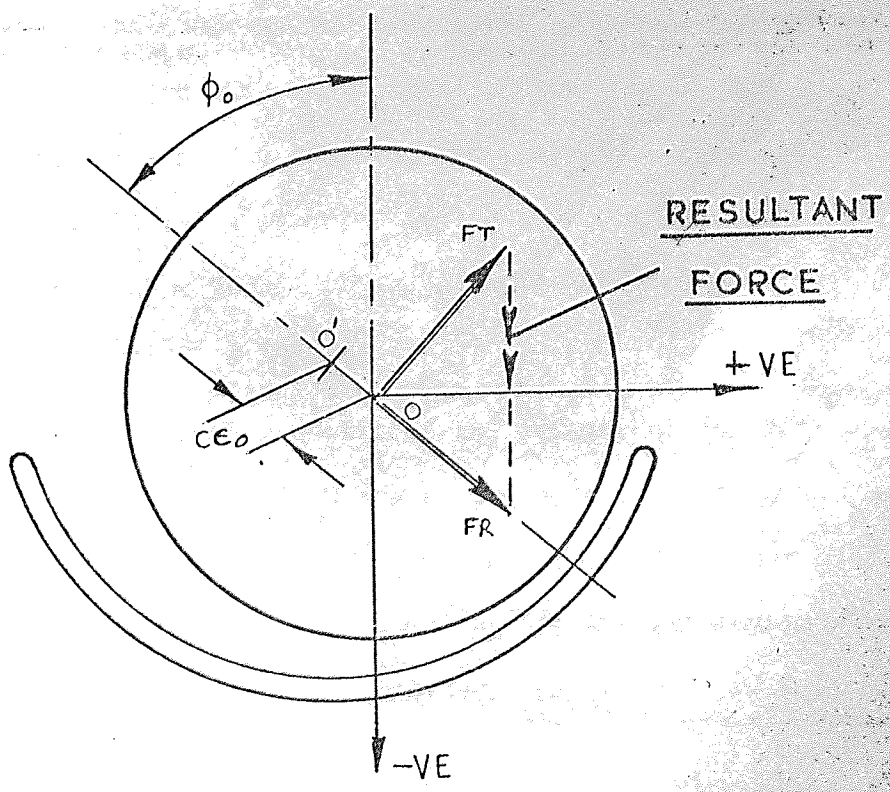

FIG 3-3 POLAR DIAGRAM OF FORCES.

CHAPTER FOUR

CHAPTER FOUR

NUMERICAL ANALYSIS

4.1 Introduction

To evaluate the resultant pressure distribution throughout the oil film, Reynolds equation was developed to include the variation in film thickness in the axial direction caused by journal misalignment. The computational procedure to accomplish this followed familiar lines of describing the steady running position of the journal midway along the bush using polar co-ordinates ϕ and ε. The value of ϕ is the angle between the vertical and the line of centres taken up by the bush centre and the journal centre, this value is referred to the attitude angle or incidence angle. The value of ε is a measure of the distance between the bush and journal centres, it is a non-dimensional value obtained by dividing the actual distance between the centres by the radial clearance, giving a number less than one, this dimensionless value is described as the eccentricity ratio.

4.2 Equations for film thickness

In figure (4-1a) let the centre of the journal at any position along the length of the bush be Q and at the centre of the bush when $Z = 0$ be equal to O'. The bearing extends to $\pm L/2$ on either side of $Z = 0$ and has its radial centre at point O. At the extreme ends of the journal the maximum tilt, measured from the central running position at any angle, is τ.

The line of centres in the mid plane is OO' from which the angular co-ordinate, at any other plane to the line of centres is OQ

at an angle δ to OO'. R_1 and R_2 are the radii of the bush and journal respectively and h is the oil film thickness at point X of the bush. It may be shown that

$$\frac{O\bar{P}}{\sin\beta} = \frac{R_2}{\sin(180 - \theta - \delta)} = \frac{\bar{OQ}}{\sin\alpha}$$

also $$\alpha = \sin^{-1}\left[\frac{\bar{OQ}}{R_2}\sin(\theta + \delta)\right]$$

from which $$\bar{JP} = \sqrt{R_2^2 - \bar{OQ}^2 \sin^2(\theta + \varepsilon)} + \bar{OQ}\cos(\theta + \delta)$$

now $$h = R_2 + c - \bar{OP}$$

Hence $$h = R_2 + c - \sqrt{R_2^2 - \bar{OQ}^2 \sin^2(\theta + \delta)} + \bar{OQ}\cos(\theta + \delta)$$

where $\bar{OQ}$ is the eccentricity of the misaligned journal at any position along the shaft. If $\bar{OQ}$ is small then $\bar{OQ}^2$ becomes negligible.

Hence $$h = c + \bar{OQ}\cos(\theta + \delta)$$

or $$\frac{h}{c} = 1 + E\cos(\theta + \delta) \qquad (4.1)$$

where $E = \bar{OQ}/c$ and is the eccentricity ratio at any position. However, it is more convenient to use the maximum tilt ratio at the ends of the bush and eliminate the variable δ.

From figure (4.1B) $O'Q = 2my/L$

and $$\frac{O'Q}{c} = 2my/Lc = \frac{2\tau y}{L}$$

where $\tau = \frac{m}{c}$ the tilt ratio.

From the triangle O, O' and Q and noting that OQ may be replaced by $\frac{2\tau y}{L}$ we have

$$\sin \delta = \frac{2\tau Z}{EL} \sin(\phi - \psi) \text{ and } \cos \delta = \frac{\varepsilon}{E} + \frac{2\tau Z}{EL} \cos (\phi - \psi)$$

when substituted into equation (4.1).

$$\frac{h}{c} = 1 + \varepsilon \cos \theta + \frac{2\tau Z}{L} \cos (\theta + \phi - \psi) \qquad (4.2)$$

thus h varies linearly with Z which is expected, and if $\tau = 0$, i.e. zero misalignment we come back to the well known formula for the oil film where the journal is parallel with the bearing bush.

4.3 Solution of Reynolds equation

Equation (3.7) is an elliptic partial differential equation and its solution can be effected by covering the bounded region by a mesh of points, establishing at every mesh point a relation deduced from the theory of finite differences the values of the required function and neighbouring points, and solving the resulting set of simultaneous equations by successive approximations. The size of the mesh was usually chosen by intuition and the accuracy of the solution obtained for each mesh point equated to equation (4.3). Further, since only the dominant term is retained in the finite difference solution and, because the resulting pressure profile had to be integrated, a reasonably large number of mesh points had to be employed, usually 32 x 32 = 1024 nodes, otherwise the phenomenon of ill-conditioning would manifest itself in the sense that relatively large changes in unknowns had little apparent effect on the residuals and accurate solutions then require an even finer mesh size, or the finite-difference equation had to be increased to include more nodes resulting in longer computational times. The ill-conditioning could

be experienced when the bearing was operating with a large eccentricity ratio and with large amounts of misalignment giving rise to steep pressure profiles as illustrated in Chapter Eight.

$$\frac{\sum_{i}^{m}\sum_{j}^{n}\left(P_{ij}^{\,r} - P_{ij}^{\,r-i}\right)}{\sum_{i}^{m}\sum_{j}^{n} P_{ij}^{\,r}} < 0.001 \qquad (4.3)$$

where r is the number of iterations performed.

Experience showed that 0.001 was the best value for the shortest computer running time and gave results to within 1.0 per cent with other published work for the load carrying capacity, where the journal is parallel with the bush.

In order to economize on the computing time a course mesh was initially chosen and all the nodes set to 0.5 and the rectangular boundaries made zero throughout the iterating process. Upon reaching the desired accuracy the mesh length was halved and the new additional nodes assigned a value equal to the mean of its surrounding nodes. Further the iterative system employed an over-relaxation factor using a method similar to Carre'(58) in order to improve the convergence rate.

To set up the finite difference grid, imagine the bearing surface to be covered by a family of lines parallel with the x and z axes. Lines parallel with the x axis corresponds to values of θ the circumferential length of the bearing and is given by

$$\theta_j = \theta_o + j\Delta\theta \quad \text{where } j = 1, 2, 3, \ldots n$$

and lines parallel with the z axis correspond to values of L along

the length of the bearing and is given by

$$L_i = L_o + i\Delta L \quad \text{where } i = 1, 2, 3 \ldots\ldots n$$

then considering intervals along the x axis Taylor Series states that in the neighbourhood of x_o

$$P(x) = P_{i,j} + \left(\frac{dP}{dx}\right)_{i,j} (x - x_{i,j}) + \frac{1}{2!}\left(\frac{d^2P}{dx^2}\right)_{i,j} (x - x_{i,j})^2$$

$$+ \frac{1}{3!}\left(\frac{d^3P}{dx^3}\right)_{i,j} (x - x_{i,j})^3$$

Putting $x = x_{i,j} + \Delta x$ and $x = x_{i,j} - \Delta x$ in turn and adding the resulting equations gives:-

$$\left(\frac{d^2P}{dx^2}\right) \simeq \left[\frac{(P_{i,j+1} - P_{i,j})}{\Delta x} - \frac{(P_{i,j} - P_{i,j-1})}{\Delta x} \right] / \Delta x \qquad (4.4)$$

It should be noted at this stage, that in Reynolds equation the pressure is also a function of the film thickness h and when considering the second order derivative of pressure with respect to x as shown in equation (4.4) a mean value for the film thickness should be taken between $P_{i,j+1}$ and $P_{i,j}$ also the same should be considered for the pressures $P_{i,j-1}$ and $P_{i,j}$. Hence using equation (4.4) the finite increments for the three partial derivatives in equation (3.7) may be written as:-

$$\frac{\partial}{\partial x}\left[h^3 \frac{\partial P}{\partial x}\right] = \left[h^3_{i,j+\frac{1}{2}} \left(\frac{P_{i,j+1} - P_{i,j}}{\Delta x}\right) - h^3_{i,j-\frac{1}{2}} \left(\frac{P_{i,j} - P_{i,j-1}}{\Delta x}\right) \right] / \Delta x$$

$$\frac{\partial}{\partial z}\left[h^3 \frac{\partial P}{\partial z}\right] = \left[h^3_{i+\frac{1}{2},j} \left(\frac{P_{i+1,j} - P_{i,j}}{\Delta z}\right) - h^3_{i-\frac{1}{2},j} \left(\frac{P_{i,j} - P_{i-1,j}}{\Delta z}\right) \right] / \Delta z$$

$$\frac{\partial h}{\partial x} = \frac{h_{i,j+\frac{1}{2}} - h_{i,j-\frac{1}{2}}}{\Delta x} \qquad (4.5)$$

Using equations (4.5) together with equations (3.7) it is possible to find the pressure $P_{i,j}$ thus:-

$$P_{i,j} = \{ 24\pi \left[\frac{h_{i,j-\frac{1}{2}} - h_{i,j+\frac{1}{2}}}{\Delta x} \right] + \left(\frac{D'}{L'}\right)^2 \left[h^3_{i+\frac{1}{2},j} \cdot \frac{P_{i+1,j}}{\Delta z^2} + h^3_{i-\frac{1}{2},j} \cdot \frac{P_{i-1,j}}{\Delta z^2} \right] + h^3_{i,j+\frac{1}{2}} \cdot \frac{P_{i,j+1}}{\Delta x^2} + h^3_{i,j-\frac{1}{2}} \cdot \frac{P_{i,j-1}}{\Delta x^2} \} \Big/ \{ \left[\frac{h^3_{i,j+\frac{1}{2}} + h^3_{i,j-\frac{1}{2}}}{\Delta x^2} \right] + \left(\frac{D'}{L'}\right)^2 \left[\frac{h^3_{i+\frac{1}{2},j} + h^3_{i-\frac{1}{2},j}}{\Delta z^2} \right] \} \quad (4.6)$$

which is in the form

$$P_{i,j} = a_0 + a_1 P_{i+1,j} + a_2 P_{i-1,j} + a_3 P_{i,j+1} + a_4 P_{i,j-1} \quad (4.7)$$

with a_0, a_1, a_2, a_3, and a_4 are given constants for each point (i,j) of the mesh, and the pressure $P_{i,j}$ is a function of these constants, together with the four surrounding pressures. For m x n points in the mesh there will be m x n simultaneous equations.

4.4 Boundary conditions

The problem here, is to decide where the oil pressure starts building up, and where it stops, these two conditions are required to evaluate the five constants in equation (4.7).

The start of the pressure curve may be taken at the point where the two surfaces start to converge in the case of a partial journal bearing this point is at the beginning of the pad i.e. θ_1 in figure (4.1A). The situation at the trailing end of the pressure profile has been the subject of considerable speculation and its precise limits are still not definitely established. The solution of

Reynolds equation for large values of eccentricity will yield negative pressures at the trailing end of the bearing pad. However, to assume that negative pressures exist within the oil film violates physical reality, as it is well known that cavitation takes place at this diverging portion and the film cannot endure negative stresses as shown by curve (1) of figure (4.2). Since cavitation exists, it leads to the suggestion that all negative pressures should be assigned the value of zero, see curve (2). Although this suggestion is more realistic it is untrue to assume the pressure gradient suddenly goes to zero, so a pressure profile which is probably more realistic is one where the slope $\partial P/\partial\theta$ = zero as shown by curve (3). Olsson(49) et al(50) (46) discuss in detail the value of curves (2) and (3). In order to keep the computing work as simple as possible all negative pressures, assuming to lie in the region of cavitation, were re-assigned the value of zero, results using this method agree closely with Pinkus and Sternkicht who used $dP/d\theta$ = zero for the trailing boundary.

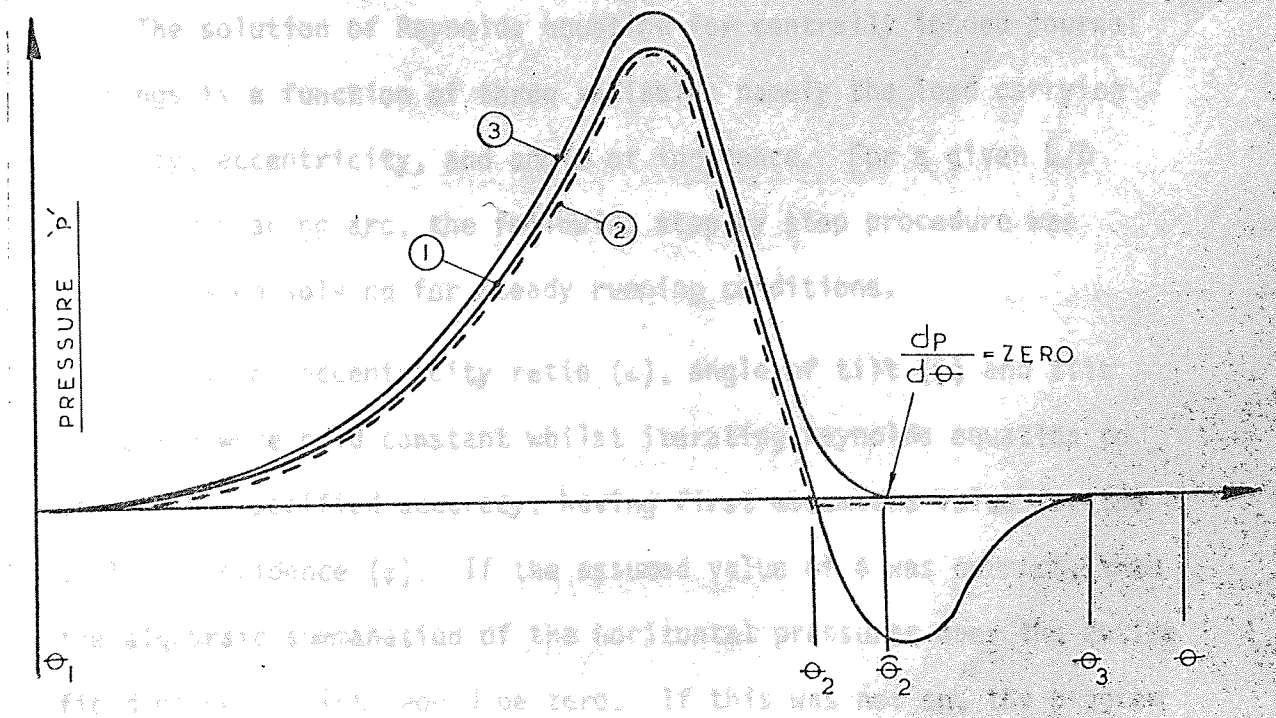

FIG. 4-2. PRESSURE PROFILE SHOWING BOUNDARY CONDITIONS FOR PARTIAL BEARINGS.

A further factor which may influence the boundary conditions, is the hydrostatic force of the oil inlet, when supplied under pressure: but because of the possibility of large variations for the oil inlet supply pressure the effects of any hydrostatic forces were neglected.

Smalley and McCallian(46) investigated the influence of the feed pressure by comparing the experimental results of a bearing having a high inlet pressure(44), and the other neglecting the feed pressure. The resulting values of minimum oil film thickness lay close to one another, having a maximum difference of 4.0 per cent. This small difference in results led to the conclusion that the extra work involved in accounting for the hydrostatic force as a result of supply pressure would not be justified. However because it was feared that the inlet pressure might affect the system, the bearing test rig was designed in a manner to allow oil to be gravity fed to the unloaded portion of the bearing.

4.5 Procedure for solving Reynolds equation

The solution of Reynolds equation for centrally loaded journal bearings is a function of three variables namely the load carrying capacity, eccentricity, and angle of incidence. For a given L/D ratio and bearing arc, the following step by step procedure was employed when solving for steady running conditions.

Values of eccentricity ratio (ε), angle of tilt (ψ) and tilt ratio (τ) were held constant whilst iterating Reynolds equation to within the specified accuracy, having first assumed a value for the angle of incidence (ϕ). If the assumed value of ϕ was correct, then the algebraic summanation of the horizontal pressures over the entire field of mesh points would be zero. If this was not so, the program

would continue by selecting another value of ϕ based upon the direction of the resulting pressure. Because the field pressures were most sensitive to small changes in ϕ the desired accuracy for steady running, was determined by checking the difference between the input and resulting ϕ; usually this difference was limited to 0.001 degrees. Figure (4.3) shows how the value ϕ converges with the number of performed iterations, and also how it changes with size of grillage.

Having obtained the field pressures and angle of incidence, to within the desired accuracy, the resulting pressure distribution was integrated numerically together with the corresponding couples to give the total direct load and couple in the radial and tangential directions as given in equations (4.8) and (4.9).

$$\text{Non-dimensional Radial force} = F_R = \Delta x \Delta z \sum_{i=1}^{m} \sum_{j=1}^{n} (P_{i,j}) \cos\theta_j$$

$$\text{Non-dimensional Tangential force} = F_T = \Delta x \Delta z \sum_{i=1}^{m} \sum_{j=1}^{n} (P_{i,j}) \sin\theta_j \qquad (4.8)$$

The resulting force is then equal to the sum of the radial and tangential components thus:-

$$\text{Resultant force} = \sqrt{F_R^2 + F_T^2}$$

Also the angle of inclination between the resultant and radial forces are given by:-

$$\alpha = \tan^{-1} (F_T/F_R)$$

and the total moment about the centre line, axially, is given by:-

$$\text{Non-dimensional Radial Moment} = M_R = -\Delta x \Delta z \sum_i^m \sum_j^n P_{i,j} \times \rho_i \cos \theta_j$$

$$\text{Non-dimensional Tangential Moment} = M_T = \Delta x \Delta z \sum_i^m \sum_j^n P_{i,j} \times \rho_i \sin \theta_j \qquad (4.9)$$

Dimensional values taken from the computer results would be for the vertical plane

$$\text{Per cent Misalignment} = (M_R \cos \phi + M_T \sin \phi)\Delta x \Delta z \times S \times 100$$

Couple = (Per cent Misalignment) x (Brg.load) x (Brg.length)

and along the horizontal plane

$$\text{Per cent Misalignment} = (M_T \cos \phi + M_R \sin \phi)\Delta x \Delta z \times S \times 100$$

Couple = (Per cent Misalignment) x (Brg.load) x (Brg.length)

where S = Sommerfeld number

Arranging Reynolds equation in non-dimensional units allows the resulting oil film pressure to be presented graphically. The dimensionless pressure is presented as a Sommerfeld number (S) and plotted against the tilt ratio (τ) for fixed values of eccentricity ratio (ε). Figure (4.4) amd (4.5) illustrates a family of such curves, for a misaligning couple in the vertical plane with the journal operating under steadily loaded conditions. Thus the radial running position of the journal bearing may be predicted; for example, knowing before

hand the amount of tilt a bearing is likely to experience under normal operating conditions, also knowing the rotational speed, the bearing loading, and oil viscosity, then by using figure (4.4) the eccentricity ratio may be determined. Figure (4.4) also allows the user to see at once the maximum amount of tilt the journal can take up, for a particular duty parameter, without metal to metal contact of the journal with the bearing bush.

If the tilt ratio is made zero figure (4.5) may be presented in a more familiar way i.e. in polar co-ordinates as shown in figure (4.6). This latter graph allows the user to see immediately the running position of the journal relative to the bush, this curve is in fact a locus of the journal which starts at the B.D.C. when the bearing is at standstill,and rising to the T.D.C. position for infinitely high running speeds. However for design purposes the writer would much prefer to present the Sommerfeld number together with the angle of incidence against eccentricity ratio as shown in figure (4.7), but it can only be presented in this manner if the tilt ratio is zero.

Although graphs are shown illustrating the angle of incidence for various values of eccentricity ratio, this information is not necessary for determining the force coefficients, however, it is of considerable value to the design engineer for establishing the minimum oil film thickness, together with the horse-power absorbed by the shearing action of the oil film wedge, which, of course, are important design criteria for any bearing.

4.6 Procedure for solving the first order stiffness and damping coefficients

The coefficients are calculated by considering the effect made upon the radial and tangential film pressures for small finite displacements $\Delta\varepsilon$ and $\Delta\phi$ and small velocities $\Delta\frac{\dot{\phi}}{\omega}$ and $\Delta\frac{\dot{\phi}}{\omega}$, given to the journal centre and measured about the steady running position ε_o, ϕ_o.

The linearized, first order, force coefficients derived in Chapter Three, Section Five, are based upon the solution of eight partial derivatives thus:-

$$\frac{\partial fR}{\partial\varepsilon},\ \frac{\partial fT}{\partial\varepsilon},\ \frac{\partial fR}{\partial\phi},\ \frac{\partial fT}{\partial\phi},\ \frac{\partial fR}{\partial\frac{\dot{\varepsilon}}{\omega}},\ \frac{\partial fT}{\partial\frac{\dot{\varepsilon}}{\omega}},\ \frac{\partial fR}{\partial\frac{\dot{\phi}}{\omega}},\ \frac{\partial fT}{\partial\frac{\dot{\phi}}{\omega}}$$

Considering the partial derivative $\frac{\partial fR}{\partial\phi}$ and $\frac{\partial fT}{\partial\phi}$. In order to calculate these derivatives two further solutions to equation (3.7) are required with ϕ and ε set to zero, then for constant values of eccentricity and tilt ratio's together with the tilt angle, equation (3.7) was solved for a new value of $\phi_1 = \phi_o + \Delta\phi_1$ but when setting up the finite difference grillage, the nodal pressures for the steady running position ε_o, ϕ_o were used for the initial guess. The iteration procedure was continued until equation (4.3) was satisfied. The above was repeated a second time but with $\phi_2 = \phi_o - \Delta\phi_2$, again the initial values of the grillage were taken from the stored values for ε_o and ϕ_o.

The values of $\Delta\phi_1$ and $\Delta\phi_2$ were sufficiently small such that variations in the resulting force magnitude remained small. Then if fR_1, fT_1, fR_2, fT_2 are the solutions to Reynolds equations then

$$\frac{\partial fR}{\partial \phi} = \frac{1}{\Delta\phi_1 + \Delta\phi_2} \left[\frac{\Delta\phi_1}{\Delta\phi_2} (fR_o - fR^2) - \frac{\Delta\phi_2}{\Delta\phi_1} (fR_1 - fR_o) \right]$$

$$\frac{\partial fT}{\partial \phi} = \frac{1}{\Delta\phi_1 + \Delta\phi_2} \left[\frac{\Delta\phi_1}{\Delta\phi_2} (fT_o - fT_2) - \frac{\Delta\phi_2}{\Delta\phi_1} (fT_1 - fT_o) \right]$$

The above equations have been weighted to improve the value of the slope, should unequal step lengths $\Delta\phi_1$, $\Delta\phi_2$ be used.

In order to evaluate $\partial fR/\partial\varepsilon$ and $\partial fT/\partial\varepsilon$ again equation (3.7) was solved with $\dot{\phi}$ and $\dot{\varepsilon}$ set to zero, but with constant values of angle of tilt, tilt ratio, and angle of incidence, then solving Reynolds equation, first with $\varepsilon_1 = \varepsilon_o + \Delta\varepsilon_1$ and a second time with $\varepsilon_2 = \varepsilon_o - \Delta\varepsilon_2$ using for the initial nodal values for the finite difference grillage those values obtained for ε_o and ϕ_2. Then if fR_3, fT_3, fR_4 and fT_4 are the final solutions

$$\frac{\partial fR}{\partial \varepsilon} = \frac{1.0}{\Delta\varepsilon_1 + \Delta\varepsilon_2} \left[\frac{\Delta\varepsilon_1}{\Delta\varepsilon_2} (fR_o - fR_4) - \frac{\Delta\varepsilon_2}{\Delta\varepsilon_1} (fR_3 - fR_o) \right]$$

Similarly for $\frac{\partial fT}{\partial \varepsilon}$

To obtain $\partial fR/\partial \frac{\dot{\varepsilon}}{\omega}$ and $\partial fT/\partial \frac{\dot{\varepsilon}}{\omega}$ equation (3.7) was solved with two values of $\pm \partial \frac{\dot{\varepsilon}}{\omega}$ having constant terms for eccentricity and tilt ratios, angle of incidence and angle of tilt. If fR_5, fT_5, fR_6 and fT_6 are the solutions then

$$\frac{\partial fR}{\partial \frac{\dot{\varepsilon}}{\omega}} = \frac{1.0}{\Delta_1 \frac{\dot{\varepsilon}}{\omega} + \Delta_2 \frac{\dot{\varepsilon}}{\omega}} \left[\frac{\Delta_1 \frac{\dot{\varepsilon}}{\omega}}{\Delta_2 \frac{\dot{\varepsilon}}{\omega}} (fR_o - fR_6) - \frac{\Delta_2 \frac{\dot{\varepsilon}}{\omega}}{\Delta_1 \frac{\dot{\varepsilon}}{\omega}} (fR_5 - fR_o) \right]$$

Similarly for $\frac{\partial fT}{\partial \frac{\dot{\varepsilon}}{\omega}}$

The solution for $\partial fR/\partial\frac{\dot{\phi}}{\omega}$ and $\partial fT/\partial\frac{\dot{\phi}}{\omega}$ was obtained in a similar manner but this time the variable $\partial\frac{\dot{\phi}}{\omega}$ was used

$$\frac{\partial fR}{\partial\frac{\dot{\phi}}{\omega}} = \frac{1.0}{\Delta_1\frac{\dot{\phi}}{\omega} + \Delta_2\frac{\dot{\phi}}{\omega}} \left[\frac{\Delta_1\frac{\dot{\phi}}{\omega}}{\Delta_2\frac{\dot{\phi}}{\omega}} (fR_o - fR_8) - \frac{\Delta_2\frac{\dot{\phi}}{\omega}}{\Delta_1\frac{\dot{\phi}}{\omega}} (fR_7 - fR_o) \right]$$

Similarly for $\frac{\partial fT}{\partial\frac{\dot{\phi}}{\omega}}$

Substituting the above derivatives into the first order terms of equation (3.10) yields the eight stiffness and damping coefficients along the x-y co-ordinate axes. The computed coefficients over an eccentricity ratio range of $\varepsilon = 0.2$ to $\varepsilon = 0.9$ are shown in figures (4.8) and (4.9), and in Appendix B for various values of misalignment acting in the vertical plane.

4.7 Procedure for solving the second order force coefficients

The remaining twenty second order coefficients formulated in equation (3.10) require the solution of the following derivatives:-

$$\frac{\partial^2 fR}{\partial\phi^2}, \frac{\partial^2 fR}{\partial\varepsilon^2}, \frac{\partial^2 fR}{\partial\frac{\dot{\varepsilon}}{\omega}^2}, \frac{\partial^2 fR}{\partial\frac{\dot{\phi}}{\omega}^2}, \frac{\partial^2 fR}{\partial\phi\partial\varepsilon}, \frac{\partial^2 fR}{\partial\varepsilon\partial\frac{\dot{\varepsilon}}{\omega}}, \frac{\partial^2 fR}{\partial\frac{\dot{\varepsilon}}{\omega}\partial\frac{\dot{\phi}}{\omega}}, \frac{\partial^2 fR}{\partial\phi\partial\frac{\dot{\phi}}{\omega}}, \frac{\partial^2 fR}{\partial\phi\partial\frac{\dot{\varepsilon}}{\omega}} \;\&\; \frac{\partial^2 fR}{\partial\varepsilon\partial\frac{\dot{\phi}}{\omega}}$$

Similarly for forces acting in the tangential direction. Using the radial and tangential oil film pressures given by finite displacements in the previous section i.e. fR_1, fR_2 etc., the following second order derivatives were obtained using the following:-

$$\frac{\partial^2 fR}{\partial\phi^2} = \frac{2.0}{\Delta\phi_1 + \Delta\phi_2} \left[\frac{(fR_1 - fR_o)}{\Delta\phi_1} + \frac{(fR_2 - fR_o)}{\Delta\phi_2} \right]$$

$$\frac{\partial^2 FR}{\partial \varepsilon^2} = \frac{2.0}{\Delta\varepsilon_1 + \Delta\varepsilon_2}\left[\frac{(fR_3 - fR_0)}{\Delta\varepsilon_1} + \frac{(fR_4 - fR_0)}{\Delta\varepsilon_2}\right]$$

$$\frac{\partial^2 FR}{\partial \frac{\dot{\varepsilon}}{\omega}^2} = \frac{2.0}{\Delta_1\frac{\dot{\varepsilon}}{\omega} + \Delta_2\frac{\dot{\varepsilon}}{\omega}}\left[\frac{(fR_5 - fR_0)}{\Delta_1\frac{\dot{\varepsilon}}{\omega}} + \frac{(fR_6 - fR_0)}{\Delta_2\frac{\dot{\varepsilon}}{\omega}}\right]$$

$$\frac{\partial^2 FR}{\partial \frac{\dot{\phi}}{\omega}^2} = \frac{2.0}{\Delta_1\frac{\dot{\phi}}{\omega} + \Delta_2\frac{\dot{\phi}}{\omega}}\left[\frac{(fR_7 - fR_0)}{\Delta_1\frac{\dot{\phi}}{\omega}} + \frac{(fR_8 - fR_0)}{\Delta_2\frac{\dot{\phi}}{\omega}}\right]$$

and in a similar manner for the tangential direction.

The second order cross product derivatives require further calculations of the oil film pressure, but this time making two increments of displacement and or velocity simultaneously. This type of partial derivative is more easily explained by the diagram shown in figure (4.10) illustrating the derivatives $\partial^2 fR/\partial\varepsilon\partial\phi$ for finite displacements $\Delta\varepsilon$ and $\Delta\phi$.

Using then $\Delta\varepsilon$ and $\Delta\phi$ and the corresponding film pressures fR_0 fR_1, fR_3, fR_9 the second order derivative may be computed from the following finite difference formula

$$\frac{\partial^2 fR}{\partial\phi\partial\varepsilon} = \frac{1}{\Delta\phi_1 \times \Delta\varepsilon_1}\left[fR_9 + fR_0 - fR_1 - fR_3\right]$$

Using the above procedure the remaining eleven, second order cross product derivatives were obtained.

The computed second order force coefficients along the x-y coordinate system are shown in figures (4.11) to (4.16) over the eccentricity ratio range of $\varepsilon = 0.2$ and $\varepsilon = 0.9$ for a journal bearing

having its journal parallel with the bearing bush. The upper limits shown in these graphs illustrate the maximum possible value of the coefficient for the maximum value of tilt in the vertical plane. A more comprehensive group of charts are given in Appendix B which are intended for design purposes where the journal tilt is some intermediate value between t = 0 to t = t_{max} acting in the vertical plane.

4.8 Layout of the computer program for solving the steady state and dynamic operating conditions

The theory has been considered extensively in order that one may readily change the geometry of the bearing, and utilize the work developed in this thesis. Although a popular bearing has been investigated, and one which is used on machines manufactured by "Parsons Peebles Limited", and of the type made by "Mitchell Bearings Co.Ltd." also "Glacier Bearings", it should be appreciated that it is by no means the only type of bearing which may be used for industrial purposes. For example, bearing having a L/D ratio larger than 1.0 are used on heavy slow speed machines; and for machines operating at high speeds often require elliptical type of bearing geometry. Therefore to allow a theoretical investigation of other types of bearings, the computer program has been included in order to provide the interested reader to make the appropriate adjustment with minimal effort.

```
      TITLEFJ1482
C
CC    THIS PROGRAM CALCULATES THE EFFECT OF JOURNAL
CC    MISSALIGNMENT ON THE STATIC LOAD CARRYING CAPACITY
CC    OF A CENTRALLY LOADED PARTIAL JOURNAL BEARING.
CC
CC    IT IS SIMILAR TO FJ1466 BUT FILM THICKNESS IS NOW
CC    DIFFERENT AT EVERY NODE.
CC
C
      DIMENSION A(30),C(25,25),D(20),TH(50),B(24,24,5),
     1EA(25),EB(25),H(24,47),TITLE(10),W(32)
      COMMON A,B,C,D,H,N1,N2,N3,N4,PI,PHI,BETA,W
      CALL HDATA(2)
      CALL GSSW
      REWIND 6
      REWIND 7
1     READ(2,2)(TITLE(I),I=1,10)
2     FORMAT(10A8)
      CALL EOF(I)
      GO TO(100,3),I
100   STOP
C
3     WRITE(3,4)(TITLE(I),I=1,10)
4     FORMAT(1H1,40HCENTRALLY LOADED PARTIAL JOURNAL BEARING
     1/12B,17HWITH MISALIGNMENT//10A8//)
      IF(TITLE(1).EQ.8H RESTART)GO TO 301
      GO TO 302
301   NCNT=1
CC    THIS SECTION GOVERNS THE RESTART MODE OF THE PROGRAM.
CC    ITEMS FROM AN ABORTED RUN HAVE BEEN STORED ON A
CC    WORK TAPE LABELLED      WHICH SHOULD BE ON
C     TAPE DRIVE 10. THIS SECTION WILL RESTART WITH 1 ITERATION.
```

```
C
      READ(7)C,A,TH,B,H,W,N1,N2,N3,N4,PI,PHI,BETA,EDOT,NCOEF,
     1LVIA,LVJA,N5,DZ,BINT,YZ,N8,YZI,BINV1,BINV2,DZI2,ZA2,A2ODZ,
     2PRED,PHIDOT,CONPID
      REWIND 7
      GO TO 31
302   PRANEWDATA
      READ(2,5)(A(I),I=1,8),(A(I),I=10,15),A(17),PRED,A(9),
     1A(21),A(22),PMULT,A(23),A(24)
5     FORMAT(8G10.0)
      EDOT=0.
      PHIDOT=0.
      NCOEF=1
      A(2)=1.0/A(2)                                          D/L
      LVIA=1
      LVJA=A(9)
      A(22)=0.01745329*A(22)                                 PSI
C     NUMBER OF SQUARES AXIALLY
      N1=A(6)
C     NUMBER OF SQUARES CIRCUMFERENTIALLY
      N2=A(7)
C     HIGH NODE AXIALLY
      N3=N1+1
C     HIGH NODE CIRCUMFERENTIALLY
      N4=N2+1
C     NODE OF CENTRAL LINE
      N5=N1/2+1
      NCNT=1
      IF(PRED-1.)61,62,62
C
C     READS IN PRESSURES AT NODES
C
62    READ(2,5)((C(I,J),I=1,N3),J=1,N4)
      LVIA=2
      GO TO 63
61    IF(LVIA-1)7,7,81
81    IF(24-2*N1)16,9,9
9     IF(24-2*N2)16,7,7
7     CALL FR2431(LVIA,N5,N6)
      LVIA=LVIA+1
```

```
C
C       SUBROUTINE SETS UP FIELD TO START AND TAKES MEANS
C       FOR NEW FIELD SIZE
C
63      PI=3.14159265
        DZ=1./A(6)                                          DZ
        BETA=0.01745329*A(3)                                BETA
        PHI=0.01745329*A(5)                                 PHI
        BINT=BETA*0.5/A(7)                                  DX
        YZ=0.5*A(6)                                         N1/2
        N8=N1-1
        YZI=1./YZ
        BINV1=1./BINT
        BINV2=1./(BINT**2)
        DZI2=1./(DZ**2)
        ZA2=A(2)**2
        A2ODZ=ZA2*DZI2
C
8       XTHETA=PI-PHI-0.5*BETA+BINT
        DIFF=PHI-A(22)
        LJ=1
C
C       K IS AN ODD/EVEN LJ INDICATOR
        K=1
21      F1=A(4)*COS(XTHETA)
C
C       F2 IS T.COS(THETA) AS (ZI/Z) IS BASED ON
C       HALF BEARING RATIO
C
        F2=A(21)*COS(XTHETA+DIFF)
        IF(K)22,22,23
C
C       EVEN VALUES OF LJ
C
22      DO 24 LI=1,N1
24      H(LI,LJ)=1.+F1+F2*YZI*(YZ+0.5-FLOAT(LI))
        GO TO 26
C
```

```
C       ODD VALUES OF LJ
C
23      DO 25 LI=1,N8
25      H(LI,LJ)=1.+F1+F2*YZI*(YZ-FLOAT(LI))
26      TH(LJ)=XTHETA
        K=-K
        LJ=LJ+1
        XTHETA=XTHETA+BINT
        IF(LJ-(2*N2-1))21,21,27
27      J=2
        CONPID=1.-2.*PHIDOT
28      M=J-1
        LJ=2*J-2
        I=2
29      K=I-1
        Z1=H(I,LJ)**3                                          I+½,J
        Z2=H(K,LJ)**3                                          2-½,J
        Z3=H(K,LJ-1)**3                                        I,J-½
        Z4=H(K,LJ+1)**3                                        I,J+½
        Z7=1./(A2ODZ*(Z1+Z2)+(Z4+Z3)*BINV2)                    DENOM
        Z5=A2ODZ*Z7
        Z6=BINV2*Z7
C       CONSTANT TERM,
        B(K,M,1)=75.39822369*BINV1*Z7*(H(K,LJ-1)-H(K,LJ+1))*CONPID      A0
C
C       ADDS EFFECT OF EDOT, WHICH IS ZERO FOR STEADY STATE CONDITION
C
        IF(EDOT)201,202,201
201     B(K,M,1)=B(K,M,1)-301.5928947*EDOT*COS(TH(LJ))*Z7
C       COEFFICIENT OF P(I+1,J)
202     B(K,M,2)=Z5*Z1                                         A1
C       COEFFICIENT OF P(I-1,J)
        B(K,M,3)=Z5*Z2                                         A2
C       COEFFICIENT OF P(I,J+1)
        B(K,M,4)=Z6*Z4                                         A3
C       COEFFICIENT OFP(I,J-1)
        B(K,M,5)=Z6*Z3                                         A4
```

```
      I=I+1
      IF(I-N1)29,29,30
   30 J=J+1
      IF(J-N2)28,28,33
   33 IF(NCOEF-2)31,31,36
C
C     READ STEADY STATE PRESSURE ARRAY
C
   36 READ(7)C
      REWIND 7
   31 MARKH1=0
   32 DO 120 J=2,N2
      M=J-1
C
C     RCS IS COS(GAMMA(J))
      RCS=COS(TH(2*J-2))
C
C     RSN IS SIN(GAMMA(J))
      RSN=SIN(TH(2*J-2))
C
      DO 12 I=2,N1
      K=I-1
C
C     EQUATION SETTING UP P(I,J)
C
      PRESS=B(K,M,1)+B(K,M,2)*C(I+1,J)+B(K,M,3)*C(I-1,J)+
     1B(K,M,4)*C(I,J+1)+B(K,M,5)*C(I,J-1)
C
C     IF PRESSURE AT NODE IS NEGATIVE MAKE IT ZERO
C
      IF(PRESS)34,34,35
   34 PRESS=0.
C
C     CHECK THAT NEW PRESSURE IS WITHIN A(8) OF OLD PRESSURE
C     IF NOT, SET MARKH1 TO 1
   35 IF(ABS(PRESS-C(I,J))-A(8))65,65,66
   66 MARKH1=1
   65 C(I,J)=C(I,J)+PMULT*(PRESS-C(I,J))
```

```
12      CONTINUE
120     CONTINUE
C
        NCNT=NCNT+1
C
C       THAT COMPLETES 1 FIELD RELAXATION. CHECK NOW WHETHER THE INDICATOR
C       MARKH1 IS 1. IF SO THE NEW PRESSURES AT EACH NODE WHERE NOT WITHIN A(8) OF
C       THE OLD PRESSURES, THEREFORE RETURN TO DO ANOTHER FIELD RELAXATION AFTER
C       CHECKING THAT ITERATION COUNT HAS NOT BEEN EXCEEDED NOR THE OPERATER
C       ABORTED THE CALCULATION
C       ABORTED THE CALCULATION
        IF(MARKH1)82,82,83
C       NOT ACCURATE ENOUGH
83      CALL SSWTCH(2,L2)
        GO TO(85,84),L2
C       SENSE SWITCH 2 SET
85      WRITE(3,151)
151     FORMAT(1H2,24HTHIS SET OF DATA ABORTED/)
C
C       THIS CALCULATION HAS BEEN ABORTED. STORE VALUES
C       IN PREPARATION FOR RESTART.
C       NOTE. IF NCOEF MORE THAN 1 PRESSURE ARRAY
C       IS ALREADY ON TAPE.
C
        IF(NCOEF-1)13,13,14
13      WRITE(7)C
        GO TO 15
14      READ(7)C
15      WRITE(7)A,TH,B,H,W,N1,N2,N3,N4,PI,PHI,BETA,EDOT,NCOEF,
       1LVIA,LVJA,N5,DZ,BINT,YZ,N8,YZI,BINV1,BINV2,DZI2,ZA2,A2ODZ,
       2PRED,PHIDOT,CONPID
        REWIND 7
        PRAHOLDTAPE.
        PRAON10AND
        PRALABELAS
        PRAMJBPRT
        PRATHENAS5
        PAUSE
```

```
      STOP
C     SENSE SWITCH 2 NOT SET
84    IF(FLOAT(NCNT)-A(1))31,31,82
C     CALCULATE FR,FT,MR,MT,PHI
C
82    DO 86 I=1,13
86    D(I)=0.
      EA(1)=0.
      EB(1)=0.
C
      DO 121 J=2,N2
      M=J-1
      D(3)=0.
      D(4)=0.
      D(11)=0.
      RCS=COS(TH(2*J-2))
      RSN=SIN(TH(2*J-2))
      DO 122 I=2,N1
      K=I-1
C
C     SUMMATE P(I,J) I=2 TO N1,J CONSTANT
      D(3)=D(3)+C(I,J)
C
C     MOMENT OF P(I,J) ABOUT CENTRAL LINE, J CONSTANT
      D(11)=D(11)+C(I,J)*FLOAT(N5-I)*YZI
122   CONTINUE
C
C     SUM D(3) IN J DIRECTION
      D(2)=D(2)+D(3)
C
C     TAKE COMPONENTS ALONG AND PERP TO PHI
      EA(J)=D(3)*RCS
      D(8)=D(8)+EA(J)
      EB(J)=D(3)*RSN
      D(9)=D(9)+EB(J)
      D(12)=D(12)+D(11)*RCS
      D(13)=D(13)+D(11)*RSN
121   CONTINUE
```

```
 8  C
        D(3)=-DZ*BINT*D(8)
        D(4)=DZ*BINT*D(9)
        D(5)=SQRT(D(3)**2+D(4)**2)
        D(6)=D(4)/D(3)                                                    TAN A
        D(6)=57.2957795*ATAN(D(6))                                        DEGREE
    C
    C       TO CHANGE DIRECTION OF RADIAL MOMENT TO + AWAY FROM BUSH
        D(12)=-D(12)
    C
        CALL SSWTCH(3,I)
        IF(I.EQ.1)WRITE(3,40)(D(I),I=1,13),A(5),PHI
    40  FORMAT(1H ,8G15.6)
    C
        IF(NCOEF.GT.1)WRITE(3,91)NCNT,A(5),A(4),EDOT,PHIDOT,
       1D(3),D(4),D(12),D(13)
        GO TO (211,212,213,214,215,216,217,228,229,
       *50,51,52,53,54,55),NCOEF
    211 IF(ABS(D(6)-A(5))-A(17))87,87,88
    C
    C       FIELD VALUE OF PHI (D(6)) DOES NOT EQUAL VALUE USED FOR
    C       FILM THICKNESS THEREFORE MODIFY INPUT PHI AND HAVE ANOTHER GO
    C
    88  A(5)=D(6)
        PHI=A(5)*0.0174532925
        GO TO 8
    C
    C       VALUE OF PHI IN AND OUT ARE EQUAL THEREFORE TEST FOR
    C       HALVING OF MESH SIZE
    C
    87  IF(LVIA-1-LVJA)61,61,16
    C
    16  WRITE(3,45)NCNT
    45  FORMAT(1H ,20HNUMBER OF ITERATIONS,5B,I6/)
        PHI=57.2957795*PHI
        SUMF=1./D(5)
        DILE=1./A(2)
        WRITE(3,46)A(21),A(22),DILE,A(4),SUMF,D(3),D(4),D(12),D(13),PHI
    46  FORMAT(1H ,2HT ,19B,1H=G15.6//
```

```
     13HPSI,18B,1H=G15.6//
     222HLENGTH/DIAMETER RATIO=G15.6//
     322HECCENTRICITY RATIO    =G15.6//
     422HSOMMERFELD NUMBER     =G15.6//
     522HRADIAL FORCE  FR      =G15.6,25H  POSITIVE AWAY FROM BUSH //
     622HTANGENTIAL FORCE  FT =G15.6,33H  POSITIVE IN DIRECTION OF MOTION//
     XN//
     722HMOMENT  MR            =G15.6,25H  POSITIVE AWAY FROM BUSH //
     822HMOMENT  MT            =G15.6,33H  POSITIVE IN DIRECTION OF MOTION//
     XN//
     922HANGLE OF INCIDENCE    =G15.6//)
      CALL SSWTCH(4,I)
      GO TO (47,224),I
47    WRITE(3,49)
49    FORMAT(1H1)
      WRITE(3,48)((I,J,C(I,J),I=1,N3),J=1,N4)
48    FORMAT(1H ,5(2HP(I2,1H,I2,2H)=G13.6)/)
C-----
C     THESE STATEMENTS CONCERN THE CALCULATION OF THE
C     LINEARIZED FORCE COEFFICIENTS
C
C-----FIRST CHECK IF COEFFICIENTS ARE TO BE FOUND IF SO STORE
C
C     A(5),FR,FT. ON W ARRAY. IF NOT STOP
C
224   IF(A(10).EQ.0..AND.A(12).EQ.0.)GO TO 1
      WRITE(3,90)
90    FORMAT(1H2,41HLINEARIZED FORCE COEFFICIENTS CALCULATION  ///
     110HITERATIONS,6B,3HPHI,8B,1HE,10B,4HEDOT,5B,6HPHIDOT,7B,2HFR,10B,
     22HFT,10B,2HMR,10B,2HMT /14B,7HDEGREES //)
      WRITE(3,91)NCNT,A(5),A(4),EDOT,PHIDOT,D(3),D(4),D(12),D(13)
91    FORMAT(1H ,I8,F14.3,3F11.6,4F12.6)                          PHI
      W(1)=A(5)                                                   FR
      W(2)=D(3)                                                   FT
      W(3)=D(4)                                                   E
      W(4)=A(4)
      NCOEF=2
      EDOT=A(14)
```

```
      WRITE(7)C
      REWIND 7
      GO TO 27
  212 W(5)=D(3)
      W(6)=D(4)
      NCOEF=3
      EDOT=-A(15)
      GO TO 27
  213 W(7)=D(3)
      W(8)=D(4)
      NCOEF=4
      EDOT=0.
      PHIDOT=A(23)
      GO TO 27
  214 W(9)=D(3)
      W(10)=D(4)
      NCOEF=5
      PHIDOT=-A(24)
      GO TO 27
  215 W(11)=D(3)
      W(12)=D(4)
      NCOEF=6
      EDOT=A(14)
      PHIDOT=A(23)
      GO TO 27
  216 W(13)=D(3)
      W(14)=D(4)
      NCOEF=7
      EDOT=0.
      PHIDOT=0.
      A(5)=W(1)+A(10)
  218 PHI=A(5)*0.0174532925
      GO TO 8
  217 W(15)=D(3)
      W(16)=D(4)
      NCOEF=8
      A(5)=W(1)-A(11)
      GO TO 218
```

FR
FT

```
228   W(17)=D(3)
      W(18)=D(4)
      NCOEF=9
      A(5)=W(1)
      A(4)=W(4)+A(12)
      GO TO 218
229   W(19)=D(3)
      W(20)=D(4)
      NCOEF=10
      A(4)=W(4)-A(13)
      GO TO 8
50    W(21)=D(3)
      W(22)=D(4)
      NCOEF=11
      A(5)=W(1)+A(10)
      A(4)=W(4)+A(12)
      GO TO 218
51    W(23)=D(3)
      W(24)=D(4)
      NCOEF=12
      A(4)=W(4)
      EDOT=A(14)
      GO TO 8
52    W(25)=D(3)
      W(26)=D(4)
      NCOEF=13
      EDOT=0.
      PHIDOT=A(23)
      GO TO 27
53    W(27)=D(3)
      W(28)=D(4)
      NCOEF=14
      A(5)=W(1)
      A(4)=W(4)+A(12)
      EDOT=A(14)
      PHIDOT=0.
      GO TO 218
54    W(29)=D(3)
```

```
12          W(30)=D(4)
            NCOEF=15
            EDOT=0.
            PHIDOT=A(23)
            GO TO 27
55          W(31)=D(3)
            W(32)=D(4)
C
C-----COEFFICIENTS CALCULATION
C
            CALL GR 482
            GO TO 1
            END
```

```
      SUBROUTINE GR482
C
CC    CALCULATES AND PRINTS PARTIAL DERIVATIVES AND
C     COEFFICIENTS FOR FJ1482.
C
      DIMENSION A(30),C(25,25),B(24,24,5),D(20),H(24,47),
     1W(32),G(28),Y(28)
      COMMON A,B,C,D,H,N1,N2,N3,N4,PI,PHI,BETA,W
      A(10)=A(10)*0.0174532925
      A(11)=A(11)*0.0174532925
      A1=1./(A(10)+A(11))
      A2=1./(A(12)+A(13))
      A3=1./(A(14)+A(15))
      A4=1./(A(23)+A(24))
      A5=1./A(10)
      A6=1./A(11)
      A7=1./A(12)
      A8=1./A(13)
      A9=1./A(14)
      A10=1./A(15)
      A11=1./A(23)
      A12=1./A(24)
      K=1
      J=2
    2 G(K)=A1*(A5*A(11)*(W(J+13)-W(J))-A6*A(10)*(W(J+15)-W(J)))
      G(K+1)=A2*(A7*A(13)*(W(J+17)-W(J))-A8*A(12)*(W(J+19)-W(J)))
      G(K+2)=A3*(A9*A(15)*(W(J+3)-W(J))-A10*A(14)*(W(J+5)-W(J)))
      G(K+3)=A4*(A11*A(24)*(W(J+7)-W(J))-A12*A(23)*(W(J+9)-W(J)))
      G(K+4)=2.*A1*(A5*(W(J+13)-W(J))+A6*(W(J+15)-W(J)))
      G(K+5)=2.*A2*(A7*(W(J+17)-W(J))+A8*(W(J+19)-W(J)))
      G(K+6)=2.*A3*(A9*(W(J+3)-W(J))+A10*(W(J+5)-W(J)))
      G(K+7)=2.*A4*(A11*(W(J+7)-W(J))+A12*(W(J+9)-W(J)))
      G(K+8)=A5*A7*(W(J+21)+W(J)-W(J+13)-W(J+17))
      G(K+9)=A7*A9*(W(J+27)+W(J)-W(J+17)-W(J+3))
      G(K+10)=A9*A11*(W(J+11)+W(J)-W(J+3)-W(J+7))
      G(K+11)=A11*A5*(W(J+25)+W(J)-W(J+13)-W(J+7))
      G(K+12)=A5*A9*(W(J+23)+W(J)-W(J+13)-W(J+3))
      G(K+13)=A7*A11*(W(J+29)+W(J)-W(J+17)-W(J+7))
```

```
      IF(K-2)1,1,3
    1 K=15
      J=3
      GO TO 2
    3 WRITE(3,4)
    4 FORMAT(1H1)
      WRITE(3,5)
    5 FORMAT (1H ,21HPARTIAL DERIVATIVES -//
     129X,2HFR,23X,2HFT)
      WRITE(3,6)(G(J),G(J+14),J=1,14)
    6 FORMAT(1H2,7HD/D.PHI,14X,G15.6,G25.6/5HD/D.E,
     116X,G15.6,G25.6/8HD/D.EDOT,13X,G15.6,G25.6/
     210HD/D.PHIDOT,11X,G15.6,G25.6/9HD2/D.PHI2,12X,
     3G15.6,G25.6/7HD2/D.E2,14X,G15.6,G25.6/
     410HD2/D.EDOT2,11X,G15.6,G25.6/12HD2/D.PHIDOT2,9X,
     5G15.6,G25.6/12HD2/D.PHI.D.E,9X,G15.6,G25.6/
     613HD2/D.E.D.EDOT,8X,G15.6,G25.6/18HD2/D.EDOT.D.PHIDOT,
     73X,G15.6,G25.6/17HD2/D.PHI.D.PHIDOT,4X,G15.6,G25.6/
     815HD2/D.PHI.D.EDOT,6X,G15.6,G25.6/
     915HD2/D.E.D.PHIDOT,6X,G15.6,G25.6)
      SS=SIN(W(1)*0.01745329)
      CC=COS(W(1)*0.01745329)
      S2=SS**2
      C2=CC**2
      SC=SS*CC
      S3=S2*SS
      C3=C2*CC
      C2S=C2*SS
      S2C=S2*CC
      E=1./W(4)
      E2=E**2
      X1=E*(W(2)-G(15))
      X2=E*(W(3)+G(1))
      X3=E*(G(1)+W(3))-G(16)
      X4=E*(G(15)-W(2))+G(2)
      X5=E*G(4)-G(17)
      X6=G(3)+E*G(18)
      X7=E2*(G(1)-0.5*G(19)+0.5*W(3))
```

```
      X8=E2*(0.5*G(5)-0.5*W(2)+G(15))
   15 X9=E*(0.5*E*(G(5)-W(2)+2.*G(15))+G(2)-G(23))
      X10=E*(0.5*E*(W(3)-G(19)+2.*G(1))-G(16)-G(9))
      X11=E*(G(9)+G(16)-0.5*W(4)*G(20))
      X12=E*(0.5*W(4)*G(6)-G(2)+G(23))
      X13=E*(G(2)-G(23))
      X14=E*(G(9)+G(16))
      X15=E*(W(4)*G(6)-G(2)+G(23)-E*(G(5)-W(2)+2.*G(15)))
      X16=E*(G(9)+G(16)-W(4)*G(20)-E*(2.*G(1)-G(19)+W(3)))
      X17=E*(0.5*W(4)*G(7)+G(25))
      X18=E*(G(11)+0.5*E*G(22))
      X19=E*(0.5*E*G(8)-G(25))
      X20=E*(G(11)-0.5*W(4)*G(21))
      X21=E*(G(25)+W(4)*G(7)-E*G(8))
      X22=E*(G(11)-W(4)*G(21)+E*G(22))
      X23=E2*(G(12)+G(18))
      X24=E*(G(13)+G(17)+G(14)-E*(G(4)-G(26)))
      X25=E*(W(4)*G(10)-G(3)+G(27)+G(28))
      X26=E2*(G(4)-G(26))
      X27=E*(E*(G(12)+G(18))+G(3)-G(27)-G(28))
      X28=E*(G(13)+G(17)+G(14)-W(4)*G(24))
      X29=E*(G(13)+G(17))
      X30=E*(W(4)*G(10)-E*(G(12)+G(18))-G(3)+G(27))
      X31=E*(G(14)-W(4)*G(24)-E*(G(4)-G(26)))
      X32=E*(G(3)-G(27))
      X33=E*(W(4)*G(10)-E*(G(12)+G(18))+G(28))
      X34=E*(G(13)+G(17)-W(4)*G(24)-E*(G(4)-G(26)))
      Y(1)=S2*G(2)+C2*X1+SC*X3
      Y(2)=SC*X4-C2*G(16)-S2*X2
      Y(3)=S2*G(3)-E*C2*G(18)+SC*X5
      Y(4)=SC*X6-C2*G(17)-E*S2*G(4)
      Y(5)=0.5*S3*G(6)+C3*X7+C2S*X9+S2C*X11
      Y(6)=S3*X8-0.5*C3*G(20)+S2C*X10+C2S*X12
      Y(7)=-S3*X14+C3*X13+S2C*X15+C2S*X16
      Y(8)=0.5*S3*G(7)-0.5*E2*C3*G(22)+C2S*X19+S2C*X20
      Y(9)=0.5*E2*S3*G(8)-0.5*C3*G(21)+C2S*X17-S2C*X18
      Y(10)=-E*S3*G(11)-E*C3*G(25)+S2C*X21+C2S*X22
      Y(11)=S3*G(10)+C3*X26+S2C*X28+C2S*X27
```

```
      Y(12)=-E*S3*G(14)+C3*X32+S2C*X33+C2S*X34
      Y(13)=S3*X23-C3*G(24)-S2C*X24+C2S*X25
      Y(14)=-S3*X29-E*C3*G(28)+S2C*X30+C2S*X31
      Y(15)=S2*G(16)+C2*X2+SC*X4
      Y(16)=S2*X1+C2*G(2)-SC*X3
      Y(17)=S2*G(17)+E*C2*G(4)+SC*X6
      Y(18)=-E*S2*G(18)+C2*G(3)-SC*X5
      Y(19)=0.5*S3*G(20)+C3*X8+S2C*X12-C2S*X10
      Y(20)=-S3*X7+0.5*C3*G(6)+S2C*X9-C2S*X11
      Y(21)=S3*X13+C3*X14-S2C*X16+C2S*X15
      Y(22)=0.5*S3*G(21)+0.5*E2*C3*G(8)+S2C*X17+C2S*X18
      Y(23)=0.5*E2*S3*G(22)+0.5*C3*G(7)+S2C*X19-C2S*X20
      Y(24)=-E*S3*G(25)+E*C3*G(11)-S2C*X22+C2S*X21
      Y(25)=S3*G(24)+C3*X23+C2S*X24+S2C*X25
      Y(26)=-S3*X26+C3*G(10)+S2C*X27-C2S*X28
      Y(27)=-E*S3*G(28)+C3*X29-S2C*X31+C2S*X30
      Y(28)=S3*X32+E*C3*G(14)-S2C*X34+C2S*X33
      WRITE(3,7)
    7 FORMAT(1H4,20HFORCE COEFFICIENTS -)
      WRITE(3,8)(Y(J),J=1,28)
    8 FORMAT(1H2,3HAXX,G23.5/3HAXY,G23.5/4HAXX.,
     1G22.5/4HAXY.,G22.5/4HAXX2,G22.5/4HAXY2,G22.5/
     24HAXXY,G22.5/5HAXX.2,G21.5/5HAXY.2,G21.5/
     36HAXX.Y.,G20.5/5HAXXX.,G21.5/5HAXXY.,G21.5/
     45HAXYY.,G21.5/5HAXYX.,G21.5/3HAYX,G23.5/3HAYY,
     5G23.5/4HAYX.,G22.5/4HAYY.,G22.5/4HAYX2,G22.5/
     64HAYY2,G22.5/4HAYXY,G22.5/5HAYX.2,G21.5/5HAYY.2,G21.5/
     76HAYX.Y.,G20.5/5HAYXX.,G21.5/5HAYYY.,G21.5/
     85HAYXY.,G21.5/5HAYYX.,G21.5)
      RETURN
      END
```

```
      SUBROUTINEFR2431(LVIA,N5,N6)                                    FJ1482
      DIMENSION A(30),B(24,24,5),C(25,25),D(20),H(24,47)
      COMMON A,B,C,D,H,N1,N2,N3,N4,PI,PHI,BETA
      IF(LVIA-1)1,1,6
    1 DO 2 I=1,N3
      C(I,1)=0.0
    2 C(I,N4)=0.0
      DO 3 J=1,N4
      C(1,J)=0.0
    3 C(N3,J)=0.0
      DO 4 I=2,N1
      DO 4 J=2,N2
    4 C(I,J)=0.5
      RETURN
    6 N1=2*N1
      N2=2*N2
      A(6)=N1
      A(7)=N2
      N3=N1+1
      N4=N2+1
      N5=N1/2+1
      N6=N3+1
      DO 7 I=1,N3
      C(I,1)=0.0
    7 C(I,N4)=0.0
      DO 8 J=1,N4
      C(1,J)=0.0
    8 C(N3,J)=0.0
    9 L1=N1-1
      L2=N2-1
      L3=N1/2
      L4=N2/2
   10 C(L1,L2)=C(L3,L4)
      L2=L2-2
      L4=L4-1
      IF(L2-3)11,10,10
```

```
      11    L2=N2-1
            L4=N2/2
            L1=L1-2
            L3=L3-1
            IF(L1-3)12,10,10
      12    L1=N1-1
            L2=N2
      13    C(L1,L2)=(C(L1,L2-1)+C(L1,L2+1))/2.0
            L2=L2-2
            IF(L2-2)14,13,13
      14    L1=L1-2
            L2=N2
            IF(L1-3)15,13,13
      15    L1=N1
            L2=N2
      16    C(L1,L2)=(C(L1+1,L2)+C(L1-1,L2))/2.0
            L2=L2-1
            IF(L2-2)17,16,16
      17    L1=L1-2
            L2=N2
            IF(L1-2)18,16,16
      18    RETURN
            END
```

FIG. 4-1A

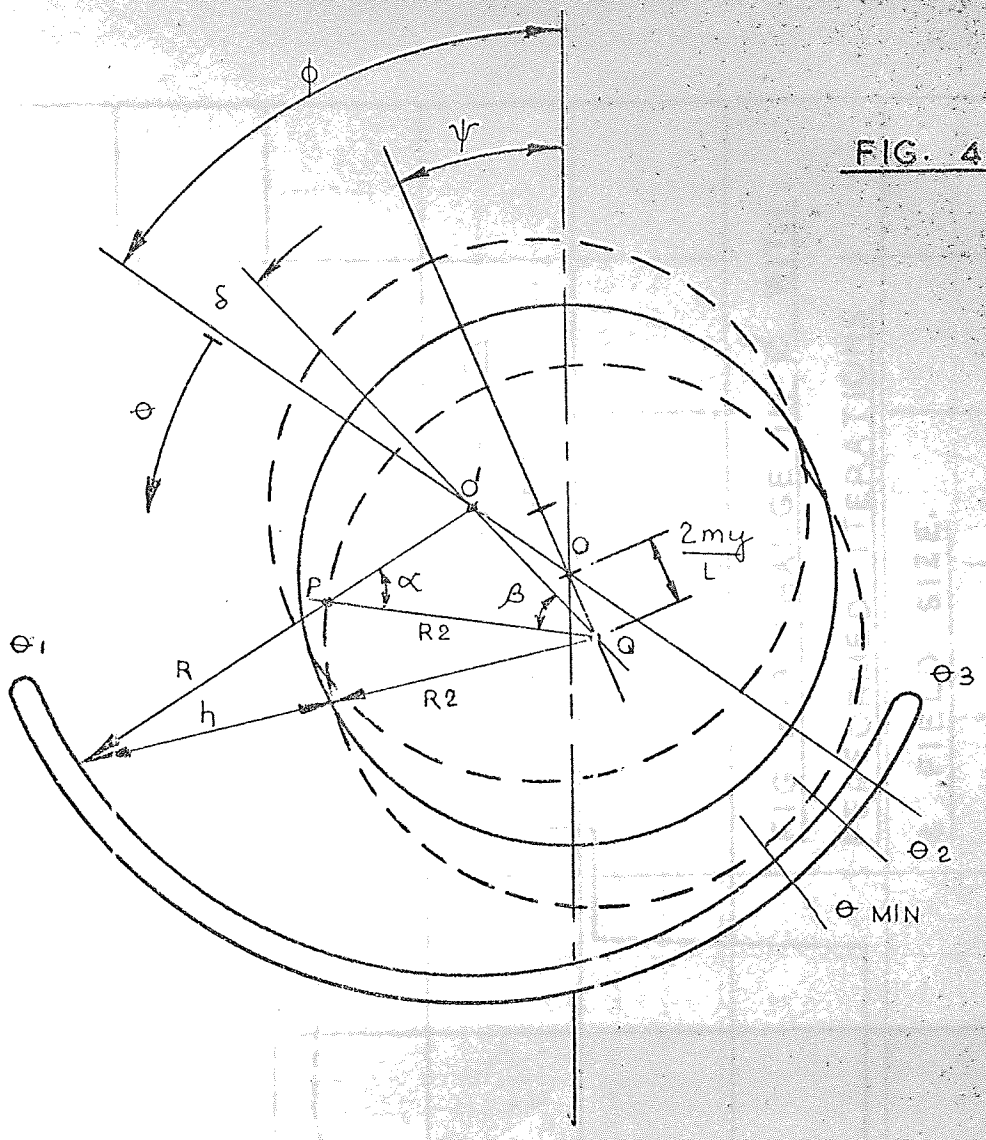

GEOMETRY OF PARTIAL JOURNAL BEARING.

FIG. 4-1B

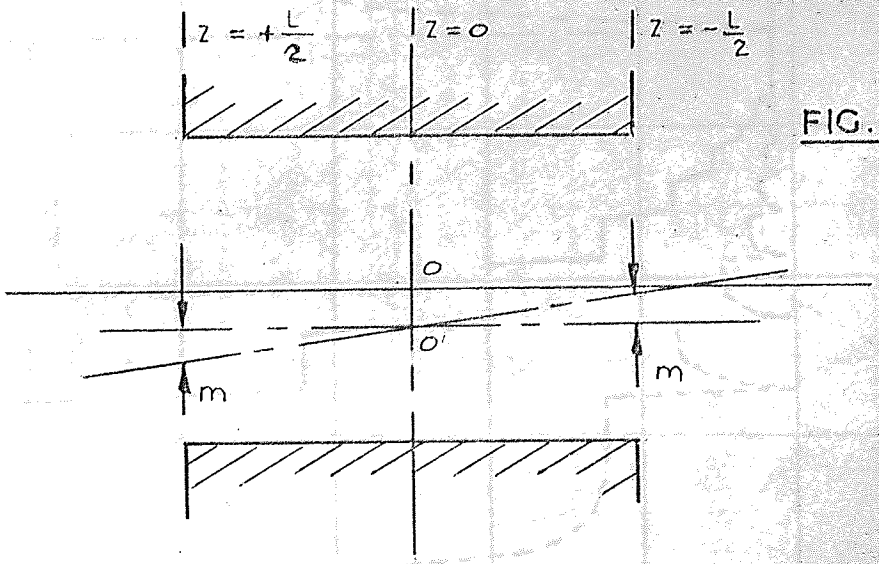

VIEW SHOWING MAXIMUM TILT INCLINED AT ψ FROM THE VERTICAL.

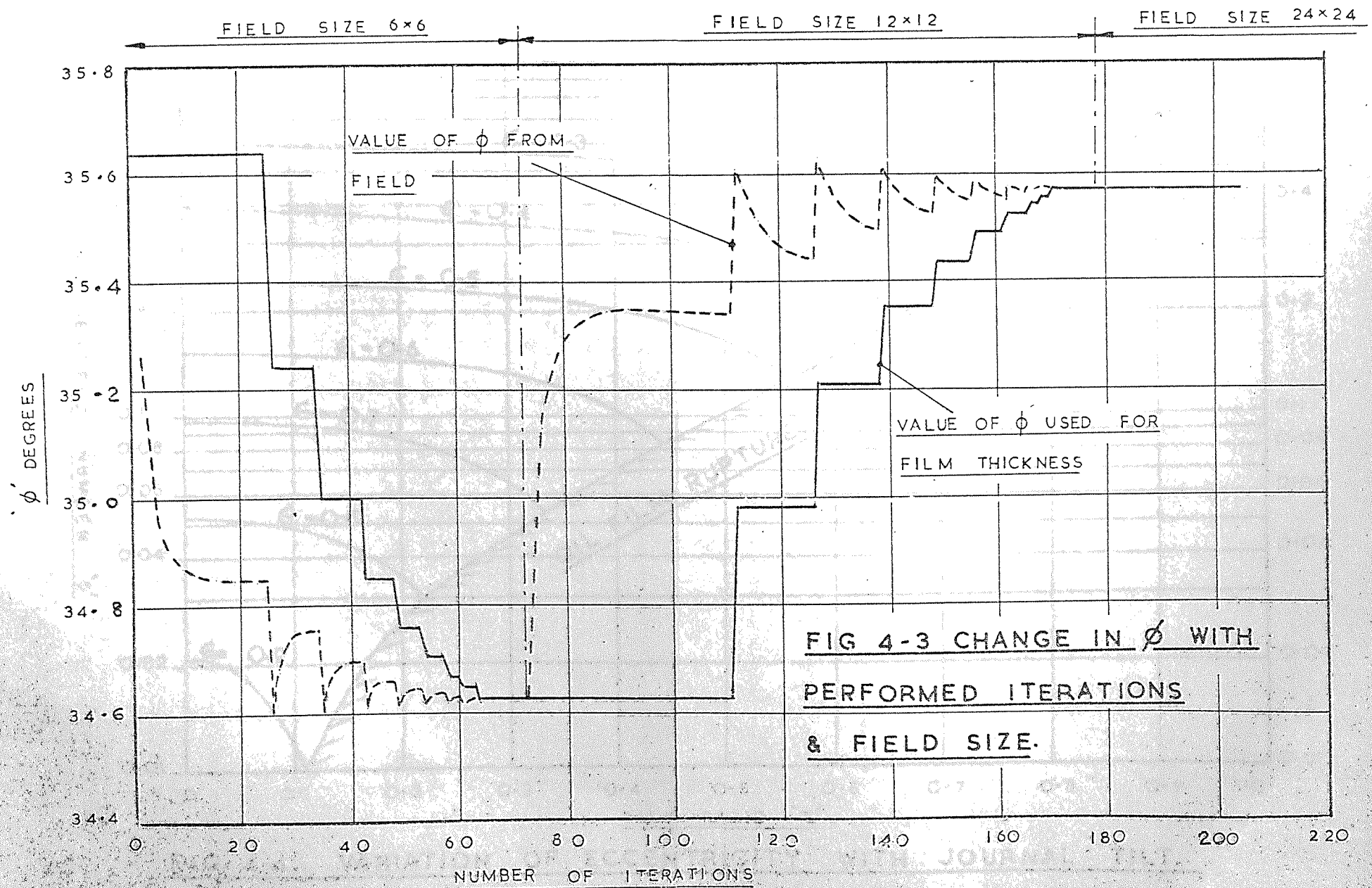

FIG 4-3 CHANGE IN ϕ WITH PERFORMED ITERATIONS & FIELD SIZE.

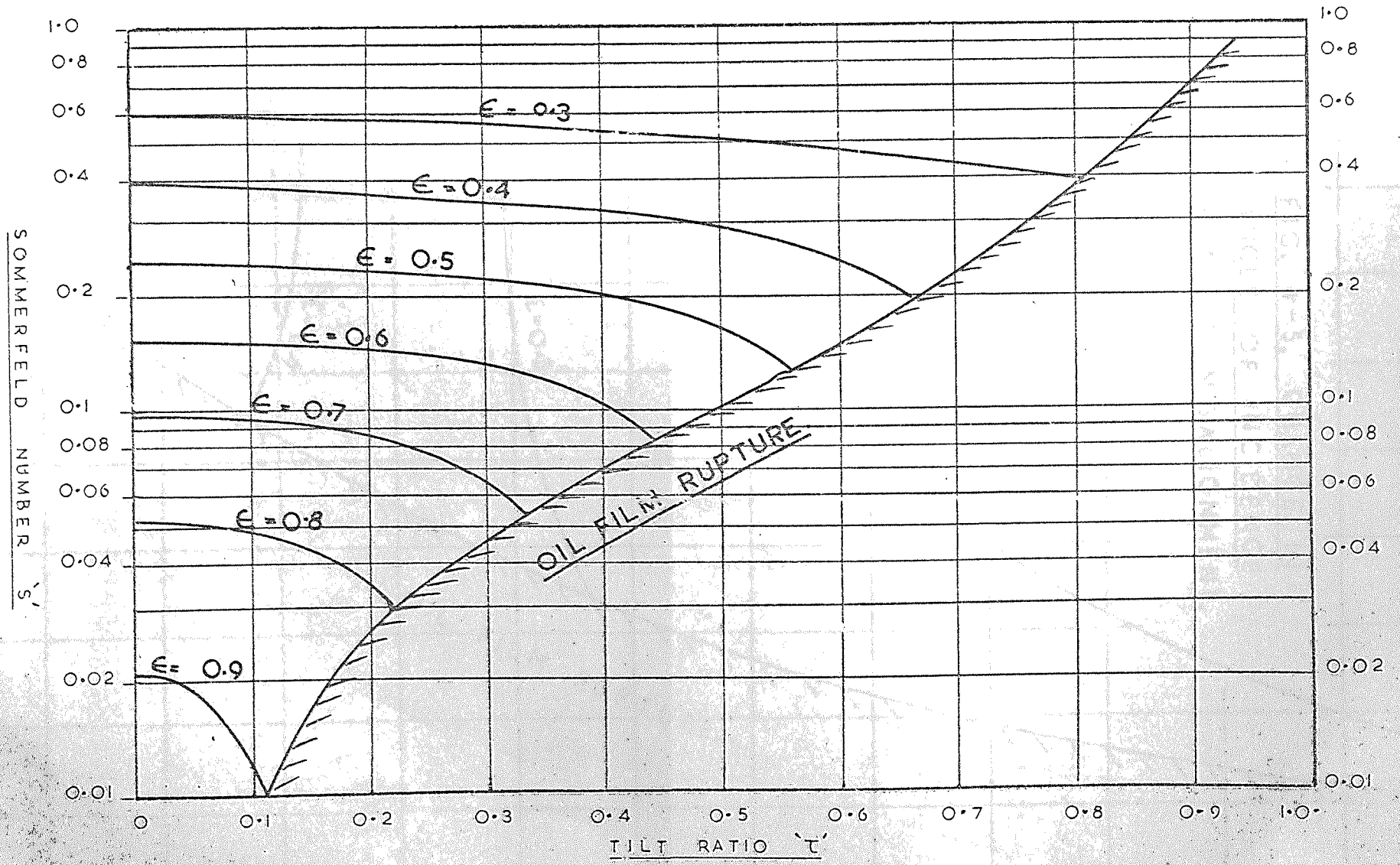

FIG. 4-4. VARIATION OF ECCENTRICITY WITH JOURNAL TILT.

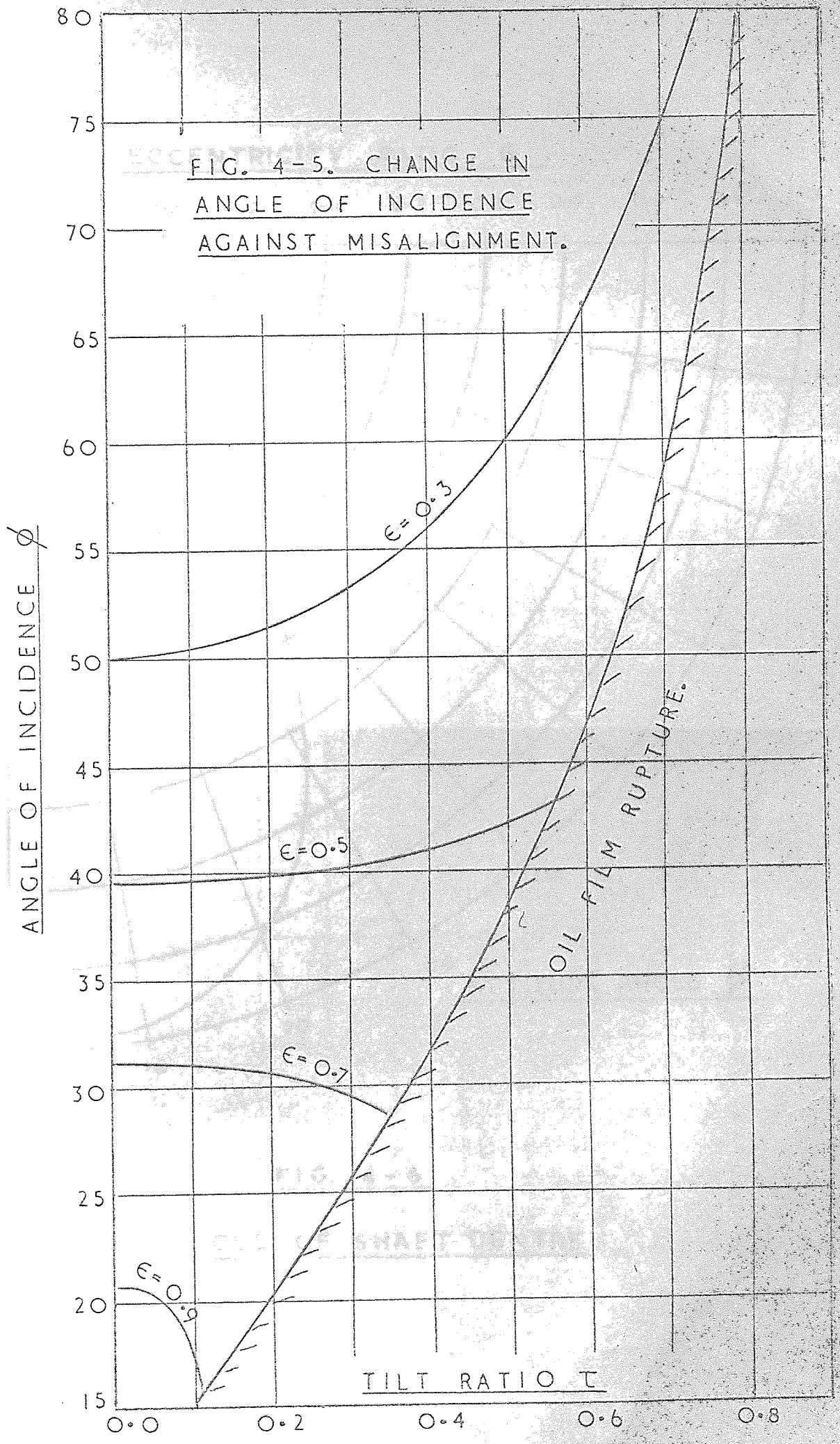

FIG. 4-5. CHANGE IN ANGLE OF INCIDENCE AGAINST MISALIGNMENT.

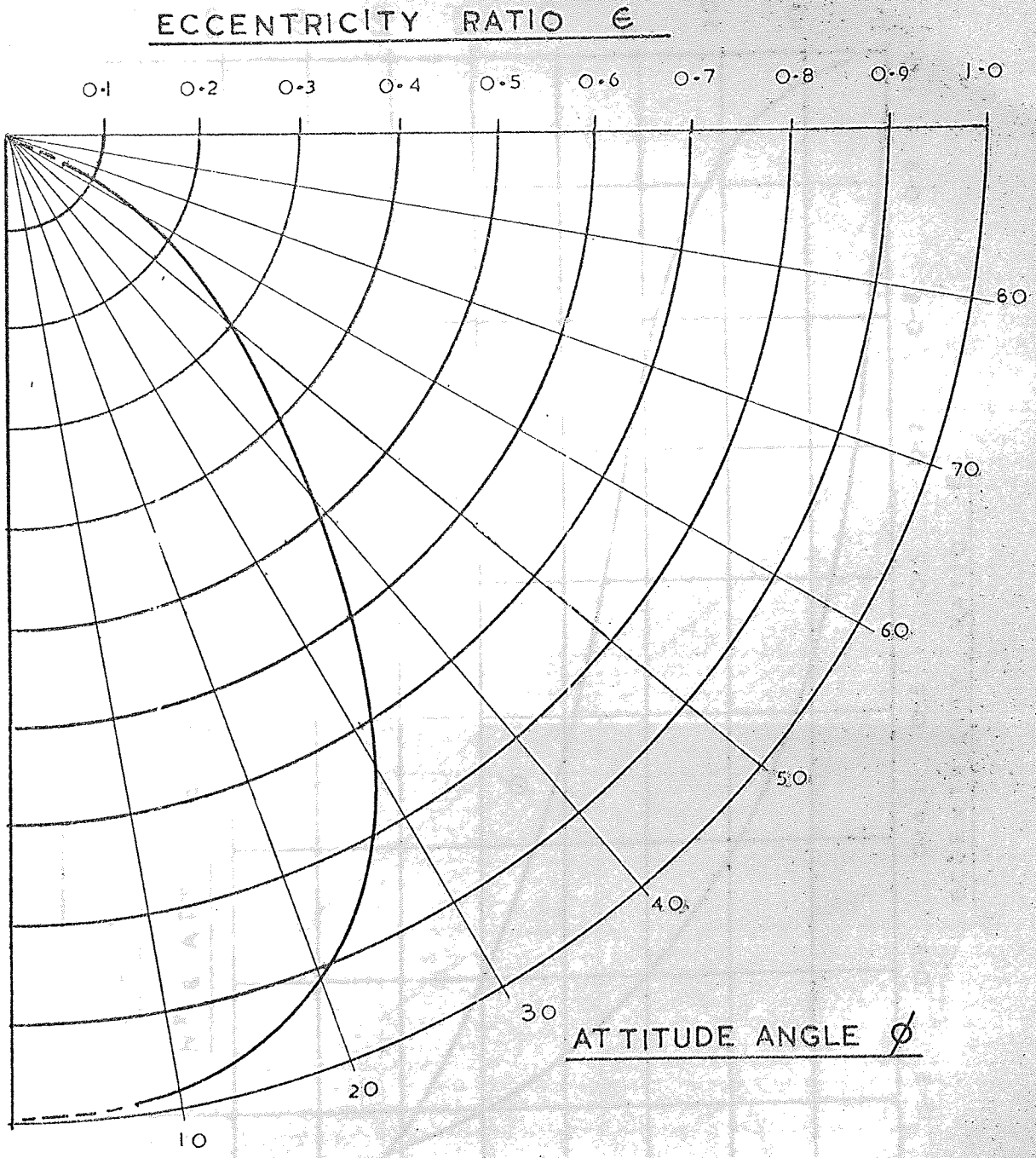

FIG. 4-6

LOCUS OF SHAFT CENTRE

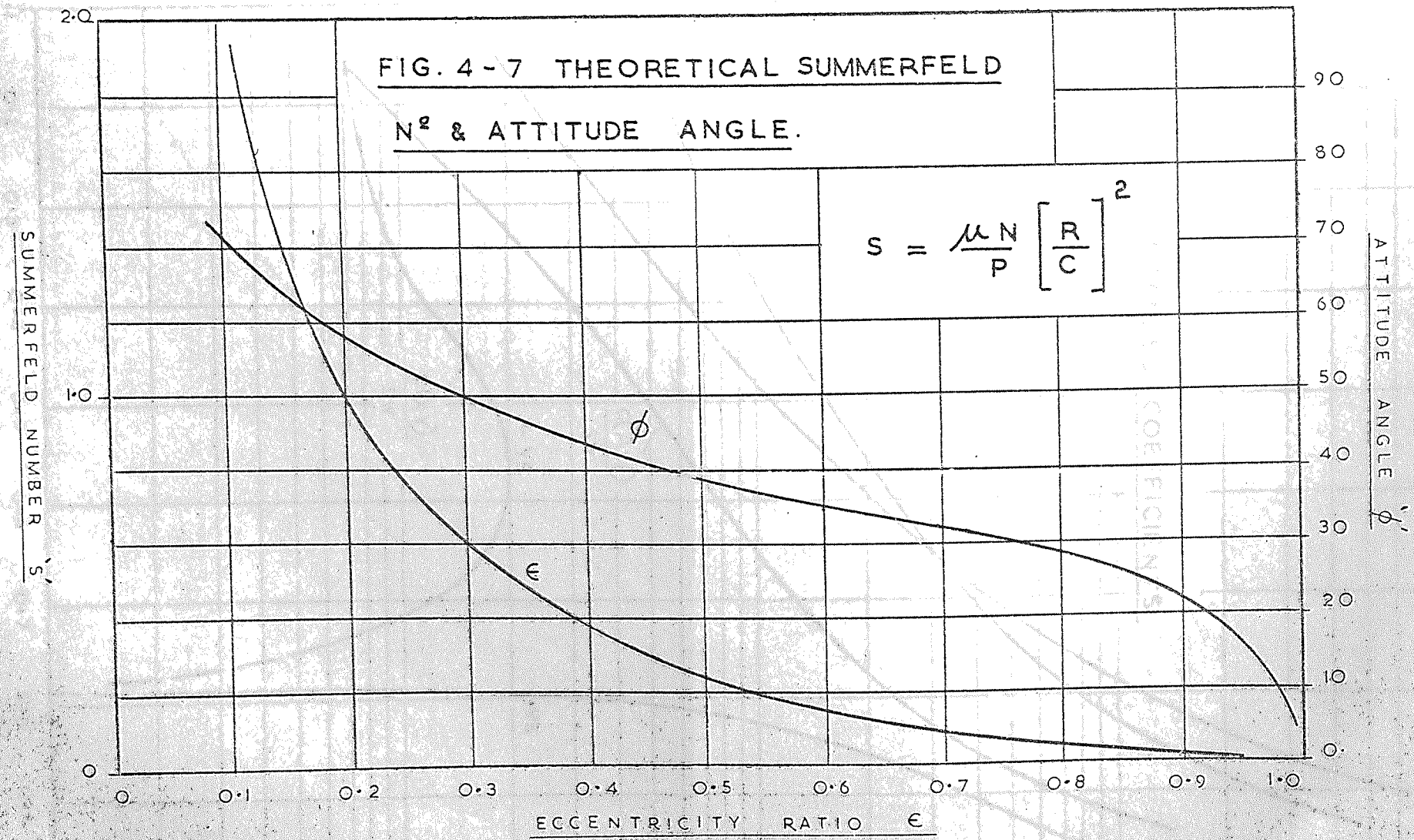
FIG. 4-7 THEORETICAL SUMMERFELD
N² & ATTITUDE ANGLE.
$S = \frac{\mu N}{P}\left[\frac{R}{C}\right]^2$
SUMMERFELD NUMBER 'S'
ATTITUDE ANGLE 'φ'
ECCENTRICITY RATIO ε
φ
ε
2·0
1·0
0
0·1
0·2
0·3
0·4
0·5
0·6
0·7
0·8
0·9
1·0
90
80
70
60
50
40
30
20
10
0·

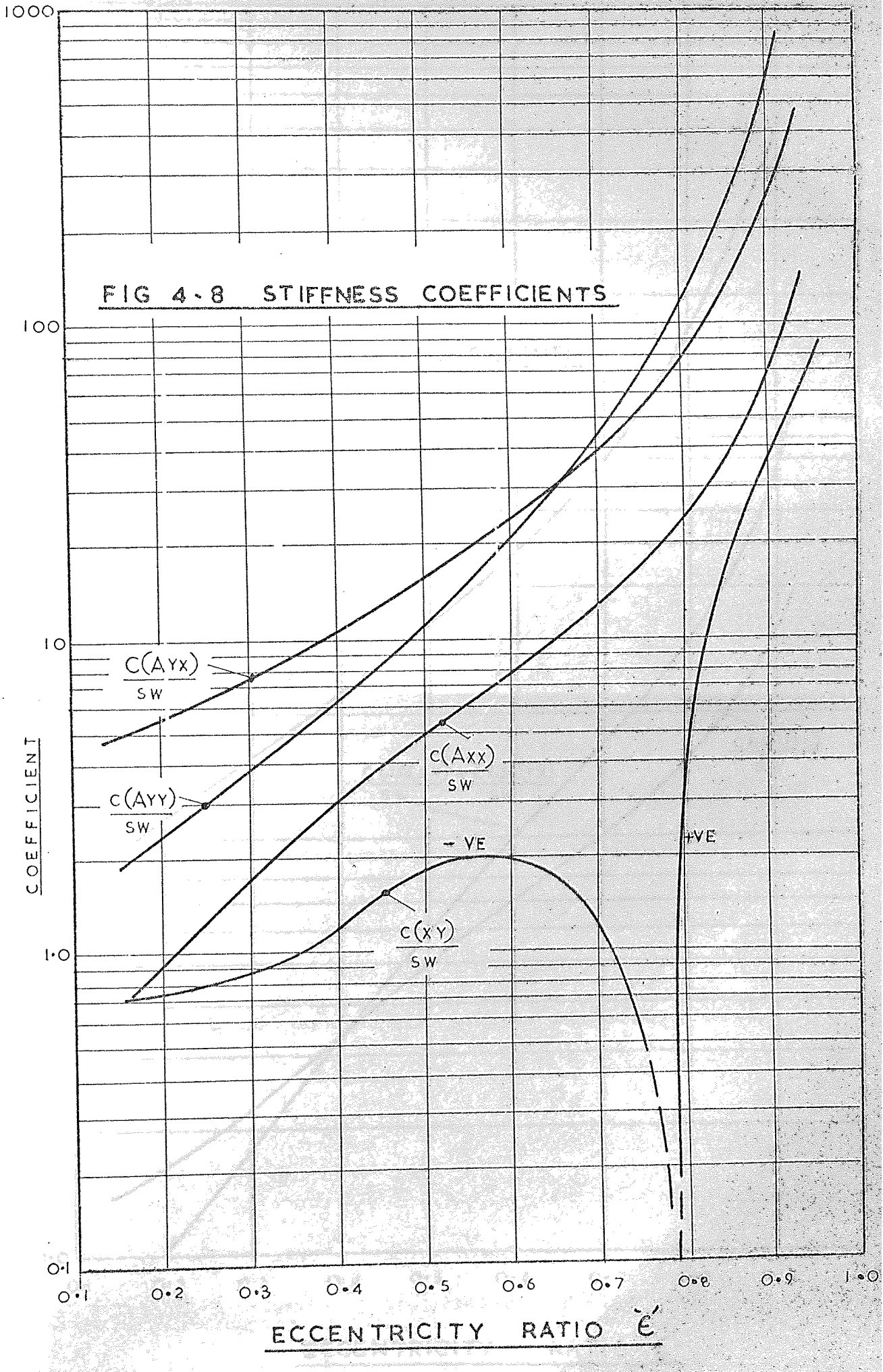

FIG 4·8 STIFFNESS COEFFICIENTS

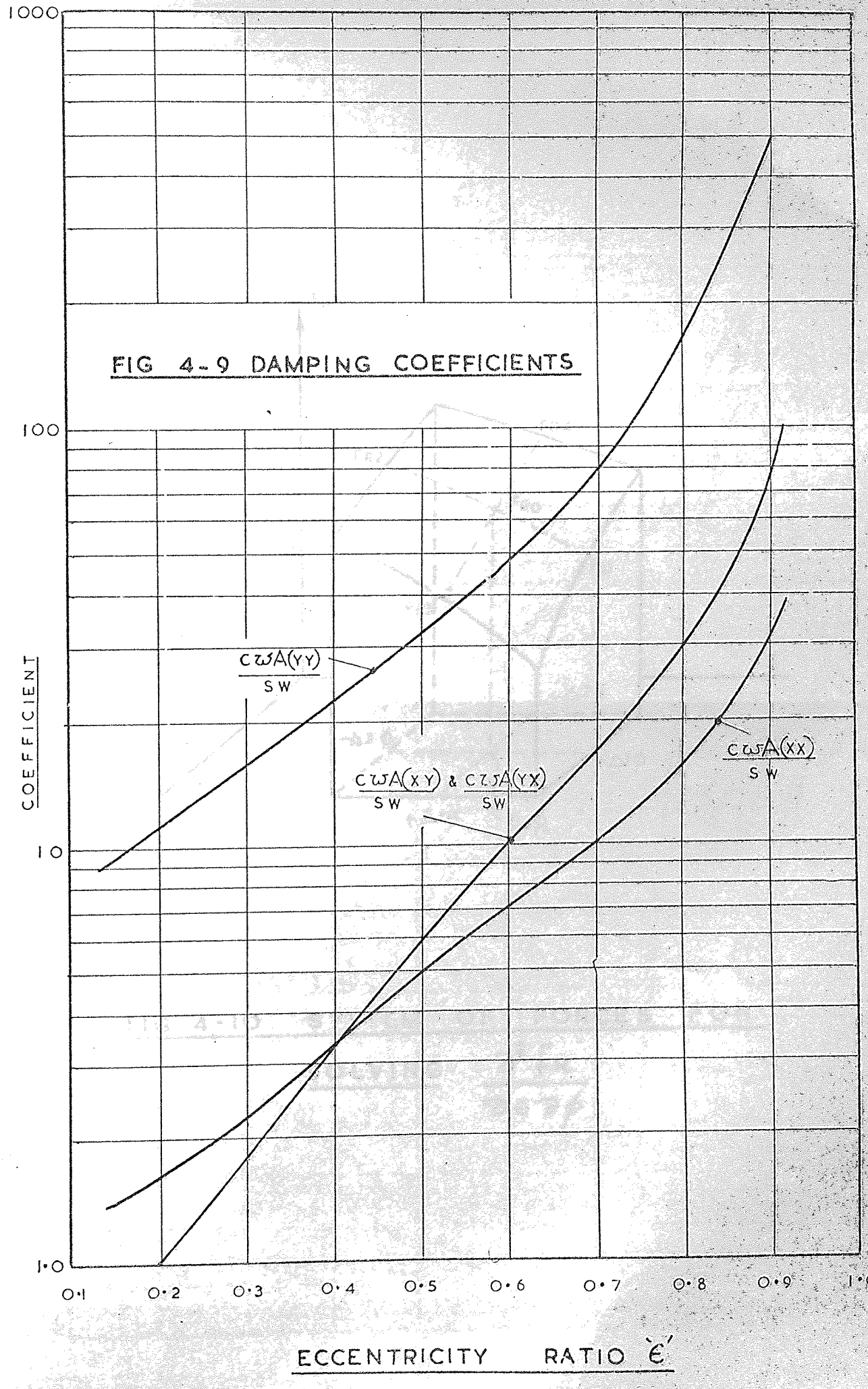

FIG 4-9 DAMPING COEFFICIENTS

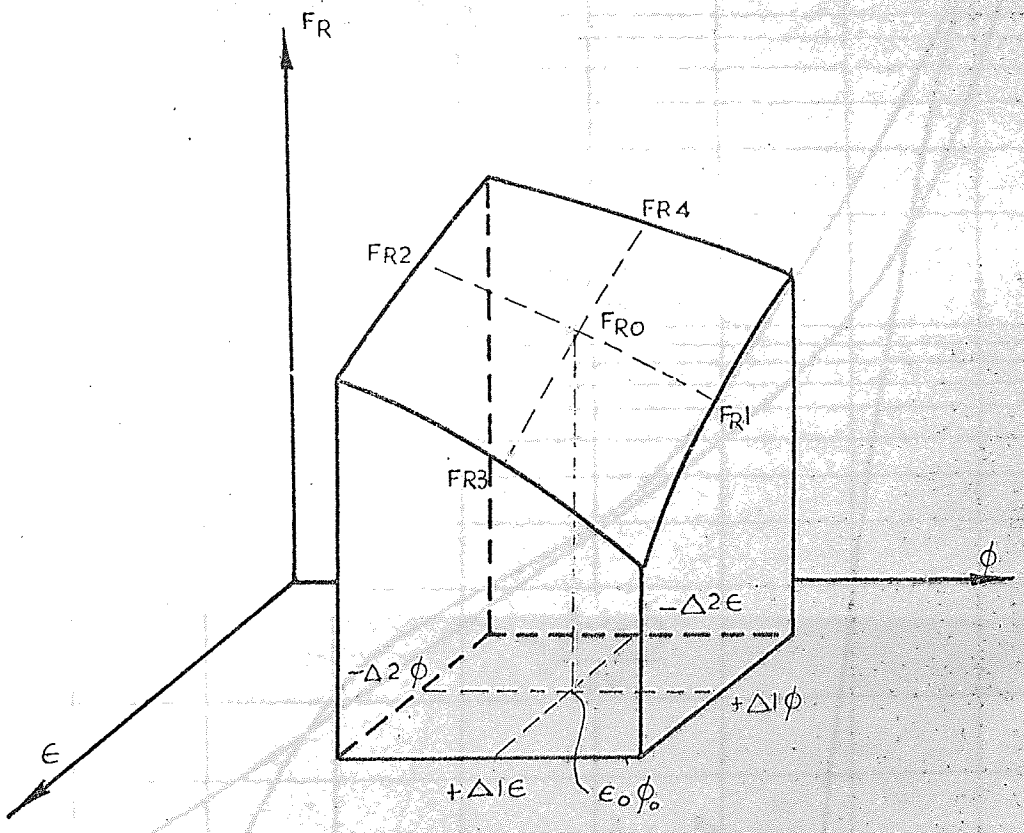

FIG 4-10 SYSTEM OF FORCES FOR SOLVING $\frac{\partial^2 f_R}{\partial \epsilon \partial \phi}$

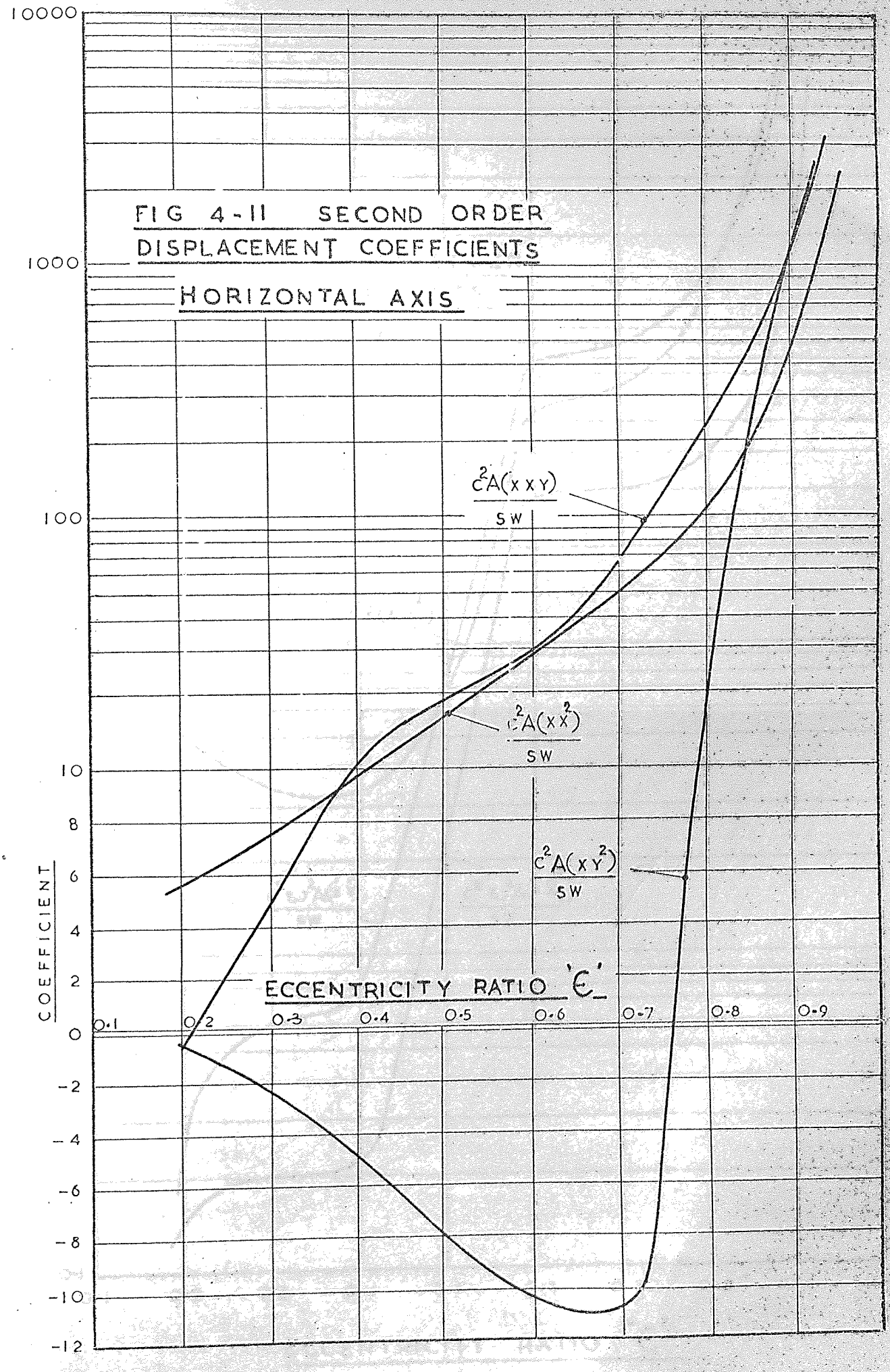
FIG 4-11 SECOND ORDER DISPLACEMENT COEFFICIENTS
HORIZONTAL AXIS
10000
1000
100
10
8
6
4
2
0
-2
-4
-6
-8
-10
-12
COEFFICIENT
$\frac{c^2 A(x x y)}{SW}$
$\frac{c^2 A(x x^2)}{SW}$
$\frac{c^2 A(x y^2)}{SW}$
ECCENTRICITY RATIO 'ε'
0·1
0·2
0·3
0·4
0·5
0·6
0·7
0·8
0·9

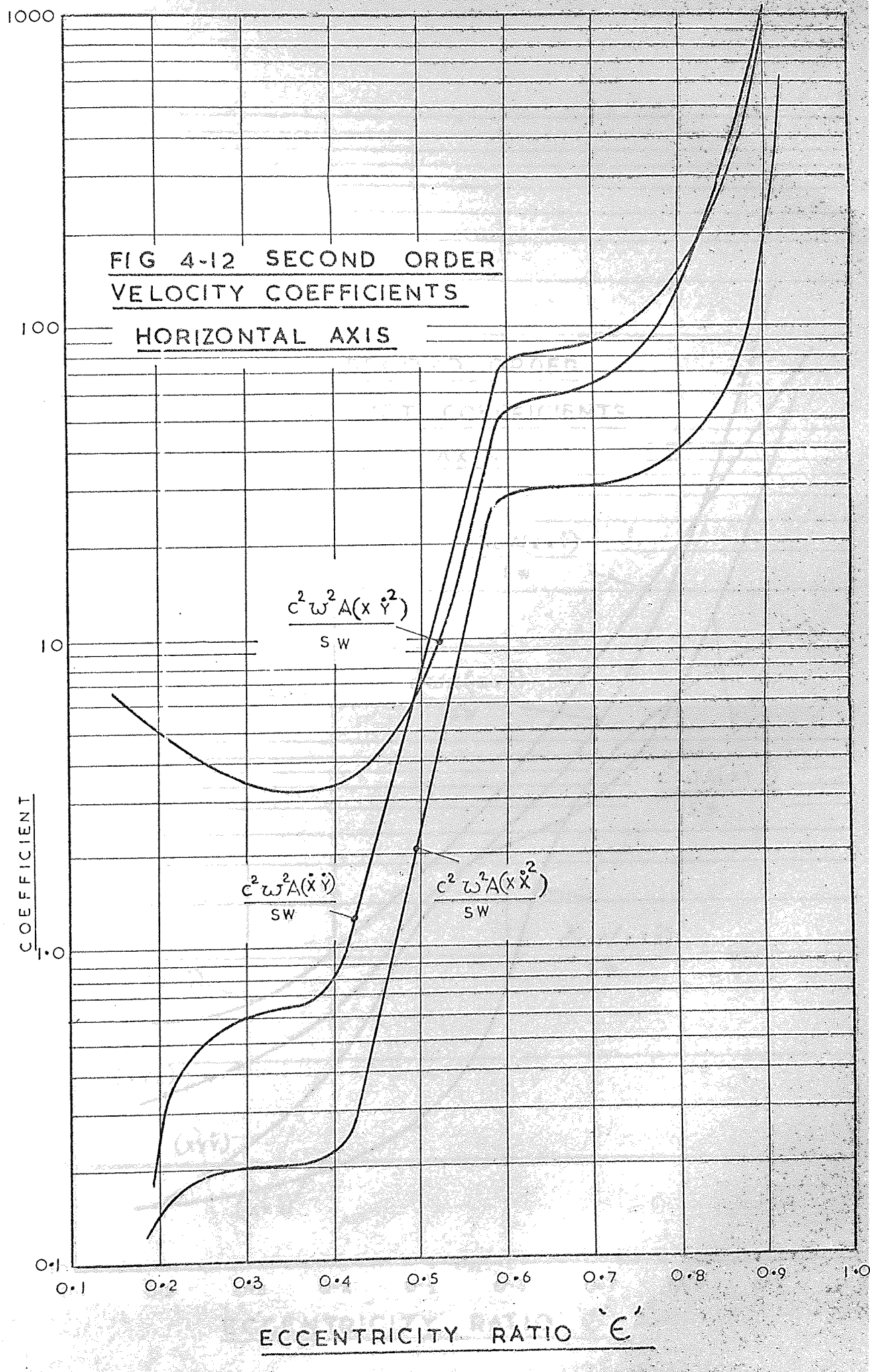

FIG 4-12 SECOND ORDER VELOCITY COEFFICIENTS HORIZONTAL AXIS

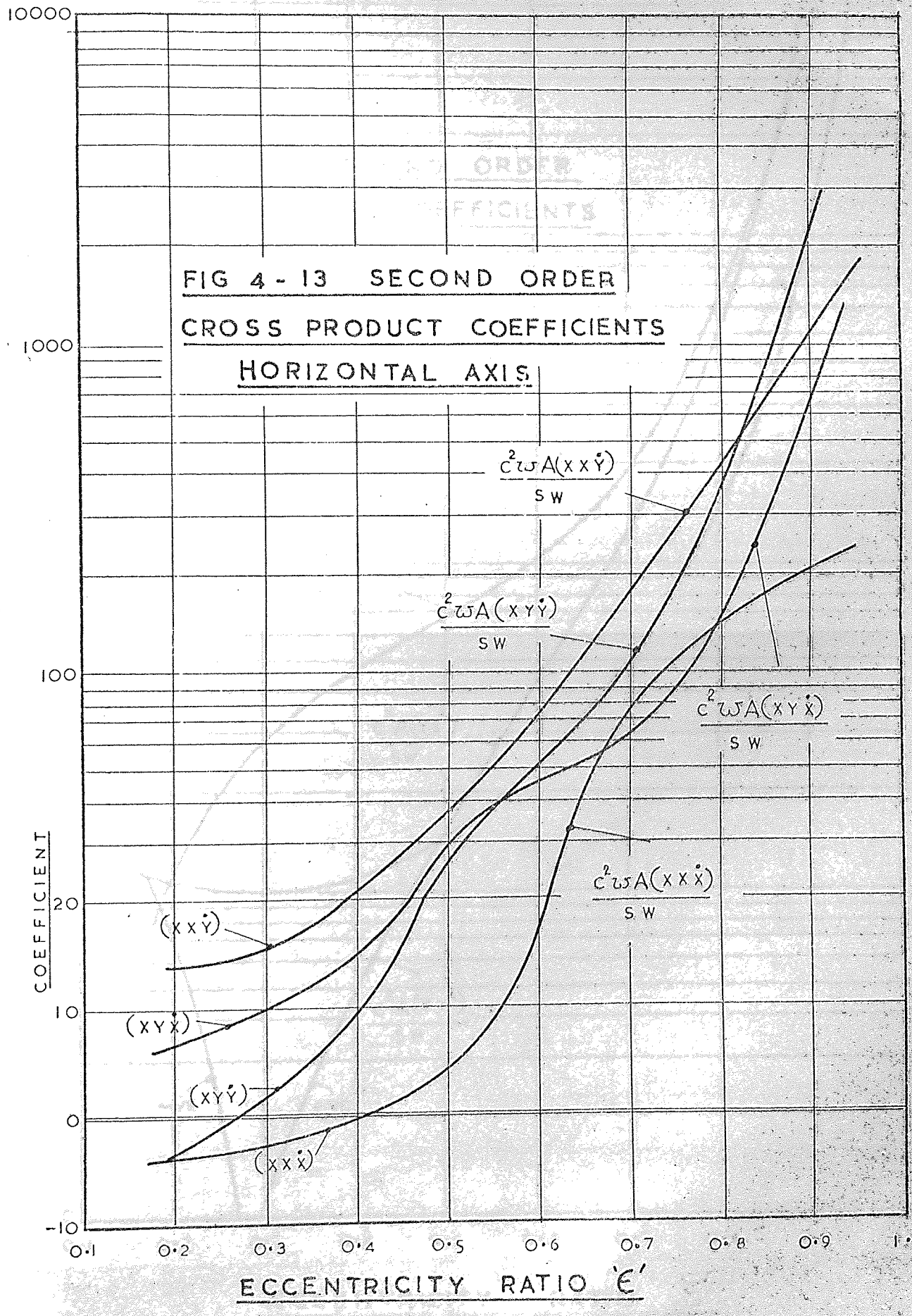

FIG 4 - 13 SECOND ORDER CROSS PRODUCT COEFFICIENTS HORIZONTAL AXIS

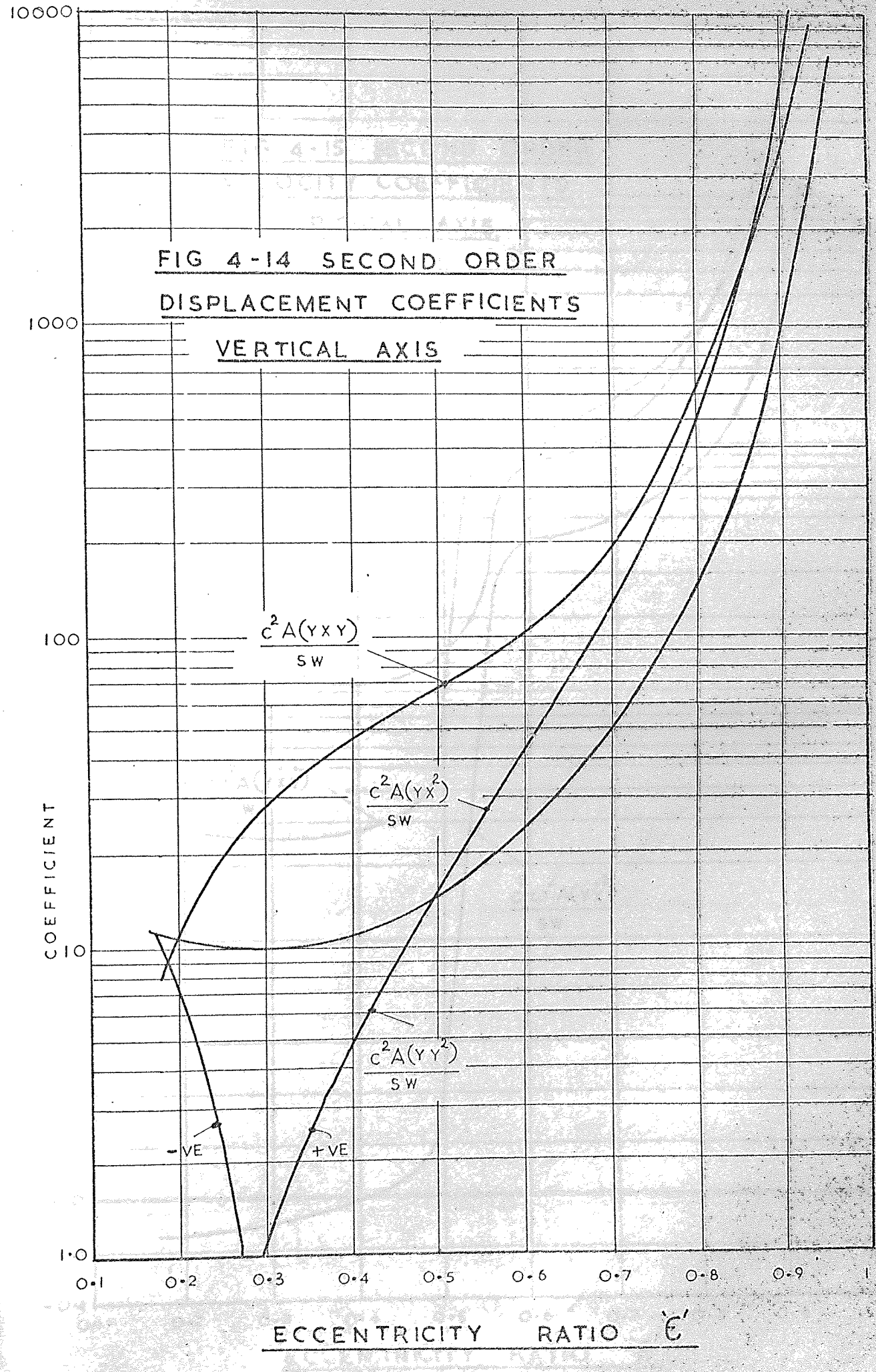

FIG 4-14 SECOND ORDER DISPLACEMENT COEFFICIENTS VERTICAL AXIS

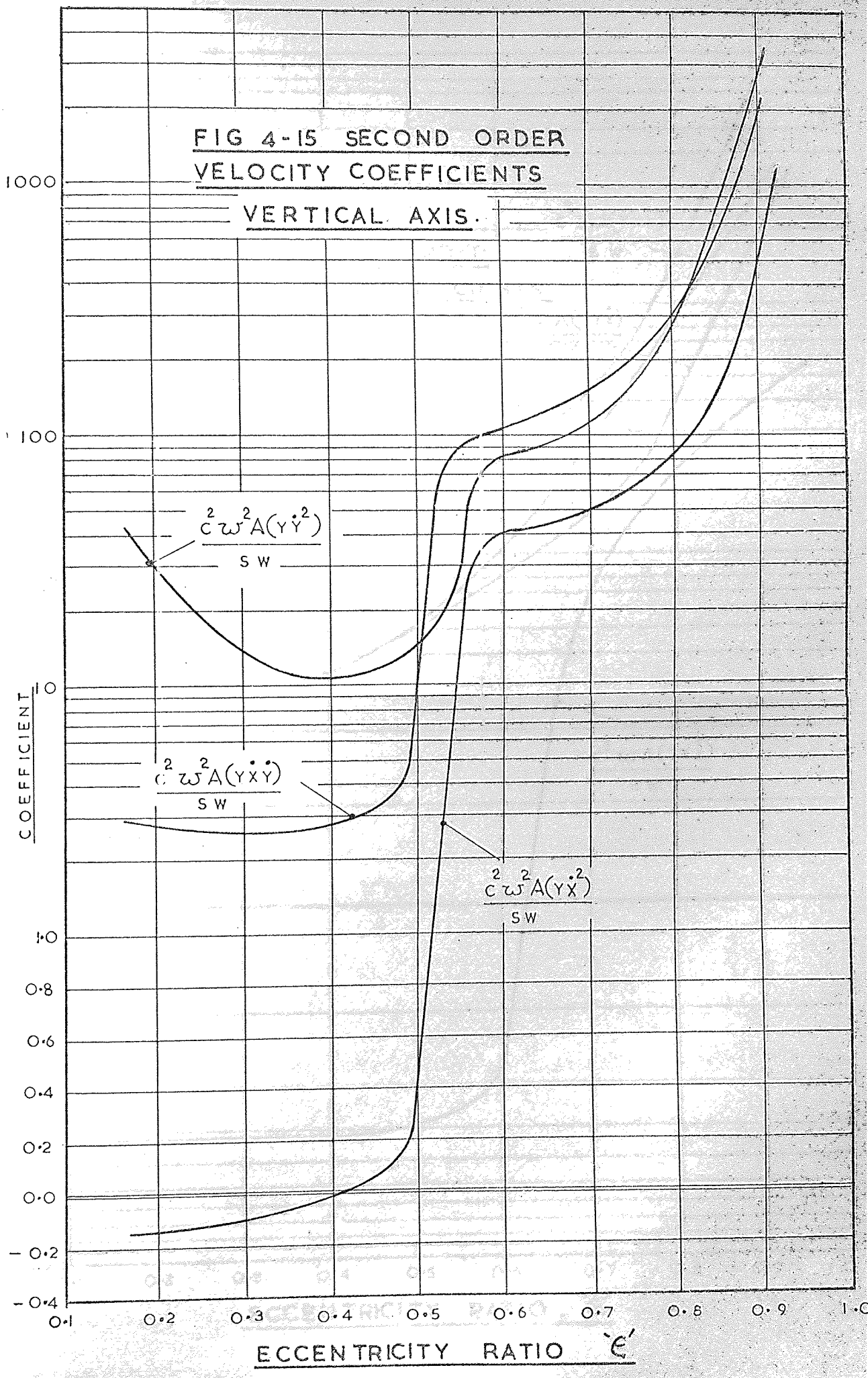
FIG 4-15 SECOND ORDER VELOCITY COEFFICIENTS
VERTICAL AXIS.
1000
100
10
1·0
0·8
0·6
0·4
0·2
0·0
- 0·2
- 0·4
COEFFICIENT
$\frac{c^2\omega^2 A(Y\dot{Y}^2)}{SW}$
$\frac{c^2\omega^2 A(Y\dot{X}\dot{Y})}{SW}$
$\frac{c^2\omega^2 A(Y\dot{X}^2)}{SW}$
0·1
0·2
0·3
0·4
0·5
0·6
0·7
0·8
0·9
1·0
ECCENTRICITY RATIO ϵ

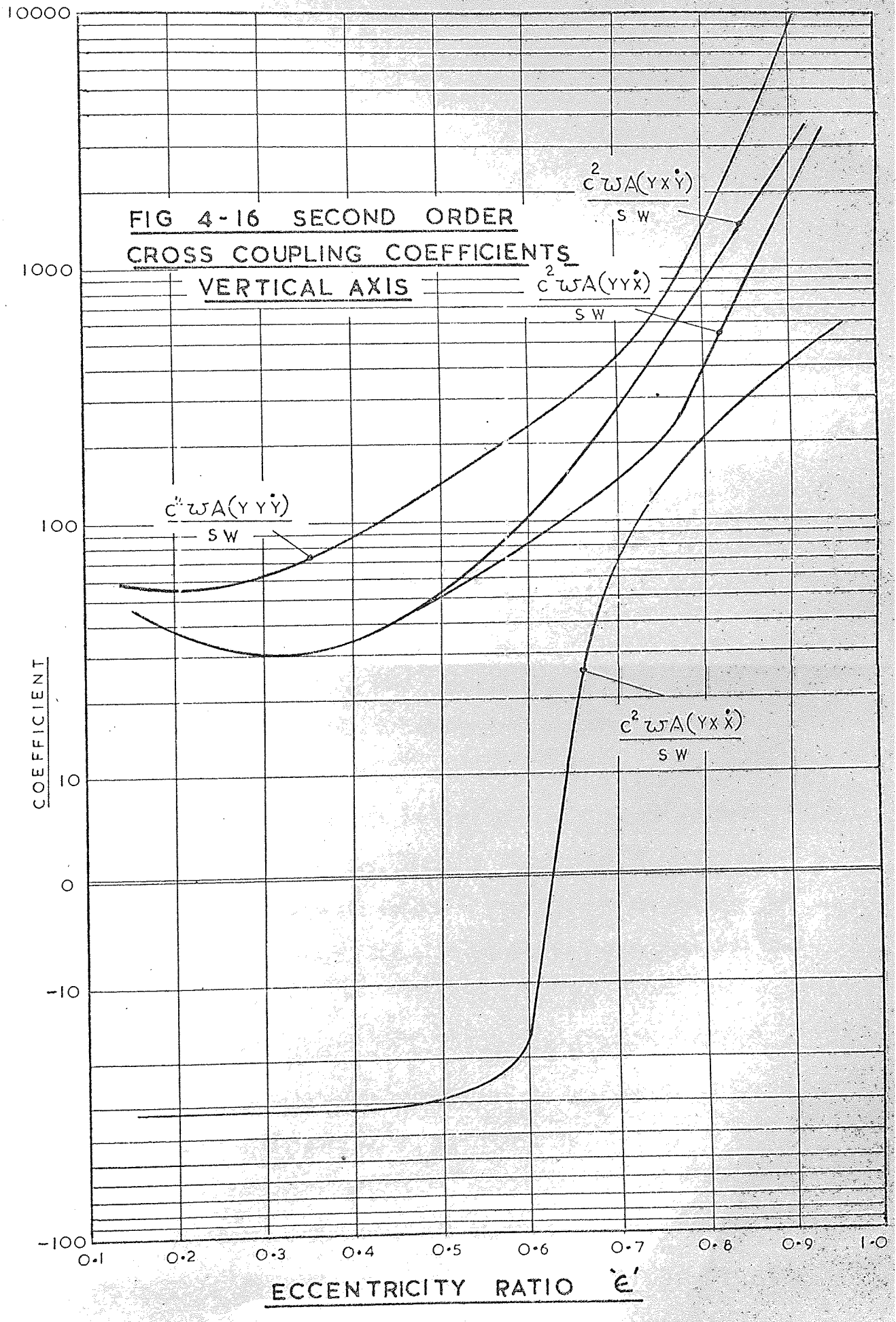

FIG 4-16 SECOND ORDER CROSS COUPLING COEFFICIENTS VERTICAL AXIS

CHAPTER FIVE

CHAPTER FIVE

SOLUTION TO LINEAR EQUATIONS OF MOTION

5.1 General equations of motion

Dynamic loading applied to bearings may vary in both magnitude and direction, in general they may be divided into four groups.

(I) Constant unidirectional load suddenly applied - as associated with shock.

(II) Variable unidirectional load - as experienced with equipment when experiencing repeated loading.

(III) Constant rotating load - unbalance, critical speed, instability.

(IV) Variable rotating load - as experienced with internal combustion engines or reciprocating compressors.

Through this thesis only Section (III) will be considered dealing exclusively with the vibration or whirling of shafts where the procession of the shaft centre is both forward and reverse to the rotation of the shaft, and also running at synchronous and non-synchronous speeds.

The oil film coefficients are highly non-linear for different running positions within the boundary of the bearing radial clearance however, the coefficients may be considered as being linear about a fixed steady state running position of the journal within the bush, i.e. ε_o ,ϕ_o provided the amplitudes of vibration are extremely small, thus limiting the second order non-linearities which are a function

of both amplitude and velocity. The system to be investigated is comprised of a journal i.e. shaft, oil film, bearing pedestal, and other supporting structure; the pedestal and its associated supporting structure may be considered as a single item having stiffness and damping properties, however, these dynamic properties are unknown and will only be included in the equations of motion as time dependent displacements together with phase of movement. The journal is considered as being rigid with its axis aligned with the axis of the bush, therefore the dynamical system may completely be described within a single plane as shown in figure (5.1).

The illustration in figure (5.2) shows the elliptical mode of free vibration being excited by a known out of balance force. The length OP represents the pedestal displacement, and point P is the steady running position ε_o, ϕ_o i.e. the position at which the journal centre would normally run without unbalance being present. It is understood that for this condition point P would coincide with point O. The length PJ is the actual displacement within the oil film wedge, having as its pole the steady state position ε_o, ϕ_o . The length JM is the radius of eccentricity of the out of balance mass m rotating with angular velocity Ω radians per second, whilst the journal may rotate about its centre of rotation J at ω radians per second, where ω need not be equal to Ω. U and V are the major and minor axis of the elliptical trajectory while x and y are the horizontal and vertical axes in which all the force coefficients discussed in the preceding sections are related. The basic assumptions made at this stage are:- (1) the journal traces an elliptical locus, and (2) the journal trajectory is closed for one complete vibrating cycle of the mass m, further all displacements are presented relative to the

bearing pedestal and all pedestal vibrations are absolute.

With these assumptions the equations of motion describing the dynamic characteristics may be expressed by eight invariant coefficients thus

$$\begin{aligned} \widehat{A(xx)}.x + \widehat{A(xy)}.y + \widehat{A(x\dot{x})}.\dot{x} + \widehat{A(x\dot{y})}.\dot{y} &= Fx \\ \widehat{A(yx)}.x + \widehat{A(yy)}.y + \widehat{A(y\dot{x})}.\dot{x} + \widehat{A(y\dot{y})}.\dot{y} &= Fy \end{aligned} \qquad (5.1)$$

where $\widehat{A(--)}$ are constant coefficients. The first letter in the closed brackets refers to the axis along which the force acts, and the second letter relates to either a displacement or velocity generating the oil film force.

Analytical expressions for the coefficients A(--) are given in Chapter Four, Section Seven, and specific values given in Appendix B. Although these coefficients have been computed together with the second order values, they do however remain unchanged if these second order terms are neglected, the remaining eight coefficients are referred to as being linear and are directly proportional to displacement, velocity and unbalance.

To check the validity of the theoretical coefficients must ultimately be from some form of correlation between the analytical results with those obtained from bearing tests or operational experiences. The method to be employed here is to compare the theoretical rotor whirl trajectory with the observed orbit. Also by considering measurements of amplitude and phase of movement in two co-ordinate directions for a known amount of unbalance for both forward and reverse directions of rotation, permits the determination of the eight oil film force coefficients.

5.2 Determination of journal whirl trajectory using eight oil film coefficients

Dealing first with theoretical predictions of the whirl orbit; for this condition the time dependent displacements have to be determined relative to the bearing bush, taking into account additional inertia forces of the test journal caused by pedestal movements.

Considering the dynamic force transmitted through the oil film, including pedestal vibrations are given by:-

$$Fx = m\Omega^2 r \sin \Omega t - M (\ddot{x} + \ddot{xp})$$
$$Fy = m\Omega^2 r \cos \Omega t - M (\ddot{y} + \ddot{yp})$$

thus the equations of motion become:-

$$M(\ddot{x} + \ddot{xp}) + \widehat{A(xx)}.x + \widehat{A(xy)}.y + \widehat{A(x\dot{x})}.\dot{x} + \widehat{A(x\dot{y})}.\dot{y} = m\Omega^2 r \cos\Omega t \quad (5.2)$$
$$M(\ddot{y} + \ddot{yp}) + \widehat{A(yx)}.x + \widehat{A(yy)}.y + \widehat{A(y\dot{x})}.\dot{x} + \widehat{A(y\dot{y})}.\dot{y} = m\Omega^2 r \cos\Omega t$$

Assuming Simple Harmonic Motion with respect to the bush, the displacements of the journal may be given as

$$x = X \sin (\Omega t - \alpha_1) \quad (4.3A)$$
$$y = Y \cos (\Omega t - \alpha_2)$$

Assuming Simple Harmonic Motion for the pedestal with respect to space, displacements for the pedestal may be given as

$$xp = Xp \sin (\Omega t - \alpha_1) \quad (5.3B)$$
$$yp = Yp \cos (\Omega t - \alpha_2)$$

Differentiating equations (5.3A) and (5.3B) and substituting into equation (5.2) and also considering two intervals of time i.e. $\Omega t = 0$ and $\Omega t = \pi/2$ gives four simultaneous equations which may be written in matrix form thus:-

$$\begin{bmatrix} (\widehat{A(xx)} - M\Omega^2) & \widehat{A(xy)} & \widehat{\Omega A(x\dot{x})} & \widehat{\Omega A(x\dot{y})} \\ -\widehat{A(yx)} & (\widehat{A(yy)} - M\Omega^2) & \widehat{\Omega A(y\dot{x})} & \widehat{\Omega A(y\dot{y})} \\ \widehat{\Omega A(x\dot{x})} & -\widehat{\Omega A(x\dot{y})} & (\widehat{A(xx)} - M\Omega^2) & \widehat{A(xy)} \\ \widehat{\Omega A(y\dot{x})} & -\widehat{\Omega A(y\dot{y})} & \widehat{A(yx)} & (\widehat{A(yy)} - M\Omega^2) \end{bmatrix}$$

$$X \begin{bmatrix} X \sin \alpha_1 \\ Y \cos \alpha_2 \\ X \cos \alpha_1 \\ Y \sin \alpha_2 \end{bmatrix} = \begin{bmatrix} 0 - M\Omega^2 Xp \sin \alpha_1 \\ m\omega^2 r + M\Omega^2 Yp \cos \alpha_2 \\ m\omega^2 r + M\Omega^2 Xp \cos \alpha_1 \\ 0 + M\Omega^2 Yp \sin \alpha_2 \end{bmatrix} \qquad (5.4)$$

which may be written as

$$[A][B] = [C]$$

$$[A]^{-1}[A][B] = [A]^{-1}[C]$$

But $$[A][A]^{-1} = [A]^{-1}[A] = [I]$$

$$[I][B] = [C][A]^{-1}$$

$$[B] = [C][A]^{-1}$$

where [A] = Coefficient matrix

[B] = Displacement matrix

[C] = Force matrix

$[A]^{-1}$ = Inverse matrix

[I] = Unit matrix

Hence by finding the inverse of the coefficient matrix it is possible to determine the displacement describing the whirl trajectory for a given unbalance. Upon determining the elements of the displacement matrix [B] we have that

$$X\sin\alpha_1 = (a);\ y\cos\alpha_2 = (b);\ X\cos\alpha_1 = (c);\ Y\sin\alpha_2 = (d)$$

$$\text{Hence}\quad \tan^{-1}\alpha_1 = \frac{(a)}{(c)} \quad \text{and} \quad \tan^{-1}\alpha_2 = \frac{(d)}{(b)}$$

$$\text{Also}\quad X = \sqrt{(a)^2 + (c)^2} \quad \text{and} \quad Y = \sqrt{(b)^2 + (d)^2}$$

The above was programmed on a Honywell H 1648 computer via a remote terminal using Fortran 4 language. The program listing is not shown, as greater part involves the inversion of a four by four matrix.

The coefficient matrix clearly demonstrates how the mass of the journal can effect the orbital response of the whirl trajectory, as also can the rotational frequency. For example, if the value of $M\Omega^2$ approached the value of A(xx) the vibrating whirl trajectory would become large along the major axis, depending upon the amount of damping present within the oil film wedge, as compared with the whirl trajectory where the value of $M\Omega^2$ is small. This phenomenon is discussed in greater detail in later sections.

5.3 Experimental methods for the determination of the eight oil film force coefficients

It is evident from the matrix (5.4) that to obtain all eight oil film coefficients a further four equations are required. Neither changes made to the magnitude of the out of balance 'm' or changes

made to the rotational frequency of the journal can be used. To change the value of the out of balance mass would produce a corresponding change in the journal whirl orbit, further as these equations specify very small deflections compared to the oil film thickness, which is difficult to obtain in practice, it is quite probable that averaged coefficients are in fact being measured due to the presence of non-linearities, therefore changes made to the vibration amplitude would unwittingly produce unknown changes in the stiffness and damping co-efficients.

To change the journal rotational frequency would most certainly affect the oil film characteristics because of influencing the Sommerfeld duty parameter, therefore it would be highly undesirable to change the journal speed in an attempt to obtain eight homogeneous simultaneous equations.

There are however several parameters which can be changed without affecting the dynamic characteristics. The first and most obvious would be to change the value of the journal mass M, however, this would only be acceptable if the value of the mass was small compared with the static weight applied to the test journal, further any change made to the journal mass must be substantially different for each group of experiments, in order to obtain distinct changes in the whirl trajectory relative to the direction of the force vector. Experimental equipment which could make such changes to the journal mass whilst still rotating as not to upset the duty parameter, would be complex.

Another method that could be employed whereby the eight invariant coefficients could be obtained, would be to introduce varying flexibility into the bearing supporting structure, thus allowing

changes to be made to the values of Xp and Yp of the matrix (5.4), this would allow changes to be made to the whirl orbit without affecting the oil film wedge, however changes made to the whirl orbit would have to be sufficiently large in order to reduce experimental error.

The last and most effective method would be to change the excitation frequency, however, in order to keep the amplitude of the journal trajectory the same, corresponding changes would have to be made to the value of the unbalanced mass, such a problem is overcome if the vibrational frequency was kept constant but reversed in rotation, this latter method is used throughout the theoretical and experimental analysis presented in this thesis. Electing then to reverse the direction of the rotating out of balance disturbing force, the dynamic forces transmitted through the oil film are

$$Fx = m\Omega^2 r \sin(-\Omega t) - M(\ddot{x} + \ddot{x}_p)$$
$$Fy = m\Omega^2 r \cos(-\Omega t) - M(\ddot{y} + \ddot{y}_p) \qquad (5.5)$$

The motion of the journal displacement, again assuming Simple Harmonic Motion, may be written as

$$x = X \sin(-\Omega t - \alpha_1)$$
$$y = Y \cos(-\Omega t - \alpha_2) \qquad (5.6A)$$

$$xp = Xp \sin(-\Omega t - \gamma_1)$$
$$yp = Yp \cos(-\Omega t - \gamma_2) \qquad (5.6B)$$

It was known beforehand that under reverse whirl conditions the journal trajectory moves in the same direction as the journal rotation,

therefore equations (5.3A) and (5.3B) could have been used which would help in simplifying the resulting matrix, however, the writer believes that the natural assumption would be to use equations (5.6A) and (5.6B) as well as equations (5.5), the final results will of course be the same.

Using the force equations (5.5) together with the displacement equations (5.6A) and (5.6B) with their appropriate derivations the following matrix is obtained - see next page

$$
\begin{bmatrix}
-X\sin\alpha_1 & Y\cos\alpha_2 & \Omega X\cos\alpha_1 & \Omega Y\sin\alpha_2 & 0 & 0 & 0 & 0 \\
X\cos\alpha_1 & Y\sin\alpha_2 & \Omega X\sin\alpha_1 & -\Omega Y\cos\alpha_2 & 0 & 0 & 0 & 0 \\
0 & 0 & 0 & 0 & -X\sin\alpha_1 & Y\cos\alpha_2 & \Omega X\cos\alpha_1 & \Omega Y\sin\alpha_2 \\
0 & 0 & 0 & 0 & X\cos\alpha_1 & Y\sin\alpha_2 & \Omega X\sin\alpha_1 & -\Omega Y\cos\alpha_2 \\
-X\sin\alpha_1 & Y\cos\alpha_2 & -\Omega X\cos\alpha_1 & -\Omega Y\sin\alpha_2 & 0 & 0 & 0 & 0 \\
-X\cos\alpha_1 & -Y\sin\alpha_2 & \Omega X\sin\alpha_1 & -Y\cos\alpha_2 & 0 & 0 & 0 & 0 \\
0 & 0 & 0 & 0 & -X\sin\alpha_1 & Y\cos\alpha_2 & -\Omega X\cos\alpha_1 & -\Omega Y\sin\alpha_2 \\
0 & 0 & 0 & 0 & -X\cos\alpha_1 & -Y\sin\alpha_2 & \Omega X\sin\alpha_1 & -\Omega Y\cos\alpha_2
\end{bmatrix}
$$

$$
X \begin{bmatrix}
\widehat{A(xx)} \\
\widehat{A(xy)} \\
\widehat{A(x\dot{x})} \\
\widehat{A(x\dot{y})} \\
\widehat{A(yx)} \\
\widehat{A(yy)} \\
\widehat{A(y\dot{x})} \\
\widehat{A(y\dot{y})}
\end{bmatrix}
=
\begin{bmatrix}
0 - M\Omega^2(X\sin\alpha_1 + X_p\sin\gamma_1) \\
m\Omega^2 r + M\Omega^2(Y\cos\alpha_2 + Y_p\cos\gamma_2) \\
m\Omega^2 r + M\Omega^2(X\cos\alpha_1 + X_p\cos\gamma_1) \\
0 + M\Omega^2(Y\sin\alpha_2 + Y_p\sin\gamma_2) \\
0 - M\Omega^2(X\sin\alpha_1 + X_p\sin\gamma_1) \\
-m\Omega^2 r - M\Omega^2(Y\cos\alpha_2 + Y_p\cos\gamma_2) \\
m\Omega^2 r + M\Omega^2(X\cos\alpha_1 + X_p\cos\gamma_1) \\
0 - M\Omega^2(Y\sin\alpha_2 + Y_p\sin\gamma_2)
\end{bmatrix}
\qquad (5.7)
$$

The matrix (5.7) may be partitioned as follows:-

$$\begin{bmatrix} A & 0 \\ 0 & A' \\ B & 0 \\ 0 & B' \end{bmatrix} \times \begin{bmatrix} \text{COEFFICIENT} \\ \text{MATRIX} \end{bmatrix} = \begin{bmatrix} \text{FORCE} \\ \text{MATRIX} \end{bmatrix} \qquad (5.8)$$

where elements A are for forward whirl

and elements B are for reverse whirl

It is now possible to obtain values of the eight invariant oil film coefficients by inverting an 8 x 8 matrix, however, when examining the matrix (5.7) it can be seen that this matrix may be partitioned by constructing a 4 x 4 matrix for the elements A and B, thus solving the coefficients along the x axis and constructing another 4 x 4 matrix for the elements A' and B' giving values for the coefficients acting along the y axis.

Clearly, unless the elements for the displacement matrix can be measured with precise accuracy the computed coefficients may fail to give satisfactory results, as indeed may be the case where non-linearities are dominate. Further, problems of ill-conditioning of equation (5.7) may give poor results, whereby necessitating in having to provide a large number of experimental results in order to obtain averaged values.

5.4 The determination of Hagg and Sankey type of coefficients from synchronous whirl vibrations

As an approximate representation, the eight oil film coefficients may be expressed in terms of four coefficients as presented by Hagg and Sankey, these latter coefficients will only

represent the orbital response for synchronous unbalance where only four independent displacements are available, further, the four computed coefficicients will only be capable of representing the dynamic response characteristics for explicit operating conditions. Unlike the equations of motion having eight invariant coefficients the equations of motion for Hagg and Sankey type of oil film coefficients are expressed along the major and minor axes of the resulting elliptical whirl orbit, these axes will of course change in angular position depending upon the particular operating conditions prevailing at the time.

As Hagg and Sankey force coefficients do not have any cross coupling terms the equations of motion may be presented as shown below, when equating forces along the Major and Minor axes respecrively.

$$M(\ddot{u} + \ddot{up}) + K(u)u + C(u)\dot{u} = m\Omega^2 r \sin(\Omega t - \xi)$$
$$M(\ddot{v} + \ddot{vp}) + K(v)v + C(v)\dot{v} = m\Omega^2 r \cos(\Omega t - \xi) \qquad (5.9)$$

Assuming S.H.M. with respect to the bearing bush, the displacements of the journal may be given as:-

$$u = u_o \sin(\Omega t - \alpha_1)$$
$$v = v_o \cos(\Omega t - \alpha_2) \qquad (5.10A)$$

Assuming S.H.M. for the pedestal with respect to space, the pedestal displacements may be given as:-

$$u_p = u_{op} \sin(\Omega t - \gamma_1)$$
$$v_p = v_{op} \cos(\Omega t - \gamma_2) \qquad (5.10B)$$

Differentiating equations (5.10A) and (5.10B) and substituting into equation (5.9) and also considering two intervals of time $\Omega t = 0$ and $\Omega t = \pi/2$ gives for simultaneous equations which may be written in matrix form thus:-

$$\begin{bmatrix} -u_o \sin\alpha_1 & \Omega u_o \cos\alpha_1 & 0 & 0 \\ 0 & 0 & v_o \cos\alpha_2 & \Omega v_o \sin\alpha_2 \\ u_o \cos\alpha_1 & \Omega u_o \sin\alpha_1 & 0 & 0 \\ 0 & 0 & v_o \sin\alpha_2 & -\Omega v_o \cos\alpha_2 \end{bmatrix} X \begin{bmatrix} K(u) \\ C(u) \\ K(v) \\ C(v) \end{bmatrix}$$

$$= \begin{bmatrix} -m\Omega^2 r \sin\zeta - M\Omega^2(u_o \sin\alpha_1 + u_{op} \sin\gamma_1) = F_1 \\ m\Omega^2 r \cos\zeta + M\Omega^2(v_o \cos\alpha_2 + v_{op} \cos\gamma_2) = F_2 \\ m\Omega^2 r \cos\zeta + M\Omega^2(u_o \cos\alpha_1 + u_{op} \cos\gamma_1) = F_3 \\ m\Omega^2 r \sin\zeta + M\Omega^2(v_o \sin\alpha_2 + v_{op} \sin\gamma_2) = F_4 \end{bmatrix} \qquad (5.11)$$

Using Cramers rule (K(u), K(v), C(u), C(v) may be evaluated in the following manner

$$\nabla = \begin{vmatrix} -u_o \sin\alpha_1 & \Omega u_o \cos\alpha_1 & 0 & 0 \\ 0 & 0 & v_o \cos\alpha_1 & \Omega v_o \sin\alpha_2 \\ u_o \cos\alpha_1 & \Omega u_o \sin\alpha_1 & 0 & 0 \\ 0 & 0 & v_o \sin\alpha_2 & -\Omega v_o \cos\alpha_2 \end{vmatrix}$$

$$K_u = \begin{vmatrix} F_1 & \Omega u_o \cos\alpha_1 & 0 & 0 \\ F_2 & 0 & v_o \cos\alpha_2 & \Omega v_o \sin\alpha_2 \\ F_3 & \Omega u_o \sin\alpha_1 & 0 & 0 \\ F & 0 & v_o \sin\alpha_2 & -\Omega v_o \cos\alpha_2 \end{vmatrix} \Big/ \nabla$$

giving $$Ku = -\frac{F_1 \sin \alpha_1}{u_o} + \frac{F_3 \cos \alpha_1}{u_o}$$

similarly $$Kv = \frac{F_2 \cos \alpha_2}{v_o} + \frac{F_4 \sin \alpha_2}{v_o}$$

$$Cu = \frac{F_3 \sin \alpha_1}{\Omega u_o} + \frac{F_1 \cos \alpha_1}{\Omega u_o}$$

$$Cv = \frac{F_2 \sin \alpha_2}{\Omega v_o} + \frac{F_4 \cos \alpha_2}{\Omega v_o}$$

substituting the above equations their respective forces gives

$$Ku = \frac{m\Omega^2 r}{u_o} \cos (\alpha_1 - \xi) + M\Omega^2 (1 + \frac{u_{cp}}{u_o} \cos (\alpha_1 - \gamma_1))$$

$$Kv = \frac{m\Omega^2 r}{v_o} \cos (\alpha_2 - \xi) + M\Omega^2 (1 + \frac{v_{op}}{v_o} \cos (\alpha_2 - \gamma_2)) \qquad (5.12)$$

$$Cu = \frac{m\Omega r}{u_o} \sin (\alpha_1 - \xi) + M\Omega (\frac{u_{op}}{u_o} \sin (\alpha_1 - \gamma_2))$$

$$Cv = \frac{m\Omega r}{v_o} \sin (\alpha_2 - \xi) + M\Omega (\frac{v_{op}}{v_o} \sin (\alpha_2 - \gamma_2))$$

If in the above equations the pedestal displacements are made zero, the resulting equations would be identical to those given by Hagg and Sankey(29).

The oil film elastic and damping properties may thus be determined from measurements of amplitude and phase in the two co-ordinate directions, measured from both the vibrating journal and

bearing pedestal, for a known out of balance force. Because of their simplicity Hagg and Sankey are often used to represent the dynamic behaviour of journal bearings presenting like for like conditions. Equations governing the whirl trajectory for a given out of balance are not given here as they are of limited value, however the interested reader may easily determine them from equations (5.11) again using Cramers rule or by using a matrix inversion for specific operating conditions.

ω = ROTATIONAL FREQUENCY OF JOURNAL

Ω = ROTATIONAL FREQUENCY OF UNBALANCE

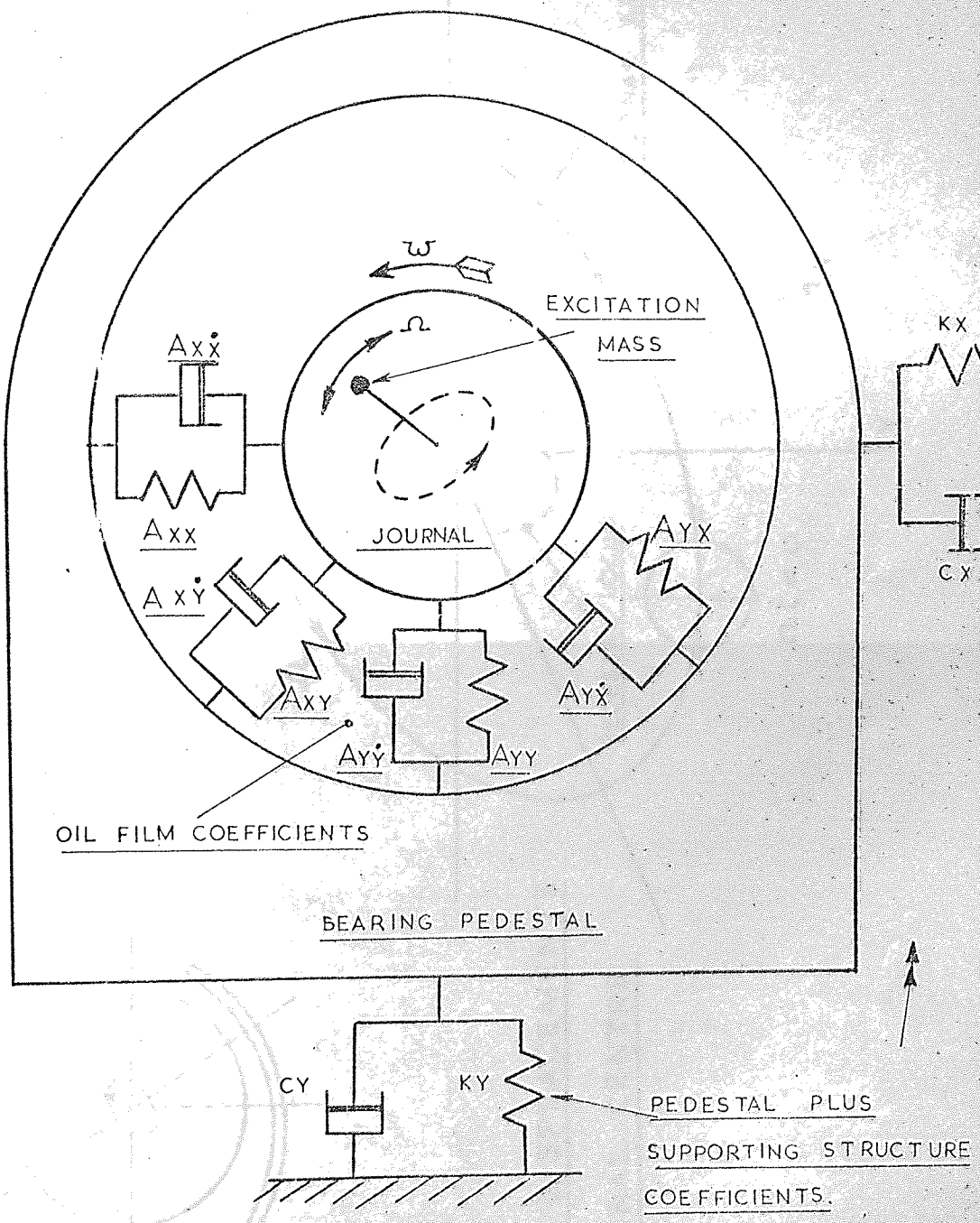

FIG 5-1 OIL FILM - PEDESTAL SYSTEM

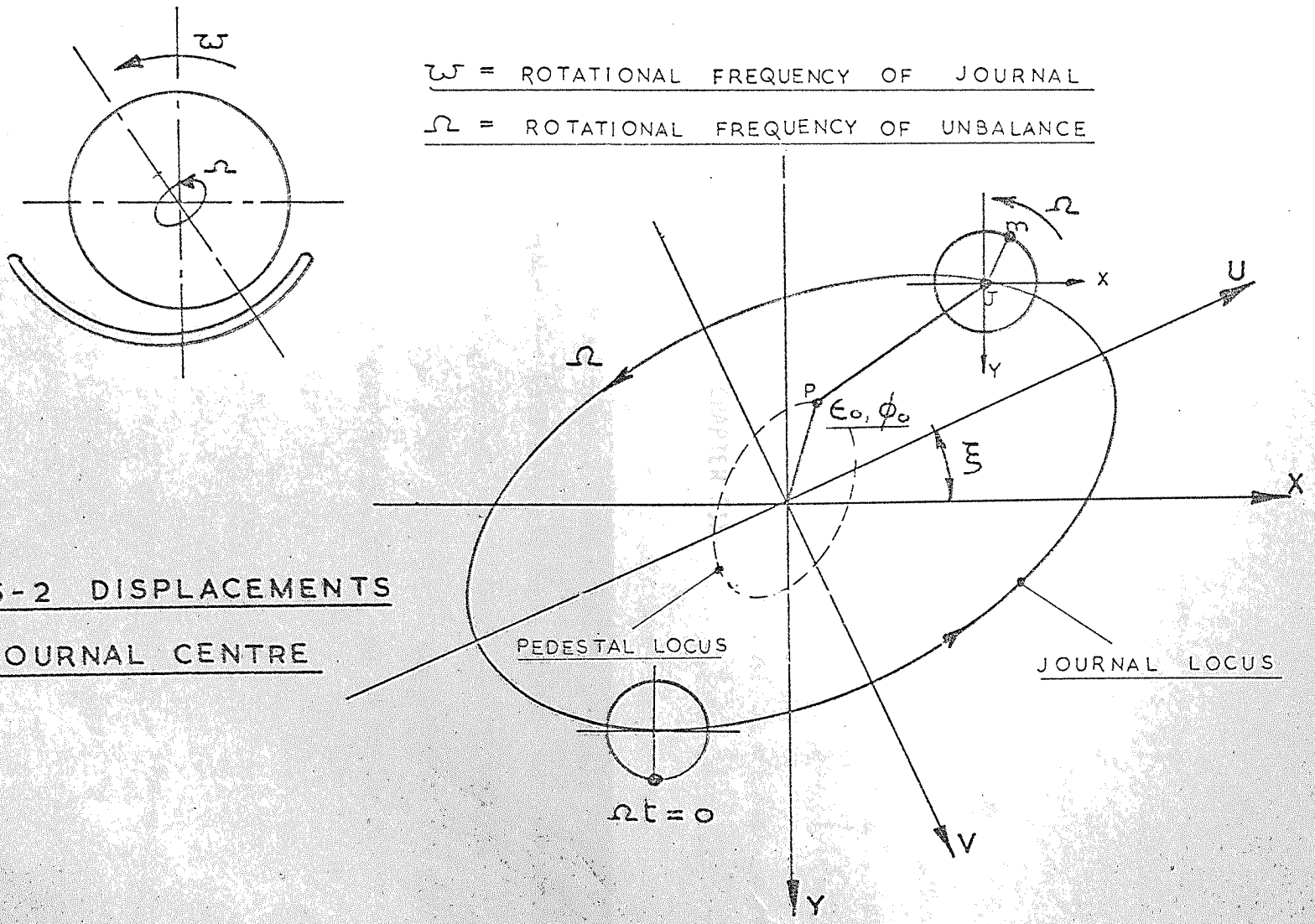

FIG 5-2 DISPLACEMENTS OF JOURNAL CENTRE

CHAPTER SIX

CHAPTER SIX

SOLUTION TO NON-LINEAR EQUATIONS OF MOTION

6.1 General equations of motion

Equations presented in Chapter Five, Section Two, for predicting the orbital response using only eight oil film coefficients, would clearly be in quantitative error if the oil film characteristics were predominantly non-linear, a better assessment of the journal trajectory would be to consider an extension of Taylor's series which the foregoing theory has been based, such an extension includes the second order terms and their associated cross coupling products of displacement and velocity. Including all these second order terms etc. into the equations of motion results in fourteen coefficients describing the film forces along the x axis, and a further fourteen along the y axis, such equations may be written as follows:-

Forces acting along the x axis

$$\begin{aligned} & M(\ddot{x} + \ddot{x}_p) + \widehat{A(xx)}x + \widehat{A(xy)}y + \widehat{A(x\dot{x})}\dot{x} + \widehat{A(x\dot{y})}\dot{y} + \widehat{A(xx^2)}x^2 \\ & + \widehat{A(xy^2)}y^2 + \widehat{A(xxy)}xy + \widehat{A(x\dot{x}^2)}\dot{x}^2 + \widehat{A(x\dot{y}^2)}\dot{y}^2 + \widehat{A(x\dot{x}\dot{y})}\dot{x}\dot{y} \\ & + \widehat{A(xx\dot{x})}x\dot{x} + \widehat{A(xx\dot{y})}x\dot{y} + \widehat{A(xy\dot{y})}y\dot{y} + \widehat{A(xy\dot{x})}y\dot{x} \\ & = M\Omega^2 r \sin \Omega t \end{aligned} \qquad (6.1A)$$

Forces acting along the y axis

$$M(\ddot{y} + \dot{y}p) + \widehat{A(yx)}x + \widehat{A(yy)}y + \widehat{A(y\dot{x})}\dot{x} + \widehat{A(y\dot{y})}\dot{y} + \widehat{A(yx^2)}x^2 + \widehat{A(yy^2)}y^2 + \widehat{A(yxy)}xy + \widehat{A(y\dot{x}^2)}\dot{x}^2 + \widehat{A(y\dot{y}^2)}\dot{y}^2 + \widehat{A(y\dot{x}\dot{y})}\dot{x}\dot{y} + \widehat{A(yx\dot{x})}x\dot{x} + \widehat{A(yx\dot{y})}x\dot{y} + \widehat{A(yy\dot{y})}y\dot{y} + \widehat{A(yy\dot{x})}y\dot{x} = M\Omega^2 r \cos \Omega t \qquad (6.1B)$$

The magnitude of the coefficients depend upon the running position of the journal relative to the bearing bush, and hence are a function of ε_o, τ and ψ. Design charts listing these coefficients in non-dimensional form are provided in Appendix B for ε = 0.2 to 0.9 and for varying amounts of misalignment confined to the vertical plane i.e. ψ = 0.

As linearisation is not a condition to be enforced when taking into account the twentyeight coefficients, the displacements of the journal trajectory need not necessarily be small, further all conditions of vibration may be considered, for example, high or low frequency of excitation at both synchronous and non-synchronous speed to the journal rotation.

6.2 The determination of the non-linear whirl trajectory using an "Analogue Simulation"

Equations (6.1A) and (6.1B) cannot be solved using direct methods whereby a solution may be obtained within a predetermined and finite number of computational steps. Available methods for solving these non-linear equations are limited and many of the few that are available become prohibitive when complying to the fundamental requirement, whichever technique is finally adopted must ensure adequate accuracy of solution without unnecessary computation, remembering

that this work is primarily intended for design engineers who usually do not have the time and perhaps the ability to involve themselves with higher mathematics.

After consultation with several mathematicians dealing in computer science, it was finally decided to investigate two methods which are relatively simple to manipulate. The first method was to simulate the configuration of an analogue computer using a digital computer. Two techniques are generally available for achieving this, the first is SLANG which was finally developed by Hawker Siddeley Dynamics and the second method considered was PARTNER i.e. Proof of analogue Results through Numerical Equivalent Routine" which was developed by the Magnet Computer Bureau Ltd., both of these methods are basically the same except for the integrating network which consists of a modified Runge-Kutta method.

The structure of the problem suitable for programming on SLANG or PARTNER consists mainly of a set of simultaneous ordinary differential equations of the form

$$x = f(x,t) \text{ where } x = \int_0^t \dot{x}\,dt + x$$

For such a problem all the integrated variables x must have an initial value x_o, these together with the other computed constants in the equations, are arranged on the right hand side, thus when solving equations (6.1A) we have that

$$\ddot{x} = f(\dot{x},x,t)$$

giving

$$\ddot{x} = (M\Omega^2 r \sin \Omega t - \widehat{A(xx)}x - \widehat{A(xy)}y \ldots\ldots \widehat{A(xy\dot{x})}y\dot{x}) \frac{1}{M}$$

and (6.2)

$$\ddot{y} = (M\Omega^2 r \cos \Omega t - \widehat{A(yx)}x - \widehat{A(yy)}y \ldots\ldots \widehat{A(yy\dot{x})}y\dot{x}) \frac{1}{M}$$

By assigning initial values to $\dot{x}$, x and $\dot{y}$,y (usually zero), together with an integrating time interval t the program proceeded to integrate the function $\ddot{x}$ thus obtaining a value for $\dot{x}$. Substituting this new found value into the original equation and integrating again, a value of x is found. Having now found values of x and $\dot{x}$ these values were substituted into the second equation describing forces acting along the y axis, and upon integrating twice values of $\dot{y}$ and y were thus obtained. This process was continued until the equations of motion were satisfied for the selected time interval. The problem here was that the full out of balance excitation force was suddenly applied, thus the problem to be solved could be likened to a transient step input, requiring extremely small intervals of time proving to be most uneconomical. A modification was later introduced to improve the computing time whereby the out of balance force was slowly applied as a "ramp input" which reached the required amplitude of force after one complete vibrationary cycle. Although this latter method was an improvement in reducing the total computing time, an investigation into one running condition took well over half an hour. It was therefore decided that only one condition of a vibrating journal would be investigated by using SLANG, and that condition would be where it was considered that non-linearities would be predominate. Figure (6.1) shows a plot of the results

demonstrating that no sub or super harmonics were present and that non-linearity had the overall effect of suppressing the whirl trajectory compared to the solution where only the linear terms were considered. The whirl orbit (1) of figure (6.1) shows results obtained by using SLANG, the orbit was not quite symmetrical either side of the major axis, suggesting that further computing time was required in order to overcome the slight amount of residual transient, or the integrating step length was too large. However because of the high cost involved further studies were not considered in view of the closeness of curve (2). The whirl orbit (2) presents results assuming the solutions to equations (6.1A) and (6.1B) may be obtained by assuming the motion of the journal about a fixed axis obeys simple harmonic motion, details of the theoretical assumptions and computational methods will be discussed in Section (6.3).

The whirl trajectories (1) and (2) do illustrate that there is little difference between these results, slight error perhaps being present in the orbit (1), indeed it could be said that the one checks the validity of the other and any physical difference being that orbit (2) is far more easily obtained and presents a method acceptable for analysing the volume of experimental results with good accuracy, remembering that the analogue simulation of the non-linear is mathematically correct thus providing a sound foundation on which solutions of orbit (2) are to be based.

The whirl trajectory (3) of figure (6.1) demonstrates the solution of the equations of motion considering the linear terms only, the trajectory obtained clearly illustrates the degree of error involved, if the oil film characteristics do not have the second order coefficients.

Further, the vibration amplitude of 0.001 in (25 μmm) is a realistic representation of amplitudes experienced by real rotors, and would be considered as smooth running with due consideration being given to the impedance of the bearing supporting structure.

6.3 Solution of the non-linear equations of motion using a modified Newton-Raphson method

In order to solve the equations (6.1A) and (6.1B) the solution was assumed to be predominantly of the first order, as suggested from the whirl trajectory obtained from the analogue simulation, therefore the journal motion along the x and y axes with respect to the bearing bush can be assumed to be behaving with Simple Harmonic Motion hence:

$$x = X \sin (\Omega t - \alpha_1)$$
$$y = Y \cos (\Omega t - \alpha_2) \qquad (6.3A)$$

and the pedestal displacements also assumed to be S.H.M. relative to space

$$xp = Xp \sin (\Omega t - \gamma_1)$$
$$yp = Yp \cos (\Omega t - \gamma_2) \qquad (6.3B)$$

Differentiating the above equations and finding their respective squares and cross products, in addition to considering two intervals of time $\Omega t = 0$ and $\Omega t = \pi/2$ gives four non-linear simultaneous equations which may be written:-

$$M\Omega^2 Xp \sin\gamma_1 = [\widehat{A(xx)} - M\Omega^2]X \sin\alpha_1 - \widehat{A(xy)}Y \cos\alpha_2 - \widehat{A(x\dot{x})}\Omega X \cos\alpha_1 - \widehat{A(x\dot{y})}\Omega Y \sin\alpha_2$$

$$- \widehat{A(xx^2)}X^2 \sin^2\alpha_1 - \widehat{A(xy^2)}Y^2 \cos^2\alpha_2 + \widehat{A(xxy)}XY \sin\alpha_1 \cos\alpha_2 - \widehat{A(x\dot{x}^2)}\Omega^2X^2 \cos^2\alpha_1$$

$$- \widehat{A(x\dot{y}^2)}\Omega^2Y^2 \sin^2\alpha_2 - \widehat{A(x\dot{x}\dot{y})}\Omega^2XY \cos\alpha_1 \sin\alpha_2 + \widehat{A(xx\dot{x})}\Omega X^2 \cos\alpha_1 \sin\alpha_1 \qquad (6.4A)$$

$$+ \widehat{A(xx\dot{y})}\Omega XY \sin\alpha_1 \sin\alpha_2 - \widehat{A(xy\dot{y})}\Omega Y^2 \cos\alpha_2 \sin\alpha_2 - \widehat{A(xy\dot{x})}\Omega YX \cos\alpha_2 \cos\alpha_1$$

$$\overline{m}\Omega^2 r + M\Omega^2 Yp \cos\gamma_2 = -\widehat{A(yx)}X \sin\alpha_1 + [\widehat{A(yy)} - M\Omega^2]Y \cos\alpha_2 + \widehat{A(y\dot{x})}\Omega X \cos\alpha_1 + \widehat{A(y\dot{y})}\Omega Y \sin\alpha_2$$

$$+ \widehat{A(yx^2)}X^2 \sin^2\alpha_1 + \widehat{A(yy^2)}Y^2 \cos^2\alpha_2 + \widehat{A(yxy)}XY \sin\alpha_1 \cos\alpha_2 + \widehat{A(y\dot{x}^2)}\Omega^2X^2\cos^2\alpha_1$$

$$+ \widehat{A(y\dot{y}^2)}\Omega^2Y^2 \sin^2\alpha_2 + \widehat{A(y\dot{x}\dot{y})}\Omega^2XY \cos\alpha_1 \sin\alpha_2 - \widehat{A(yx\dot{x})}\Omega X^2 \cos\alpha_1 \sin\alpha_1 \qquad (6.4B)$$

$$- \widehat{A(yx\dot{y})}\Omega XY \sin\alpha_1 \sin\alpha_2 + \widehat{A(yy\dot{y})}\Omega Y^2 \cos\alpha_2 \sin\alpha_2 + \widehat{A(yy\dot{x})}\Omega YX \cos\alpha_2 \sin\alpha_1$$

$$m\Omega^2 r + M\Omega X p \cos\gamma_1 = \widehat{A(x\dot{x})}\Omega X \sin\alpha_1 - \widehat{A(x\dot{y})}\Omega Y \cos\alpha_2 + [\widehat{A(xx)} - M\Omega^2]X \cos\alpha_1 + \widehat{A(xy)}Y \sin\alpha_2$$

$$+ \widehat{A(x\dot{x}^2)}\Omega^2X^2 \sin^2\alpha_1 + \widehat{A(x\dot{y}^2)}\Omega^2Y^2 \cos^2\alpha_2 - \widehat{A(x\dot{x}\dot{y})}\Omega^2XY \sin\alpha_1 \cos\alpha_2 + \widehat{A(xx^2)}X^2 \cos^2\alpha_1$$

$$+ \widehat{A(xy^2)}Y^2 \sin^2\alpha_2 + \widehat{A(xxy)}XY \cos\alpha_1 \sin\alpha_2 + \widehat{A(xx\dot{x})}\Omega X^2 \cos\alpha_1 \sin\alpha_1 \qquad (6.4C)$$

$$+ \widehat{A(xy\dot{x})}\Omega XY \sin\alpha_1 \sin\alpha_2 - \widehat{A(xy\dot{y})}\Omega Y^2 \cos\alpha_2 \sin\alpha_2 - \widehat{A(xx\dot{y})}\Omega YX \cos\alpha_2 \cos\alpha_1$$

$$M\Omega Y p \sin\gamma_2 = \widehat{A(y\dot{x})}\Omega X \sin\alpha_1 - \widehat{A(y\dot{y})}\Omega Y \cos\alpha_2 + \widehat{A(yx)}X \cos\alpha_1 + [\widehat{A(yy)} - M\Omega^2]Y \sin\alpha_2$$

$$+ \widehat{A(y\dot{x}^2)}\Omega^2X^2 \sin^2\alpha_1 + \widehat{A(y\dot{y}^2)}\Omega^2Y^2 \cos^2\alpha_2 - \widehat{A(y\dot{x}\dot{y})}\Omega^2XY \sin\alpha_1 \cos\alpha_2 + \widehat{A(yx^2)}X^2 \cos^2\alpha_1$$

$$+ \widehat{A(yy^2)}Y^2 \sin^2\alpha_2 + \widehat{A(yxy)}XY \cos\alpha_1 \sin\alpha_2 + \widehat{A(yx\dot{x})}\Omega X^2 \cos\alpha_1 \sin\alpha_1 \qquad (6.4D)$$

$$+ \widehat{A(yy\dot{x})}\Omega XY \sin\alpha_1 \sin\alpha_2 - \widehat{A(yy\dot{y})}\Omega Y^2 \cos\alpha_2 \sin\alpha_2 - \widehat{A(yx\dot{y})}\Omega YX \cos\alpha_2 \cos\alpha_1$$

Equations (6.4) present four non-linear equations, each equation having fourteen constants being a function of the following unknowns $x \sin \alpha_1$, $x \cos \alpha_1$, $y \sin \alpha_2$ and $y \cos \alpha_2$. To accomplish their solution a modified version of the Newton-Raphson process was adopted using the technique of successive approximations for the improved estimate of the required root. In this method the function is assigned initial value, then by using Taylor's series whose tangent is extended giving an intersection with the horizontal axis, then the value at this intersection is used as the improved estimate and the process is repeated until the desired accuracy is obtained. The convergence rate of the above method was further improved by considering the second order derivatives, also the solution should normally converge over a wider range than Newton-Raphson method.

Presenting equations (6.4) in the following form:-

$$\left.\begin{aligned} &F(\omega, x, y, z) \\ &G(\omega, x, y, z) \\ &H(\omega, x, y, z) \\ &K(\omega, x, y, z) \end{aligned}\right\} = 0 \text{ at the roots} \qquad (6.5)$$

Taylor's expansion of functions of several variables (ω, x, y, z) may be extended to take into account the second order approximations thus:-

$$F(\omega + \delta\omega, x + \delta x, y + \delta y, z + \delta z) = \Big[F + F'_\omega \delta\omega + F'_x \delta x + F'_y \delta y + F'_z \delta z$$

$$+ \frac{1}{2}\left(F''_{\omega\omega}\delta^2\omega + F''_{xx}\delta^2 x + F''_{yy}\delta^2 y + F''_{zz}\delta^2 z + 2F''_{\omega x}\delta\omega\delta x\right.$$

$$\left. + 2F''_{\omega y}\delta\omega\delta y + 2F''_{\omega z}\delta\omega\delta z + 2F''_{xy}\delta x\delta y + 2F''_{xz}\delta x\delta z + 2F''_{yz}\delta y\delta z\right)\Big]_{\omega_o, x_o, y_o, z_o}$$

$$G(\omega + \delta\omega, x + \delta x, y + \delta y, z + \delta z) = [\, G \ldots\ldots\ldots 2G''_{yz}\delta y\delta z)]_{\omega_o, x_o, y_o, z_o}$$

$$H(\omega + \delta\omega, x + \delta x, y + \delta y, z + \delta z) = [\, H \ldots\ldots\ldots 2H''_{yz}\delta y\delta z)]_{\omega_o, x_o, y_o, z_o} \qquad (6.6)$$

$$K(\omega + \delta\omega, x + \delta x, y + \delta y, z + \delta z) = [\, K \ldots\ldots\ldots 2K''_{yz}\delta y\delta z)]_{\omega_o, x_o, y_o, z_o}$$

Suppose that estimated $(\omega_o, x_o, y_o, z_o)$ of the equations (6.5) are known. If these estimates are incremented respectively by changes $\delta\omega$, δx, δy, δz, then the resulting changes in $F(\omega,x,y,z)$ $G(\omega,x,y,z)$ etc. are given by the total differentials

$$F = [F'_\omega \delta\omega + F'_x \delta x + F'_y \delta y + F'_z \delta z + \tfrac{1}{2}(F''_{\omega\omega}\delta\omega^2 + F''_{xx}\delta x^2 + F''_{yy}\delta y^2$$

$$+ F''_{zz}\delta z^2 + 2F''_{\omega x}\delta\omega\delta x + 2F''_{\omega y}\delta\omega\delta y + 2F''_{\omega z}\delta\omega\delta z + 2F''_{xy}\delta x\delta y \qquad (6.7)$$

$$+ 2F''_{xz}\delta x\delta z + 2F''_{yz}\delta y\delta z)]_{\omega_o, x_o, y_o, z_o}$$

Similarly for δG, δH and δK

A solution of equation (6.5) can be obtained by determining $\delta\omega$, δx, δy, δz such that δF, δG, δH, δK satisfy the constants:-

$$\begin{aligned} \delta F &= -F(\omega_o, x_o, y_o, z_o) \\ \delta G &= -G(\omega_o, x_o, y_o, z_o) \\ \delta H &= -H(\omega_o, x_o, y_o, z_o) \\ \delta K &= -K(\omega_o, x_o, y_o, z_o) \end{aligned} \qquad (6.8)$$

Equating equations (6.8) and (6.7) and factorizing the right hand side, the following expressions may be obtained:-

$$-F(\omega_o, x_o, y_o, z_o) =$$

$$\left(\frac{\partial F}{\partial \omega} + \frac{\partial^2 F}{\partial \omega^2}\frac{\delta\omega}{2} + \frac{\partial^2 F}{\partial \omega \partial x}\frac{\delta x}{2} + \frac{\partial^2 F}{\partial \omega \partial y}\frac{\delta y}{2} + \frac{\partial^2 F}{\partial \omega \partial z}\frac{\delta z}{2}\right)\delta\omega$$

$$+ \left(\frac{\partial F}{\partial x} + \frac{\partial^2 F}{\partial x^2}\frac{\delta x}{2} + \frac{\partial^2 F}{\partial \omega \partial x}\frac{\delta \omega}{2} + \frac{\partial^2 F}{\partial x \partial y}\frac{\delta y}{2} + \frac{\partial^2 F}{\partial x \partial z}\frac{\delta z}{2}\right)\delta x$$

$$+ \left(\frac{\partial F}{\partial y} + \frac{\partial^2 F}{\partial y^2}\frac{\delta y}{2} + \frac{\partial^2 F}{\partial \omega \partial y}\frac{\delta \omega}{2} + \frac{\partial^2 F}{\partial x \partial y}\frac{\delta x}{2} + \frac{\partial^2 F}{\partial y \partial z}\frac{\delta z}{2}\right)\delta y$$

$$+ \left(\frac{\partial F}{\partial z} + \frac{\partial^2 F}{\partial z^2}\frac{\delta z}{2} + \frac{\partial^2 F}{\partial \omega \partial z}\frac{\delta \omega}{2} + \frac{\partial^2 F}{\partial x \partial z}\frac{\delta x}{2} + \frac{\partial^2 F}{\partial y \partial z}\frac{\delta y}{2}\right)\delta z$$

and

$$-G(\omega_o, x_o, y_o, z_o)$$

$$\left(\frac{\partial G}{\partial \omega} + \frac{\partial^2 G}{\partial \omega^2}\frac{\delta\omega}{2} + \frac{\partial^2 G}{\partial \omega \partial x}\frac{\delta x}{2} + \frac{\partial^2 G}{\partial \omega \partial y}\frac{\delta y}{2} + \frac{\partial^2 G}{\partial \omega \partial z}\frac{\delta z}{2}\right)\delta\omega$$

$$+ \left(\frac{\partial G}{\partial x} + \frac{\partial^2 G}{\partial x^2}\frac{\delta x}{2} + \frac{\partial^2 G}{\partial \omega \partial x}\frac{\delta \omega}{2} + \frac{\partial^2 G}{\partial x \partial y}\frac{\delta y}{2} + \frac{\partial^2 G}{\partial x \partial z}\frac{\delta z}{2}\right)\delta x$$

$$+ \left(\frac{\partial G}{\partial y} + \frac{\partial^2 G}{\partial y^2}\frac{\delta y}{2} + \frac{\partial^2 G}{\partial \omega \partial y}\frac{\delta \omega}{2} + \frac{\partial^2 G}{\partial x \partial y}\frac{\delta x}{2} + \frac{\partial^2 G}{\partial y \partial z}\frac{\delta z}{2}\right)\delta y$$

$$+ \left(\frac{\partial G}{\partial z} + \frac{\partial^2 G}{\partial z^2}\frac{\delta z}{2} + \frac{\partial^2 G}{\partial \omega \partial z}\frac{\delta \omega}{2} + \frac{\partial^2 G}{\partial x \partial z}\frac{\delta x}{2} + \frac{\partial^2 G}{\partial y \partial z}\frac{\delta y}{2}\right)\delta z$$

Similarly for $-H(\omega_o, x_o, y_o, z_o)$

and $-K(\omega_o, x_o, y_o, z_o)$

If $\delta\omega$, δx, δy and δz inside the brackets are approximated respectively by $-\frac{F}{\frac{\partial F}{\partial \omega}}$, $-\frac{F}{\frac{\partial F}{\partial x}}$, $-\frac{F}{\frac{\partial F}{\partial y}}$, $-\frac{F}{\frac{\partial F}{\partial z}}$ in the first equation and for the second equation use $-\frac{G}{\frac{\partial G}{\partial \omega}}$, $-\frac{G}{\frac{\partial F}{\partial x}}$, $-\frac{G}{\frac{\partial F}{\partial y}}$, $-\frac{G}{\frac{\partial F}{\partial z}}$ and similarly for the remaining equations, we have that

$$-F(\omega_o, x_o, y_o, z_o) =$$

$$\left(\frac{\partial F}{\partial \omega} - \frac{1}{2}\cdot\frac{\partial^2 F}{\partial \omega^2}\cdot\frac{F}{\frac{\partial F}{\partial \omega}} - \frac{1}{2}\cdot\frac{\partial^2 F}{\partial \omega \partial x}\cdot\frac{F}{\frac{\partial F}{\partial x}} - \frac{1}{2}\cdot\frac{\partial^2 F}{\partial \omega \partial y}\cdot\frac{F}{\frac{\partial F}{\partial y}} - \frac{1}{2}\cdot\frac{\partial^2 F}{\partial \omega \partial z}\cdot\frac{F}{\frac{\partial F}{\partial z}}\right)\delta\omega$$

$$+\left(\frac{\partial F}{\partial x} - \frac{1}{2}\cdot\frac{\partial^2 F}{\partial x^2}\cdot\frac{F}{\frac{\partial F}{\partial x}} - \frac{1}{2}\cdot\frac{\partial^2 F}{\partial \omega \partial x}\cdot\frac{F}{\frac{\partial F}{\partial \omega}} - \frac{1}{2}\cdot\frac{\partial^2 F}{\partial x \partial y}\cdot\frac{F}{\frac{\partial F}{\partial y}} - \frac{1}{2}\cdot\frac{\partial^2 F}{\partial x \partial z}\cdot\frac{F}{\frac{\partial F}{\partial z}}\right)\delta x \qquad (6.9A)$$

$$+\left(\frac{\partial F}{\partial y} - \frac{1}{2}\cdot\frac{\partial^2 F}{\partial y^2}\cdot\frac{F}{\frac{\partial F}{\partial y}} - \frac{1}{2}\cdot\frac{\partial^2 F}{\partial \omega \partial y}\cdot\frac{F}{\frac{\partial F}{\partial \omega}} - \frac{1}{2}\cdot\frac{\partial^2 F}{\partial x \partial y}\cdot\frac{F}{\frac{\partial F}{\partial x}} - \frac{1}{2}\cdot\frac{\partial^2 F}{\partial y \partial z}\cdot\frac{F}{\frac{\partial F}{\partial z}}\right)\delta y$$

$$+\left(\frac{\partial F}{\partial z} - \frac{1}{2}\cdot\frac{\partial^2 F}{\partial z^2}\cdot\frac{F}{\frac{\partial F}{\partial z}} - \frac{1}{2}\cdot\frac{\partial^2 F}{\partial \omega \partial z}\cdot\frac{F}{\frac{\partial F}{\partial \omega}} - \frac{1}{2}\cdot\frac{\partial^2 F}{\partial x \partial z}\cdot\frac{F}{\frac{\partial F}{\partial x}} - \frac{1}{2}\cdot\frac{\partial^2 F}{\partial y \partial z}\cdot\frac{F}{\frac{\partial F}{\partial y}}\right)\delta z$$

the remaining equation for G, H and K take the same form.

Equations (6.9A/B/C/D) can be solved directly as linear simultaneous equations for $\delta\omega$, δx, δy and δz, thus $(\omega + \delta\omega)$, $(x + \delta x)$, $(y + \delta y)$ and $(z + \delta z)$ should be an improved estimate for the solution of equations (6.4A/B/C/D). The accuracy of these results depends upon the number of iterations and for the work contained in this thesis the computer program was allowed to continue iterating

equations (6.9) until the absolute values of $\delta\omega$, δx, δy and δz had reached an accuracy of 1×10^{-8}, further the results obtained using this method are all real.

At first sight the evaluation of the second order derivatives would seemingly be time consuming, however, equations (6.4) are such that the values of $\partial^2 F/\partial\omega^2$, $\partial^2 F/\partial x^2$ etc., are equal to the value of 2.0 and the second order cross product terms are all equal to 1.0, hence equation (6.9) may be simplified as shown below:

$$F(\omega_o, x_o, y_o, z_o) =$$

$$\left[\frac{\partial F}{\partial \omega} - \frac{F}{2}\left(\frac{2}{\frac{\partial F}{\partial \omega}} + \frac{1}{\frac{\partial F}{\partial x}} + \frac{1}{\frac{\partial F}{\partial y}} + \frac{1}{\frac{\partial F}{\partial z}}\right)\right] \delta\omega$$

$$+ \left[\frac{\partial F}{\partial x} - \frac{F}{2}\left(\frac{2}{\frac{\partial F}{\partial x}} + \frac{1}{\frac{\partial F}{\partial \omega}} + \frac{1}{\frac{\partial F}{\partial y}} + \frac{1}{\frac{\partial F}{\partial z}}\right)\right] \delta x \qquad (6.10A)$$

$$+ \left[\frac{\partial F}{\partial y} - \frac{F}{2}\left(\frac{2}{\frac{\partial F}{\partial y}} + \frac{1}{\frac{\partial F}{\partial \omega}} + \frac{1}{\frac{\partial F}{\partial x}} + \frac{1}{\frac{\partial F}{\partial z}}\right)\right] \delta y$$

$$+ \left[\frac{\partial F}{\partial z} - \frac{F}{2}\left(\frac{2}{\frac{\partial F}{\partial z}} + \frac{1}{\frac{\partial F}{\partial \omega}} + \frac{1}{\frac{\partial F}{\partial x}} + \frac{1}{\frac{\partial F}{\partial y}}\right)\right] \delta z$$

$$G(\omega_o, x_o, y_o, z_o)$$

$$\left[\frac{\partial G}{\partial \omega} - \frac{G}{2}\left(\frac{2}{\frac{\partial G}{\partial \omega}} + \frac{1}{\frac{\partial G}{\partial x}} + \frac{1}{\frac{\partial G}{\partial y}} + \frac{1}{\frac{\partial G}{\partial z}}\right)\right] \delta\omega$$

$$+ \left[\frac{\partial G}{\partial x} - \frac{G}{2}\left(\frac{2}{\frac{\partial G}{\partial x}} + \frac{1}{\frac{\partial G}{\partial \omega}} + \frac{1}{\frac{\partial G}{\partial y}} + \frac{1}{\frac{\partial G}{\partial z}}\right)\right] \delta x$$

$$+ \left[\frac{\partial G}{\partial y} - \frac{G}{2}\left(\frac{2}{\frac{\partial G}{\partial y}} + \frac{1}{\frac{\partial G}{\partial \omega}} + \frac{1}{\frac{\partial G}{\partial x}} + \frac{1}{\frac{\partial G}{\partial z}}\right)\right] \delta y \qquad (6.10B)$$

$$+ \left[\frac{\partial G}{\partial z} - \frac{G}{2}\left(\frac{2}{\frac{\partial g}{\partial z}} + \frac{1}{\frac{\partial G}{\partial \omega}} + \frac{1}{\frac{\partial G}{\partial x}} + \frac{1}{\frac{\partial G}{\partial y}}\right)\right] \delta z$$

Similarly for $H(\omega_o, x_o, y_o, z_o)$

$K(\omega_o, x_o, y_o, z_o)$

The improved estimate will now be

$$\omega(n + 1) = \omega n + \delta\omega$$

$$x(n + 1) = xn + \delta x$$

$$y(n + 1) = yn + \delta y$$

$$z(n + 1) = zn + \delta z$$

Equations (6.10) may now be used to solve the non-linear equations of motion equation (6.4), whereby the unknowns may be written as:-

$$x \sin \alpha_1 = \omega \text{ - (A)}$$

$$y \cos \alpha_2 = x \text{ - (B)}$$

$$x \cos \alpha_1 = y \text{ - (C)}$$

$$y \sin \alpha_2 = z \text{ - (D)}$$

However, to avoid unnecessary complication of the computer program, the trigonometric terms were replaced with the letters (A), (B), (C) and (D) as illustrated above, a complete listing of the computer is given, as it is only by making use of this program that the non-linear whirl trajectories may be obtained.

In addition to the above method of solution, a further method was formulated as a result of an M.Sc. research project undertaken in the Department of Computer Sciences at the University of Aston in Birmingham. The results obtained were in complete agreement with those obtained using the method described above.

```
 TITLEFJ1412
C      JOURNAL RESPONSE FOR CRITICAL SPEEDS AND UNBALANCE
       DIMENSION XM(4,4),X(4),D(4),C(4,15),XN(4,4),TITLE(10)
       CALL HDATA(2)
      *CALL GSSW
      *CALL SSWTCH(1,NS)
 1     READ(2,2)(TITLE(I),I=1,10)
 2     FORMAT(10A8)
      *CALL EOF(I)
       GO TO (100,3),I
 100   STOP
 3     WRITE(3,4)(TITLE(I),I=1,10)
 4     FORMAT(1H1,50HJOURNAL RESPONSE FOR CRITICAL SPEEDS AND UNBALANCE
      1//10A8//)
       DO 10 I=1,4
 10    READ(2,500)(C(I,J),J=1,15)
 500   FORMAT(8G10.0)
       VAL1=1.E-8
       GO=1.
       READ(2,500)A1,B1,C1,D1
       READ(2,500)AK
       NK=AK
       WRITE(3,140)
 140   FORMAT(1H0,13HFORWARD WHIRL)
 120   A0=A1
       B0=B1
       C0=C1
       D0=D1
       K=1
 60    IF(K-NK)61,61,62
 62    WRITE(3,63)
 63    FORMAT(1H ,14HTOO MANY ITNS.)
       GO TO 64
```

```
      DO 20 I=1,4
      D(I)=-(C(I,1)*A0**2+C(I,2)*B0**2+C(I,3)*C0**2+C(I,4)*D0**2
     1+C(I,5)*A0*B0+C(I,6)*A0*C0+C(I,7)*A0*D0+C(I,8)*B0*C0
     2+C(I,9)*B0*D0+C(I,10)*C0*D0+C(I,11)*A0+C(I,12)*B0
     3+C(I,13)*C0+C(I,14)*D0-C(I,15))
      XM(I,1)=2.*C(I,1)*A0+C(I,5)*B0+C(I,6)*C0+C(I,7)*D0+C(I,11)
      XM(I,2)=2.*C(I,2)*B0+C(I,5)*A0+C(I,8)*C0+C(I,9)*D0+C(I,12)
      XM(I,3)=2.*C(I,3)*C0+C(I,6)*A0+C(I,8)*B0+C(I,10)*D0+C(I,13)
   20 XM(I,4)=2.*C(I,4)*D0+C(I,7)*A0+C(I,9)*B0+C(I,10)*C0+C(I,14)
      DO 33 I=1,4
      A2=1./XM(I,1)
      A3=1./XM(I,2)
      A4=1./XM(I,3)
      A5=1./XM(I,4)
      XN(I,1)=XM(I,1)-.5*D(I)*(2.*A2+A3+A4+A5)
      XN(I,2)=XM(I,2)-.5*D(I)*(A2+2.*A3+A4+A5)
      XN(I,3)=XM(I,3)-.5*D(I)*(A2+A3+2.*A4+A5)
   33 XN(I,4)=XM(I,4)-.5*D(I)*(A2+A3+A4+2.*A5)
     * CALL GE4(XN,D,X,4,4,DET)
      A0=A0+X(1)
      B0=B0+X(2)
      C0=C0+X(3)
      D0=D0+X(4)
      K=K+1
      IF(NS.EQ.1)WRITE(3,55)A0,B0,C0,D0
   55 FORMAT(1H ,70X,4G12.5)
      J=1
      DO 40 I=1,4
      VAL=ABS(X(I))
      IF(VAL.LT.VAL1)GO TO 12
```

```
13      J=2
12      CONTINUE
40      CONTINUE
        GO TO (50,60),J
50      WRITE(3,600)A0,B0,C0,D0
600     FORMAT(1H ,8HSOLUTION/5H A = ,G13.6/5H B = ,G13.6/
       15H C = ,G13.6/5H D = ,G13.6//)
64      GC = GO +1.
        IF(GO.GT.2.)GO TO 1
        WRITE(3,130)
130     FORMAT(1H0,13HREVERSE WHIRL)
        READ(2,500)(C(I,15),I=1,4)
        GC TO 120
        END
```

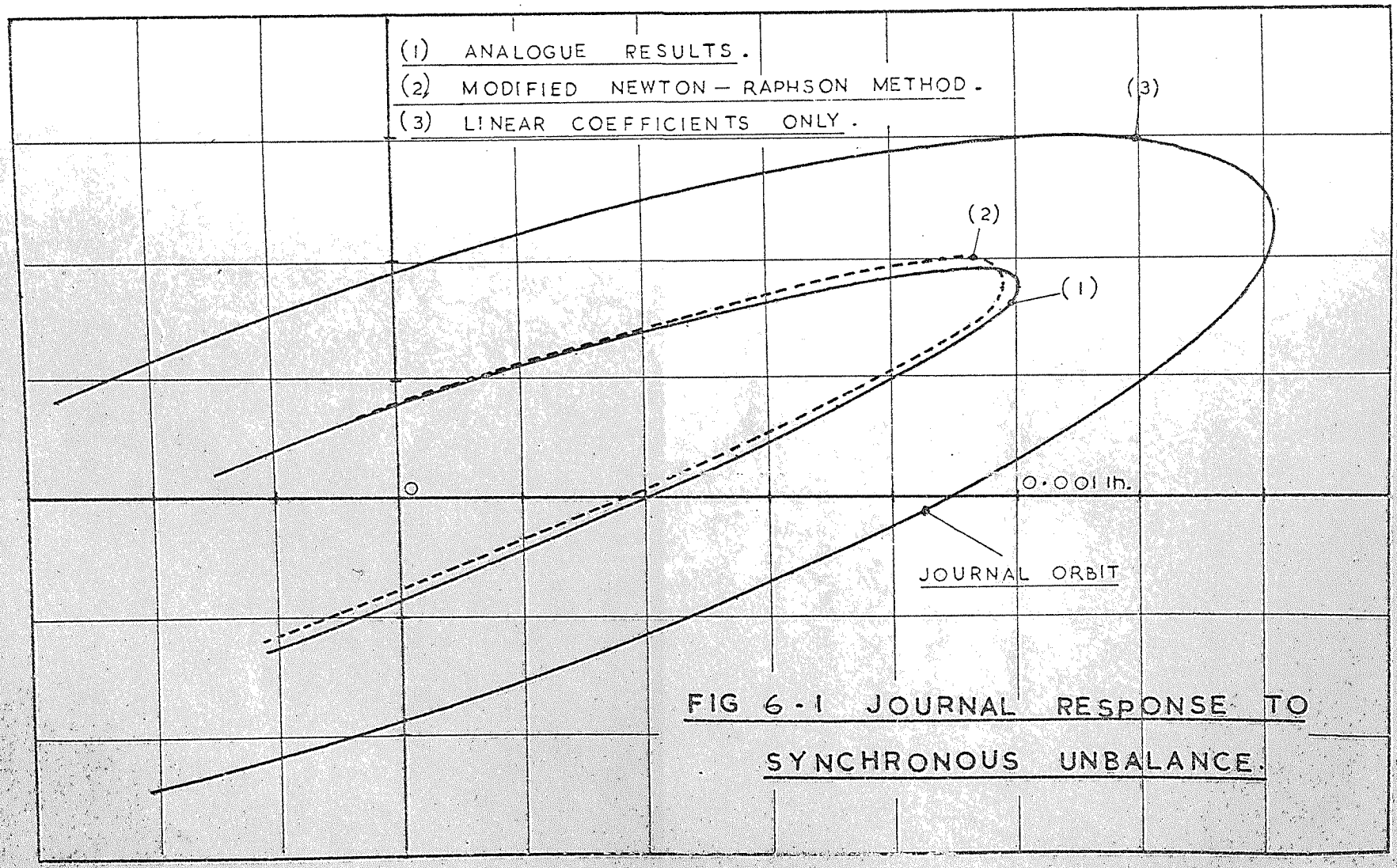

FIG 6-1 JOURNAL RESPONSE TO SYNCHRONOUS UNBALANCE.

CHAPTER SEVEN

CHAPTER SEVEN

THEORETICAL RESULTS FOR THE OIL FILM PRESSURE DISTRIBUTION

7.1 Oil film pressure distribution, aligned conditions

The strength of the computer program described in Chapter Four lies in its ability to determine with a good degree of accuracy the pressures generated within the oil film wedge, and also to detect the rapid rate of change of the film pressure when the bearing is operating under misaligned conditions; unless this first stage can be achieved, little value can be placed in the remaining work. It is also important to determine when cavitation occurs within the working face of the bush, values of eccentricity experiencing oil film cavitation may be subjected to an error due to the boundary condition $dP/d\theta \neq$ zero being used in the general solution. By using this boundary value assumption, there exists a possibility of an abrupt change in the journal running position, when cavitation commences at the trailing boundary, which can be expected to exist at an eccentricity ratio of approximately 0.6 and above.

Figures (7.1A/B/C) illustrate the oil film pressures for eccentricity ratios of 0.5, 0.7 and 0.9 respectively, the oil film grillage represents the bearing pad shown at the top of this diagram. Figure (7.1a) clearly shows the entire working face of the bearing to be completely effective in supporting an oil film wedge, and is representative of a bearing supporting moderate loads. The ratio

of the peak pressure to the averaged pressure is 2.63. Figure(7.1B) shows the oil pressures to be more dependent upon the effects of side leakage and also shows the trailing edge of the bearing to be non-effective due to the presence of cavitation, these are conditions normally experienced by the more heavily loaded journal bearing operating at speeds of approximately 1500 R.P.M. Figure (7.1C) demonstrates the severity of the pressure profile for very heavily loaded bearings illustrating how the side leakage drastically lowers the load carrying capacity of the bearing, and also the zero pressure region of the bearing pad becomes enlarged. The ratio of the peak to the averaged pressure under these conditions is increased to 4•3 for an eccentricity ratio of 0.9.

7.2 Pressure distribution for misaligned conditions

The effect of misalignment when acting in the vertical plane is demonstrated by introducing a misaligning couple to the bearing illustrated in figure (7.1B) which has an eccentricity ratio of 0.7. Changes made to the oil film pressure profile for this same eccentricity is shown in figure (7.1D), this figure clearly illustrates the considerable changes made to the oil film wedge, not only by introducing localized high intensity of pressure, but also changes made to the cavitation region, further, it can be seen that a considerable change is also made to the non-dimensional specific pressure. This latter phenomenon is also demonstrated by figure (4.4) which upon the introduction of misalignment reduces the value of eccentricity for a fixed Sommerfeld duty parameter, the reverse of this is also true, for example, for a fixed eccentricity ratio the duty parameter is reduced.

Figures (7.2A/B/C/D) demonstrate more fully the effect made to the oil film pressure distribution due to the introduction of misalignment. For example figure (7.2B) illustrates misalignment applied in the vertical plane resulting in an increase of the maximum oil film pressure from 17 units to 30 units, whilst at the same time having the effect of lowering the Sommerfeld duty parameter to 82 per cent of its original value. A further interesting phenomenon is although the misaligning couple is applied in the vertical plane, the redistribution of the oil film pressure is such that a couple is generated in the horizontal plane, equivalent to 4.0% of the applied couple. At first this was considered to be an error in the computer program, however, this residual unbalance couple was also experienced on the test rig, indeed trim weights had to be introduced during the misalignment tests in order to ensure that misalignment was confined to the vertical plane. The magnitude of the misaligning couple can be best described by replacing the couple by a percentage movement of the vertical load line away from the bush centre-line, thus zero per cent misalignment places the main load at the centre of the bearing, and 50 per cent misalignment places the main load at the extreme edge of the bearing bush; therefore in figure (7.2B) the misaligning couple is equivalent to 23.0 per cent. The severity of misalignment is considered in greater detail in the discussion.

Figure (7.2C) shows the pressure profile for the same tilt ratio, but inclined at 45^{o} to the vertical centre line, here the Sommerfeld duty parameter is reduced to 80% of the original in-line value, and as to be expected the couple acting in the horizontal

plane is increased to 19.5 per cent of the vertical couple. Because the minimum oil film thickness is reduced even further, by inclining the journal tilt, the vertical misaligning couple has been increased by approximately 13.0 per cent compared with that shown in figure (7.2B). By changing the tilt ratio from positive 45 degrees to minus 45 degrees increases the minimum oil film thickness, thereby reducing the severity of the oil film pressure distribution, which is indeed illustrated by the pressure distribution in figure (7.2D).

The theoretical results presented in figures (7.2A/B/C/D) clearly emphasizes the importance of controlling the degree of journal misalignment if accurate results are to be obtained.

7.3 Comparison with other published work

Studies are made in this section to investigate the practicability of obtaining an analytical solution for the pressure profile of the oil film wedge for a misaligned journal bearing. The solution to Reynolds differential equation for the misaligned case requires integrations by numerical methods of the oil film pressure grillage, first for the pressure distribution and subsequently for the loads and couples. Under misaligned conditions three parameters are necessary to describe the film thickness, in contrast with one parameter for bearings without misalignment. The three parameters for describing the position of the misaligned journal are central eccentricity ratio (ε), tilt ratio (T) and inclination of the tilt (ψ). Numerical methods used in performing the integrations requires considerable computer time and to consider all the individual cases for varying amounts of ε, T and ψ would make the work voluminous,

even if results were obtained from analytical investigations, methods of plotting these results would be complex. However, a knowledge of how the pressures of the oil film wedge changes for various conditions of misalignment is necessary if their importance is to be fully appreciated. Further, the accuracy of the theoretical force coefficients for both aligned and misaligned conditions depends upon accurately determining the oil film pressures.

To design a test bearing to record oil film pressures would be at the expense of rigidity, and as Du Bois, Mabie and Ocvirk, ref(43) have published a comprehensive list of results of oil film pressures listing in detail all relevant information making it possible to compute theoretical pressures,it was decided to use these measured results to check the validity of those determined using a finite difference grillage, further this publisned work investigated the effects of misalignment, thus making the results most attractive to the investigation at hand.

Results published by ref.(43) present oil film pressures for a bearing 1.62 in dia. by 1.62 in long, having a bearing arc of 180 degrees. The speed of the test journal was 5000 R.P.M. having a specific pressure of 850 lb/in^2 (600 N/cm^2). By introducing seven pressure sampling holes 0.25 in apart along the length of the bush and by rotating the bush, allowed oil pressures to be recorded whilst the bearing was operating. To check the computer program used in this thesis like conditions were set up, and by arranging the output data to print the pressures over the entire grillage having 650 nodes allowed a detailed investigation to be made. The theoretical results for the above experiment are presented in figure (7.3).

Using the results displayed in figure (7.3) allowed direct comparison between the pressure sampling points along the length of the test bearing, and theoretical predictions. The magnitude of the twisting misaligning couple about the load line was equivalent to the central load displaced 16.0 per cent of the bearing length, which are conditions likely to be experienced under real operating conditions, results are given in figures (7.4A/B). The experimental results illustrated in figure (7.4) are the best test data taken from a total of four experiments all having the same operating conditions.

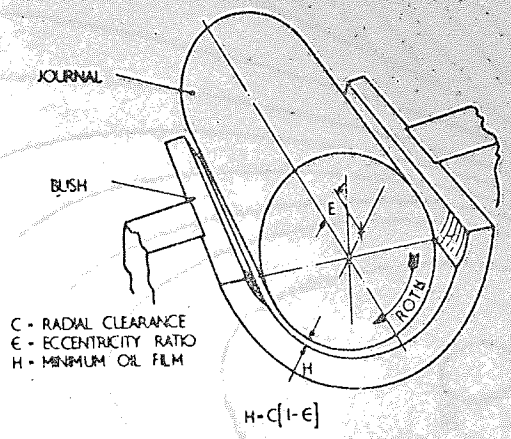

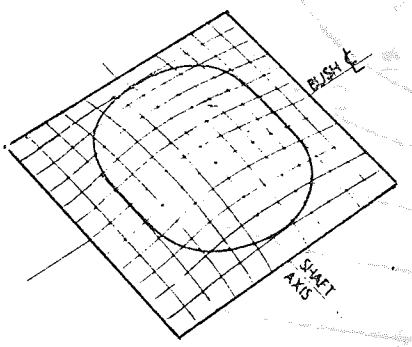

FIG. 1A — PEAK PRESSURE 10·5 UNITS
SPECIFIC PRESSURE 4 UNITS
ECCENTRICITY RATIO 0·5

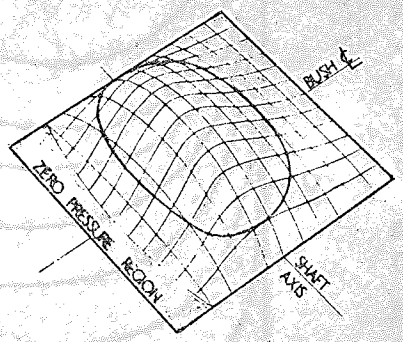

FIG. 1B — PEAK PRESSURE 30·9 UNITS
SPECIFIC PRESSURE 10 UNITS
ECCENTRICITY RATIO 0·7

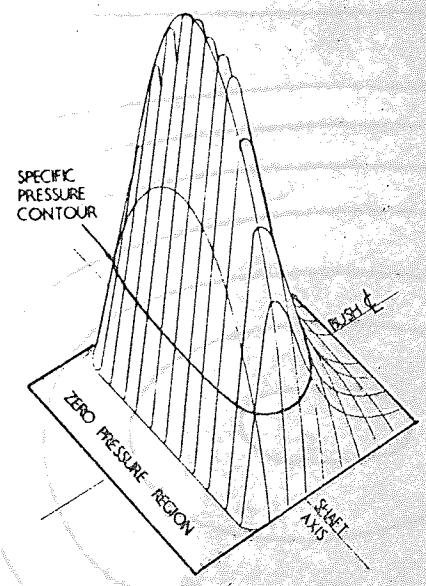

FIG. 1C — PEAK PRESSURE 205 UNITS
SPECIFIC PRESSURE 48 UNITS
ECCENTRICITY RATIO 0·9

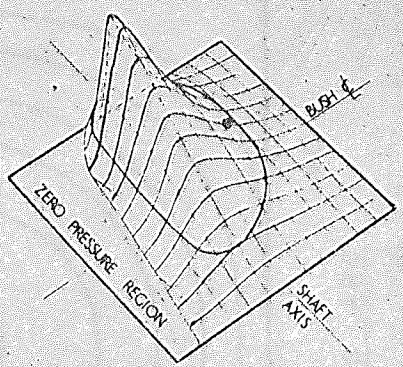

FIG. 1D — PEAK PRESSURE 65·6 UNITS
SPECIFIC PRESSURE 14·5 UNITS
ECCENTRICITY RATIO 0·7

RHB

FIG. 7-1. OIL FILM PRESSURE 'GRILLAGE.

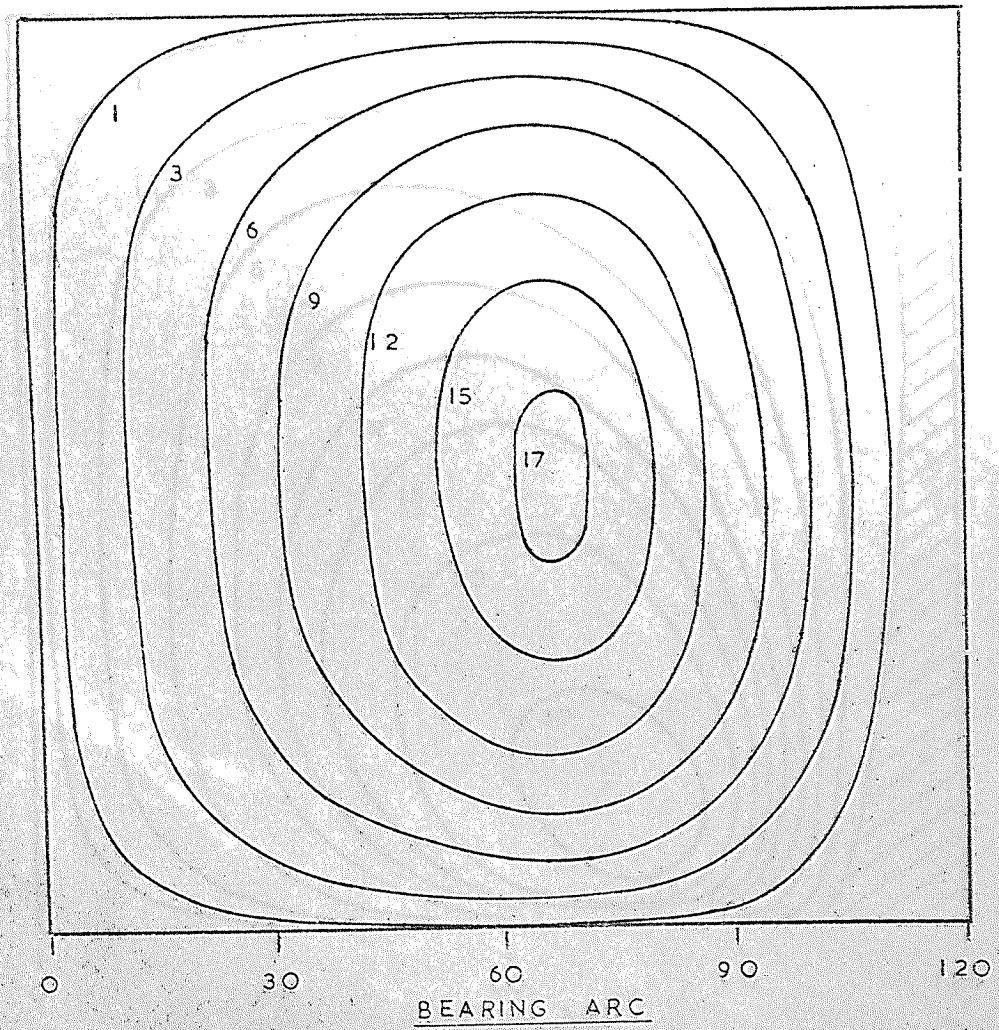

FIG 7-2A $\epsilon = 0.6$; $\tau = 0.0$; $\psi = 0$; $\phi = 35.67$

$P_{(AVE)} = 6.1$ MR = 0 ; MT = 0

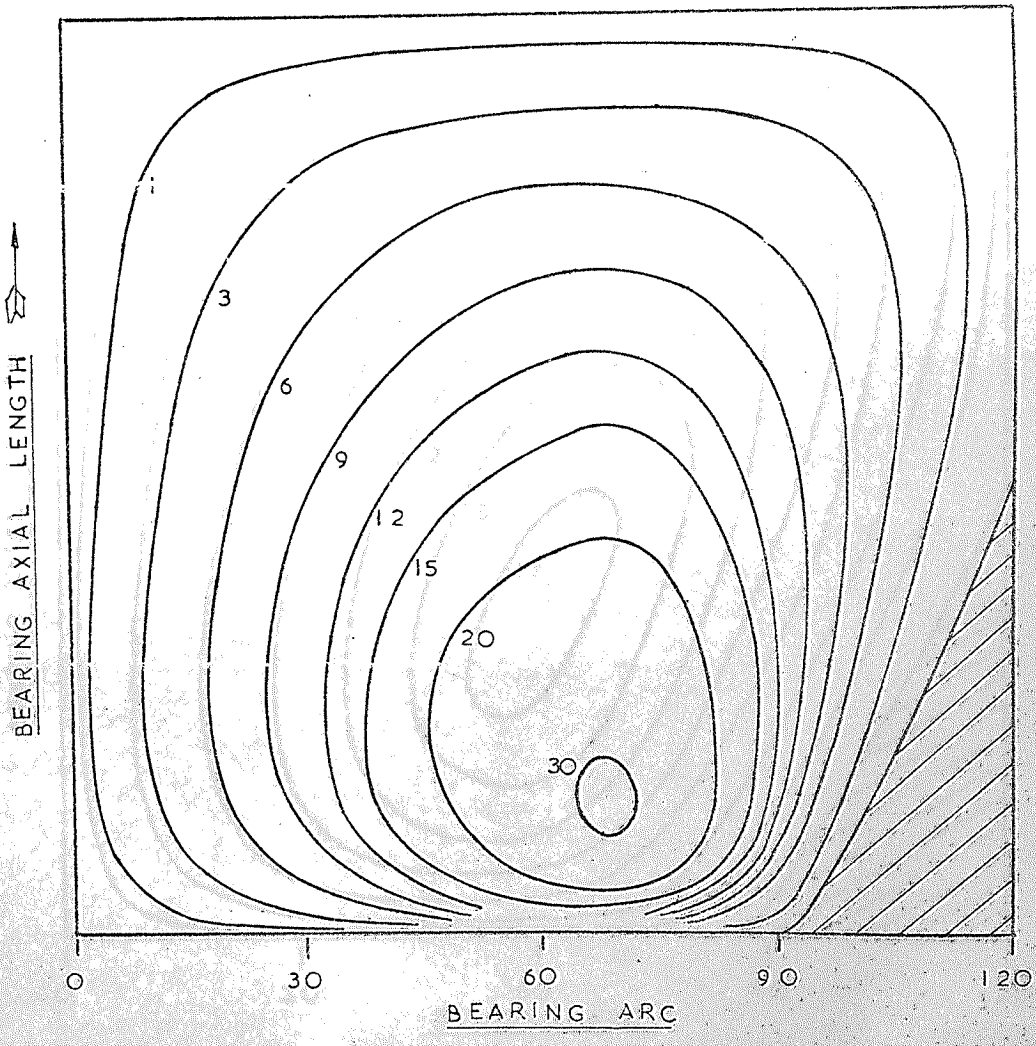

FIG 7-2B $\epsilon = 0.6$; $\tau = 0.3$; $\psi = 0$; $\phi = 36.18$

$P_{(AVE)} = 7.4$ MR = 733.8 ; MT = 582.9

NON-DIMENSIONAL PRESSURE PROFILE

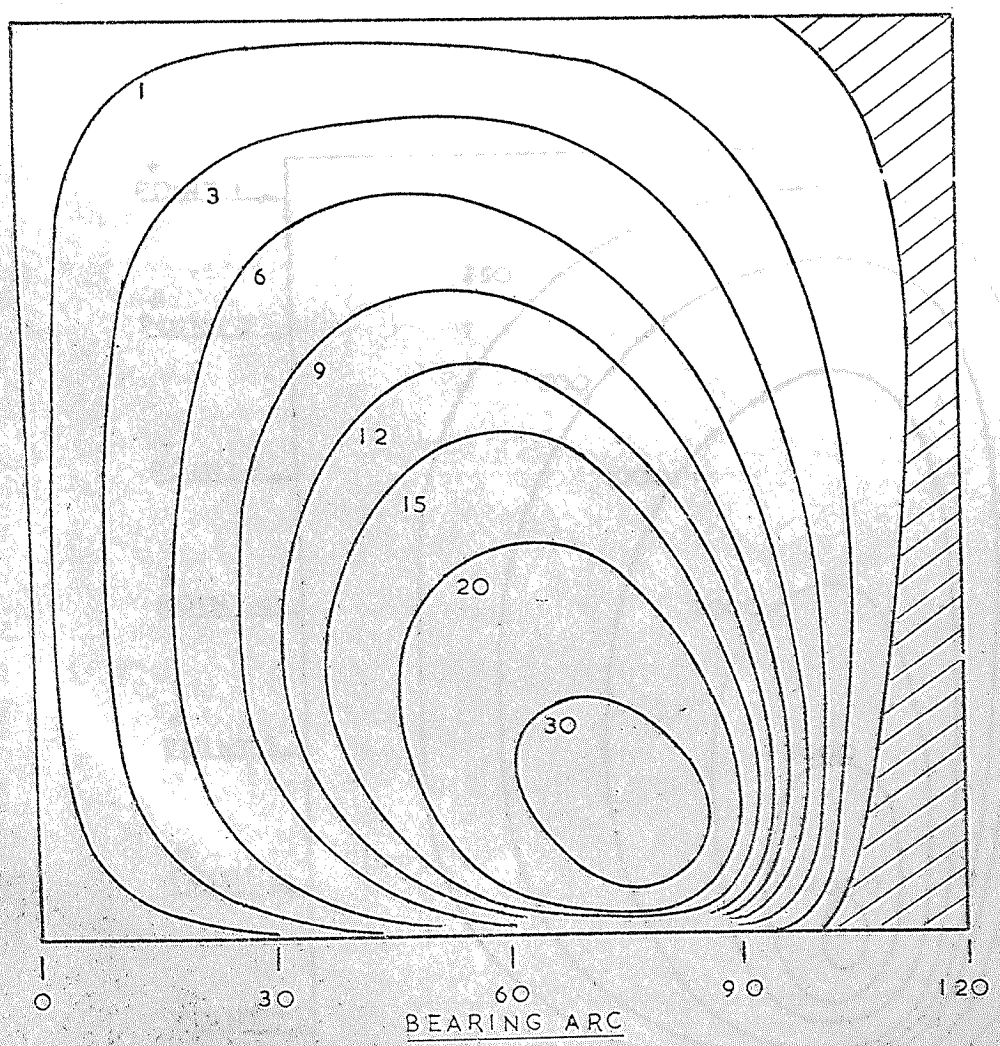

FIG 7-2C $\epsilon = 0.6$; $\tau = 0.3$; $\psi = 45$; $\phi = 29.7$

$P_{(AVE)} = 7.75$ MR = 1130.6 ; MT = 459.7

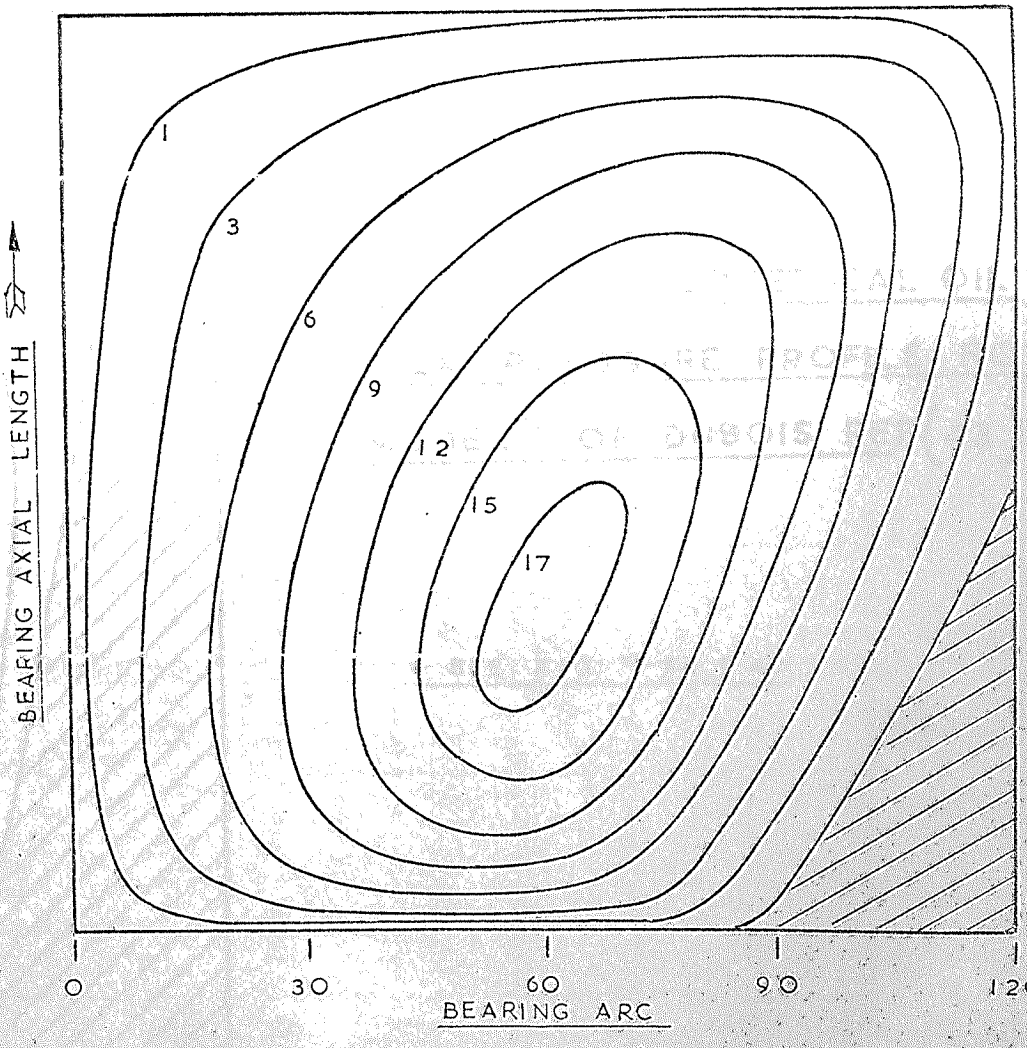

FIG 7-2D $\epsilon = 0.6$; $\tau = 0.3$; $\psi = -45$; $\phi = 36.4$

$P_{(AVE)} = 6.3$ MR = 6.6 ; MT = 242.6

NON-DIMENSIONAL PRESSURE PROFILE.

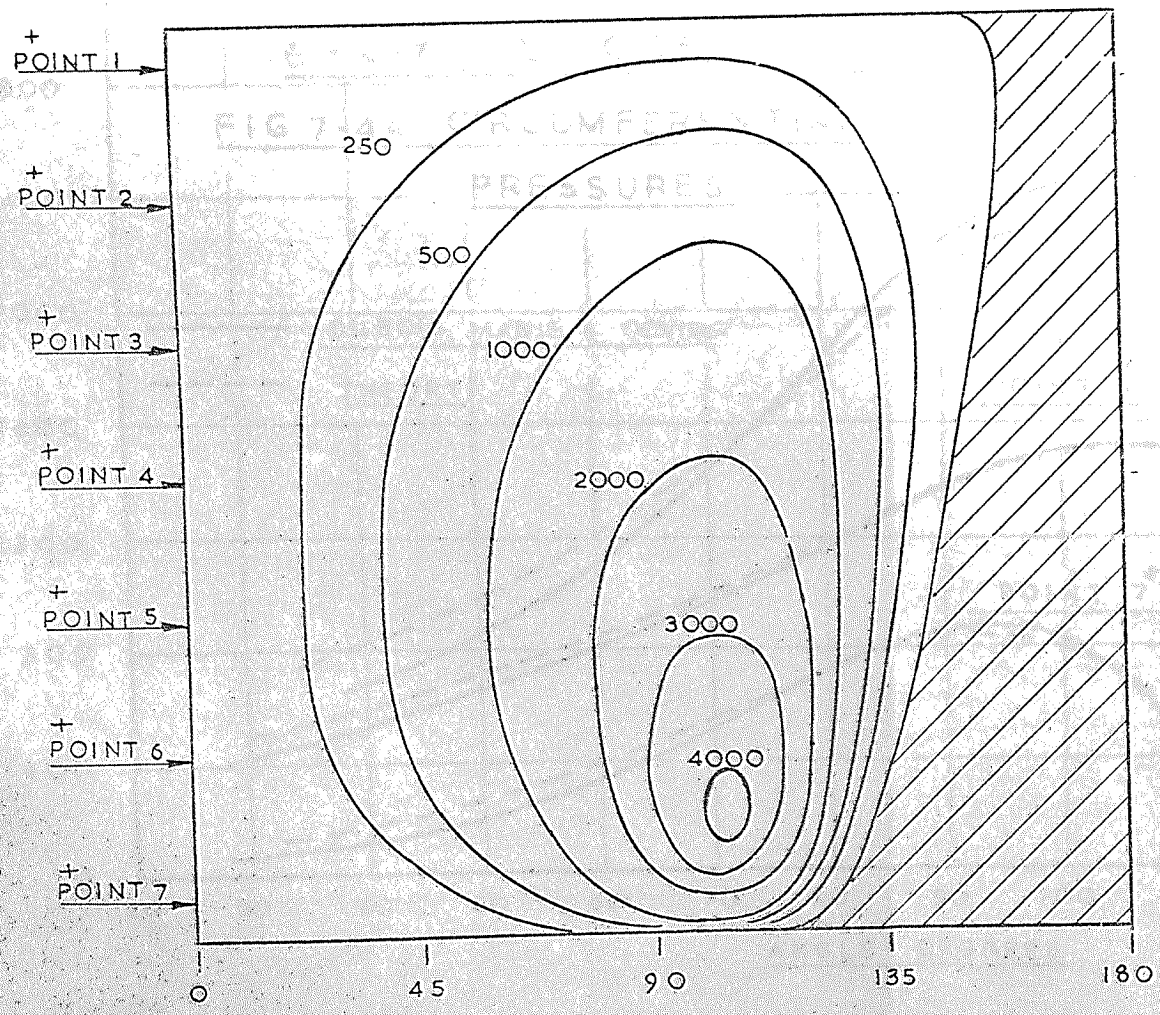

FIG 7-3 THEORETICAL OIL FILM PRESSURE PROFILE FOR MODEL '1' OF DUBOIS REF(43)

+ SEE FIG 7-4A & 4B

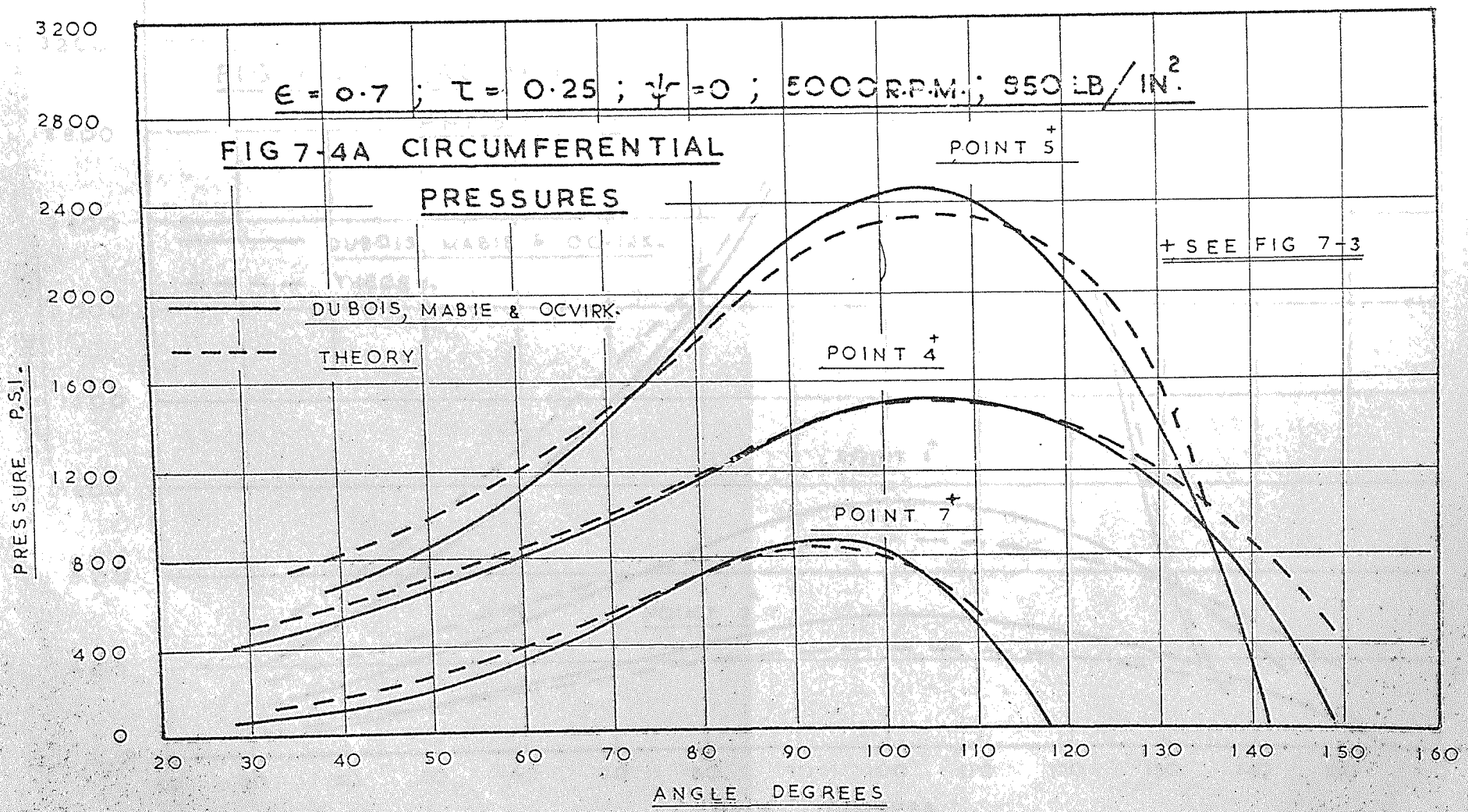
ε = 0·7 ; τ = 0·25 ; ψ = 0 ; 5000 R.P.M. ; 950 LB/IN.²
FIG 7-4A CIRCUMFERENTIAL PRESSURES
POINT 5 +
POINT 4 +
POINT 7 +
+ SEE FIG 7-3
DUBOIS, MABIE & OCVIRK.
THEORY
PRESSURE P.S.I.
3200
2800
2400
2000
1600
1200
800
400
0
20 30 40 50 60 70 80 90 100 110 120 130 140 150 160
ANGLE DEGREES

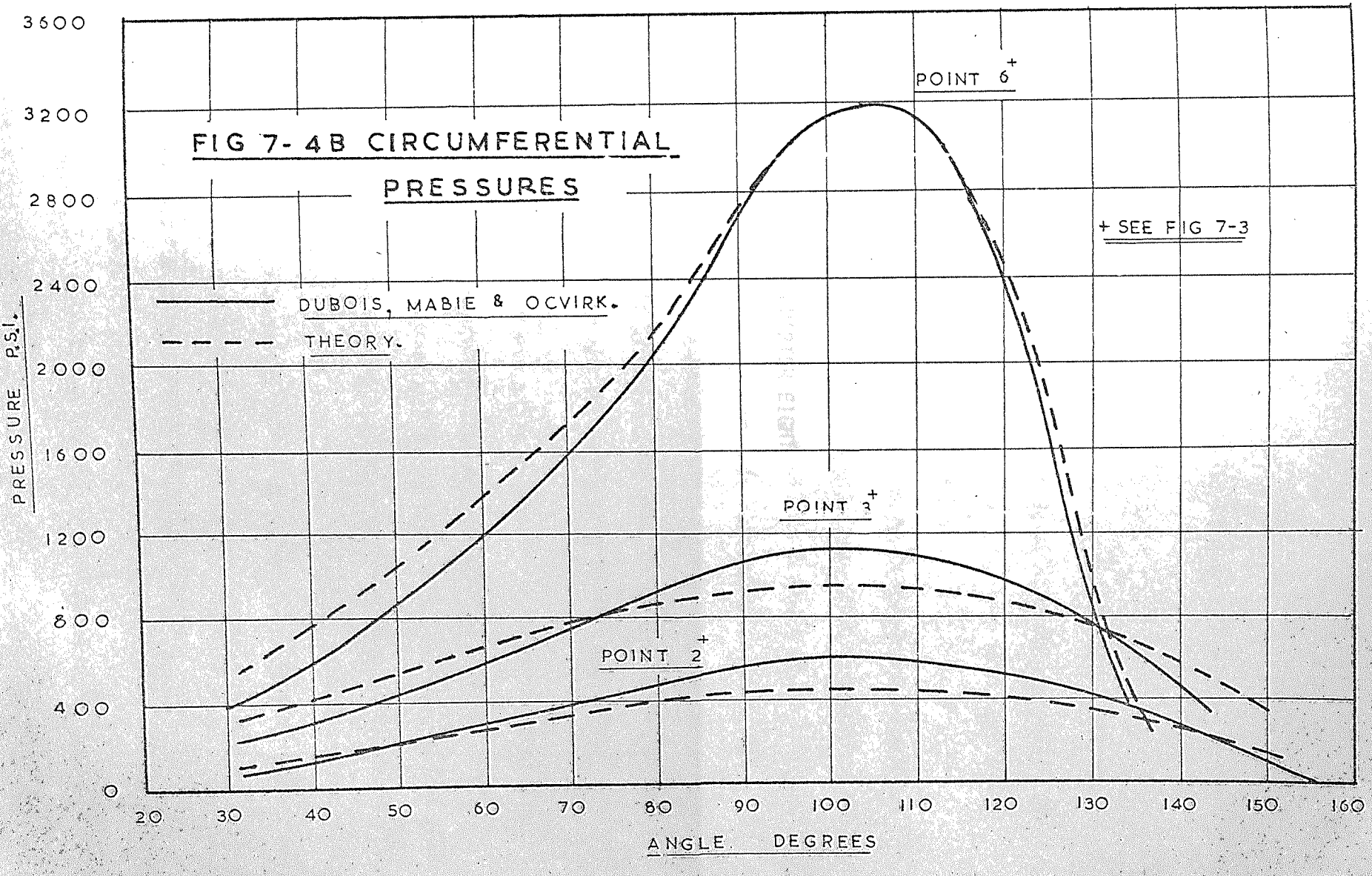
FIG 7-4B CIRCUMFERENTIAL PRESSURES
POINT 6+
+ SEE FIG 7-3
DUBOIS, MABIE & OCVIRK.
THEORY.
POINT 3+
POINT 2+
PRESSURE P.S.I.
3600
3200
2800
2400
2000
1600
1200
800
400
0
20
30
40
50
60
70
80
90
100
110
120
130
140
150
160
ANGLE DEGREES

CHAPTER EIGHT

CHAPTER EIGHT

EXPERIMENTAL TEST EQUIPMENT

8.1 Design considerations

The basic philosophy adopted throughout the design of all the component parts of the experimental test rig, was to ensure that their natural frequencies were well above the rotational and vibrational frequency of the journal. This basic requirement was to eliminate any dynamical forces generated either from the rotating shaft or any component attached to the shaft which might introduce a coupling effect. To implement this requirement necessitated having a rigid shaft supported by a single bearing, rather than a two bearing plus shaft system. This then forms the format of the design requirements for the remaining part of the test rig.

The theoretical treatment in Chapter five suggested that the journal should be capable of being excited over a range of frequencies compared to the rotational frequency of the journal, and should be further capable of having the vibratory unbalance force running in the reverse direction to the journal rotation, as well as in the same direction. In addition to the above the test journal should be designed to allow the excitation force to be applied without stopping the journal, and also be capable of being reversed, again without affecting the speed or stopping the journal.

The most effective method of exciting the journal, and where the magnitude of the force can be measured or calculated with accuracy, is to use an out of balance of a known mass and radius from the axis of rotation, thus allowing the centrifugal force to be computed for a given vibratory frequency. The unbalance force would also have to be applied in such a manner not to cause a conical whirl.

8.2 Test Journal and Bearing Bush

To achieve the above requirement for applying a vibratory unbalance force, would mean having to employ a hollow journal to allow an inner shaft capable of driving the unbalance without passing through, or running close to a critical speed. Figure (8.1) shows a sectional arrangement of the test journal and supporting structure, together with the inner shaft system driving a disc to which the unbalance was attached. A photograph showing this same disc assembled inside the journal is shown in figure (8.2).

The bearing bush used throughout the experimental investigation was a thin walled split bearing five inches in diameter by five inches long, consisting of a 0.050 in thickness of whitemetal bonded onto a steel shell having a wall thickness of 0.375 inches. The bush was machined to provide a 120 degree arc pad having 0.006 in diameteral clearance. The bottom half of the bush was secured to the pedestal by two button stops diagonally opposite, and the upper half of the bush clamped into position by the top pedestal cap. Fitted at the extreme ends of the bearing bush, and at 45 degrees

to the horizontal split, were the displacement transducers which were locked into position with araldite, see figure (8.3).

Fitted into the whitemetal of the bearing in the bottom half of the bush, were nine thermocouples, with the one set of three placed at the bottom dead centre, and the other two sets of three placed at 45 degrees either side of the B.D.C. Each set of the three thermocouples were positioned axially, with the one placed half way along the length of the bush, the other two set two inches either side of the central thermocouple.

The journal was loaded by two pneumatic pistons which offered negligible inertia to the vibrating journal. Because of the rubber sealing rings around the pistons, the additional stiffness offered to the test journal was also of second order, figure (8.4) shows the air pistons fitted to the underside of the cast iron support blocks. The force exerted by the pneumatic pistons was finally applied to the test journal via two sets of double row self-aligning ball bearings, positioned equidistant about the centre-line of the journal, thus allowing the journal to take up its free vibrating running position, without any external constraint other than applied force.

A strain gauge load cell was fitted between the air piston and the double row self-aligning bearing, which was primarily included to measure both the steady load plus any additional fluctuating load. However, it was to be found later that fluctuating loads were so small that they could not be recorded.

To allow misalignment to be introduced to the test bearing, the air pistons could be loaded independently to each other, by introducing a combined air pressure regulating valve and dial gauge which recorded the air pressure on the supply pipe leading to the pneumatic piston. In addition to the piston force, trim weights could also be added to the test journal acting in the same direction as the piston force, also trim weights could be added acting along the horizontal plane which was necessary in order to confine the misalignment in the vertical plane. The method of applying the external trim weights etc. and the regulating pressure valve may be seen in figure (8.5).

The bearing was driven by a Heenan and Froude dynamic excitation unit employing a five horsepower electric motor and an eddy current coupling which allowed a fine speed control over the entire working range up to the maximum speed of 2,700 R.P.M. The journal was driven from the drive side of the eddy current coupling via a Hardy Spicer coupling, thus avoiding any extraneous restraint applied to the test journal. The drive to the vibrator, i.e. the internal shafting, was again from a five horsepower Heenan and Froude unit, but the speed range was increased by taking the drive through a belt and pulley system, the maximum speed being in excess of 6000 R.P.M. However, because of the high excitation speeds, the final drive was taken through a hooks joint manufactured from plastic, which built a mechanical fuse into the system, this latter driving arrangement may also be seen in figure (8.5).

8.3 Lubricating System

The bearing and oil circulating system was designed in such a manner not to require a forced oil supply, which might cause the journal to be forced over within the bearing bush under lightly loaded conditions. The oil inlet supply was taken to an upper reservoir within the bearing pedestal where it was allowed to flow under the influence of gravity to the working face of the bearing via slots in the jointed surface between the two bearing halves, and distributed along the bush by means of grooves which ran axially at each side of the assembled bearing.

The oil was supplied to the upper reservoir of the test bearing from a header tank, in which a heater was fitted in order to bring the working temperature to its equilibrium value in the shortest possible time, and also to extend the viscosity range of the oil. The oil having passed through the bearing was allowed to drain into a lower tank and then pumped back up into the header tank thus completing the circulating system.

8.4 Measurements of shaft displacements

To completely describe the position of the journal relative to the bearing bush, assuming that no geometric distortion existed, it was necessary to measure in at least two planes spaced along the axis of the bearing, and at least two coordinates in each plane. To meet this requirement inductive transducers were used positioned at 45 degrees to the horizontal and arranged normal to one another.

The displacement transducers were type TW 12-2/A manufactured by Vibro-Meter AG having an approximate inductivity of 2.5 to 2.9mHy and an impedance of 130 to 150 ohm, and were capable of operating up to a maximum temperature of 180°C. Linearity was improved together with output by arranging the transducers in push-pull, i.e. a pair of transducers used in a half bridge circuit, thus a change of inductance was the difference of the changes in the two transducers, since the air gap of one transducer increased as the other decreased. A further improvement was obtained by purchasing matched pairs of transducers as non-linearities tend to cancel when operating under push-pull conditions.

By providing an initial air gap of C.5 mm gave a linearity to within 2 per cent for the complete bearing clearance of 0.006 in. (0.152 mm) and a relative sensitivity of 72 mv per 0.001 in. valve voltmeter and 29 M/M per 0.001 in. for the U.V. recorder.

The principle of operation was that a change in journal position caused a change in impedance unbalancing an A.C. bridge of which they were part. The bridge was supplied with a stabilized voltage at 3 kHz, thus changes in transducer inductance resulted in amplitude modulation of the energising carrier voltage. The bridge output, modulated by the journal movement, was amplified by an A.C. amplifier coupled through a 60 DB attenuator having twenty 3 DB steps, thus allowing the output of all four channels to be equalized. The amplified output was taken to a phase sensitive demodulator which in turn drove the U.V. recorder type 1050 and also a Nagard type 311 two channel oscilloscope. The bridge, oscillator, amplifiers and

demodulator were all housed in one cabinet.

The four vectors of displacement were displayed on the oscilloscope by using a Nagard four beam switched pre-amplifier type P311Q. The four independent displays were achieved by devoting the pre-amplifiers channels (1) and (2) to the "upper" channel of the oscilloscope, and channels (3) and (4) to the "lower" channel. When selected, electronic switching circuitry alternately connected channels (1) and (2) to the upper channel of the oscilloscope on a time sharing basis and similarly connecting channels (3) and (4) to the lower oscilloscope channel. The oscilloscope was also capable of being switched to display two sets of Lissajous figures, again on a time sharing basis.

In order to measure absolute displacements, a second set of transducers were used to measure pedestal movement. These transducers were arranged with only one active transducer, the second remained passive and was placed at a fixed distance of 0.5 M/M away from a dummy cap. This second set of transducers were supported by a flexibly mounted framework which had previously been monitored using accelerometers for the vibration range of the test journal, and rubber mounts selected accordingly.

8.5 Shaft speed control and counter

The rotational speed of the journal and vibrator shaft was controlled by each of the Heenan and Froude dynamic excitation units, both consisting of an electric motor driving through an eddy-current

coupling. The speed was varied by the amount of excitation to the coupling and the fine speed control was achieved by driving a tachogenerator from the driving end of the eddy-current coupling, which supplied a reference voltage to the servo speed control unit.

The rotational speeds were counted by using a tachometer type G308. This type of tachometer was a non-contact unit, the sensing element of which produced a pulse of constant amplitude generated from the teeth of a gear wheel, the output was then taken to a Southern digital voltmeter/counter type M 1155. By switching, it was possible to make a speed count of either the journal speed or the vibration frequency.

8.6 Shaft position indicator

The position of the unbalance weight, relative to the journal displacement, was also recorded by a tachometer type G308, the output of which was taken to the U.V. recorder.

8.7 Measurement of the oil film temperature

The oil film temperature, in the bottom half of the bearing bush was measured by nine thermocouples, together with a hot junction held at a constant temperature of $45^{o}C$. All of the thermocouples were connected to a switching unit which measured each in turn using a milli-voltmeter which when calibrated gave the following relationship:

$$\text{Temperature } {}^{o}C = 45 + 8.5 \text{ (M.V.)}$$

8.8 Calibration of displacement transducers

To calibrate the bearing proximity transducers via the U.V. recorder, oscilloscope and valve voltmeter, required moving the journal in incremental displacements, rather than moving the transducer itself, as once the bearing pedestal top cap had been placed into position it was not possible to get direct access to the transducers. Therefore by arranging dial gauges in the vertical and horizontal planes at both ends of the test journal, which were capable of recording to within 0.0002 in, and by moving the journal along the vertical plane by means of a simple lever system, allowed all the transducers to be calibrated at the same time. The array of levers used in jacking the journal are shown in figure (8.5).

Calibration was undertaken both at room temperature, and also after the bearing had been operating with a film temperature of over 80^{o}C for several hours. However, the sensitivity of the transducers did not change for these two extreme conditions, also for the full radial clearance the sensitivity remained linear.

By switching the output of each transducer to the valve voltmeter in turn allowed the D.C. component to be measured, which gave the steady state running position of the journal relative to the bearing bush, whilst the U.V. recorder was only used to measure the A.C. component which represented the whirling amplitude of vibration. The oscilloscope was only used for general display purposes.

The transducers recording the pedestal displacements, were mounted on micrometer heads, therefore it was a simple matter to calibrate them upon completion of each test.

8.9 Balancing the test journal

Before commencing the test programme the test journal was balanced to well within 1.0 gramme at each end of the journal. The method employed was first to determine the magnitude and direction, of the unbalanced displacement vector from the U.V. recorder. Then to attach a known calibration weight to the test journal and obtain a second displacement vector which contained the unknown plus the known unbalance, then from vector algebra it was possible to determine the magnitude and circumferential position of the inherent unbalance within the journal. The above procedure was repeated at the maximum running speed of the test rig until the unbalance was to within 1.0 gramme.

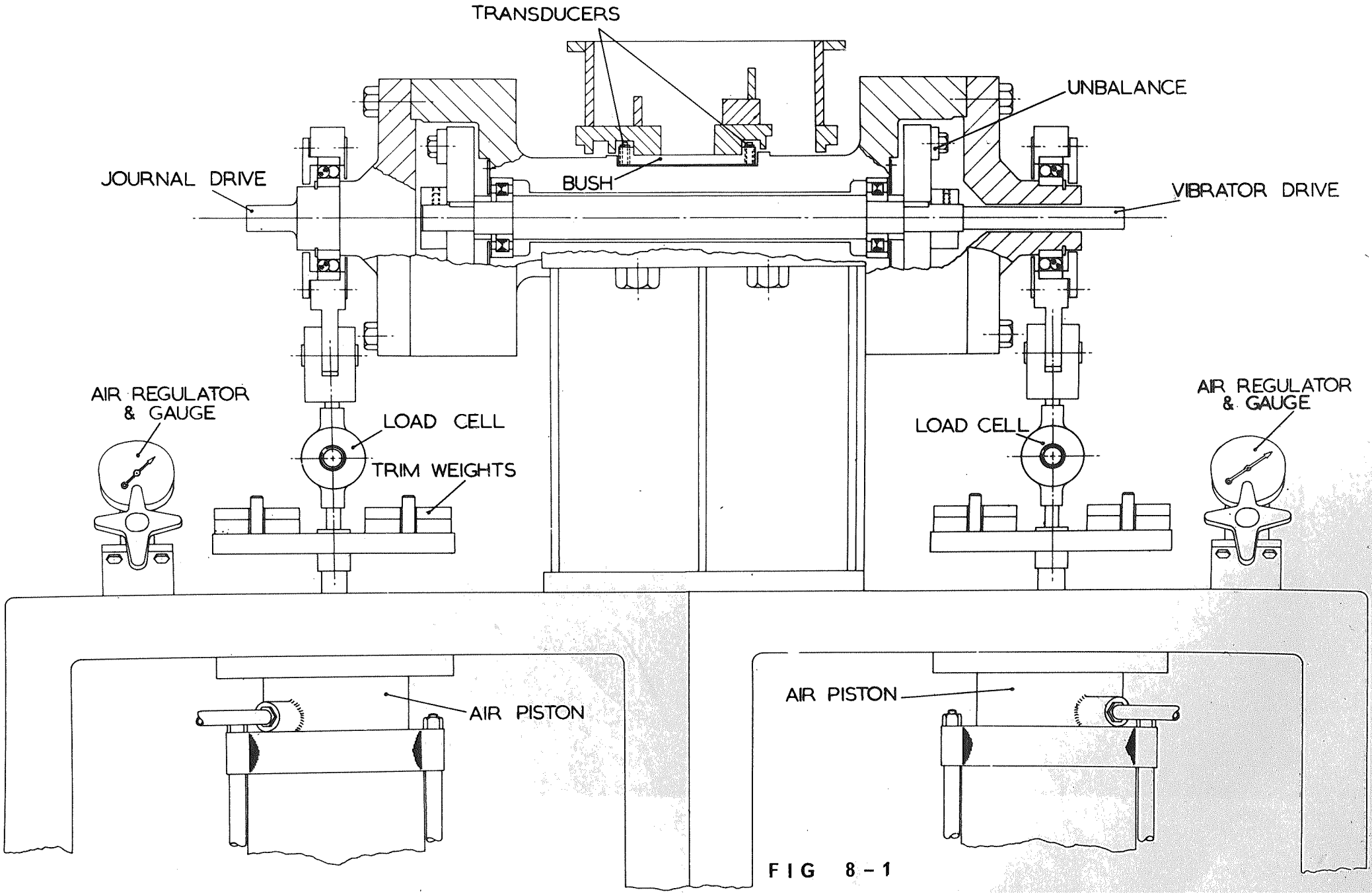
TRANSDUCERS
UNBALANCE
JOURNAL DRIVE
BUSH
VIBRATOR DRIVE
AIR REGULATOR & GAUGE
LOAD CELL
TRIM WEIGHTS
LOAD CELL
AIR REGULATOR & GAUGE
AIR PISTON
AIR PISTON

FIG 8-1

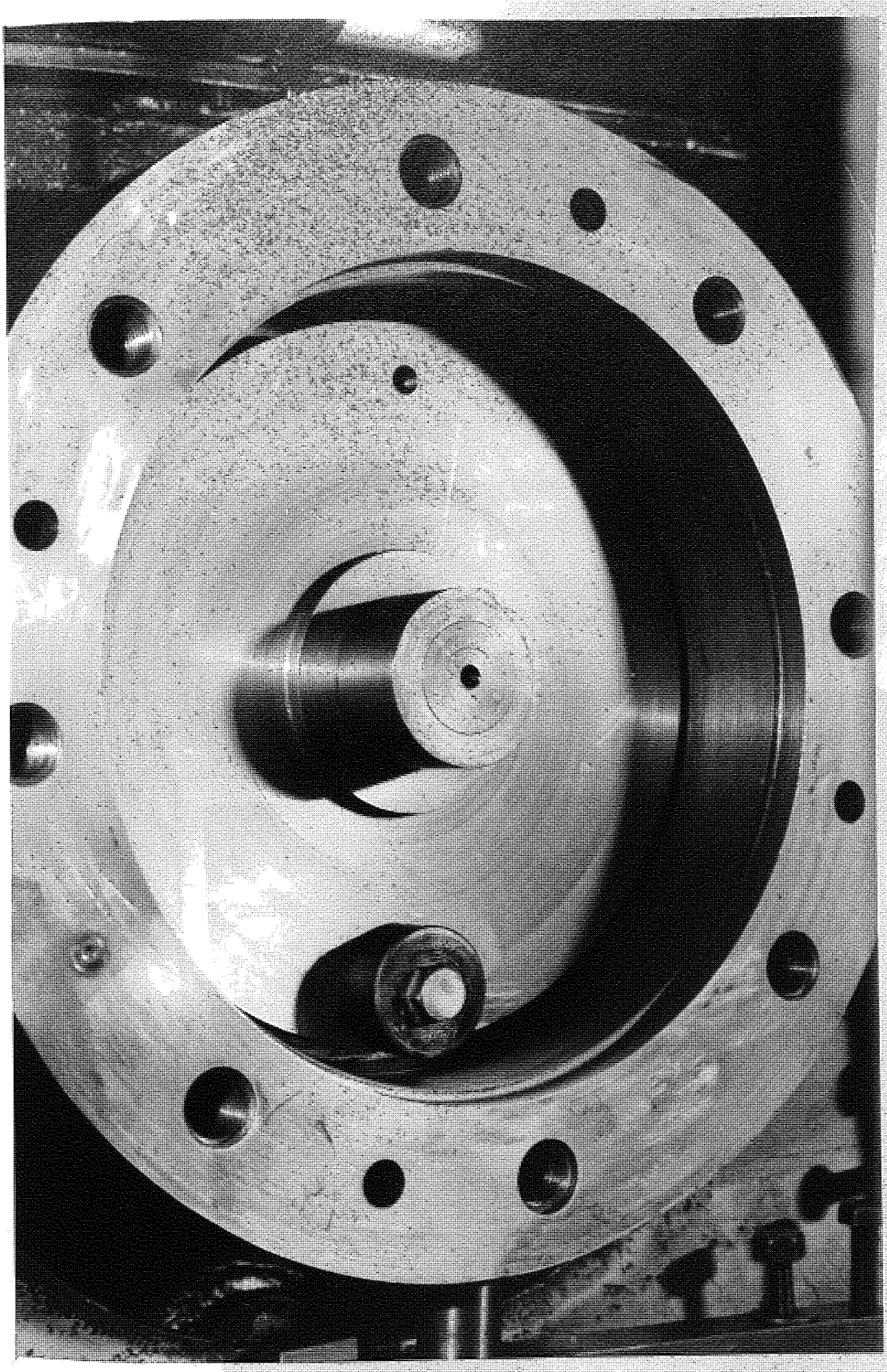

FIG 8-2

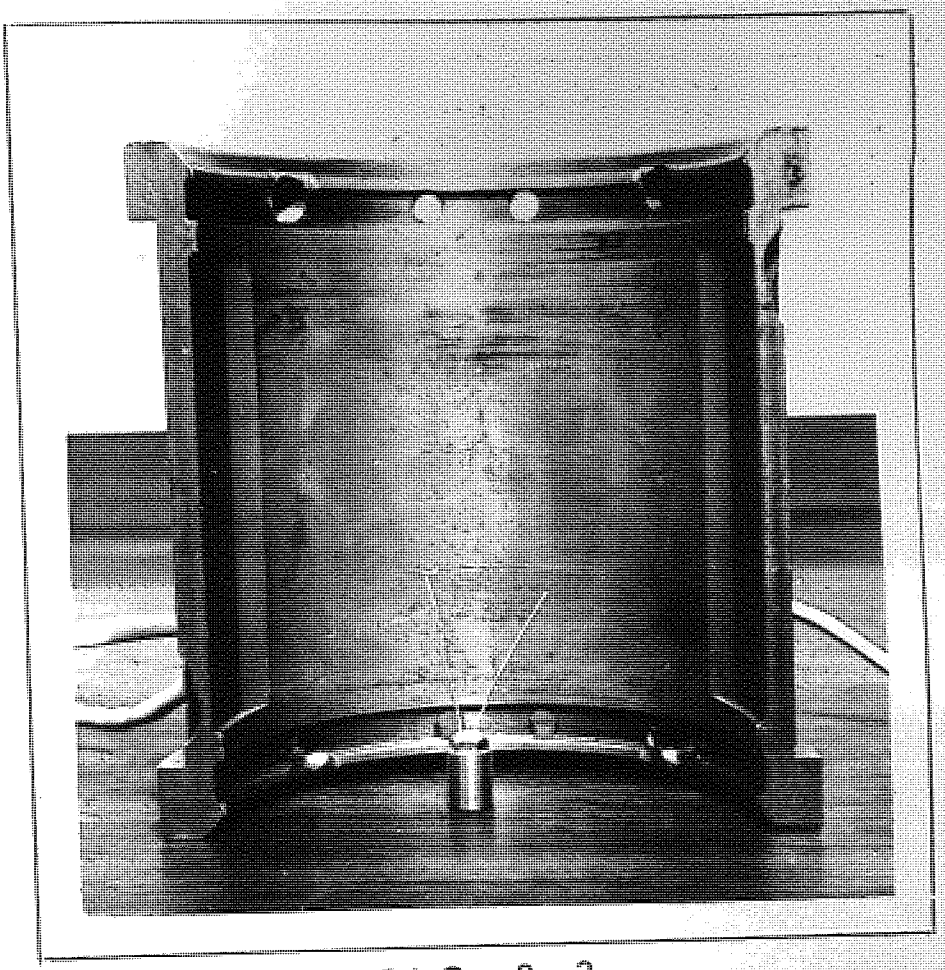

FIG 8-3

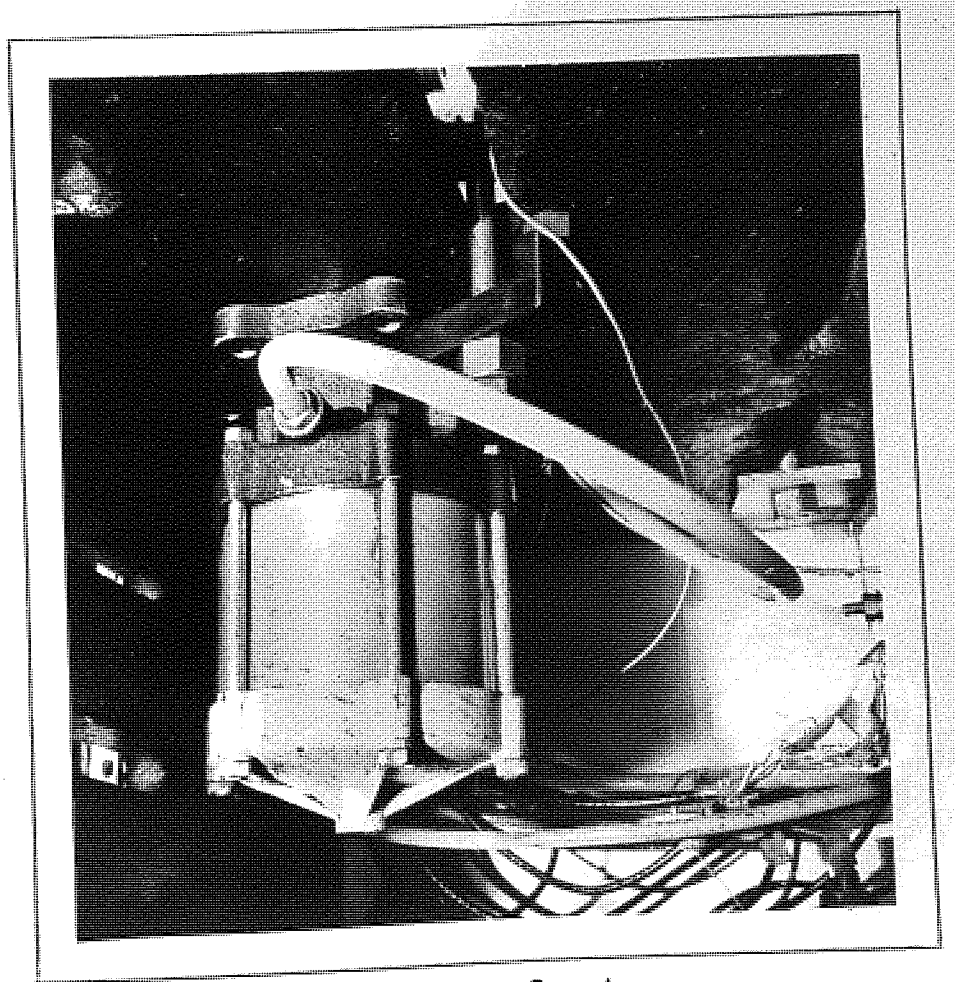

FIG 8-4

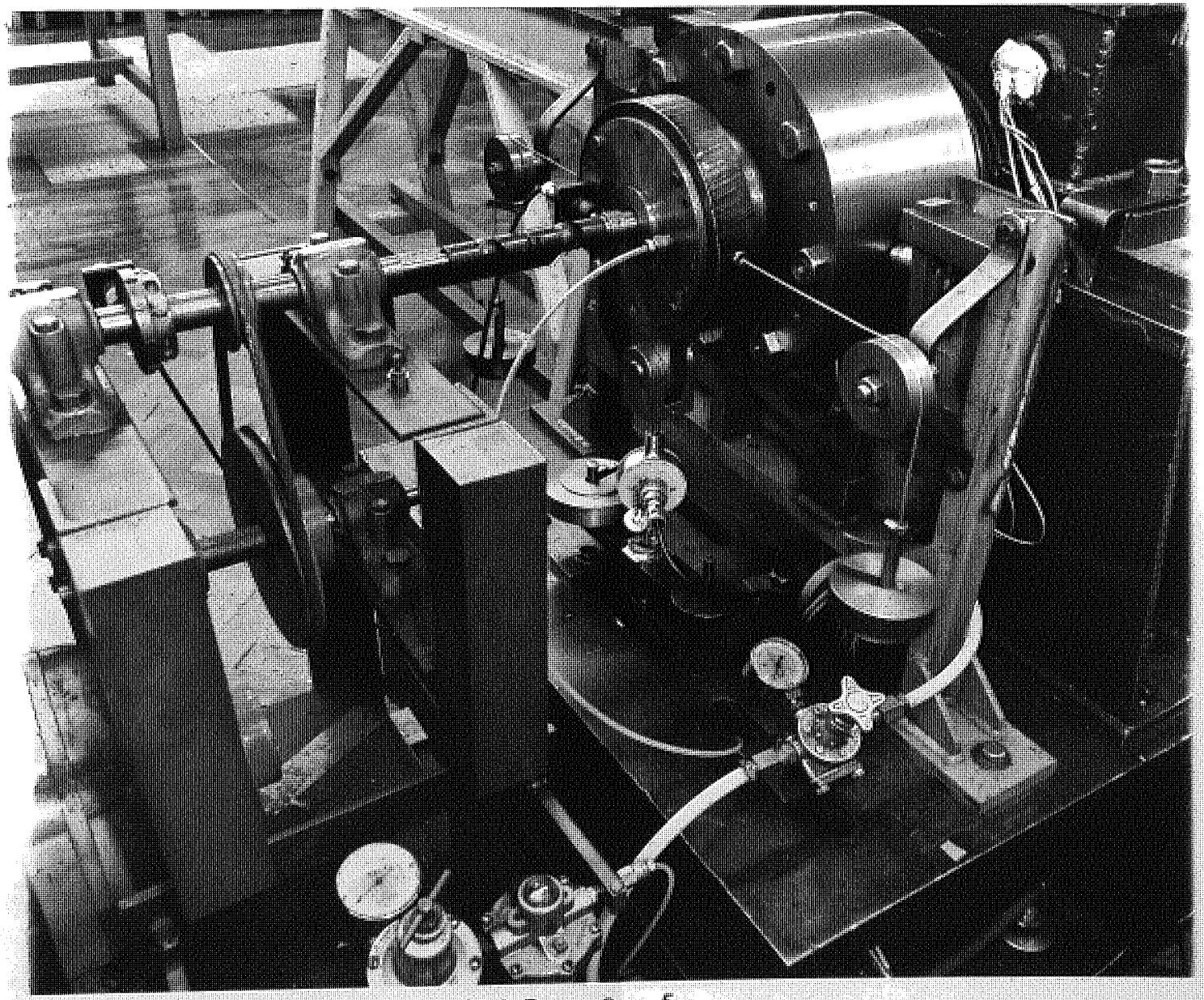

FIG 8-5

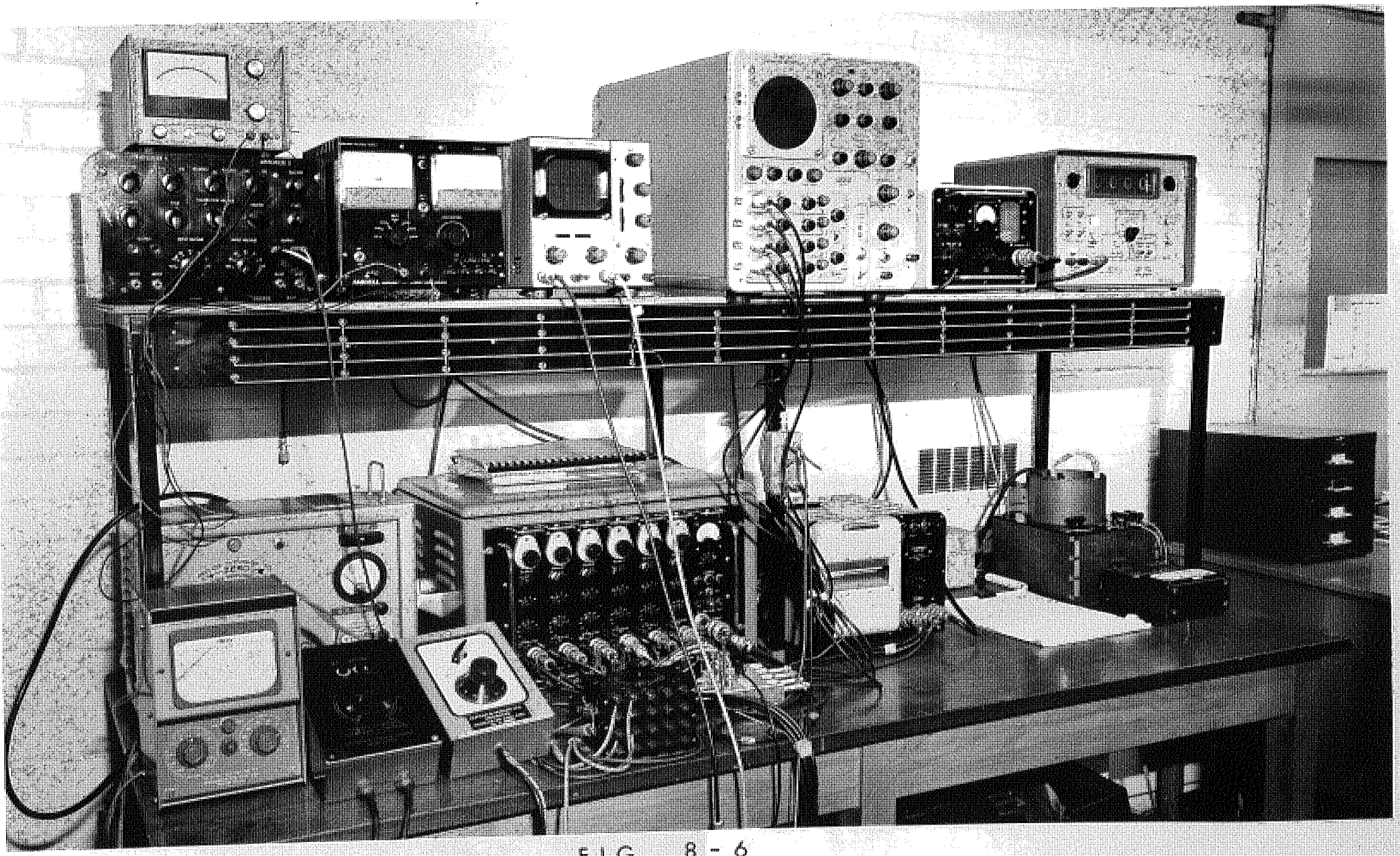

FIG 8-6

FIG 8-7

CHAPTER NINE

CHAPTER NINE

EXPERIMENTAL RESULTS FOR THE STEADY STATE RUNNING CONDITIONS

9.1 Locus of shaft centre - aligned conditions

The operation of a journal bearing is completely determined by the position taken up by the journal centre, caused by the wedging action of the oil film. For each such position the load, speed, viscosity, and radial clearance are related to the duty parameter. The relationship between these variables must be considered if it is to be made possible to quantify the dynamic characteristics of the bearing.

Experimental results illustrating the change in the steady state running position of the journal centre, for various operating conditions of the bearing, are presented in figure (9.1). The results plotted illustrated the changes in eccentricity ratio and angle of incidence for various values of Sommerfeld duty parameter. A better appreciation of the journal centre characteristics is obtained by presenting the eccentricity ratio and attitude angle in polar co-ordinates as shown in figure (9.2). The latter presentation of results is usually favoured by the researcher, whilst the former presents information suiting the requirements of the design engineer; because the friction factor and side leakage are also functions of the eccentricity ratio.

An essential requirement when conducting the tests to determine the steady state conditions, was to ensure thermal stability, by

allowing the bearing to run continuously for approximately three hours at the required speed and loading, thus eliminating thermal transient conditions before accepting the final test results. In order to accelerate thermal equilibrium, the oil inlet supply was heated by means of an emersion heater fitted in the oil header tank. Heating the oil inlet supply also allowed a wider range of duty parameter to be investigated.

To allow for thermal expansions of the test journal, possibly giving rise to a false datum, a zero reference check was made upon completion of each test by measuring the standstill position of the journal i.e. point A in figure (9.2).

Scatter of the results presented in figures (9.1) and (9.2) would seemingly be large, however, it should be remembered that for the radial clearance used, an eccentricity ratio of 0.1 corresponds to a displacement of 0.0006 in. It is with awareness of this that accuracy of results may be judged.

9.2 Locus of shaft centre under misaligned conditions

To plot the locus of the journal centre for different duty parameters, together with different amounts of journal tilt acting in the vertical plane is a very difficult task, due to the degree of accuracy required. Theoretical results presented in figure (9.3) clearly illustrates that small changes in eccentricity would have to be measured for relatively large changes in the tilt ratio. Therefore unless the loading applied to the test journal can be controlled with precision, changes in eccentricity would not be obtained to within the required accuracy. To overcome this problem

the test bearing was designed such that having obtained the desired running equilibrium position, weights could easily be transferred from one end of the test journal to the other, thus introducing a misalign -ing couple to the journal without affecting the resulting vertical loading. It should be explained however, that this method of transferring weights would not be acceptable under dynamically loaded conditions, as the size of the weight involved would effect the inertia force acting at each end of the test journal, therefore these results demonstrating changes in eccentricity with the introduction of a misaligning couple were utilized when investigating dynamically loaded conditions.

To improve the accuracy of results the journal running position was first recorded with zero misalignment, then with the D.C. millivolt meter switched to give three times the normal amplifications, small amounts of misalignment were introduced, and only the difference in journal position recorded. This particular method was adopted, as theoretical reasoning showed that when the bearing was operating with a small eccentricity, the changes in eccentricity with the introduction of misalignment would be extremely small, and would only become more apparent when the bearing was operating with an eccentricity ratio above 0.5.

Experimental results obtained for a number of conditions are presented in figure (9.3), together with theoretical predictions. As these results were only required to prove the reliability of the Sommerfeld duty parameter, the test program did not allow for a large number of results to be obtained, providing the initial recordings gave good correlation with theory.

By applying the misaligning couple in the reverse direction, such that during the first test the one end of the journal was forced vertically down, and for the second test run was forced in an upward direction, would not only prove the correctness of the computer program for the steady loaded conditions, but also check for any machining errors across the axial length of the bearing causing an unevenness in the oil film wedge.

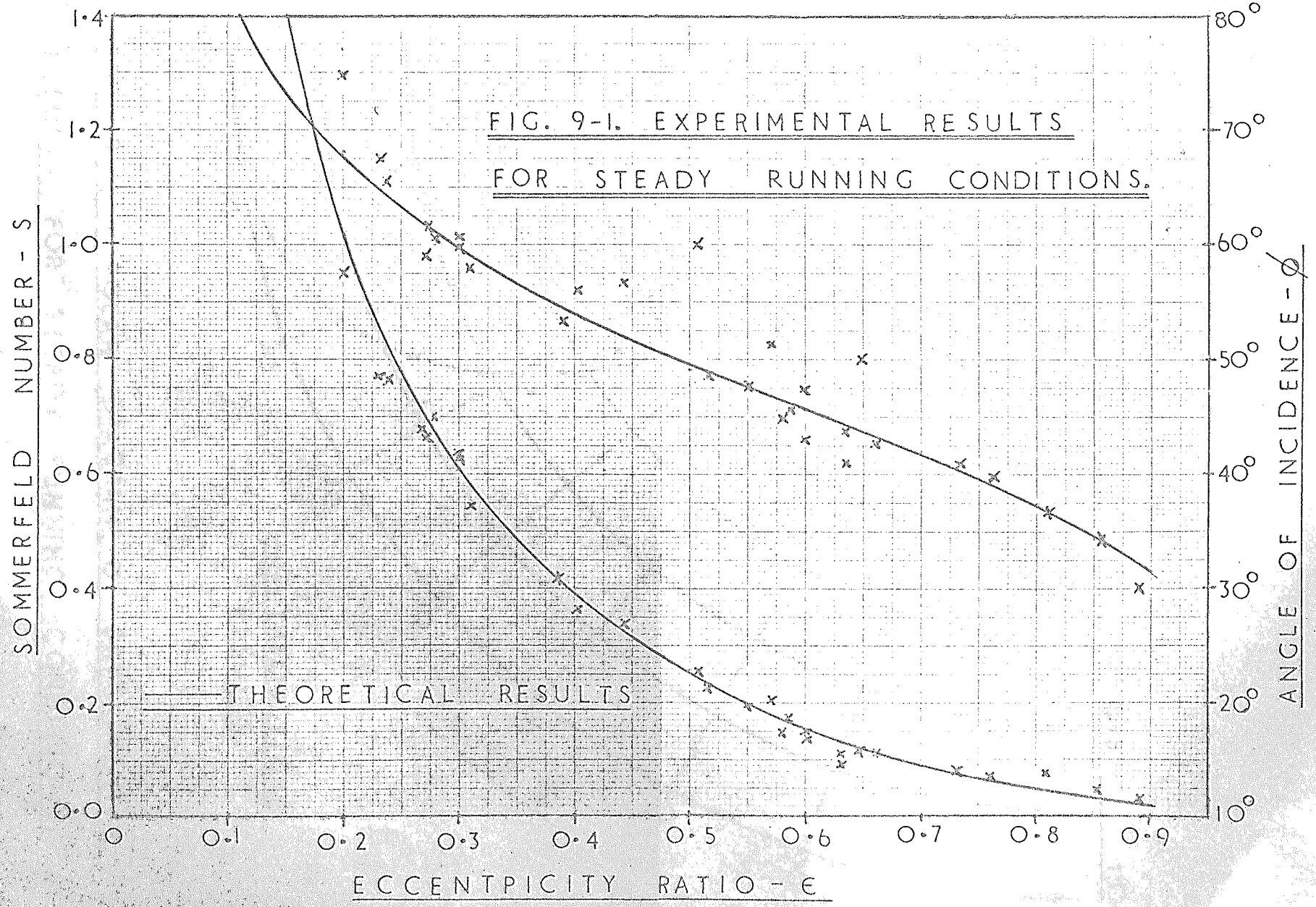
FIG. 9-1. EXPERIMENTAL RESULTS
FOR STEADY RUNNING CONDITIONS.
THEORETICAL RESULTS
SOMMERFELD NUMBER - S
ANGLE OF INCIDENCE - ∅
ECCENTPICITY RATIO - ∈
1·4
1·2
1·0
0·8
0·6
0·4
0·2
0·0
80°
70°
60°
50°
40°
30°
20°
10°
0
0·1
0·2
0·3
0·4
0·5
0·6
0·7
0·8
0·9

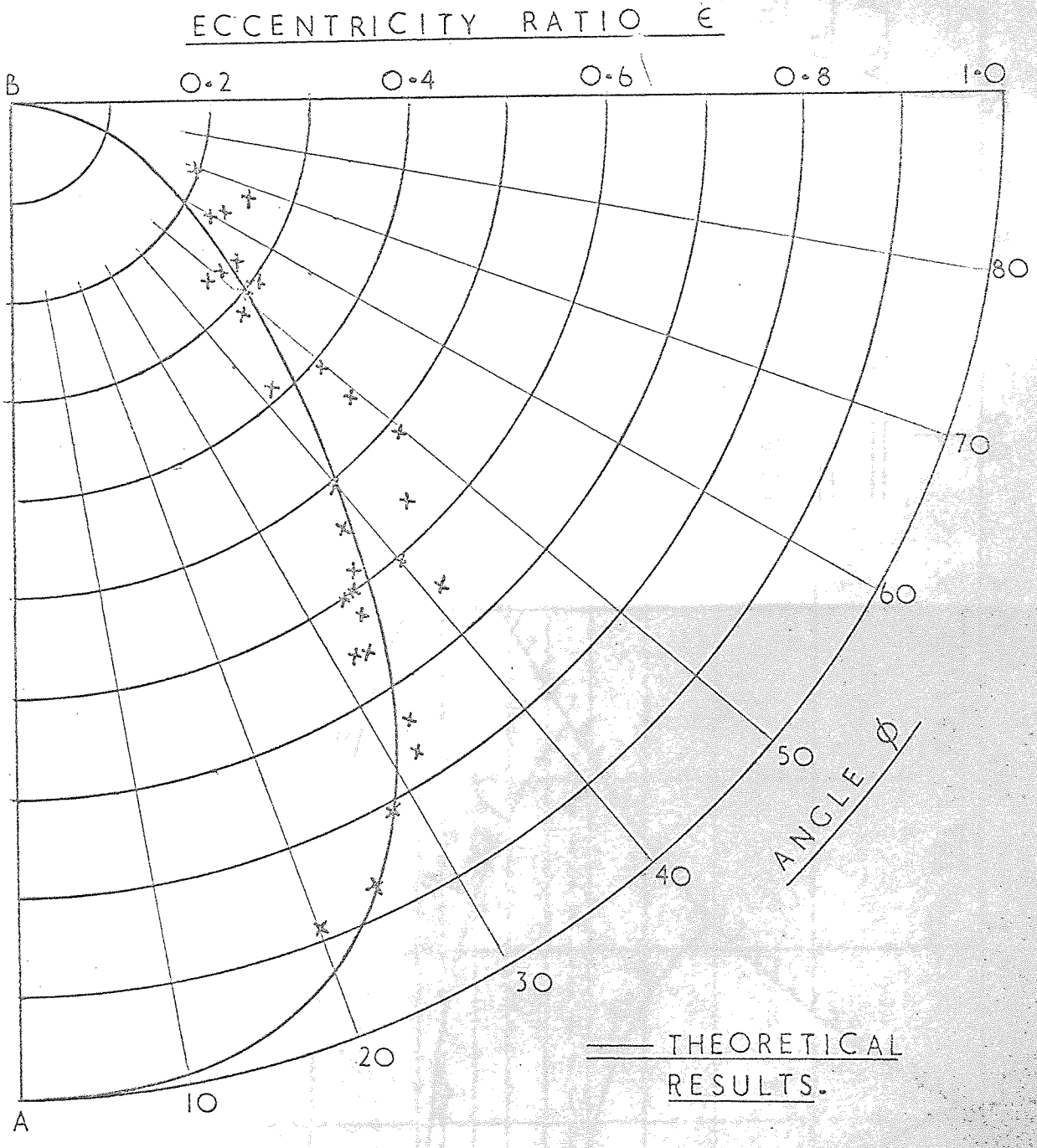

FIG. 9-2. POLAR DIAGRAM OF EXPERIMENTAL RESULTS FOR STEADY RUNNING CONDITIONS.

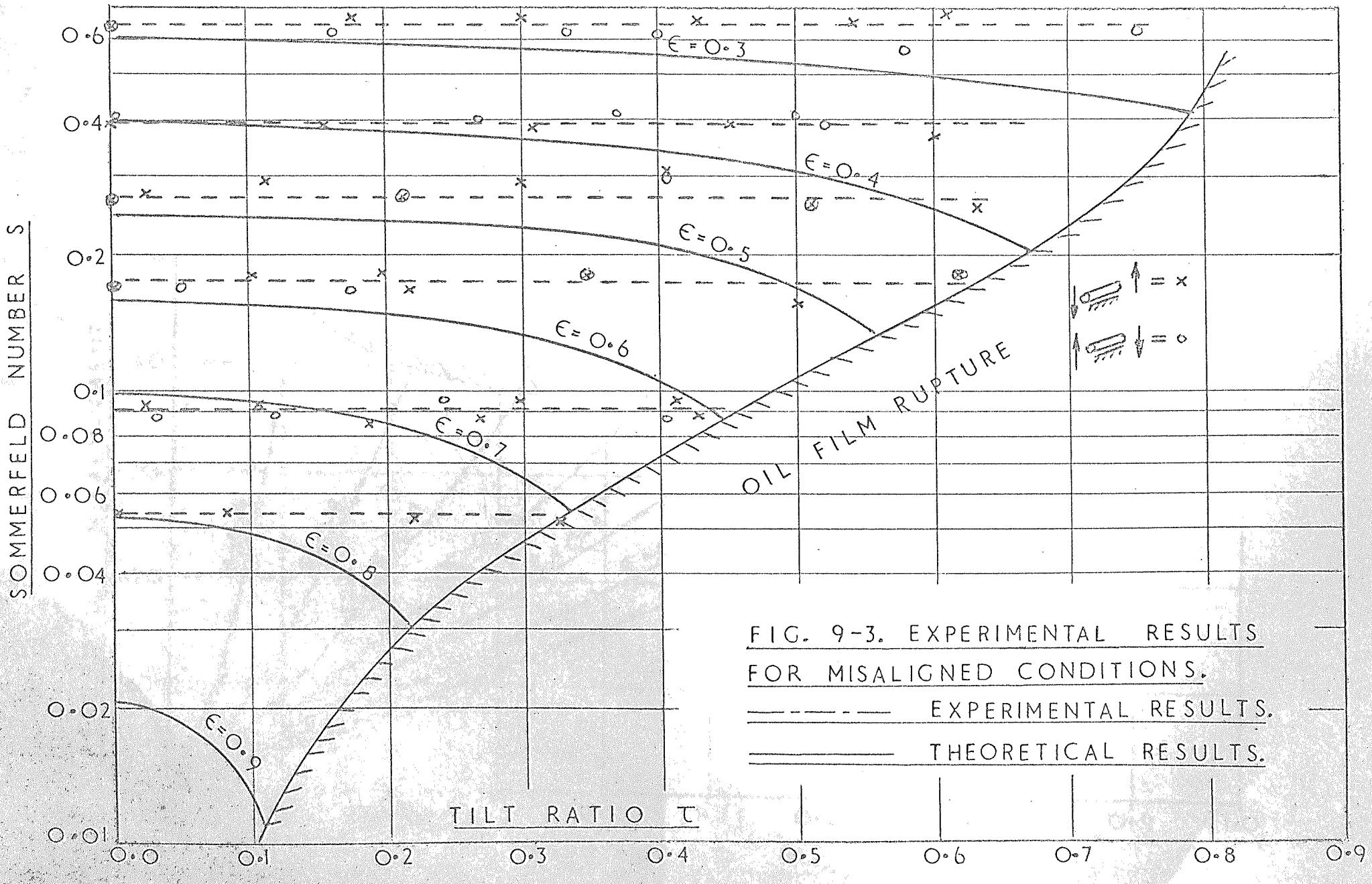

FIG. 9-3. EXPERIMENTAL RESULTS FOR MISALIGNED CONDITIONS.

EXPERIMENTAL RESULTS.

THEORETICAL RESULTS.

FIG. 9-4 AXIAL MOVEMENT OF CENTRE OF PRESSURE AGAINST JOURNAL TILT.

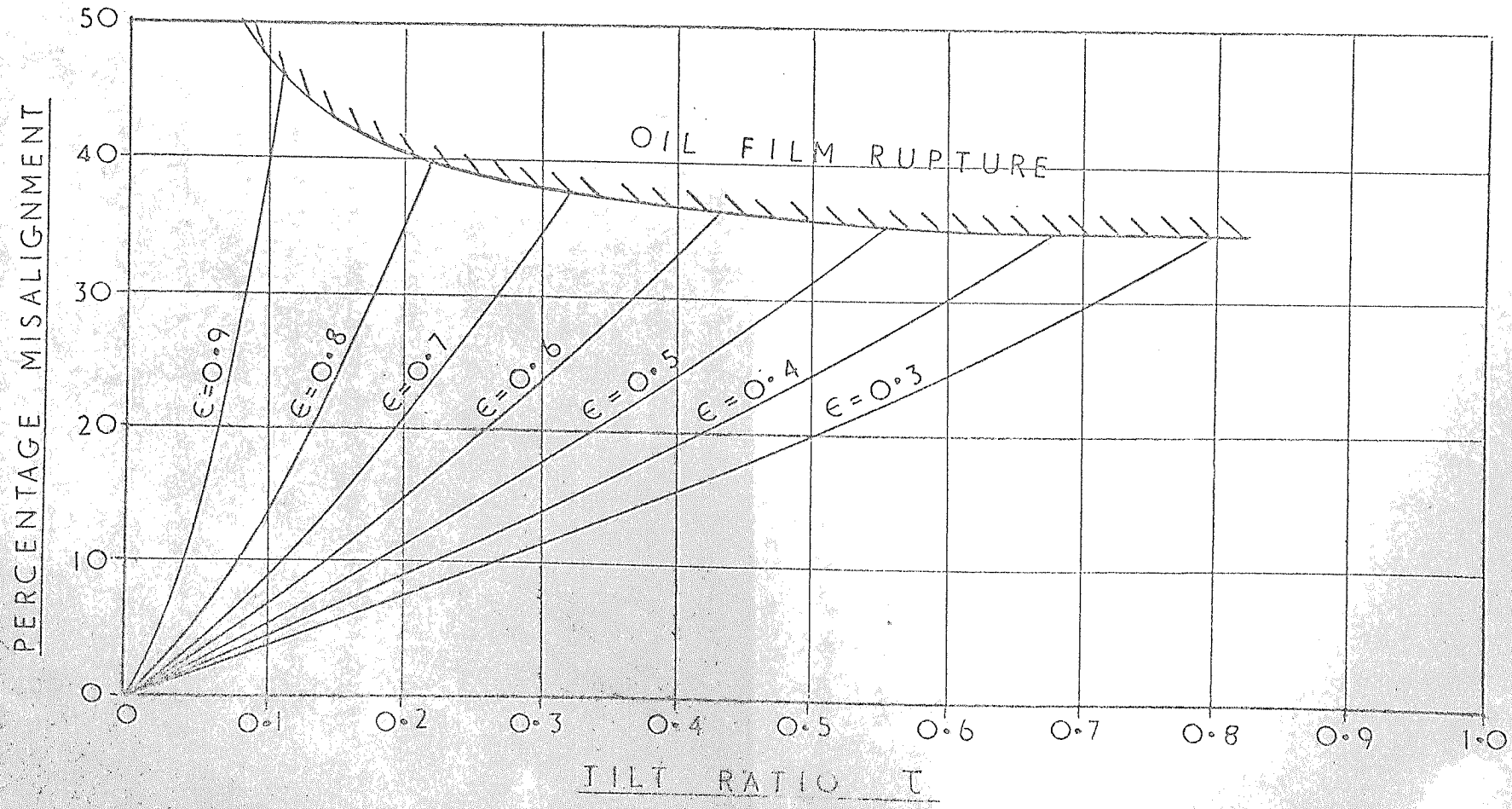

CHAPTER TEN

CHAPTER TEN

THEORETICAL-EXPERIMENTAL FORCE COEFFICIENTS

10-1. Hagg and Sankey type of coefficients (i.e. four coefficients)

The writer has failed to find any completely satisfactory method for accurately dealing with equations of journal motion involving only four coefficients, such equations were found to be of limited use when presenting the bearing dynamic characteristics for heavy rotors running at high speeds, further such coefficients are limited to synchronous vibrating forces. Nevertheless, as information dealing with four coefficients has been published, consideration to this presentation is necessary.

Experimental work published by Hagg and Sankey reference (28) and (29) presents dynamic coefficients observed from the elliptical orbital response, excited by a known out-of-balance force. By using test equipment of rigid construction, thus eliminating additional degrees of freedom, it was possible, by applying a known disturbing force and measuring the resulting amplitude and phase in two co-ordinate directions, to obtain two force-displacement coefficients and two force-velocity coefficients along the major and minor axis of the whirl trajectory.

In setting up the problem the above authors made two unfounded assumptions, allowing inaccuracies in their experimental results.

For example, it was assumed that the dynamic characteristics of the oil film was not influenced by conditions external to the bearing, thus accelerating forces other than unbalance were made zero. This assumption is hardly permissible when considering a rotor of a machine, as the adjoining masses to the bearing are several times greater than the small mass of the journal. The second assumption made, was that tests were conducted with a pure out-of-balance disturbing force, thus allowing the cross coupling terms to be equal to each other, allowing components of force to be taken when presenting the major and minor coefficients. However, the unbalance force also generates acceleration forces produced by the mass of the journal, the resultant of which is no longer a vector of fixed magnitude rotating at shaft speeds, suggesting therefore that consideration must be given to the cross-coupling spring and velocity terms if accurate results are to be obtained.

It is because Hagg and Sankey type of force coefficients are easily obtained by employing synchronous unbalance, that they are favoured by most industries engaged in the manufacturing of rotating equipment, therefore if such measurements are taken, careful consideration must be given to the inertia forces of the vibrating journal and supporting structure, and only like for like conditions should be considered.

In order to demonstrate the effects of inertia force upon Hagg and Sankey coefficients, the following theoretical analysis was made. By considering components of the hydrodynamic oil film forces as derived by expanding Taylors series giving the resulting equations of motion as shown in equations (6.1) and by equating to zero all

second order terms, the following equations of forces were obtained for the motion of the journal

$$M\ddot{x} + A(xx)x + A(xy)y + A(x\dot{x})\dot{x} + A(x\dot{y})\dot{y} = m\omega^2 r\sin t$$
$$M\ddot{y} + A(yx)x + A(yy)y + A(y\dot{x})\dot{x} + A(y\dot{y})\dot{y} = m\omega^2 r\sin t \qquad (10.1)$$

The above analysis was made on the assumption that all journal displacemerts are sufficiently small as to permit linearisation of the oil film forces, this assumption will be shown later not to be true except for extremely small displacements, but is a necessary requirement for this analysis in order to use the eight linear force coefficients.

Introducing a given set of operating conditions and by using equations (10.1) the orbital response may be determined for a synchronous disturbance, excited by a known out-of-balance force, from these results simulated Hagg and Sankey force coefficients may be determined by selecting two displacement and two damping coefficients which will produce identical response characteristics. The results of this investigation are given in figures (N-1,2,3 and 4).

Figure (10.1) illustrates the change in the minimum oil film stiffness for different values of eccentricity ratio. The contained curves show very little change in the oil film elasticity even for large changes made to the value $m\omega^2$, and may thus be neglected. Curve (4) in figure (10.1) i.e. $m\omega^2 = A(yy)$ is most unlikely to be experienced in practice, and is only presented to demonstrate extreme conditions. However, it is clear from figure (10.2) that if $m\omega^2$ had been given a value greater than zero, but less than A(xx), when solving

equations (10.1) Hagg and Sankey values could have been obtained, indeed these curves do suggest that the magnitude of the mass of the test journal used by Hagg and Sankey must have been small. This conclusion is further verified by illustrations of the test rig used by H & S which suggests that the 3.0 in dia. test journal was hollow.

Figure (10.2) demonstrates the influence of $m\omega^2$ upon the magnitude of the maximum oil film stiffness, the larger the value of $m\omega^2$ the weaker the equivalent film stiffness becomes, to the extent that it becomes weaker than the oil film stiffness along the major axis of vibration. The physical implication here, is that the out of balance force is no longer constant but is affected by the acceleration force generated by the mass of the journal, thus the stiffness is masked by the presence of the cross coupling terms and because the phase change becomes more predominate for the larger values of $m\omega^2$.

This last statement may not be readily appreciated unless the whirl trajectory is shown illustrating the journal displacement vector, relative to the angular position of the unbalance force vector. Figure (10.5) illustrates the response to an out of balance disturbance acting in the same direction as the journal rotation, and figure (10.6) again shows the response to an unbalance force, but this time acting in the reverse direction to the journal rotation, referred to in this thesis as reverse whirl. Both figure (N-5) and (N-6) were determined using identical duty parameters. It should be noted that the radial force at the position of maximum and minimum amplitudes of vibration is acting towards the centre of rotation which is due to a 90^{o} phase angle.

The obvious features of the orbital ellipse is that the force vector leads the displacement vector by an angle dependent upon the eccentricity ratio, also the ellipse closes for one complete cycle of the excitation force, thus following conventional theory of vibrations. Further, the ratio of the major to the minor axis of vibration is notably larger for the higher eccentricity ratio which provides a "tell-tale" indication of the steady running position of the journal relative to the bearing bush. A further interesting phenomenon is that although the excitation force is rotating in the reverse direction, to the journal rotation, the whirl trajectory continues to rotate in the same direction as the journal rotation, thus offering a stabilizing effect to the vibration amplitudes. Assigning some value to $m\omega^2$ the journal response changes, the degree of change is demonstrated in figures (10.7) and (10.8) which illustrates the journal whirl in the forward and reverse directions. The noticeable changes being the angle of inclination between the force and displacement vectors and also the increased amplitude of displacements, again this behaviour is conclusive with vibration theory.

Returning to the discussion on the four H & S coefficients, the effects upon the damping coefficients for a change in magnitude of $m\omega^2$ are basically the same as with the stiffness coefficients. For example curve (1) of figures (10.3) and (10.4) shows the values obtained by H & S and curve (2) are results obtained using equation (10.1) but with $m\omega^2$ equal to zero. It can be seen that assigning a value to $m\omega^2$ the resulting damping curve tends to approach the H & S results, slight discrepancies being attributed to scatter in the experimental results obtained by H & S.

10.2 Consideration to equations of motion having eight force coefficients

In the previous section (10.1) dealing with only four coefficients, the u and v axes were orientated as to provide the maximum and minimum amplitudes of vibration, as illustrated in figure (10.7); for example for $\varepsilon = 0.5$ the major axis is 23.2 degrees from the horizontal and of course the minor axis is normal to the major. However, when considering eight coefficients the incremental forces are considered along the x and y cartesian coordinate axes as given by equations (5.1).

When using the eight force coefficients, the basic assumption made is that although the coefficients are extremely non-linear throughout the running range of the bearing, they do however remain linear for a fixed value of εo, ϕo. Although this assumption is always made when considering the experimental and theoretical investigations, it is by no means self-evident that it is an accurate one. Usually this assumption is further qualified by stating that all force displacement-velocity relations are linear for journal motions having small amplitudes of vibration, compared with the oil film thickness. The validity of this assumption can only ultimately be proved, or disproved, by comparing analytical results with results obtained from a series of tests conducted over a wide range of operating conditions, including forward and reverse synchronous vibration, and for vibration frequencies above and below the rotational frequency of the journal.

In order to produce a direct comparison between theoretical force coefficients, with those obtained experimentally, it would be

more informative to illustrate the measured and calculated orbital whirl trajectories for a given disturbing force, compared to a series of curves, giving the non-dimensional force coefficients. Indeed the latter presentation could be misleading as the magnitude of the displacement could be masked by the presence of heavy damping. Figures (10.9) and (10.10) illustrate the orbital response for synchronous vibration in the same direction as the journal rotation, and reverse to the journal rotation respectively. The speed of the journal rotation during the tests was maintained at a constant speed of 2,700 R.P.M. and also the centrifugal force was kept constant at 192 lbs force (853 Newtons). Also throughout all the tests presented in this section the journal was parallel with the bearing bush.

A comparison of the elliptical orbital response for forward and reverse whirl at a particular eccentricity ratio, illustrates the angular position of the force vector relative to the displacement vector to be altogether different, also it becomes obvious that reverse whirl has a stabilizing effect by reducing the amplitudes of the journal vibration particularly along the minor axis of the elliptical orbit.

There is very good correlation between the theoretical and experimental results for the general shape of the whirl trajectory, and to some extent for the angular position of the force vector. However, the experimental response orbit has a considerable reduction in amplitude compared to the response deduced from theory. These results also illustrate how the motion of the journal is affected by the duty parameter caused by changing the specific pressure of the bearing, and to a lesser extent a change made to the

oil film viscosity caused by a corresponding change in the thermal balance of the bearing. Clearly, all the experimental response orbits are suppressed by a considerable amount, varying between 20 to 30 per cent reduction compared to the theoretical results, indicating that for synchronous whirl conditions, there is, at this stage of the investigation, some unknown factor influencing the journal response.

The test results illustrated in figure (10.11) and (10.12) are again for a journal having a constant speed of 2700 R.P.M. but having the frequency of the excitation force kept as low as possible, such that the centrifugal force produced a measurable journal vibration whilst ensuring that measuring errors are minimal. Comparing these results with those in figures (10.9) and (10.10) clearly shows a dramatic change in the angular position of the force vector, and also the angle of inclination of the major axis of the whirl trajectory to the horizontal. The amplitude of vibration over the range of eccentricity ratios, for the low frequency whirl, are shown to be approximately of equal magnitude, this is because it was decided beforehand that 0.0005 in (0.0127 mm) was a reasonable low amplitude of vibration which the vibrating journal could go down to without loss of accuracy. To achieve this, it was necessary to increase the amplitude of the vibrating out of balance force, whenever the specific pressure on the bearing was increased.

10.3 Consideration to equations of motion having 28 force coefficients

By considering the xy cartesian coordinate system of axes described in the foregoing section, and using the equations of motion as shown by equations (6.1),theoretical whirl orbits of the journal

bearing may be simulated for a given disturbance excited by a known out of balance force. Throughout the following section the condition of parallelism of the journal with the bearing bush is retained.

As stated previously the introduction of the twenty additional force coefficients, being of second order, caters for any non-linearities generated within the oil film. A simple test to illustrate the degree of non-linearity would be to simulate a journal having different amounts of unbalance and to correlate the resulting vibrating amplitudes. If the oil film stiffness is of the HARD TYPE as suggested beforehand, then one would expect the resulting amplitudes of vibration to be less than proportional to the excitation force, showing an equivalent increase in the film stiffness for an increase in vibration amplitude. If the non-linearity is located in the damping effect of the oil film, and the equations of motion suggest that some of it is, then the magnitude of the orbital response will also be sensitive to the rotational frequency of the vibrating force, which would account for the results presented in figures (10.11) and (10.12) when compared with figures (10.9) and (10.10).

To demonstrate the behaviour of non-linearity with vibration amplitude, whirl trajectories were computed for varying amounts of unbalance which are presented in figure (10.15). Bearing operating conditions were chosen which were capable of being reproduced on the test bearing, namely a reactive force of 1141 lb (5050 Newtons) operating at a constant speed of 1680 R.P.M. vibrating at synchronous speed with varying amounts of unbalance. Curve (1) of figure (10.15) demonstrates the theoretical orbital response for an out of balance force of 250 lb.f (1110 Newtons) using the eight oil film force

coefficients, and curve (4) is for identical conditions but with an unbalance of 500 lb.f (2220 Newtons). The amplitude of the major and minor axis of vibration for curve (4) is exactly twice that of curve (1), also the angular position of the force vector remains unchanged for both whirl trajectories. These results are in complete accord with linear theory, and thus demonstrates the correctness of the computation. Curve (2) has the same conditions of exertation as curve (1) but with the addition of the twenty non-linear terms into the equations of motion, and curve (3) has the same unbalance as curve (4) but again with the addition of the non-linear terms into the equations of motion. Comparing curves (1) and (2) which both have an unbalance disturbing force of 250 lb.f, but clearly the addition of the non-linear coefficients have considerable effect in suppressing the whirl amplitudes. Also the angular position of the force vector for the non-linear equations of motion is approximately 20 degrees in advance compared to the force vector for the linear whirl orbit, indicating that the second order terms involving velocity are influencing the journal motion.

By comparing the major axis of vibration for the 250 lb.f with the same axis for the 500 lb.f i.e. curves (2) and (3) respectively, illustrates the extent of the non-linearity upon the amplitude of vibration; where twice the unbalance force using eight oil film coefficients gave twice the displacement, using the example illustrated in figure (10.15), twice the unbalance force using the twenty-eight coefficients only gave sixty per cent more deflection, thus demonstrating the effect of the second order terms in suppressing the amplitude of whirl. Indeed, the orbital whirl employing the second

order terms and an unbalance of 500 lb.f, is suppressed to such a degree, that its amplitude is practically the same as if only 250 lb.f had been used with the eight linear force coefficients, i.e. curves (3) and (1) respectively.

Although curves (1) to (4) are theoretical, the accuracy of this mathematical model is verified by curve (5) being obtained from experimental results. By comparing the experimental results, curve (5), with theoretical predictions using twentyeight coefficients i.e. curve (2), it can be seen that extremely good results can be obtained.

If having shown that the second order terms are important when determining the dynamic response of a journal bearing, it is equally important to recognise when, and if, they should be used. Normally only small displacements of the journal centre from its equilibrium position are considered, and theorists when predicting the theoretical dynamic response, or force coefficients, assume that forces involved are linearized. It is therefore necessary to take to the limit the work presented in figure (10.15) by reducing the magnitude of the disturbing force, and comparing the results obtained using the twentyeight coefficients with those only having eight coefficients. Only by making such a detailed study, is it possible to appraise what is considered to be a sufficiently small displacement in order to evoke the theory of linearized forces.

Table (10.1) lists the percentage reduction of the non-linear whirl orbit compared with the theoretical orbit for both the major and minor axis of vibration, together with the amount the non-linear force vector leads the linear force vector.

This investigation clearly demonstrates that in order to obtain experimental results to within 2 per cent error, the maximum displacement of the major axis must be limited to 0.00005 in which for this type of bearing would be quite unrealistic if meaningful results are to be obtained. Even if such small amplitudes could be measured successfully, it is most doubtful if phase of movement in the two coordinate directions could be measured, indeed the surface irregularities of the journal would be in the order of displacement measurements to be taken.

In order to ascertain if the above phenomenon is valid over the entire running range of the journal bearing, further tests were undertaken with a reactive loading of 2791 lbs (12391 Newtons) and a speed of 2700 R.P.M., producing an eccentricity ratio of up to 0.62, thus all the variables of the Sommerfeld duty parameter have in some way been changed.

Comparing the results in tables (10.1) and (10.2) the difference in percentage reduction for vibrations measured along the major axis, is only in the order of 2.0 per cent and 3.5 per cent along the minor axis for a non-linear displacement. It is therefore quite clear that even for the smaller amplitudes of vibration, it is essential for the second order coefficients to be included in the equations of motion.

In reference (40) Orcutt and Arwas presented measured and calculated whirl trajectories for a 110 degree centrally loaded journal bearing, having an L/D ratio of unity, their results by experimental and theoretical predictions are shown in figure (10.16). This reference demonstrates, quite independently, the seriousness of omitting the non-linear second order terms in the theoretical analysis, thus

substantiating the validity and accuracy of results presented in figure (10.5) and tables (10.1) and (10.2). Unfortunately the above authors did not compare the angular position of the force vector between experimental and calculated results, therefore it would be difficult to draw any conclusions from the results given in figure (10.16) as to the extent of any phase error.

The magnitude of the second order force coefficients are comparable for both the displacement and velocity components of vibration, as indeed are the cross coupling velocity/displacement coefficients. It is therefore necessary to include in this investigation the effects of velocity upon the dynamic orbital response, as well as the displacement as previously described. It is also important to illustrate that the assumption made by conventional theory of linearized dynamic characteristics is again invalid, and is dependent not only upon the amplitude of vibration but also upon the velocity of the exciting force. In order to demonstrate the effects of velocity upon the behaviour of the orbital response, the same mathematical model was used as in figure (10.15) but with the excitation frequency of the distributing force equal to twice the rotational frequency of the rotating journal i.e. $k = \Omega/\omega = 2.0$. (N.B. for synchronous vibration $k = 1.0$).

As to be expected the orbital response was more elliptical with a corresponding decrease in the angle of inclination of the major axis of vibration to the horizontal, together with a shift in the phase angle of the exciting force and the journal displacement. Using the same notation as in figure (10.15), curves (1) and (2) show the orbital response for an unbalance force of 250 lb (1100

Newtons) for the linearized eight coefficients, and the non-linear coefficients, and curves (3) and (4) represents an unbalance of 500 lb.f(2220 Newtons) for the linear and non-linear coefficients.

At first it would seem that the percentage reduction of the non-linear orbit compared with the linear results has improved, however, this is not so if one takes into account the magnitude of the whirl trajectory, remembering that non-linearity is a function if displacement. By making a direct comparison with tables(10.1) and (10.2) it can be shown that the percentage reduction of the non-linear orbit is of the same order as for a given amplitude of non-linear whirl.

A further important factor which may be deduced from figures (10.15) and (10.17) is that by increasing k=1.0 to k=2.0 the amplitude of the variation is reduced by the following ratios, Major axis - 50 per cent and Minor axis - 25 per cent, thus indicating that oil film damping plays a very predominant role in machine vibration by absorbing a great deal of the journal vibration, and thus lowering the dynamic magnifier. Whilst still discussing damping, the degree of damping is represented by the angular position of the force vector relative to the direction of the journal displacement, and for the model illustrated in figure (10.17) has a damping error of 27.6 degrees between linear and non-linear results for an unbalance of 500 lb.f and an error of 28.8 degrees for an unbalance of 250 lb.f clearly demonstrating the influence of the velocity coefficients.

If the theory of non-linearity for the velocity coefficients is to be taken to its limit, then values of k less than 1.0 should provide results similar to those illustrated in figures (10.11) and

(10.12) and in order to provide uniformity in results the same operating conditions for the journal are used.

Curves (1) and (2) in figure (10.18) presents the whirl trajectory for an unbalance disturbing force of 250 lb for the linear and non-linear force coefficients respectively, having a value of k equal to 0.5. A comparison between these two curves clearly shows the error between the two response orbits to be small, for example, for a linearized displacement along the major axis of 0.002 in suppresses the non-linear orbit by 8.5% and by approximately the same amount along the minor axis of vibration.

By increasing the disturbing force to 500 lb produces an amplitude of vibration of 0.0044 in along the major axis using the linear force coefficient, and upon using the non-linear coefficients only suppresses the vibration amplitude by 30 per cent along the major axis and 32 per cent along the minor axis. Results given in figure (10.18) suggest that provided both the amplitude of vibration and also the frequency of the exciting force are kept to an absolute minimum, then it is possible to check the accuracy of the eight linearized force coefficients without too much difficulty. However, because of the inherent phase error some discrepancies are to be expected in obtaining the velocity coefficients from the experimental recordings.

Curves presented in figures (10.15), (10.16) and (10.18) are based upon theoretical coefficients, which are non-linear in damping; however, they are not non-linear to the extent that displacements along the cartesian coordinate axis are forced to be non-harmonic, if

this was so it would violate the basic assumptions evoked for the solution of the equations of motion. Therefore in order to illustrate that displacements are "simple harmonic motion" and hence the velocity, ultra violet recordings are presented in figures (10.19) and (10.20) for low frequency and for synchronous frequency of vibration, these recordings being typical of the results obtained verify that assumptions made for the determination of the non-linear dynamic response orbits of vibration are indeed correct.

10.4 Further experimental evidence

Results presented in figures (10.21 A/B) and (10.22 A/B) were obtained experimentally from the test bearing, operating over a wide range of running conditions, and also with the disturbing force running synchronously with the journal in both the forward and reverse directions respectively. Theoretical results are also shown, and provide an ultimate check on the value of using the twentyeight force coefficients. The computed results were obtained using both the measured eccentricity ratio and also checked using the calculated Sommerfeld duty parameter.

Further results are presented in figures (10.23 A/B) and (10.24 A/B) again showing a comparison between theoretical and experimental results, but with the frequency of the exciting force kept sufficiently low as to permit measurable amplitudes of vibration.

All results presented in figures (10.21 A/B) to (10.24 A/B) are based on the background outlined in the foregoing sections, and are aimed primarily at showing the accuracy of using the twentyeight force

coefficients in the equations of motion. In order not to unnecessarily burden the reader with a mass of experimental results all leading to the same conclusion, only a limited number are presented, but sufficient in number as to allow an examination of a journal bearing operating within the normal range of service conditions, usually experienced with rotating machines where the oil flow within the oil film wedge is laminar.

10.5 Effects of journal misalignment upon the dynamic characteristics

Even where bearing test rigs are employed to measure coefficient values, it is doubtful whether service conditions are always adequately duplicated. Thus between design charts produced from test results, and physical reality, there is a possibility for a considerable margin for error and to the uninitiated designer could give a false indication as to the operational performance of a particular rotor system under investigation. A single contributing factor influencing design charts is the introduction of misaligning couples externally applied to the journal bearing, indeed slight amounts of misalignment must be inherent in all journal bearing assemblies; therefore it is necessary to take into consideration the effects of misalignment when investigating the force coefficients generated within the oil film.

It is obviously impracticable to construct design charts to include all variables of misalignment, covering components in both the vertical and horizontal planes, therefore consideration is only given to misaligning couples acting in the vertical plane, which is considered to be the type of misalignment experienced in practice.

The experimental method adopted throughout this section of the practical investigation, was to check the accuracy of the design charts providing force coefficients for varying amounts of misalignment, by comparing the theoretical and experimental whirl trajectories, and also to provide visual evidence of how the elliptical response orbit is suppressed by the presence of misalignment within the oil film. Although this makes the presentation of the results clumsy, nevertheless it does clearly display the importance of obtaining the degree of misalignment if accurate results are to be obtained.

In order to ensure that a direct comparison may be made between the perfectly aligned and misaligned journal, it was essential throughout both tests to ensure that the eccentricity ratio remained constant. To achieve this requirement the misaligned tests were conducted immediately after completing the tests for the aligned journal. It was also found necessary to add trim weights on the horizontal plane to ensure that misalignment was totally confined to the vertical plane, the magnitude of these weights was usually in the order of 1 to 2 lb.f i.e. 4.4 to 8.8 Newtons, at each end of the test journal, which compared to the total reactive weight was very small, thus any change made to the inertia force was negligible.

To conduct tests starting with a perfectly aligned journal, and repeating the tests with gradual increments of misalignment until full misalignment is achieved would be a formidable task if the full operating range of the bearing is to be investigated. If however, near extreme conditions of misalignment could be investigated with qualitative results, it would be reasonable to assume that intermediate force coefficients could be accepted as being correct without further qualification.

Experimental and theoretical results for misaligned conditions are presented in figure (10.25 A/B) and (10.26 A/B) for synchronous vibration in the same direction as the journal rotation and reverse to the journal rotation respectively. In all the results displayed, the larger elliptic orbit was for the perfectly aligned journal, and the smaller orbit represented the response for the misaligned condition. Also results are presented in figure (10.27) for forward whirl, but with the frequency of vibration kept as low as possible, without prejudicing the accuracy of the vibrations being measured.

10.6 Oil film temperature distribution

It was almost impossible to vary any single item of the duty parameter during testing, without simultaneously varying the temperature field of the lubricant. This was because the heat generated within the bearing is a function of any one of the following:- oil inlet supply temperature, ambient temperature of the surrounding air, speed and loading of the journal and viscosity index of the lubricant used. Therefore, before commencing the tests the film temperature distribution was recorded and again upon completion. To determine the duty parameter for the tests conducted, the oil film viscosity was calculated from the averaged bearing temperature data, and in order to isolate any variation in viscosity, and therefore minimize the difficulty in correlation between performance and theoretical predictions, tests were only considered valid if the averaged viscosity before and after testing was to within 1.0 per cent. To achieve this accuracy usually necessitated in running the bearing for three to four hours when commencing from the cold condition, and between one to one and one half hours between successive tests.

The temperature distribution over the working surface of the bearing bush is given in figure (10.28). From these results it can be seen that the maximum film temperature occurs adjacent to the oil film in the vicinity of the minimum oil film thickness, as indicated by the thermocouples 7, 8 and 9. Also, whilst conducting the tests it was possible to check for parallelism of the journal relative to the bush by checking if thermocouples 1, 4 and 7 were equal in magnitude to 3, 6 and 9, thus providing a check for any drift of the transducer amplifiers.

Introducing misalignment into the system clearly affects the temperature distribution, again the maximum temperature occured in the vacinity of the minimum oil film thickness. This was demonstrated by the increase in temperature of thermocouples 6 and 9 with respect to 4 and 7, correctly suggesting that misalignment was introduced in such a manner as to lift the journal, relative to the bush, at the driving end, and to lower the journal at the opposite driving end.

If a comparison is made between the averaged temperature of the oil film for the aligned and misaligned conditions, it will be noticed that misalignment does little to change the averaged temperature of the oil film, the worst condition being an increase in the misaligned condition having a 1.2 degree centigrade rise. Such information is most important to the design engineer as it allows the direct use of the duty parameter ZN/P, without further modification when predicting the misaligned running conditions. It further suggests that friction within the oil film also remains unchanged, again such information is of paramount importance to the designer when assessing the power generated by the shearing action of the oil

film wedge; it is based on such information that quantities of cooling oil are computed.

The variation of the temperature field also illustrates the importance of measuring the bush temperature with thermocouples positioned as close to the oil film as possible, and not by recording the oil outlet temperature from the bush, as has been the practice of many other researchers.

Throughout the tests the oil film temperature was found to remain unchanged with the introduction of journal vibration, however, temperature recordings were always made with the journal vibrating at the required amplitude and frequency.

10.7 Journal response about the steady running position i.e. about ε_o and ϕ_o.

Assumptions made in section (5.1) were that journal displacements, excited by a known out of balance force, should take the form of an ellipse, having as its pole the steady state running position ε_o and ϕ_o, further, the elliptic orbit closes when one full cycle of the disturbing force is made. As this was the starting point when evaluating the force coefficients, and hence the theoretical prediction of the dynamic whirl orbit, it is therefore necessary to demonstrate that these assumptions are indeed valid, if confidence is to be placed in the numerical analysis.

The test rig was designed in such a manner as to easily demonstrate this first assumption, by allowing the journal to operate at its steady running position and to apply the disturbing force without

having to stop the journal or adjust any of the operating parameters, thus allowing the superposition of the two running conditions, i.e. the first being the steady running position and secondly the dynamic running conditions. By monitoring the displaced journal centre on the C.R.O. allowed polaroid photographs to be taken, and by taking a double exposure of the two running conditions, would clearly demonstrate the relative running positions of the journal centre. Further if the exposure time was set equal to the inverse of the exciting frequency, would provide evidence of the latter assumption described above. However, this is better illustrated on the u.v. recordings i.e. figure (10.19) and (10.20).

Typical polaroid photographs are displayed in figure (10.29) selected over a wide range of running conditions. The bright centre dot represents the position of the journal running at speed under steady loaded conditions. The largeness of this centre dot is due to machining inaccuracies of the journal but mostly due to the carrier frequency of the oscillator breaking through, however, this effect is negligible when compared with the whirl orbit surrounding it.

Except for very slight discrepancies which may be attributed to a rocking motion of the journal, the results leave no doubt what-so-ever, that the whirl trajectory has as its pole the steady state condition.

10.8 Further visual evidence of the effect of misalignment upon the orbital response

Results presented in figures (10.25) to (10.27) were obtained from ultra violet traces providing an accurate method of obtaining a

semi-permanent recording. Further only near extreme conditions were considered, this being the misaligned condition close to oil film rupture. Therefore, in order to provide additional evidence of the effects of misalignment upon the dynamic response characteristics between extreme conditions, polaroid photographs were taken illustrating varying amounts of misalignment by making a number of re-exposures for each increment of the induced misaligning couple. The centre orbit of each photograph illustrates the vibrating journal when perfectly aligned, upon the introduction of a misaligning couple the two traces separate, the upper trace represents the end of the journal which experiences an equivalent reduction in load, and the lower trace represents the equivalent increase in load caused by the couple.

The dynamic whirl trajectories given in figure (10.30)are not intended to provide an accurate comparison between experimental and theoretical predictions, but only to show changes in whirl amplitudes, further, it was not possible to increase the amplitude of the elliptical orbit if the change in eccentricity at both ends of the journal was to be recorded simultaneously. Some of the orbits are blurred, again due to the carrier frequency breakthrough. However these photographs do provide a good indication of how the whirl orbit is suppressed due to the introduction of misalignment in the vertical plane, and to what extent the mean eccentricity changes.

Unbalance force (lbs)	Linear Coefficient		Non-Linear Coeff.		Percentage Error		Phase Error Degrees
	Major Axis	Minor Axis	Major Axis	Minor Axis	Major Axis	Minor Axis	
500.0	0.005116	0.002512	0.002485	0.001178	51.4	53.1	26.5
250.0	0.002558	0.001256	0.001538	0.00068	39.9	45.8	21.5
50.0	0.0005116	0.0002512	0.0004315	0.000193	15.7	23.3	9.0
5.0	0.0000511	0.00002512	0.000050	0.000024	1.5	2.8	1.5

TABLE 10.1 SUPPRESSION OF WHIRL AMPLITUDE AND PHASE ERROR DUE TO THE INTRODUCTION OF THE SECOND - ORDER (NON-LINEAR) FORCE COEFFICIENTS.

OPERATING CONDITIONS:- JOURNAL SPEEDS=1680 R.P.M., JOURNAL LOAD = 1141 lbs.

ECCENTRICITY RATIO = 0.2.

Unbalance force (lbs)	Linear Coefficient		Non-Linear Coeff.		Percentage Error		Phase Error Degrees
	Major Axis	Minor Axis	Major Axis	Minor Axis	Major Axis	Minor Axis	
500.0	0.001935	0.000969	0.001297	0.000618	33.0	36.1	26.3
250.0	0.0009674	0.000485	0.000755	0.000353	22.0	27.2	17.7
125.0	0.0004837	0.000242	0.0004207	0.000198	13.0	18.2	11.5
25.0	0.0000967	0.0000485	0.0000937	0.0000462	3.0	4.8	2.1

TABLE 10.2 SUPPRESSION OF WHIRL AMPLITUDE AND PHASE ERROR DUE TO THE INTRODUCTION OF THE SECOND-ORDER (NON-LINEAR) FORCE COEFFICIENTS.

OPERATING CONDITIONS:- JOURNAL SPEED = 2700 R.P.M., JOURNAL LOAD = 2791 lbs.
ECCENTRICITY RATIO = 0.62.

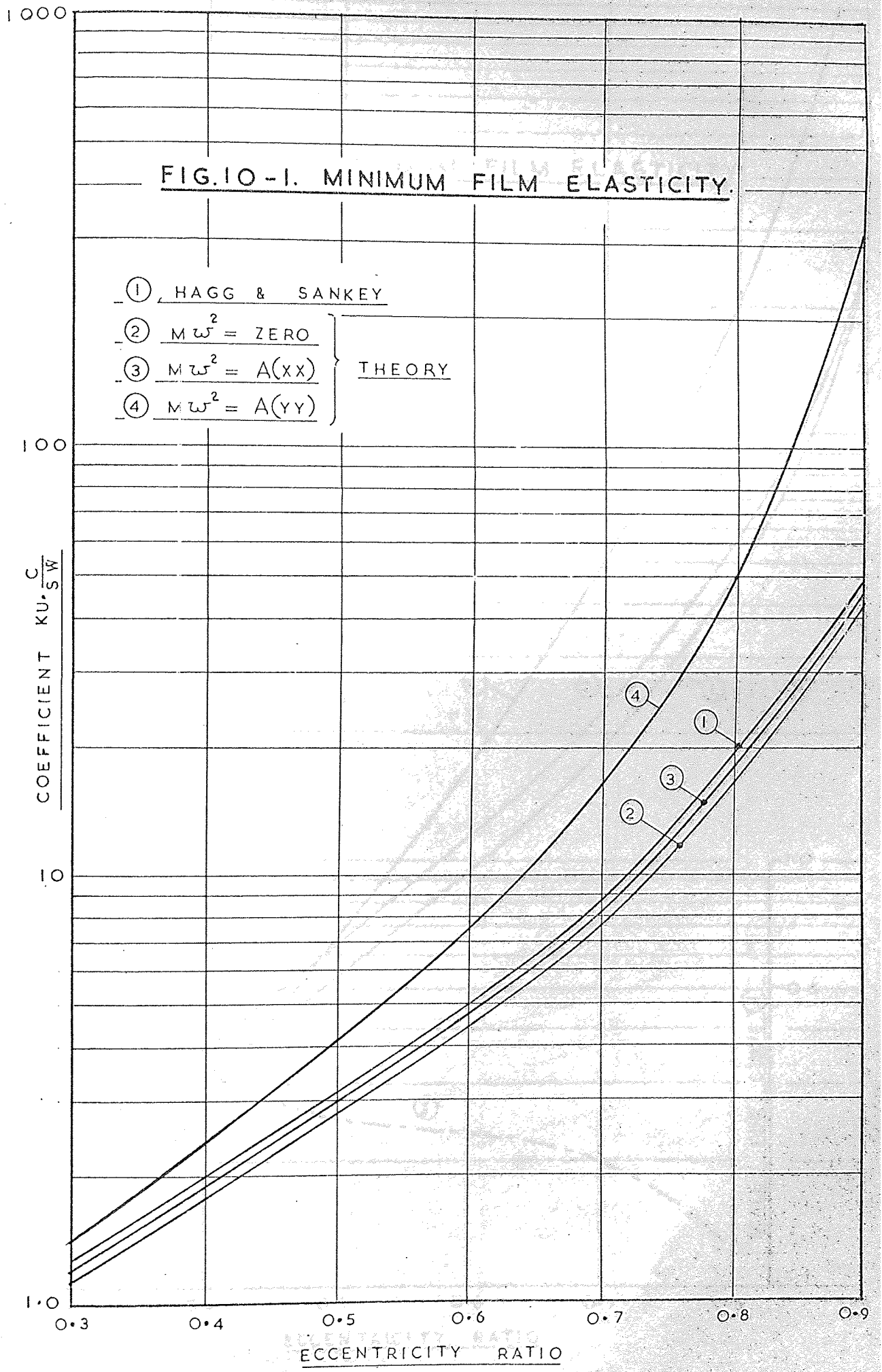

FIG. 10-1. MINIMUM FILM ELASTICITY.

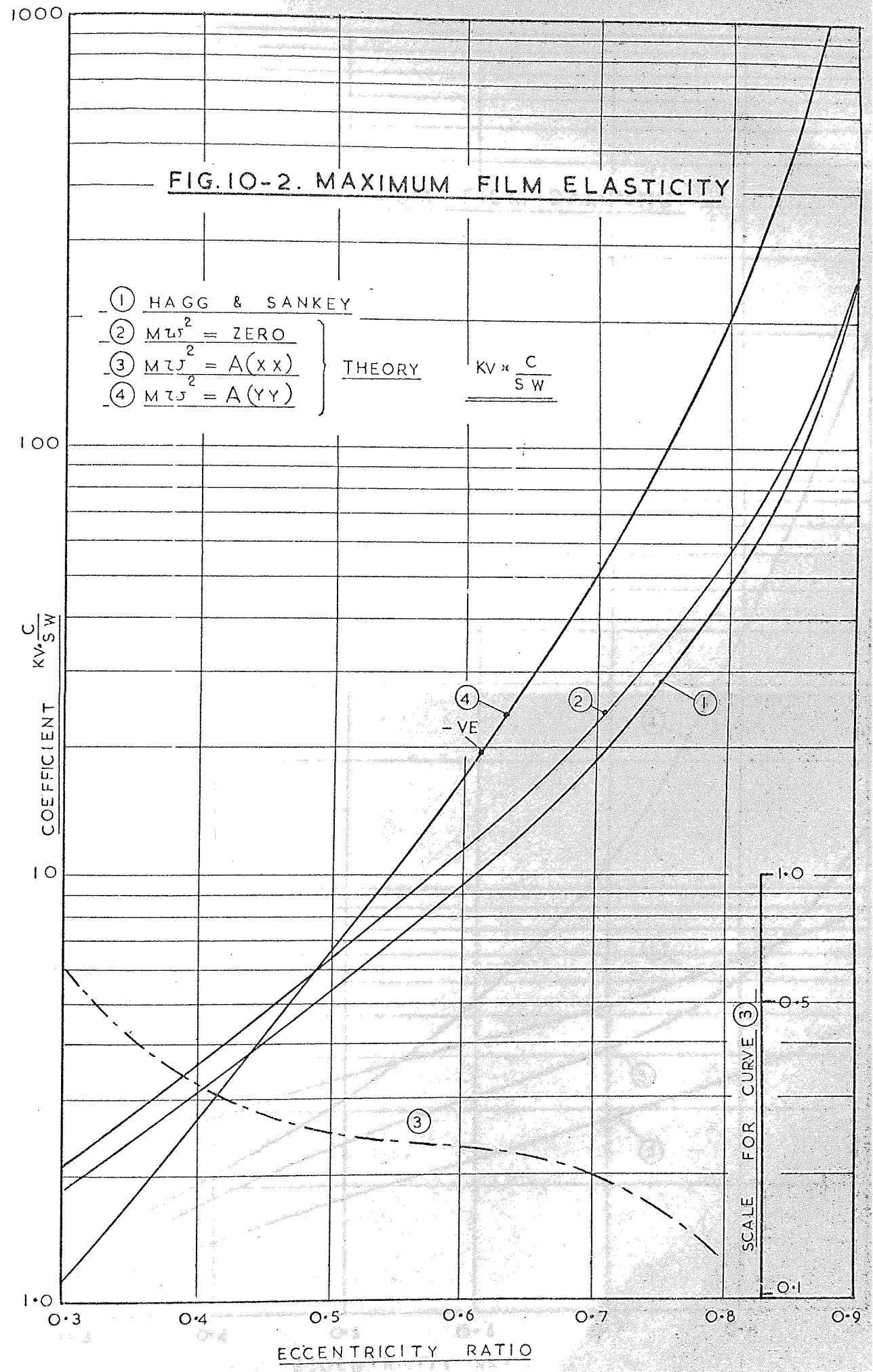
FIG. 10-2. MAXIMUM FILM ELASTICITY
1 HAGG & SANKEY
2 Mr²ω² = ZERO
3 Mr²ω² = A(XX)
4 Mr²ω² = A(YY)
THEORY
KV ∝ C/SW
1000
100
10
1·0
KV = C/SW COEFFICIENT
4
2
1
-VE
3
SCALE FOR CURVE (3)
1·0
0·5
0·1
0·3
0·4
0·5
0·6
0·7
0·8
0·9
ECCENTRICITY RATIO

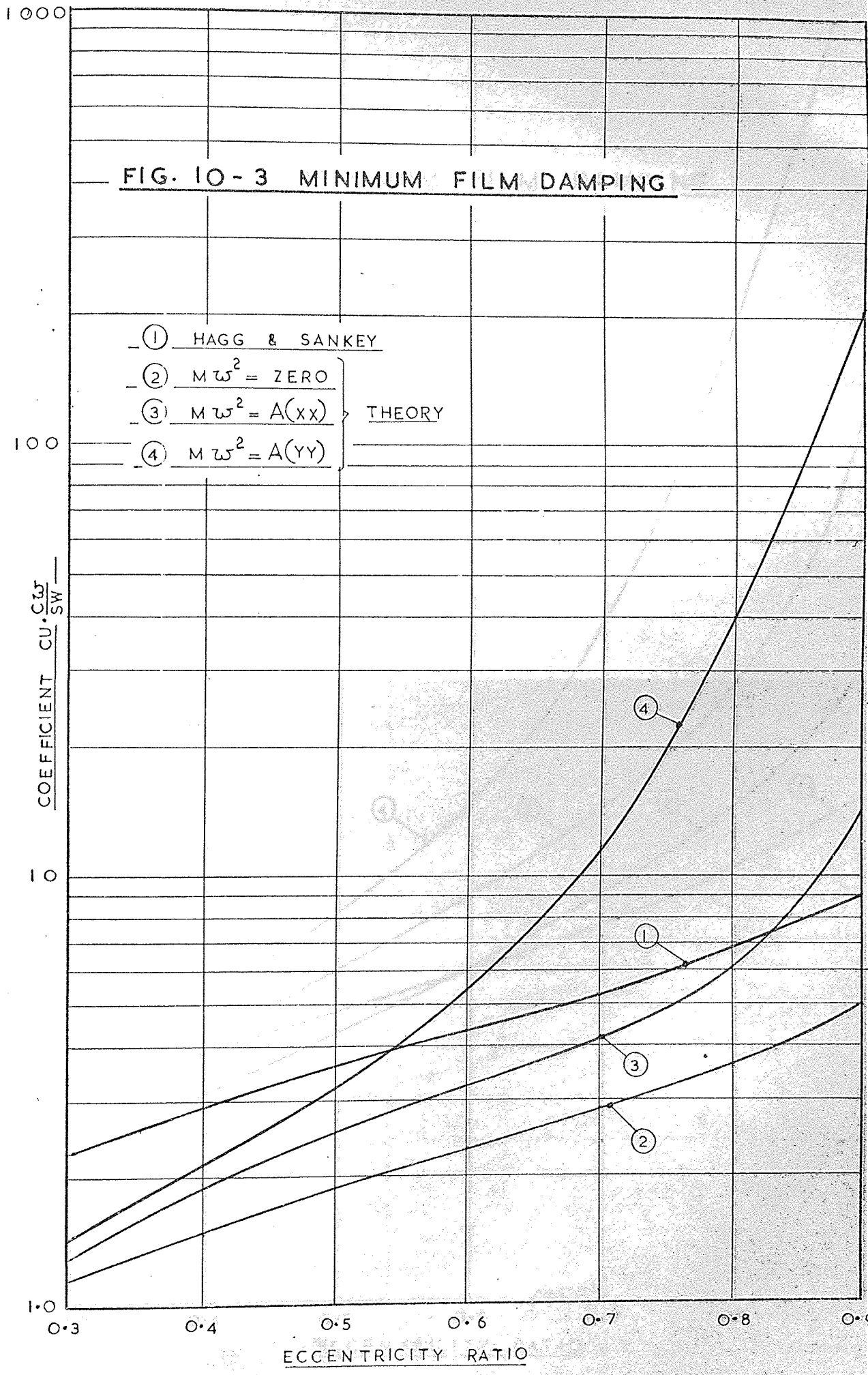

FIG. 10-3 MINIMUM FILM DAMPING

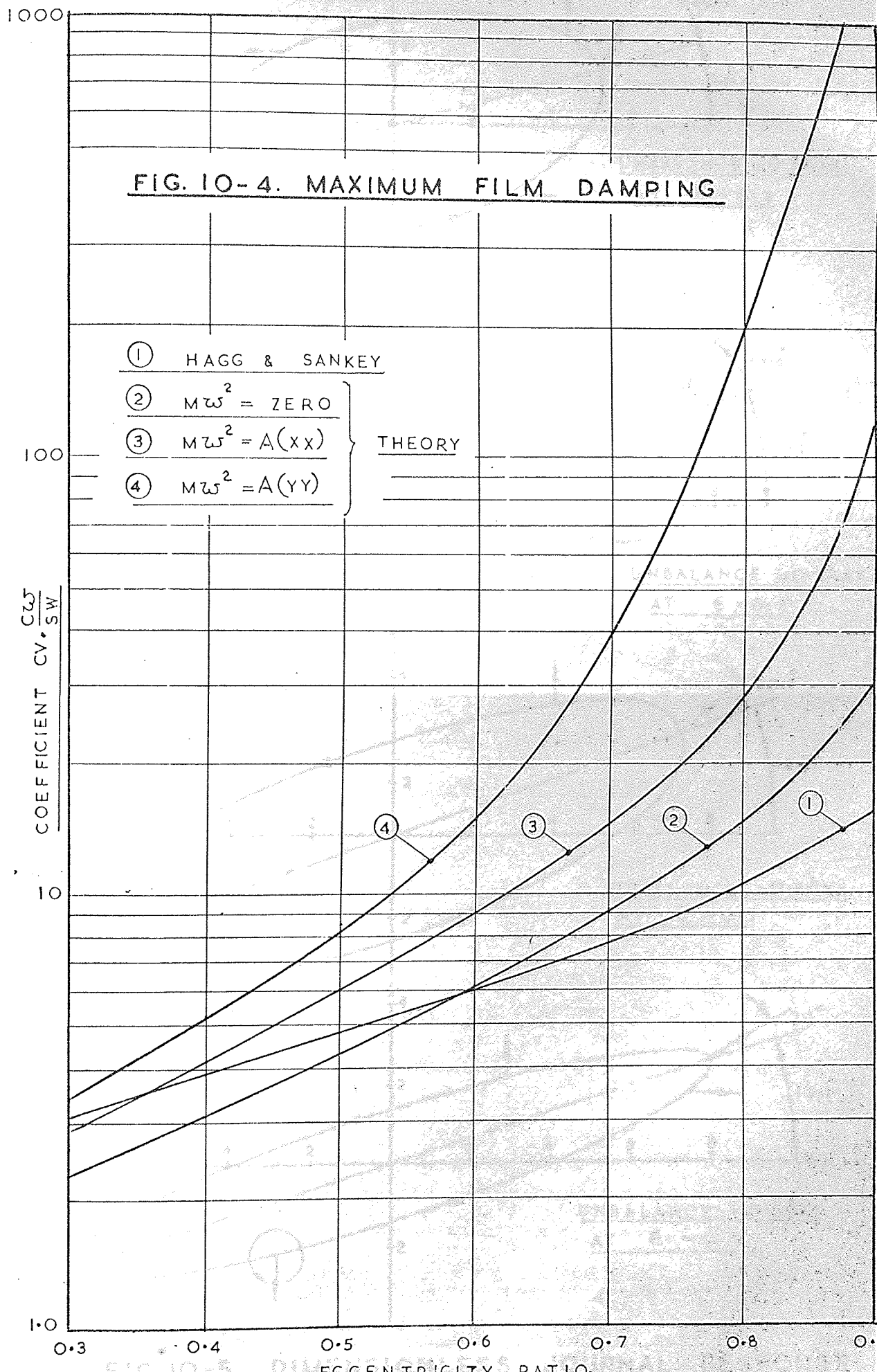
FIG. 10-4. MAXIMUM FILM DAMPING
1000
100
10
1·0
COEFFICIENT CV. $\frac{C\omega}{SW}$
① HAGG & SANKEY
② $M\omega^2$ = ZERO
③ $M\omega^2 = A(XX)$
④ $M\omega^2 = A(YY)$
THEORY
0·3
0·4
0·5
0·6
0·7
0·8
ECCENTRICITY RATIO

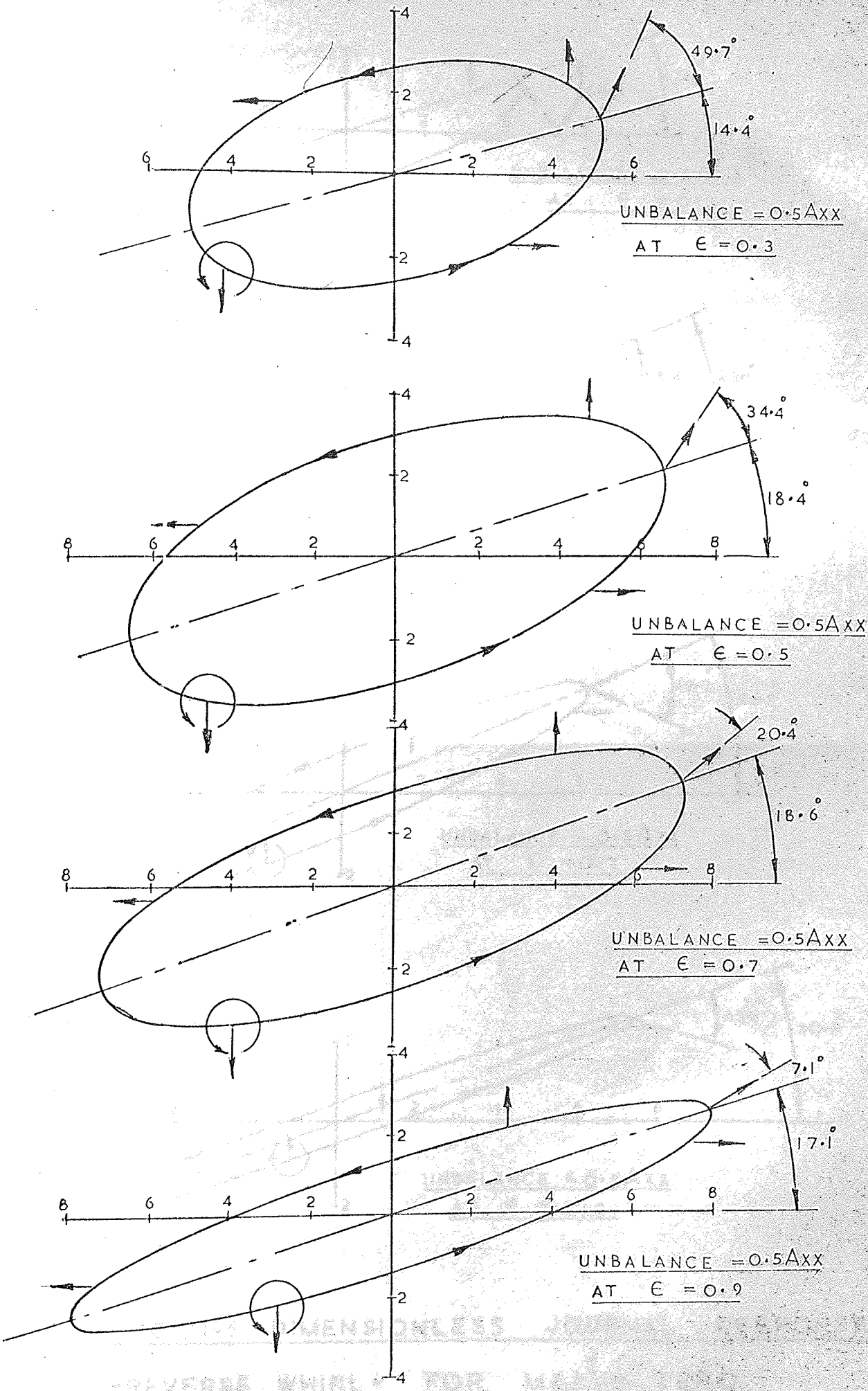

FIG. 10-5 DIMENSIONLESS JOURNAL RESPONSE -FORWARD WHIRL- FOR $M\omega^2 = Axx$.

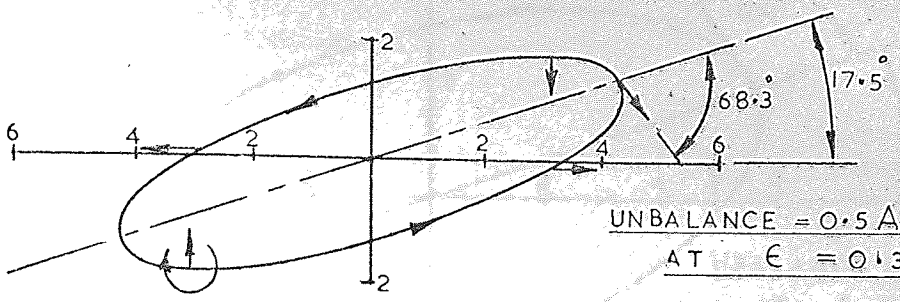

UNBALANCE = 0·5 A XX
AT ϵ = 0·3

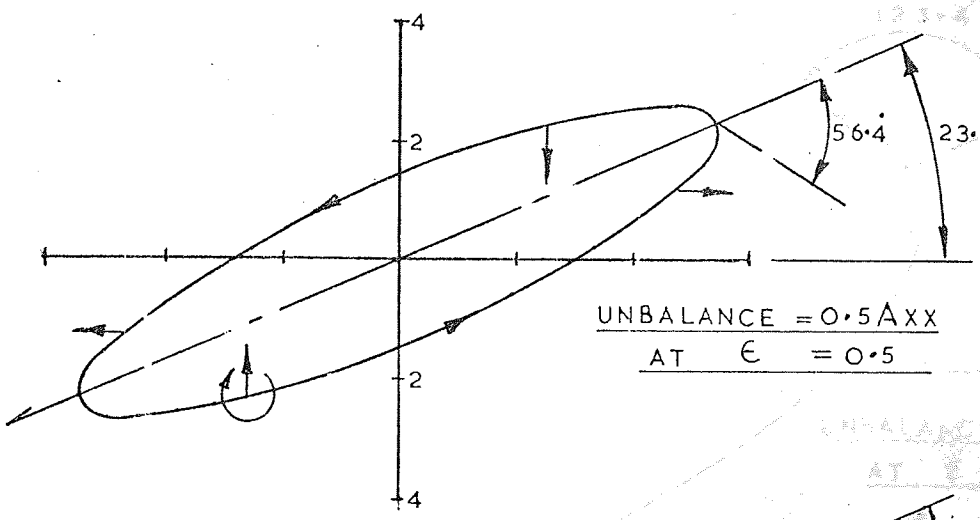

UNBALANCE = 0·5 A XX
AT ϵ = 0·5

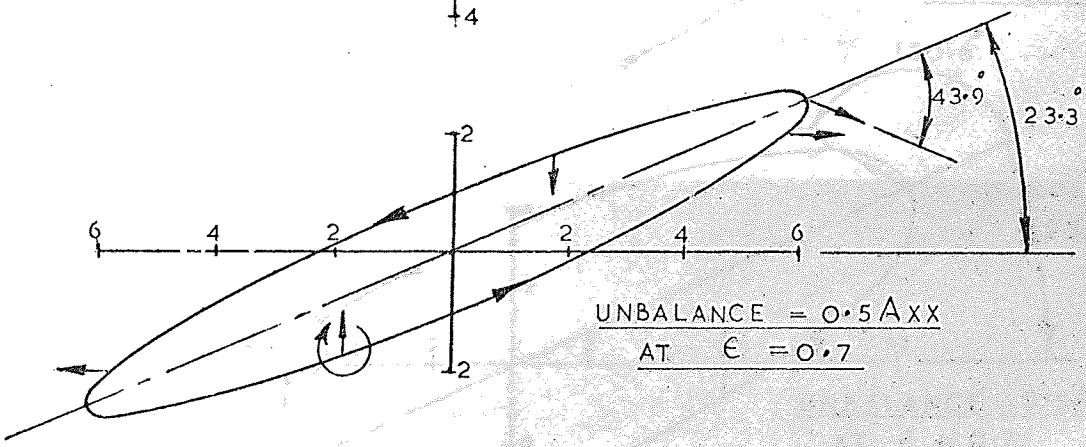

UNBALANCE = 0·5 A XX
AT ϵ = 0·7

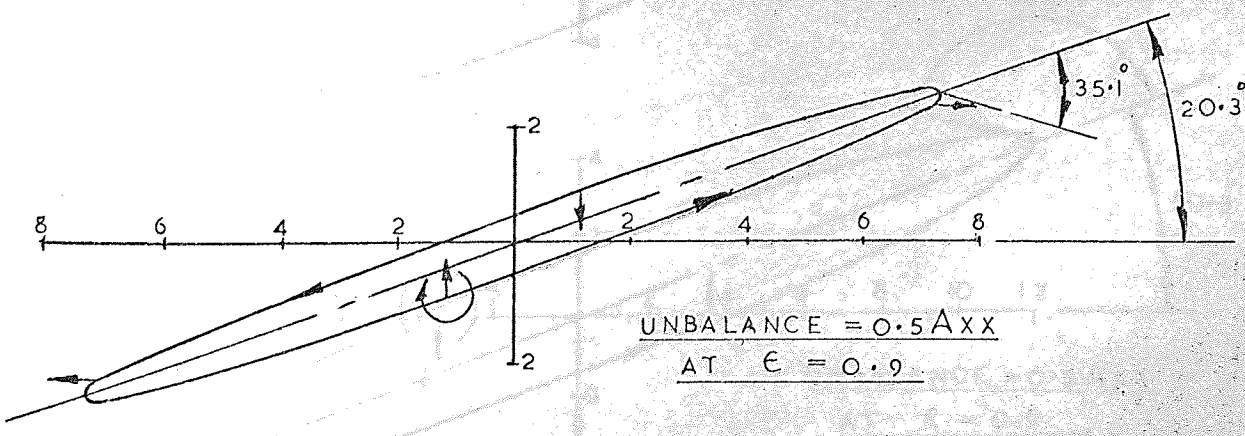

UNBALANCE = 0·5 A XX
AT ϵ = 0·9

FIG.10-6. DIMENSIONLESS JOURNAL RESPONSE -REVERSE WHIRL- FOR $M\omega^2$ = ZERO

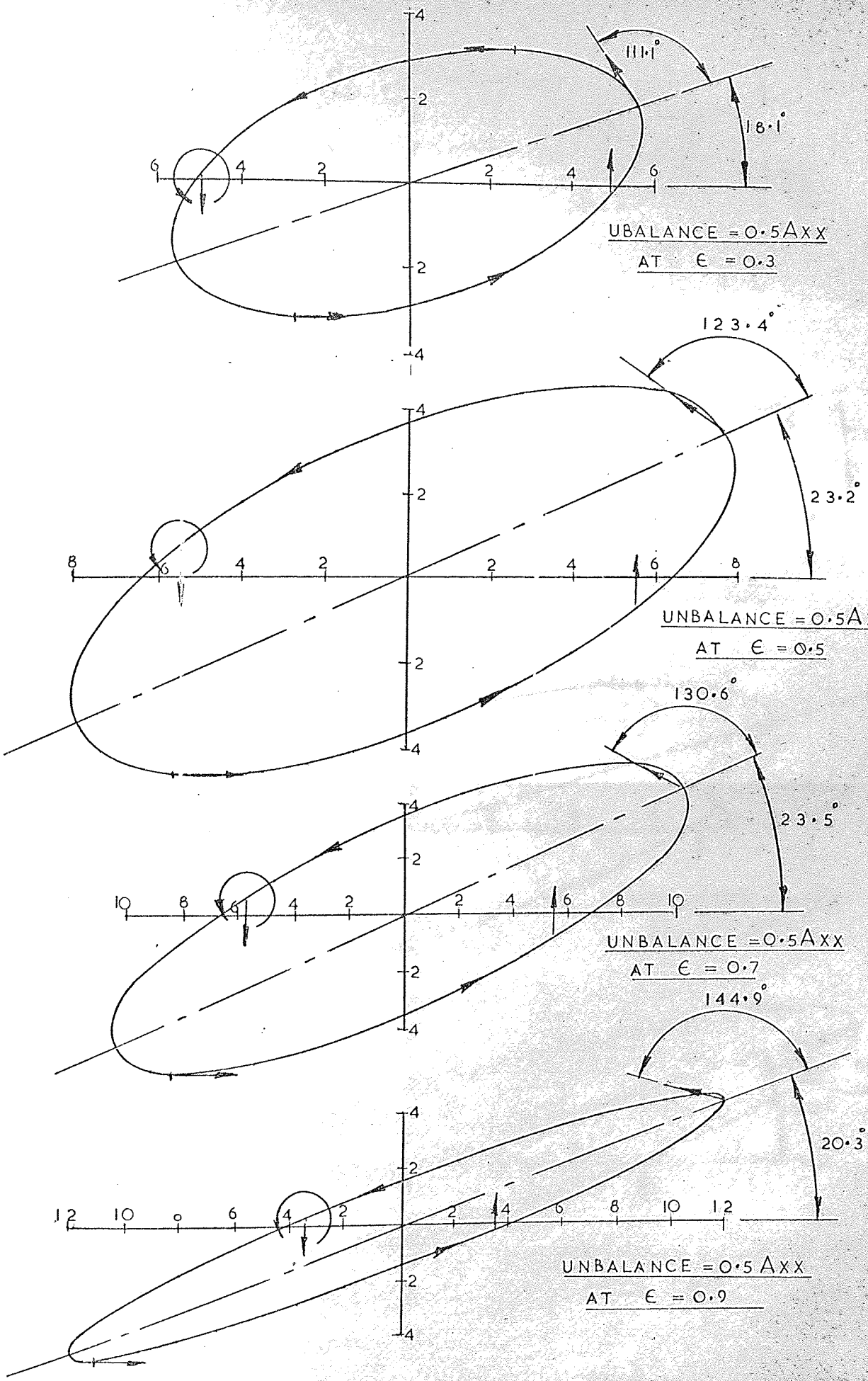

FIG. 10-7 DIMENSIONLESS JOURNAL RESPONSE -FORWARD WHIRL- FOR $M\omega^2$ = ZERO.

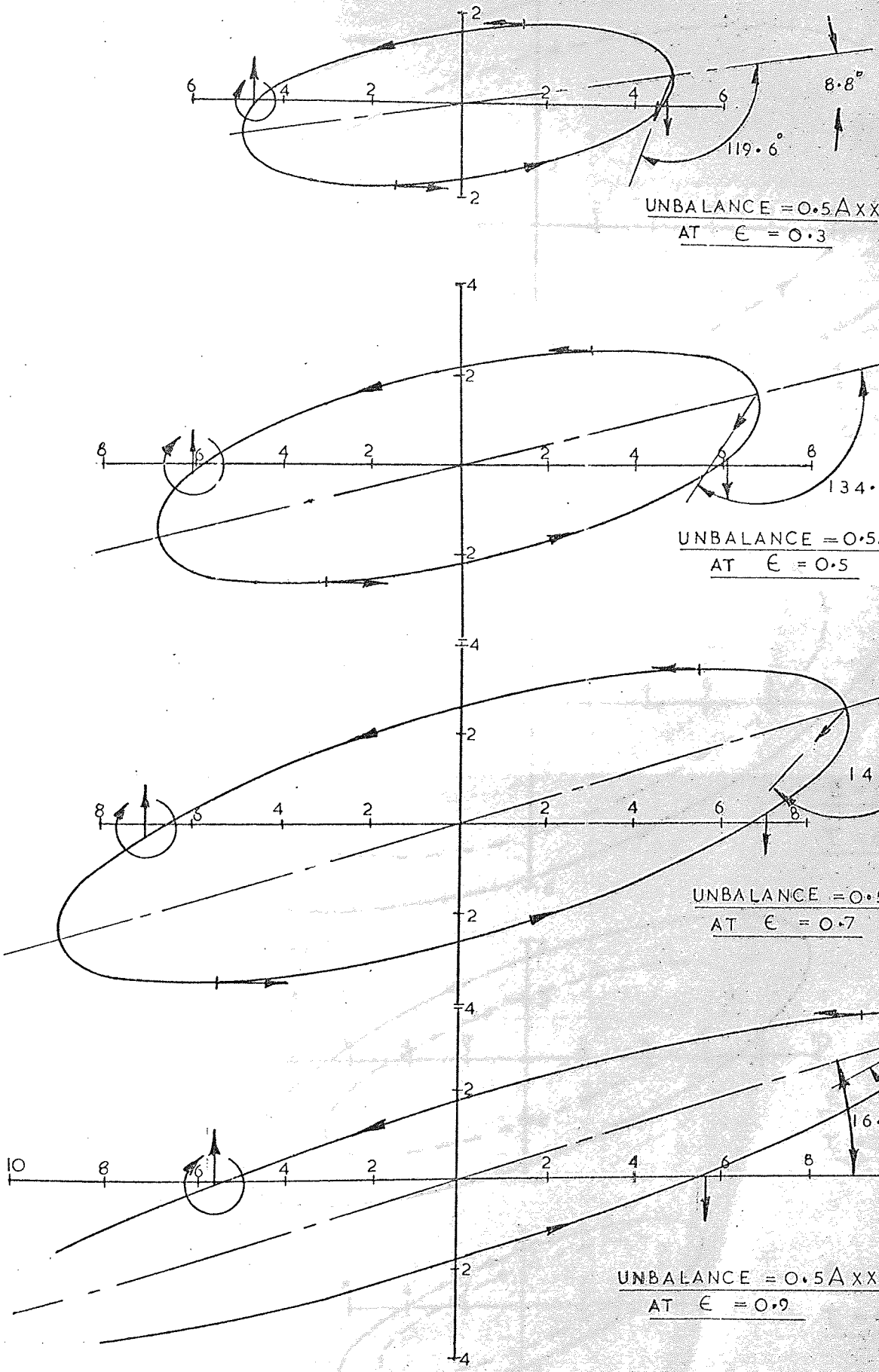

FIG. 10-8. DIMENSIONLESS JOURNAL RESPONSE -REVERSE WHIRL- FOR $M\omega^2 = Axx$.

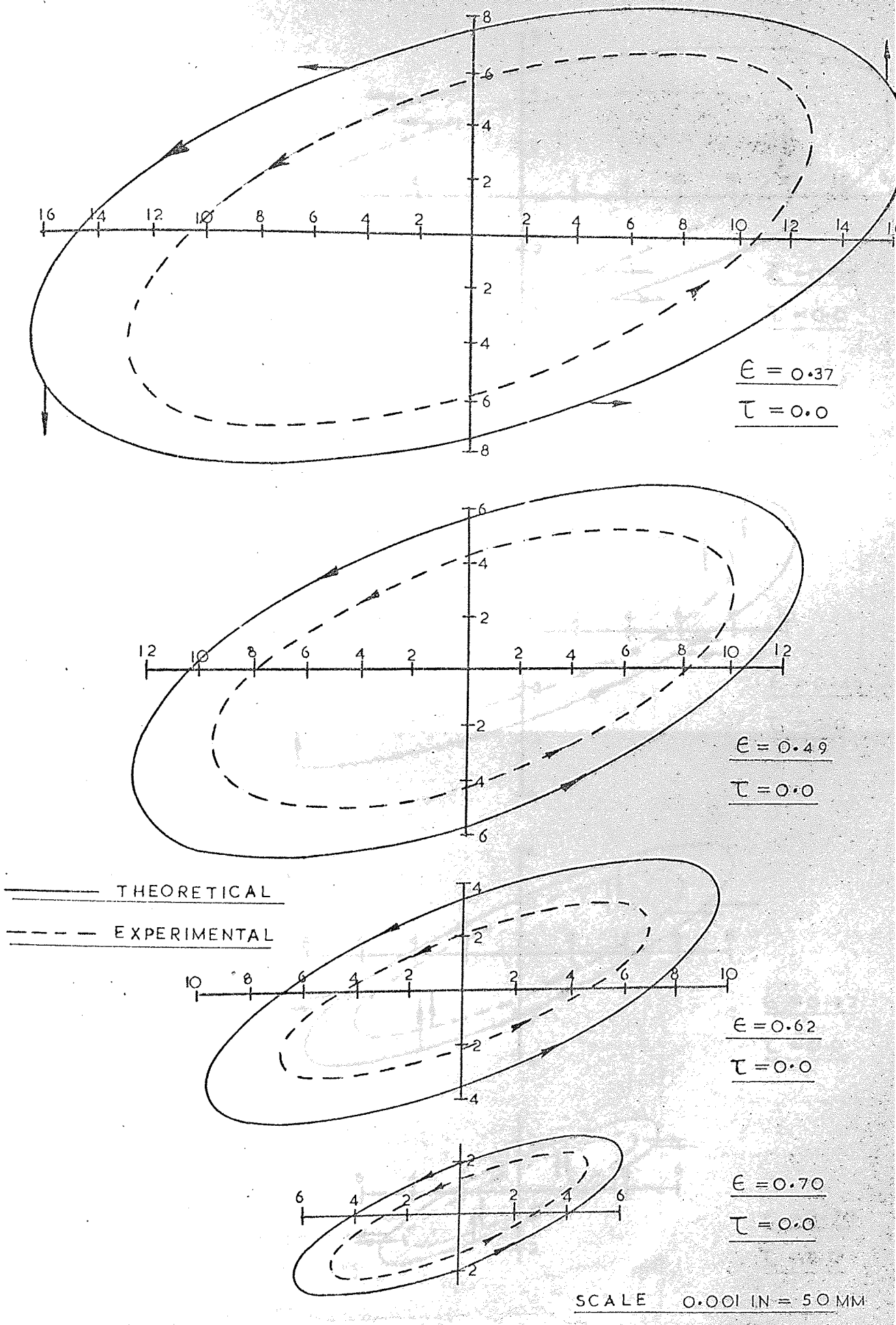

FIG. 10-9. FORWARD WHIRL SYNCHRONOUS SPEED 2700 R.P.M; UNBALANCE 192 LBF.

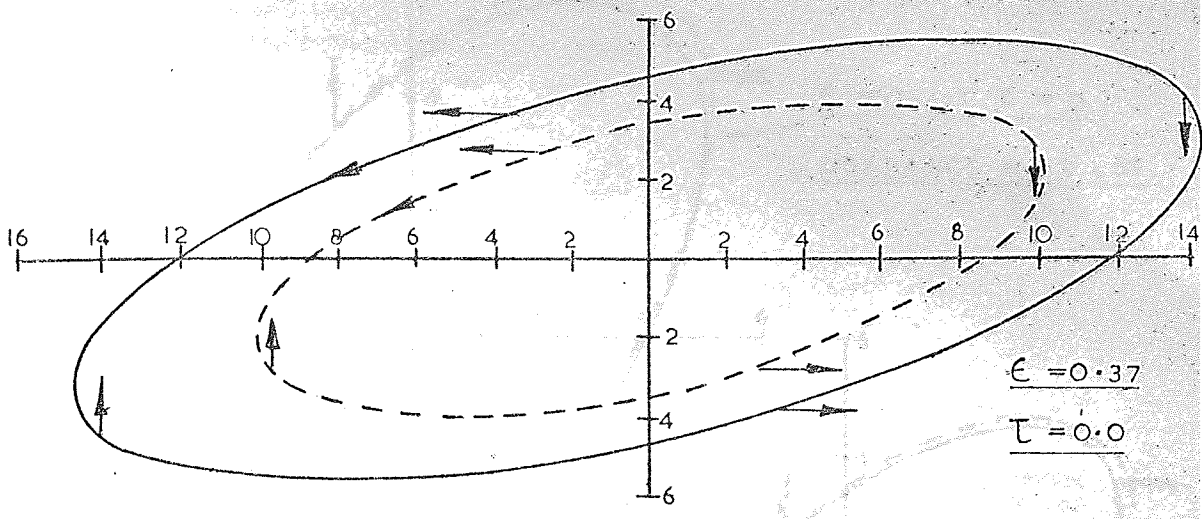

$\epsilon = 0.37$

$\tau = 0.0$

SCALE 0·001 IN = 50 MM

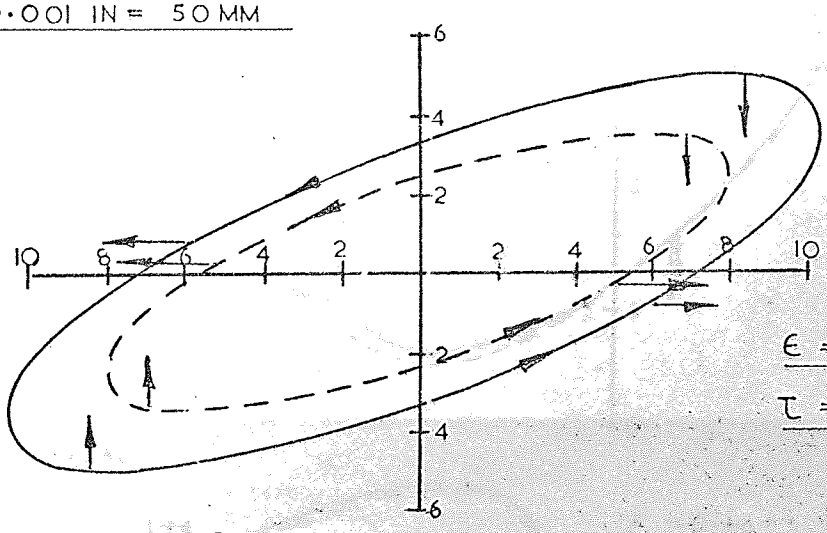

$\epsilon = 0.49$

$\tau = 0.0$

——— THEORETICAL

– – – – – EXPERIMENTAL

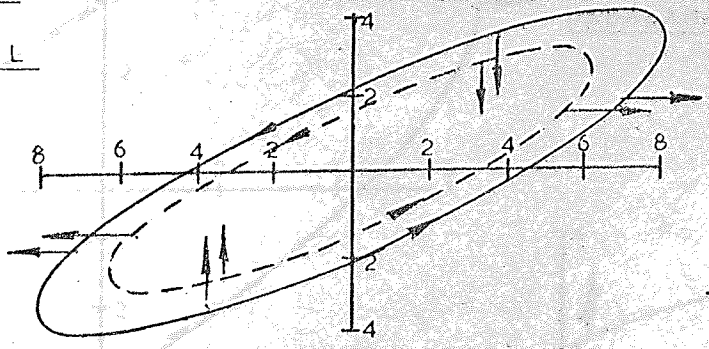

$\epsilon = 0.62$

$\tau = 0.0$

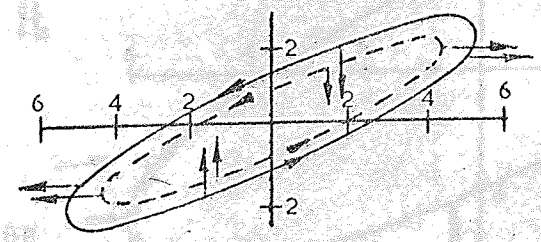

$\epsilon = 0.70$

$\tau = 0.0$

FIG. 10-10. REVERSE WHIRL 'SYNCHRONOUS'

SPEED 2700 RPM. UNBALANCE 192 LB.F.

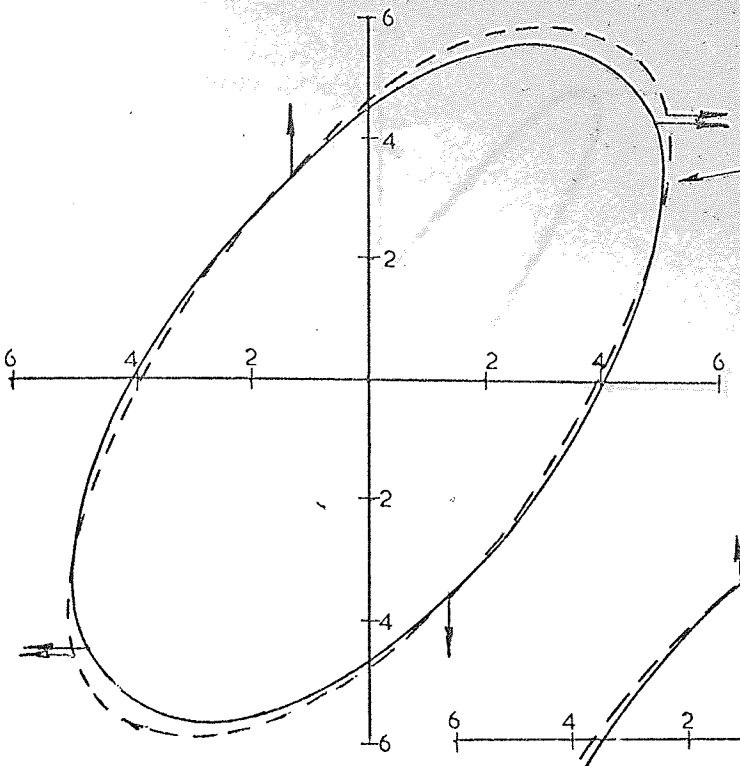

$\epsilon = 0.41$; $\tau = 0$

UBALANCE = 112 LBF

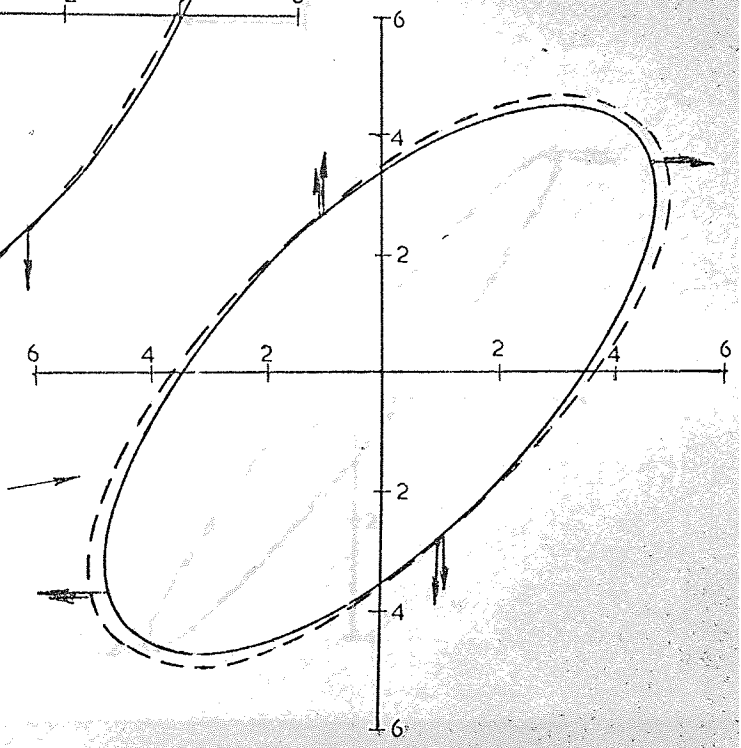

$\epsilon = 0.51$; $\tau = 0$

UNBALANCE = 157 LBF

——— THEORETICAL

– – – – – EXPERIMENTAL

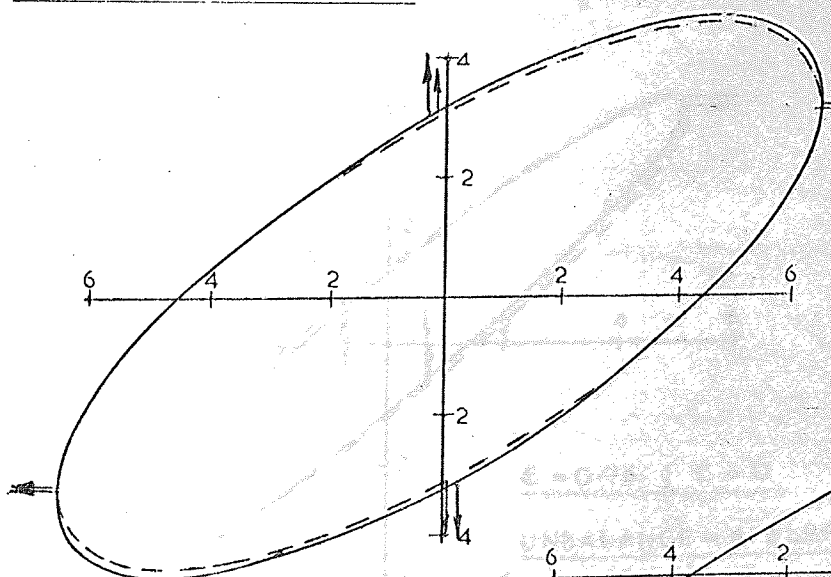

$\epsilon = 0.66$; $\tau = 0$

UNBALANCE = 281 LBF

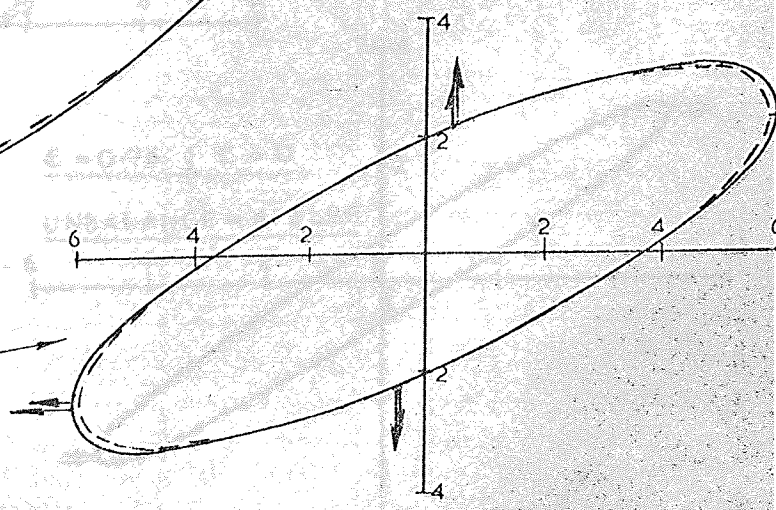

$\epsilon = 0.76$; $\tau = 0$

UNBALANCE = 412 LBF

FIG. 10-11 FORWARD WHIRL

LOW FREQUENCY IE $\Omega < \omega$

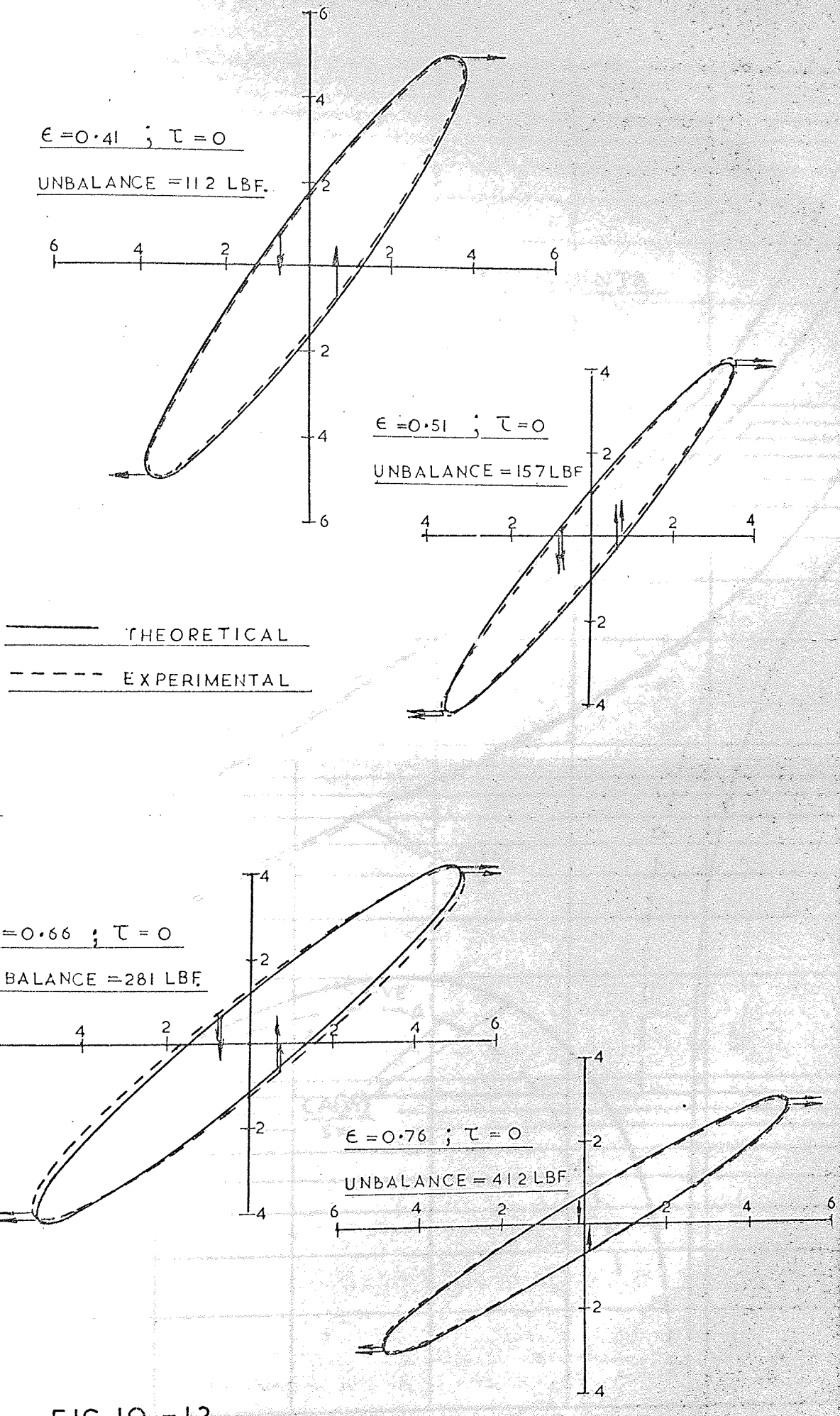

FIG. 10 - 12.

REVERSE WHIRL LOW FREQUENCY i.e. $\Omega < \omega$

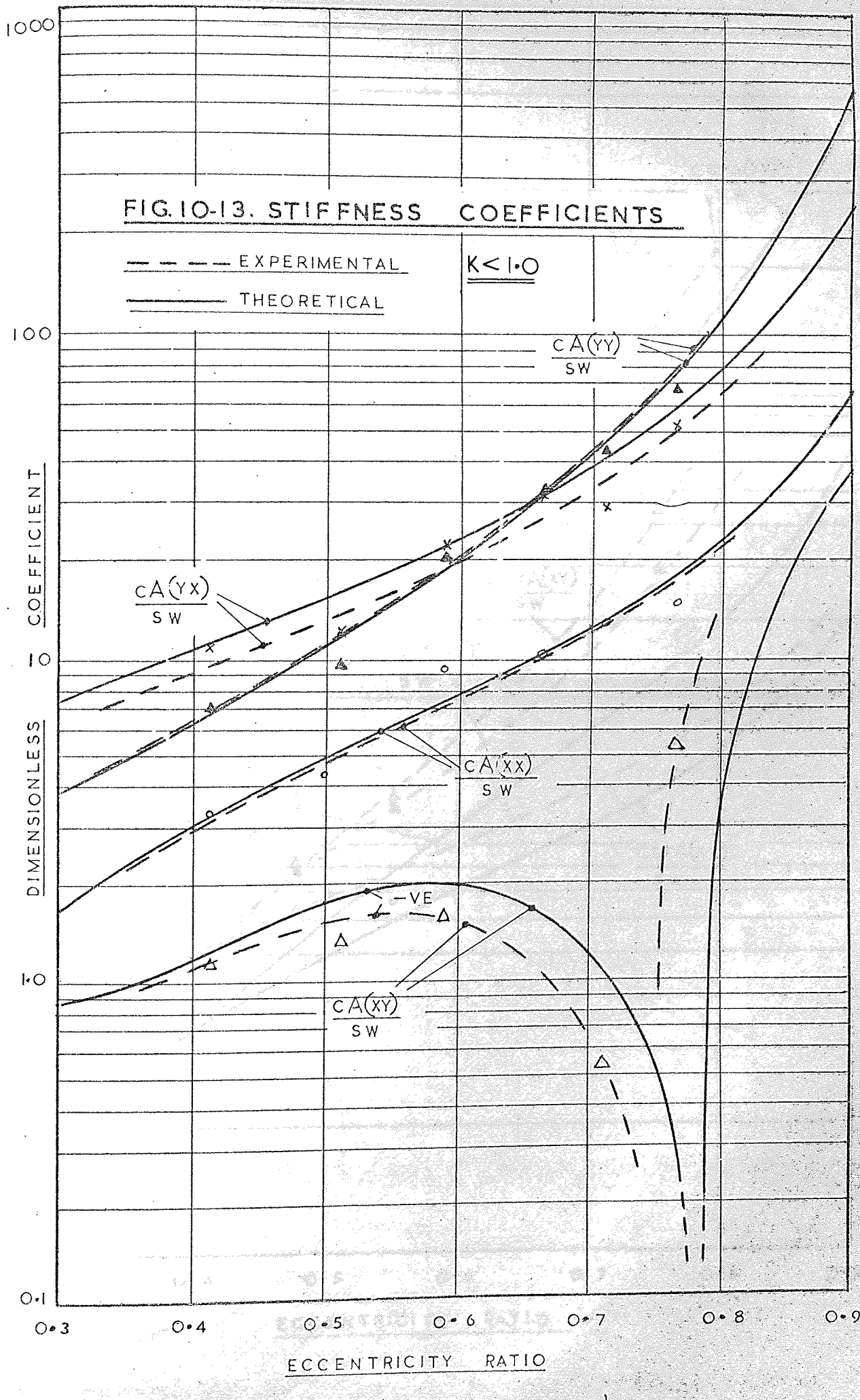
FIG. 10-13. STIFFNESS COEFFICIENTS
EXPERIMENTAL
THEORETICAL
K < 1·0
1000
100
10
1·0
0·1
DIMENSIONLESS COEFFICIENT
cA(YY)/SW
cA(YX)/SW
cA'(XX)/SW
cA(XY)/SW
-VE
0·3
0·4
0·5
0·6
0·7
0·8
0·9
ECCENTRICITY RATIO

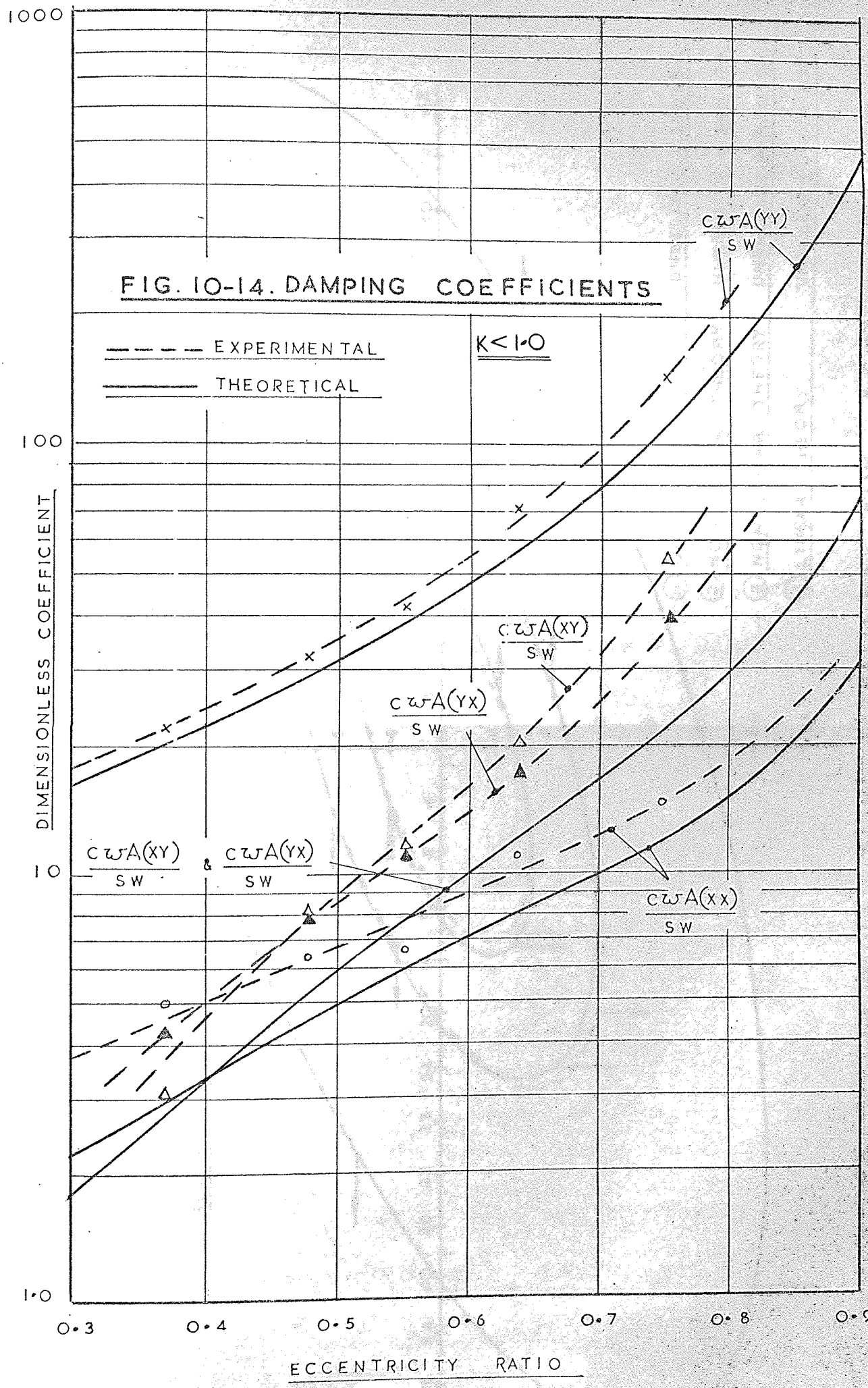

FIG. 10-14. DAMPING COEFFICIENTS

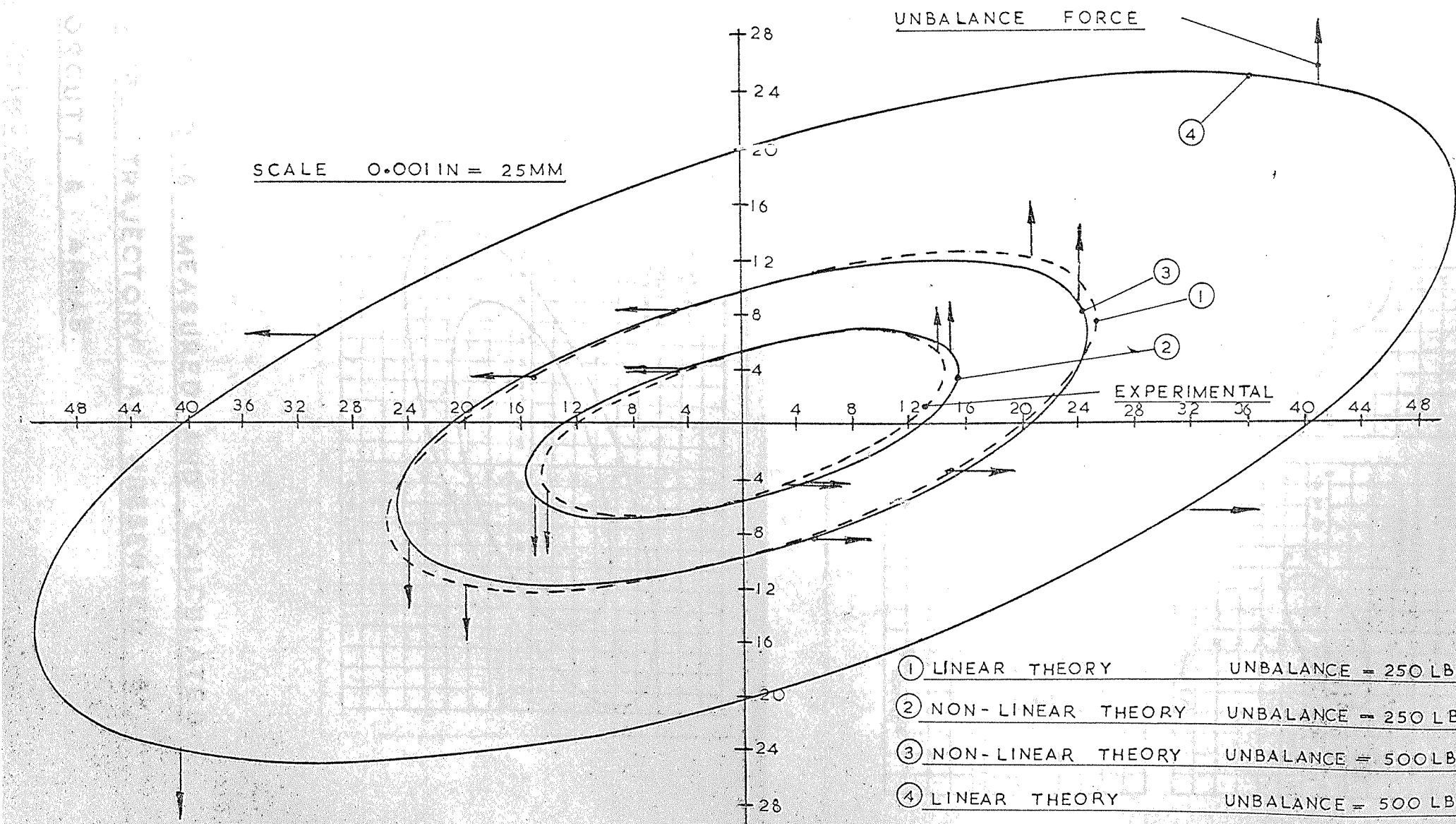

1. LINEAR THEORY — UNBALANCE = 250 LBF.
2. NON-LINEAR THEORY — UNBALANCE = 250 LBF.
3. NON-LINEAR THEORY — UNBALANCE = 500 LBF.
4. LINEAR THEORY — UNBALANCE = 500 LBF

FIG. 10-15. SYNCHRONOUS WHIRL VIBRATIONS FOR K = 1·0

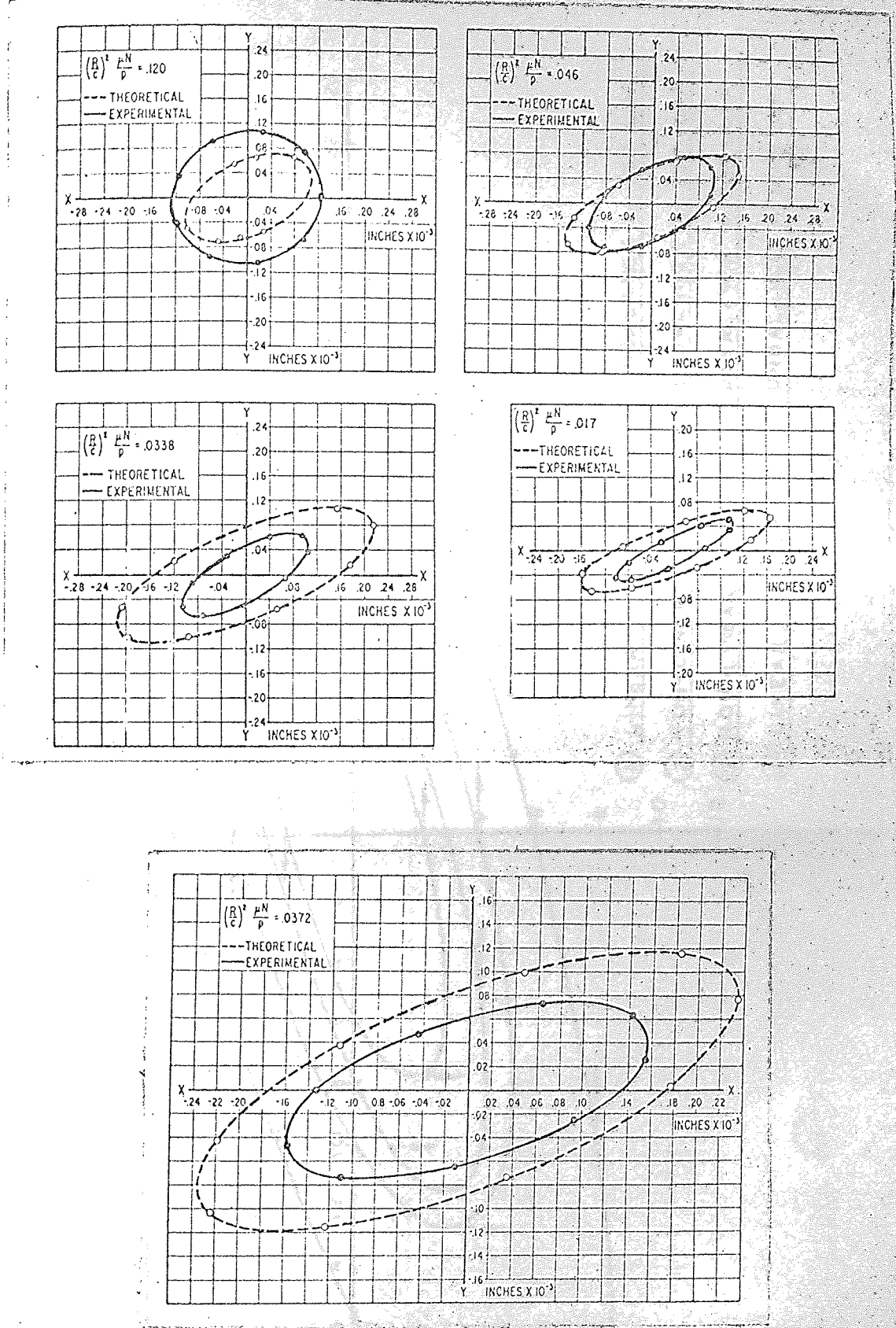

FIG. 10-16. MEASURED AND CALCULATED WHIRL TRAJECTORY AS PRESENTED BY ORCUTT & ARWAS.

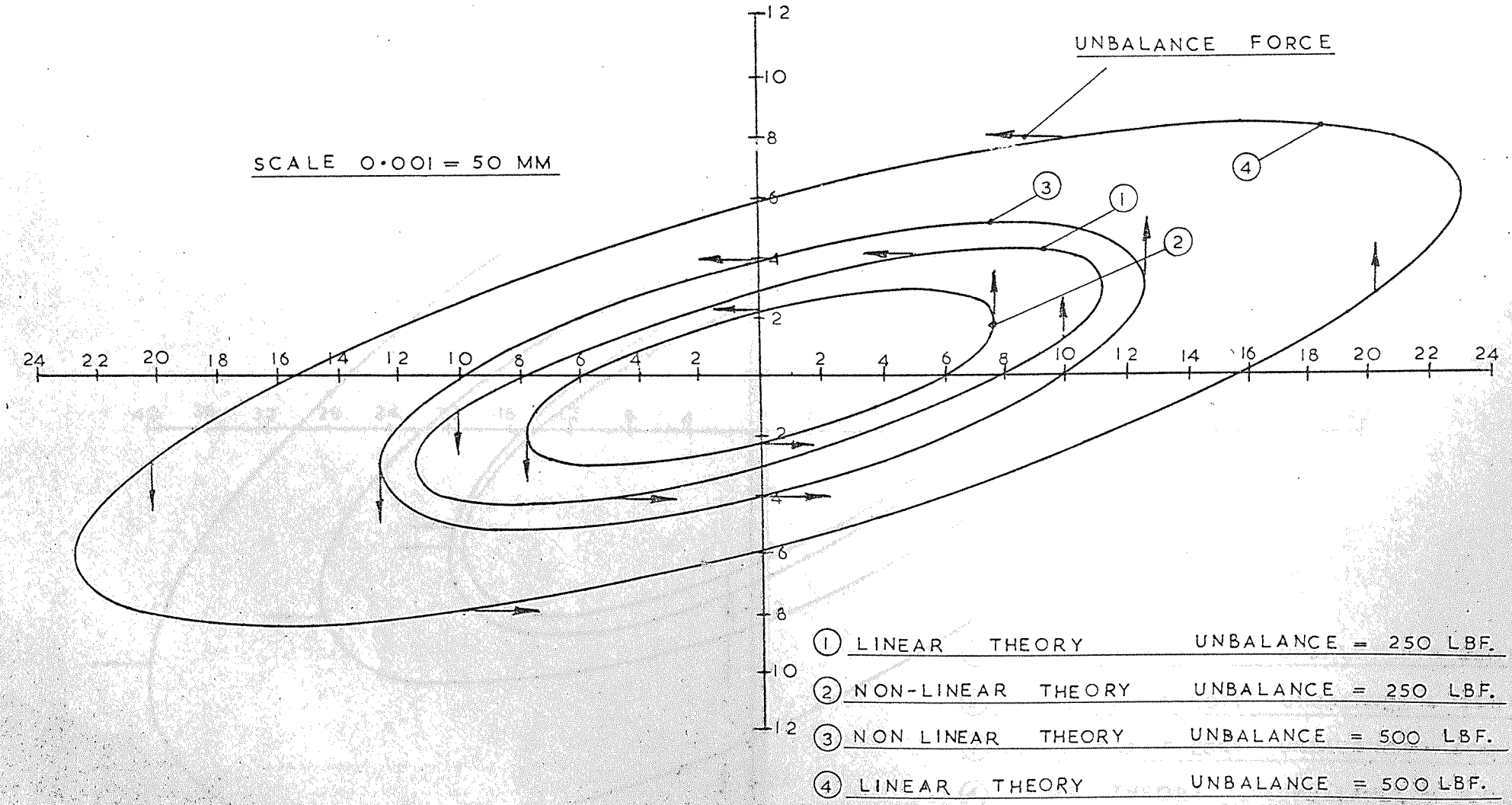

FIG. 10-17. NON SYNCHRONOUS WHIRL VIBRATIONS FOR K=2·0

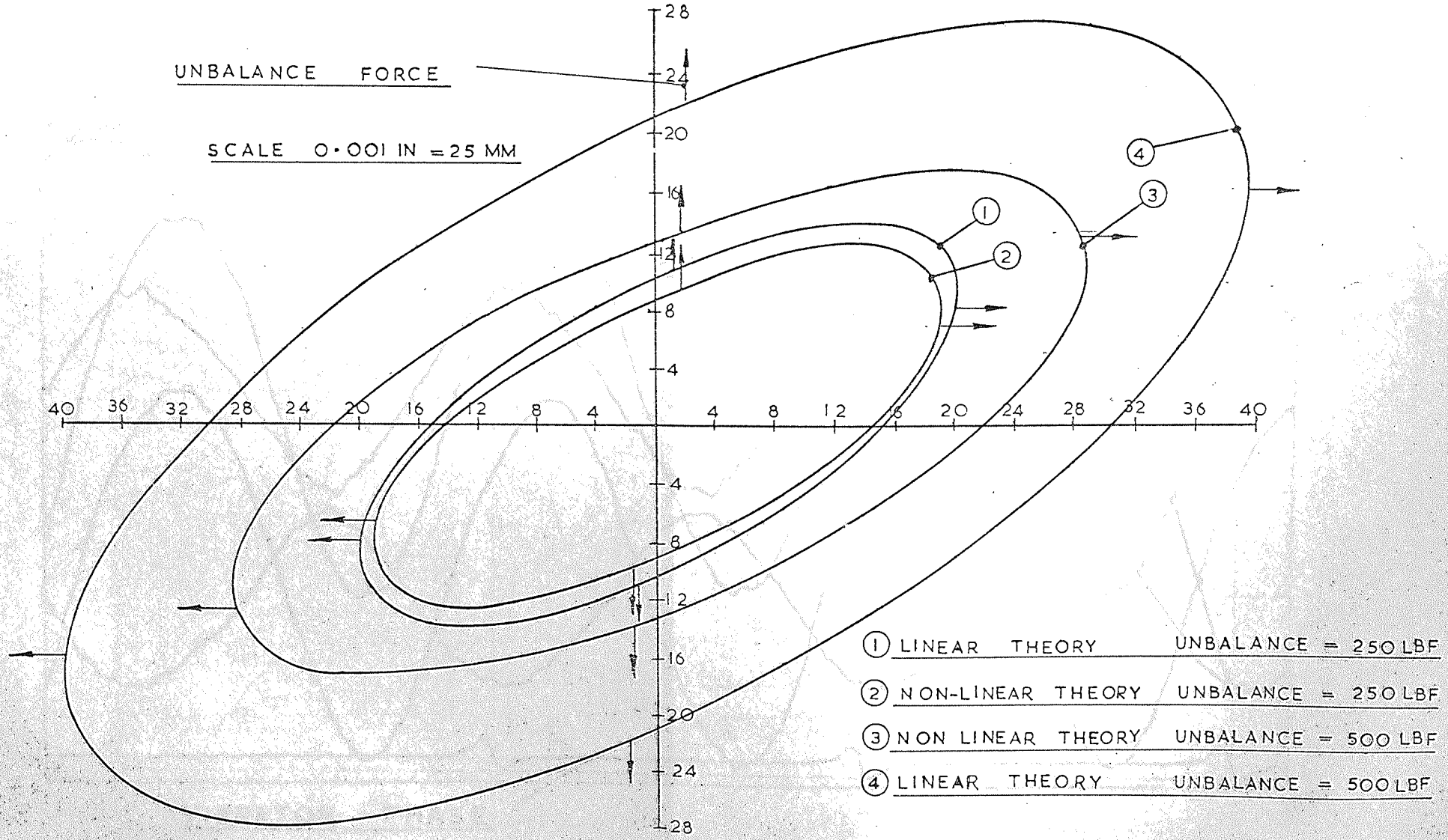

FIG. 10-18. NON SYNCHRONOUS WHIRL VIBRATIONS FOR K 0·5

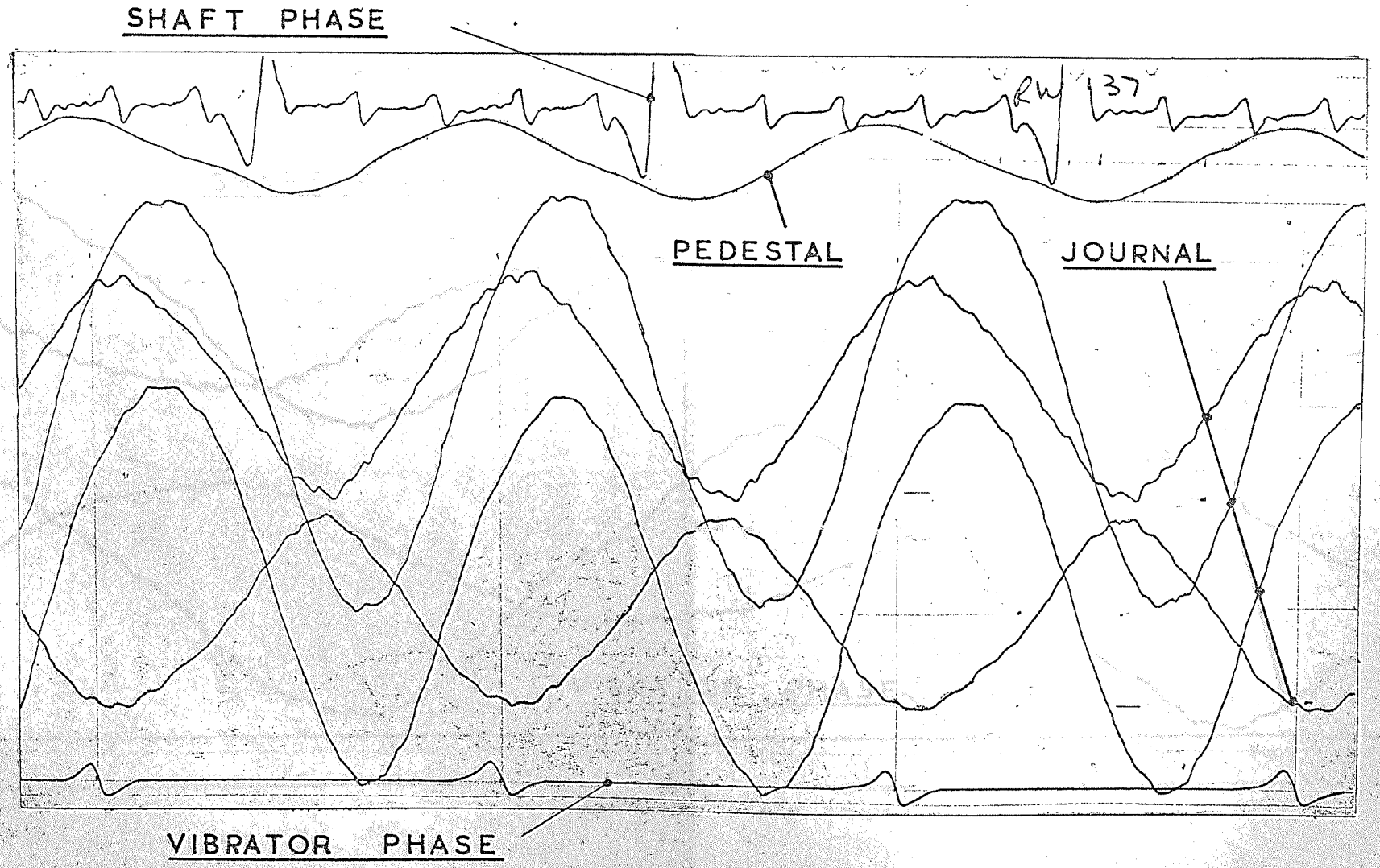

FIG. 10-19. TYPICAL U.V. RECORDING.

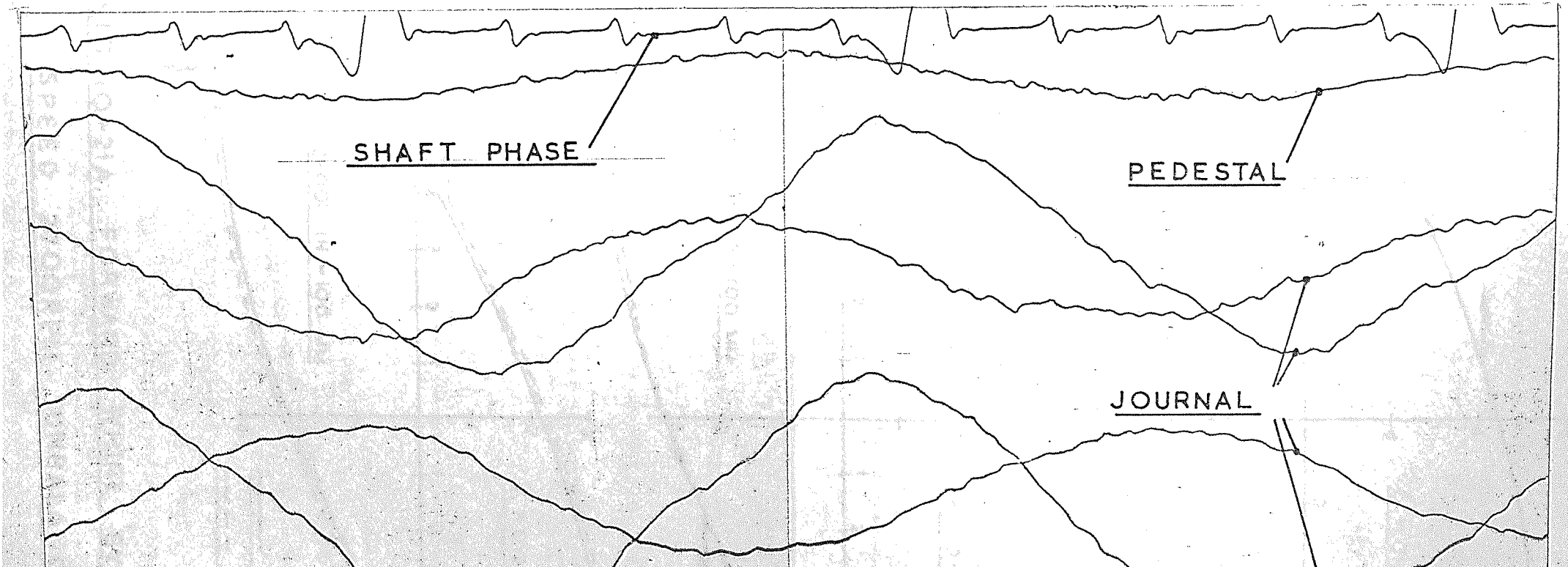

FIG. 10-20. TYPICAL U.V. RECORDING.

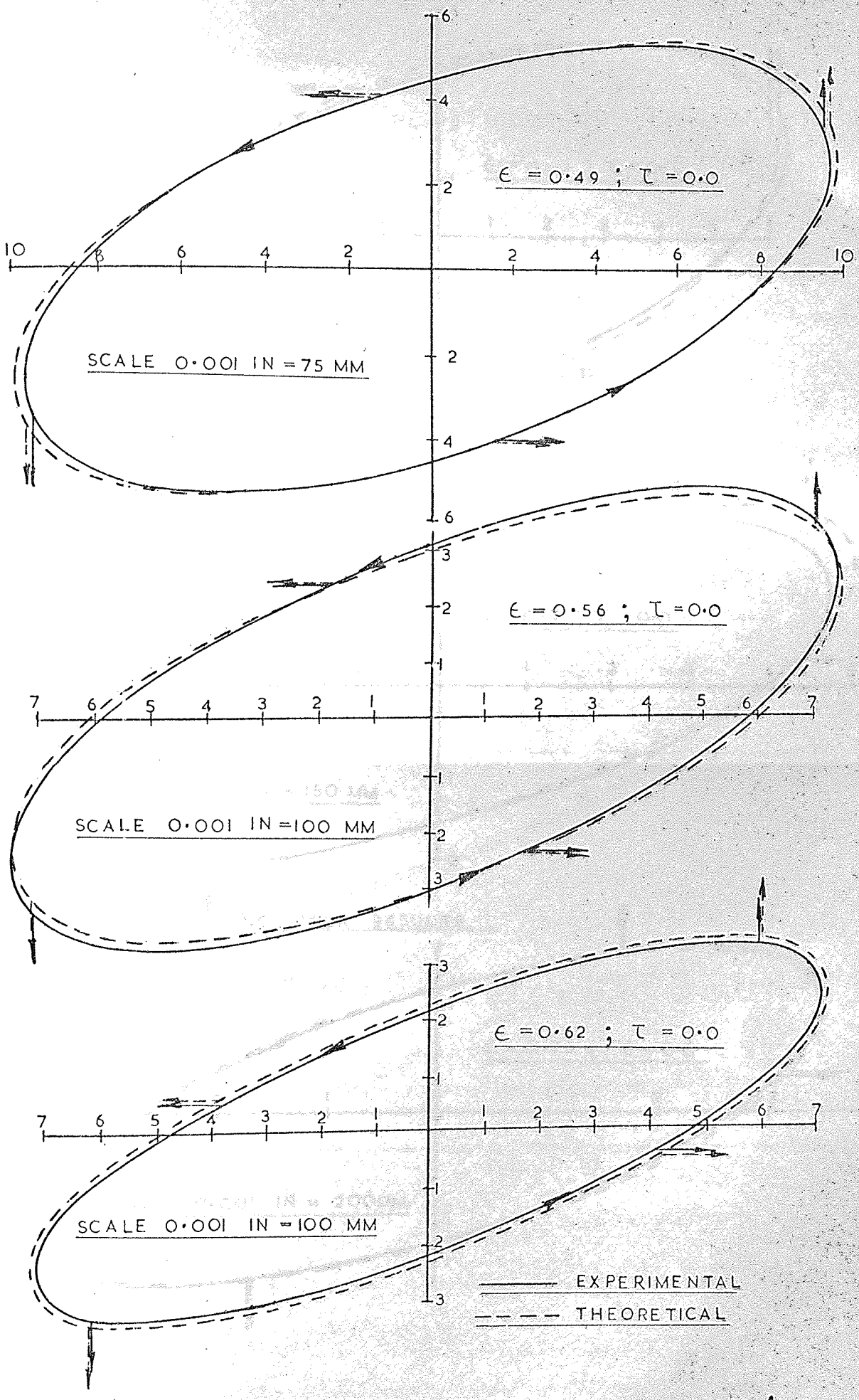

FIG. 10-21A. FORWARD WHIRL 'SYNCHRONOUS' SPEED 2700RPM. UNBALANCE 192 LB.F.

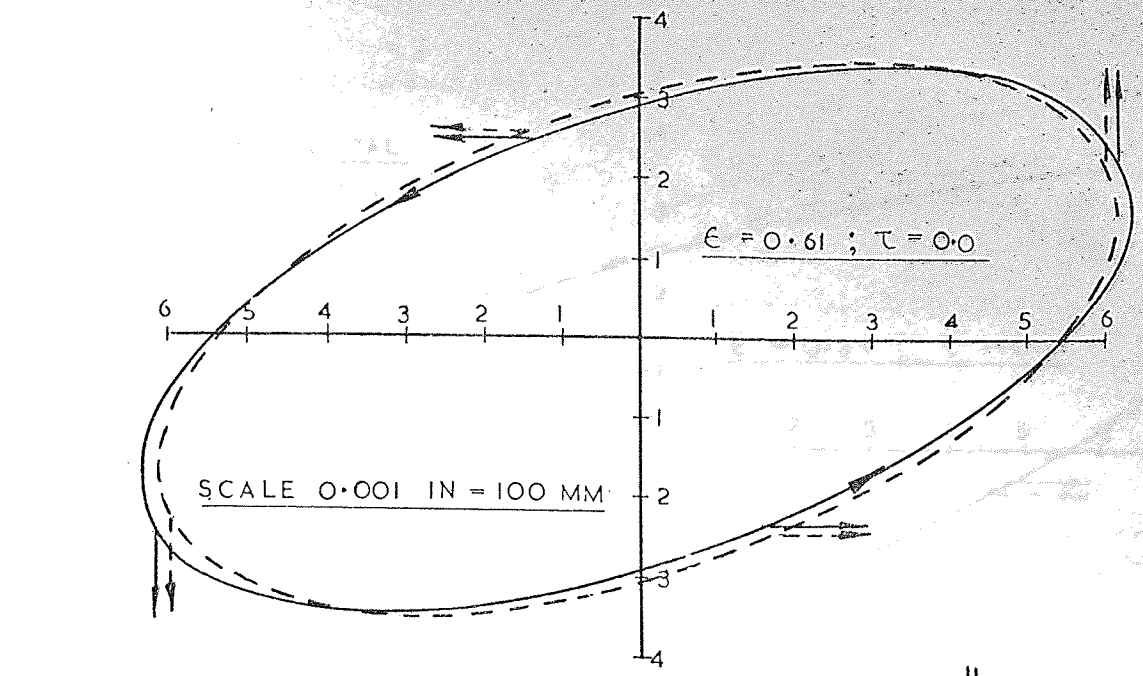

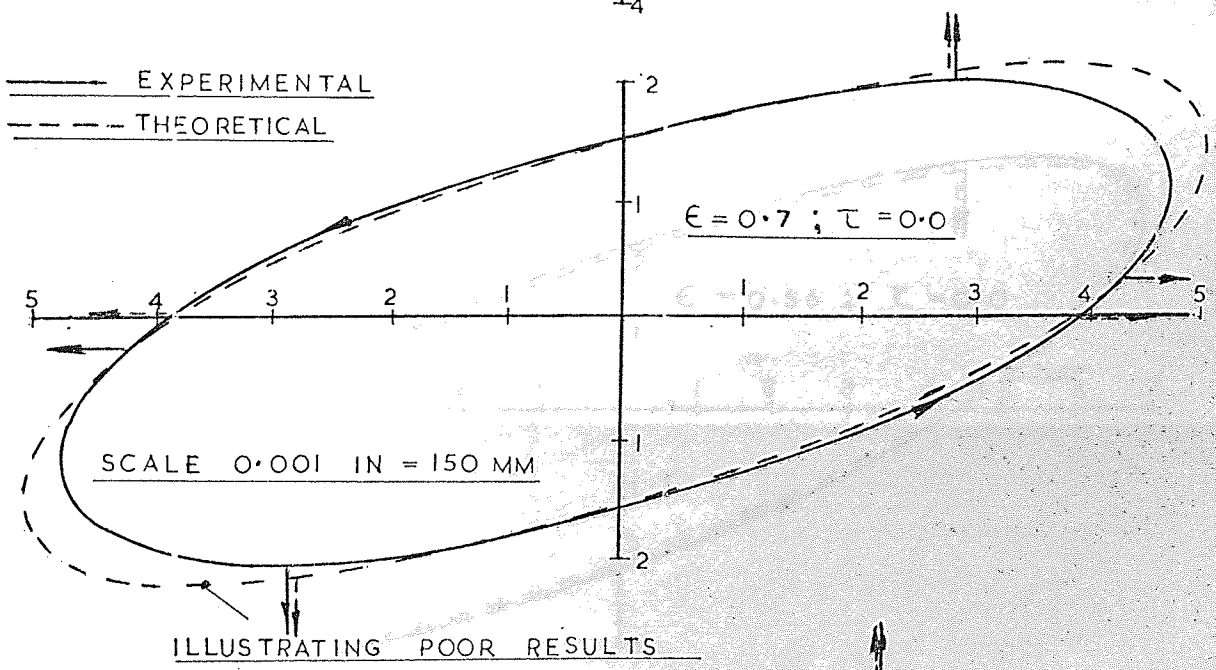

ILLUSTRATING POOR RESULTS

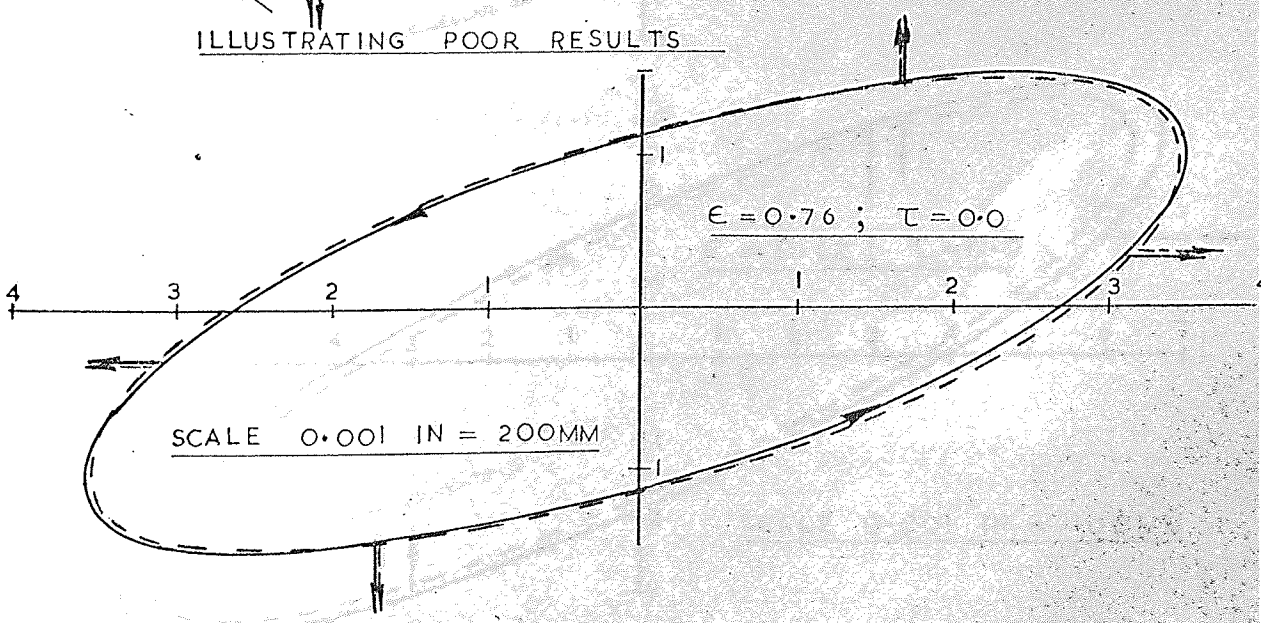

FIG. 10-21B. FORWARD WHIRL SYNCHRONOUS SPEED 1500 RPM. UNBALANCE 197 LB.F.

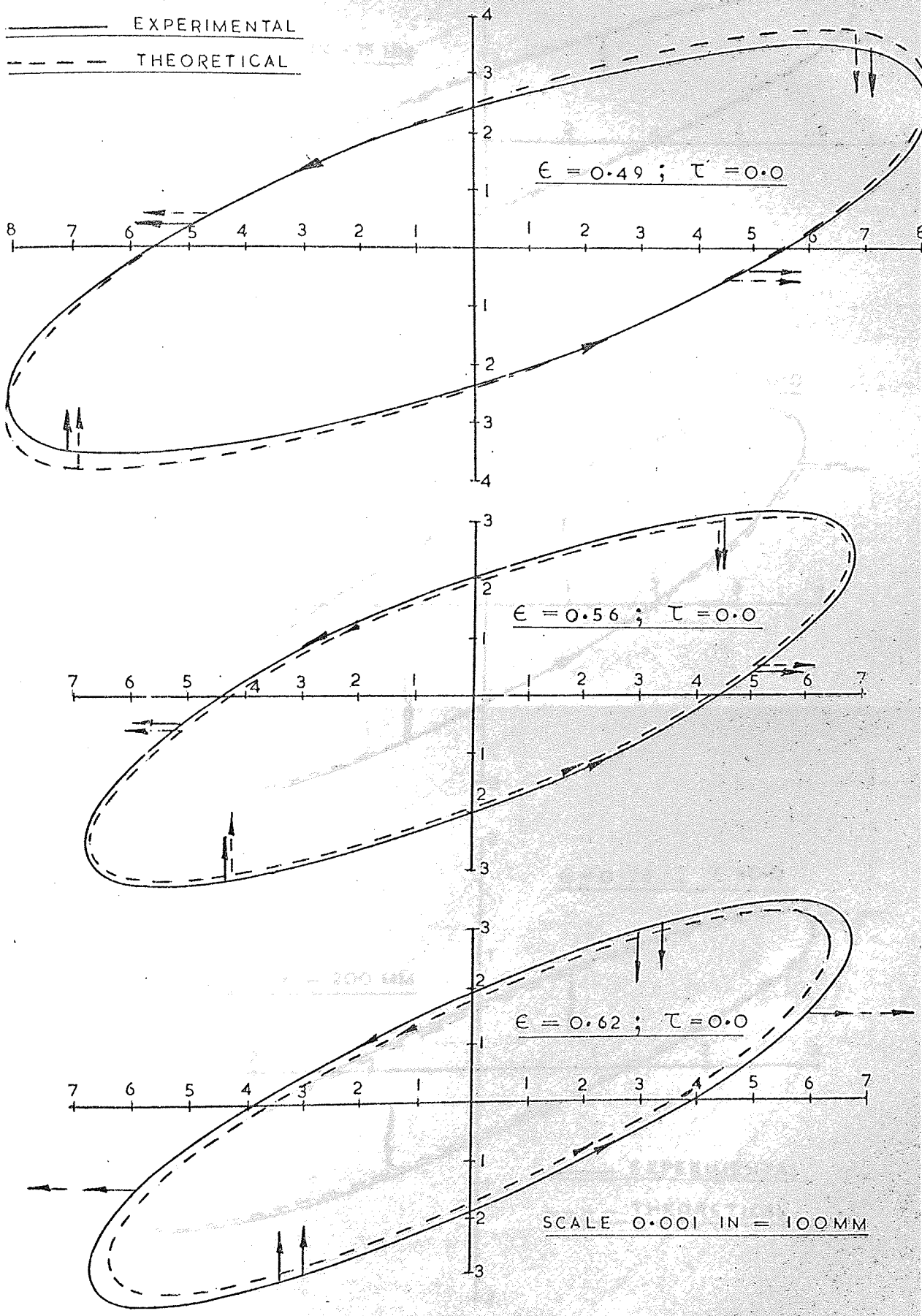

FIG. 10-22A. REVERSE WHIRL SYNCHRONOUS SPEED 2700 R.P.M. ; UNBALANCE 192 LB.F.

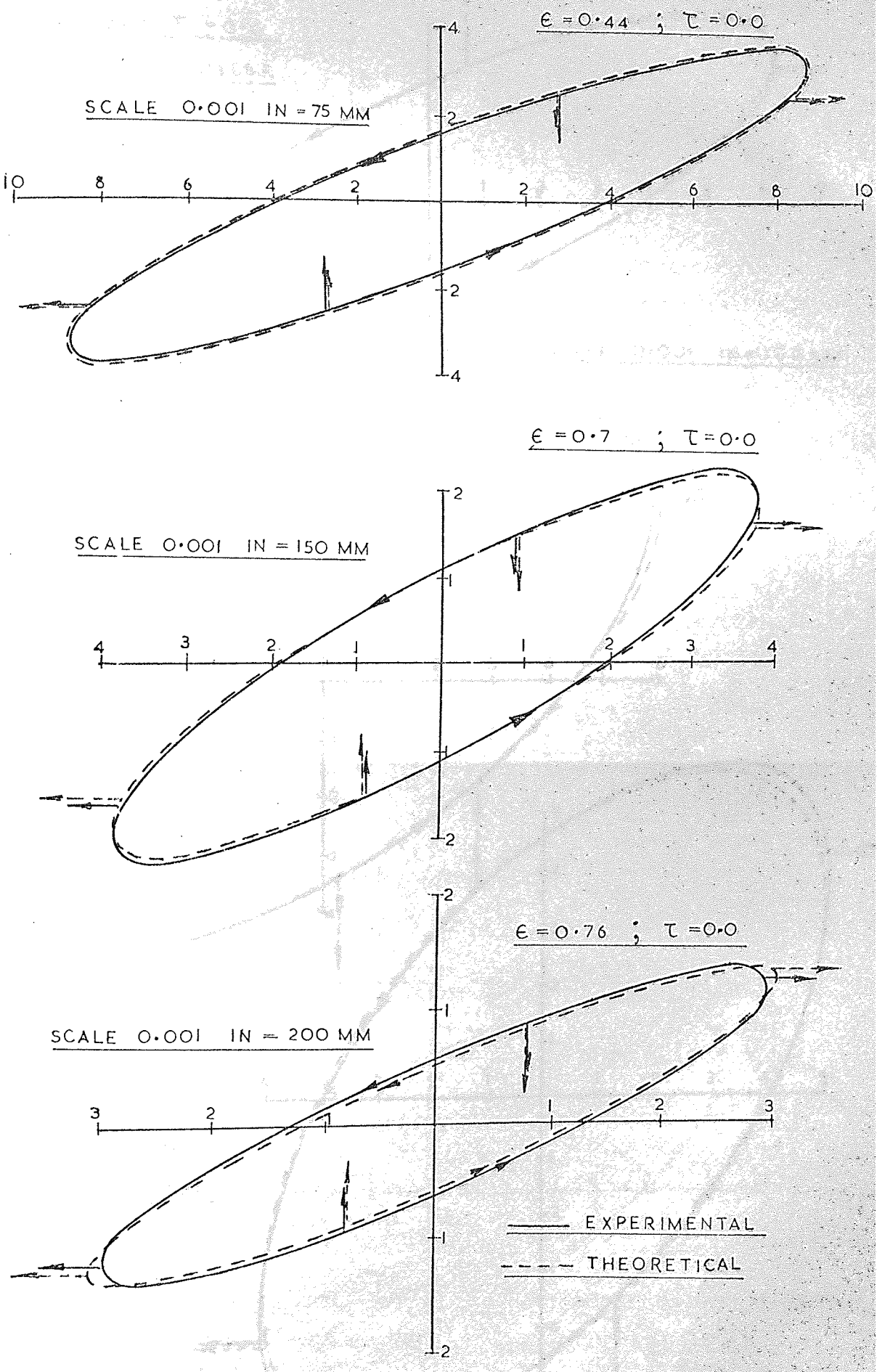

FIG. 10-22B. REVERSE WHIRL - SYNCHRONOUS SPEED 1500 RPM. UNBALANCE 197 LB.F.

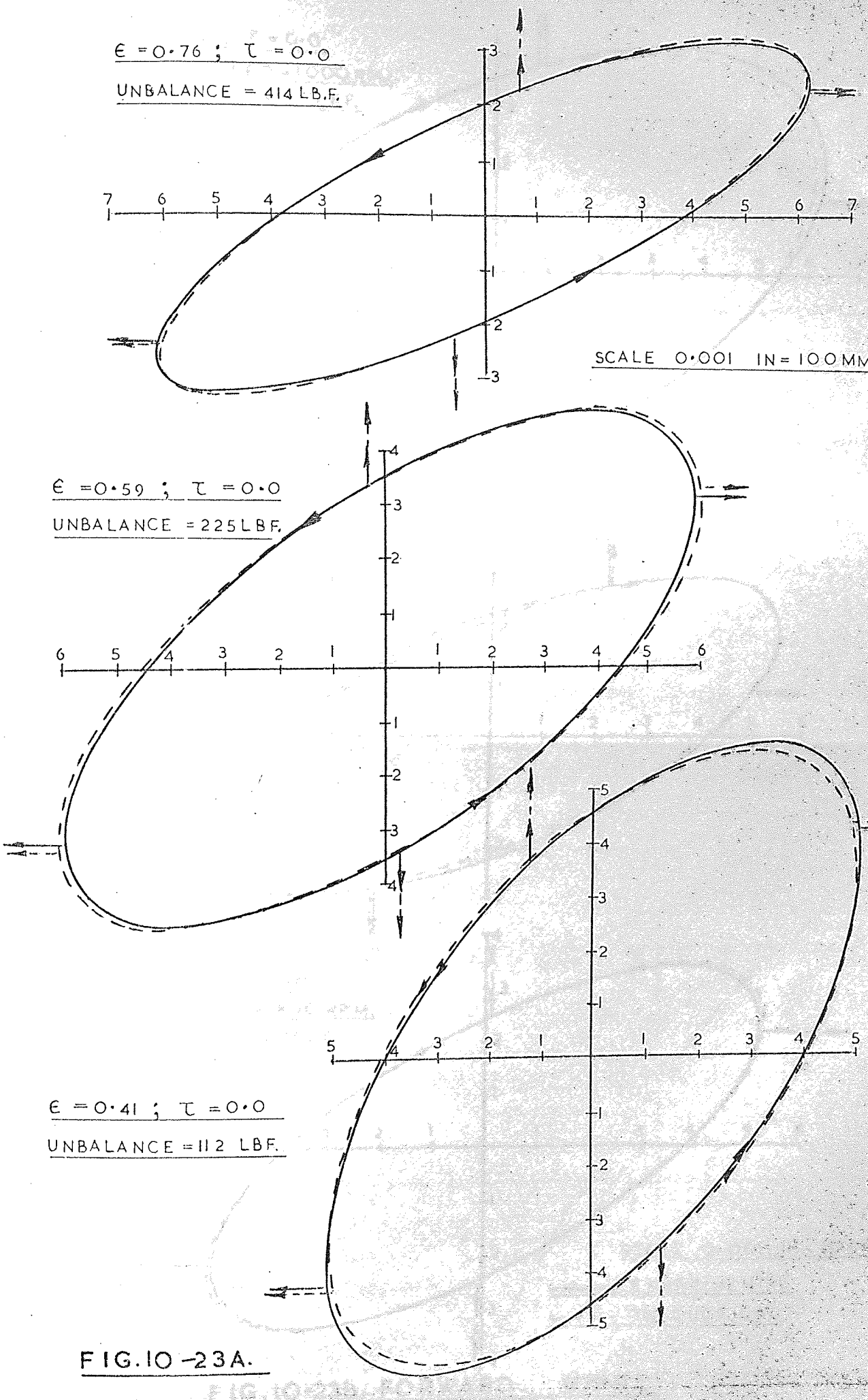

FIG. 10-23A.

FORWARD WHIRL LOW FREQUENCY i.e. $\Omega < \omega$

$\epsilon = 0.4$; $\tau = 0.0$

SHAFT SPEED = 1000 RPM.

UNBALANCE = 73 LBF.

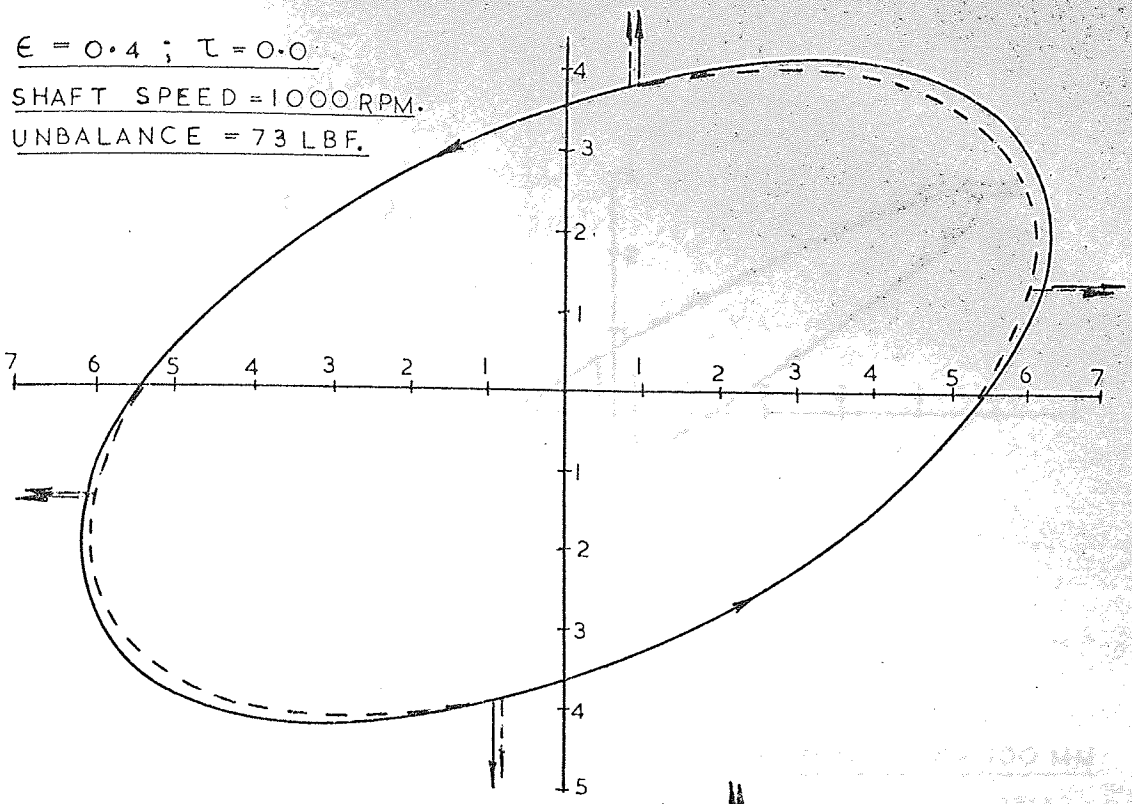

$\epsilon = 0.54$; $\tau = 0.0$

SHAFT SPEED = 1000 RPM.

UNBALANCE = 137 LBF.

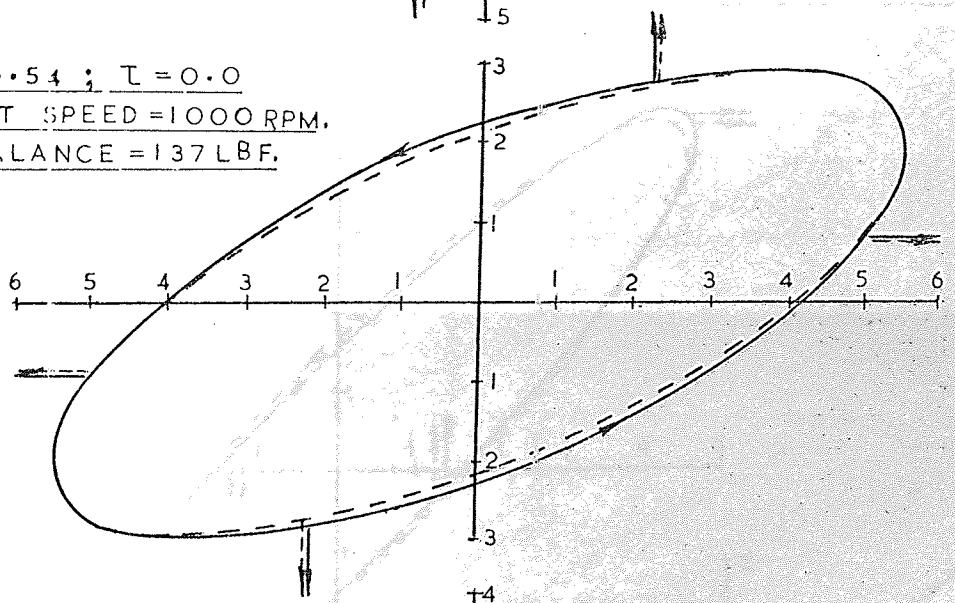

$\epsilon = 0.63$; $\tau = 0.0$

SHAFT SPEED = 1800 RPM.

UNBALANCE = 204 LBF.

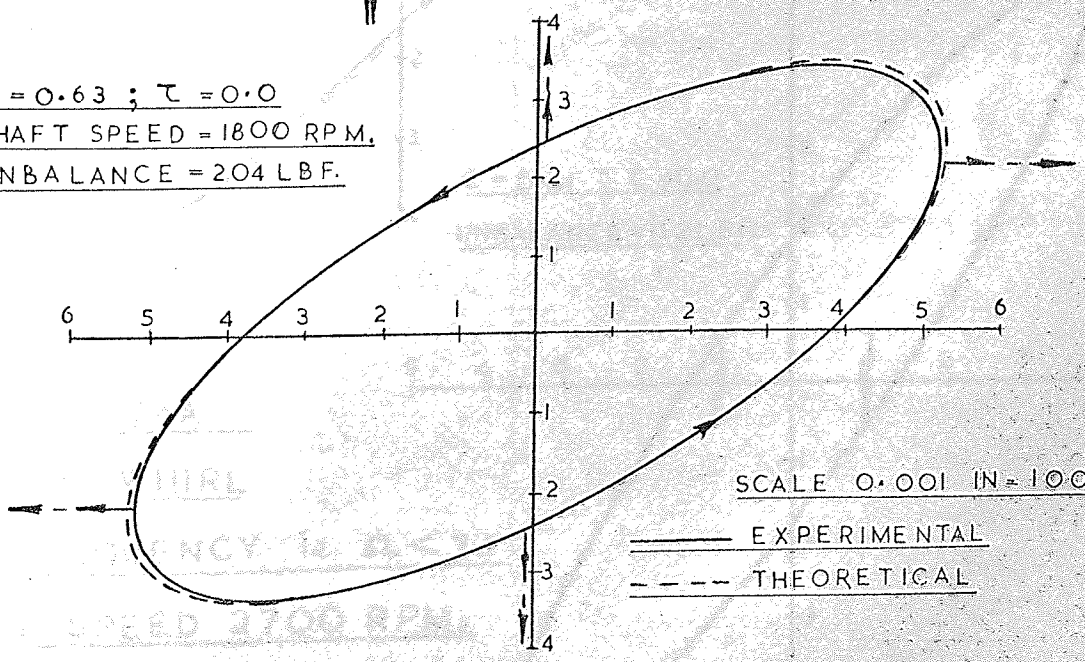

SCALE 0.001 IN = 100MM

——— EXPERIMENTAL

– – – – THEORETICAL

FIG. 10-23B. FORWARD WHIRL

LOW FREQUENCY i.e. $\Omega < \omega$

$\epsilon = 0.76$; $\tau = 0.0$

UNBALANCE = 414 LBF.

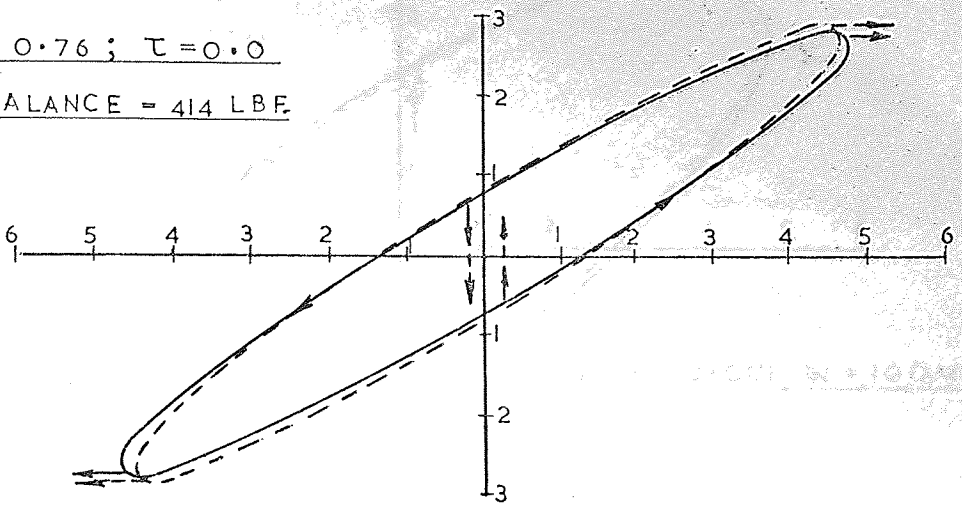

——— EXPERIMENTAL

– – – – THEORETICAL

SCALE 0·001 IN = 100 MM

$\epsilon = 0.59$; $\tau = 0.0$

UNBALANCE = 225 LBF.

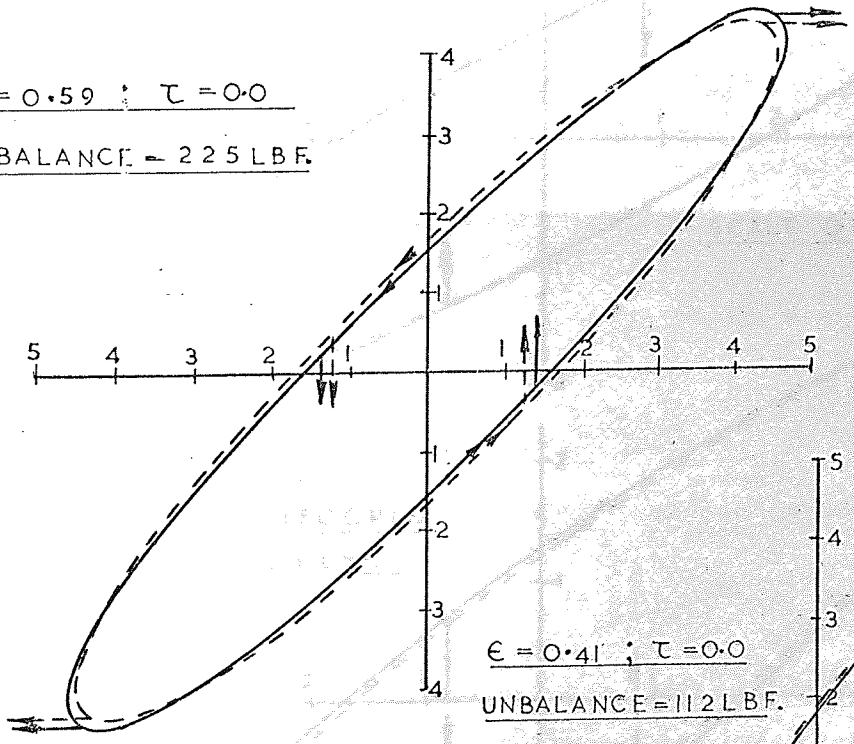

$\epsilon = 0.41$; $\tau = 0.0$

UNBALANCE = 112 LBF.

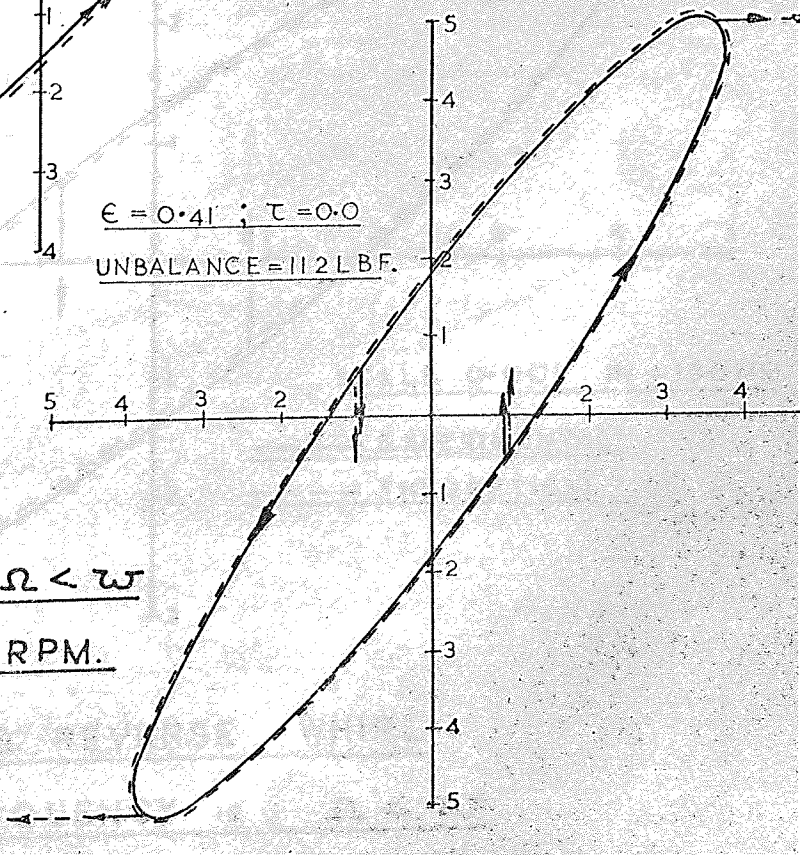

FIG. 10-24A.

REVERSE WHIRL

LOW FREQUENCY ie $\Omega < \omega$

SHAFT SPEED 2700 RPM.

ϵ = 0·4 ; τ = 0·0

SHAFT SPEED = 1000 RPM.

UNBALANCE = 73 LBF.

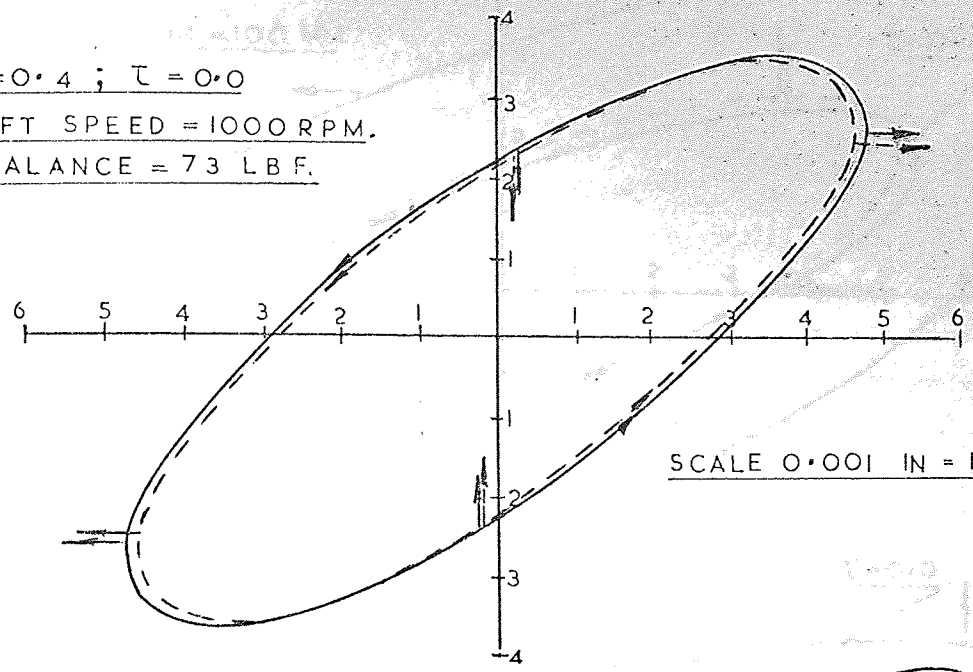

SCALE 0·001 IN = 100 MM

ϵ = 0·54 ; τ = 0·0

SHAFT SPEED = 1000 RPM.

UNBALANCE = 137 LBF.

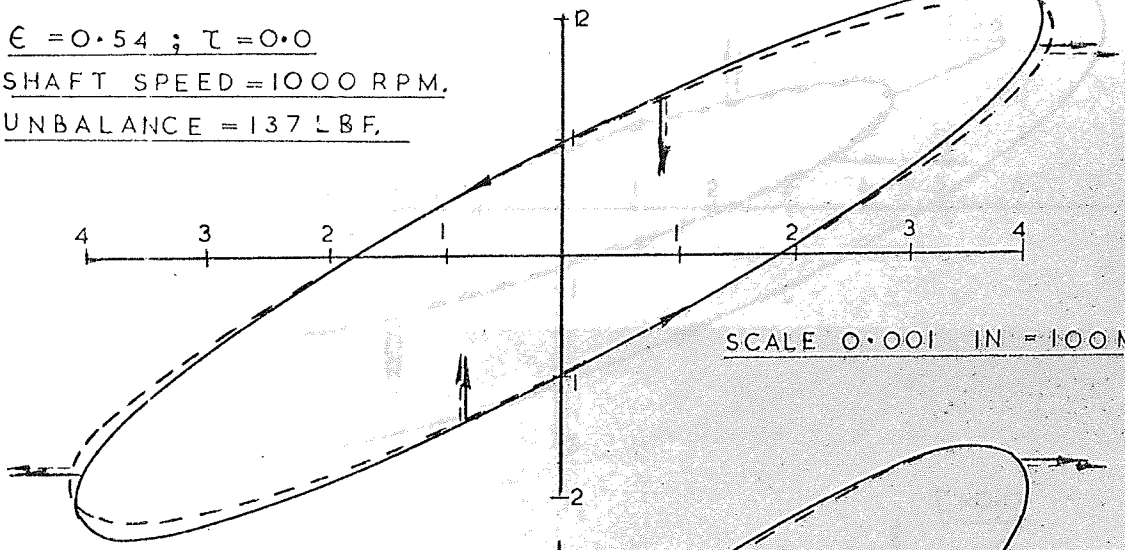

SCALE 0·001 IN = 100 MM

ϵ = 0·63 ; τ = 0·0

SHAFT SPEED = 1800 RPM.

UNBALANCE = 204 LBF.

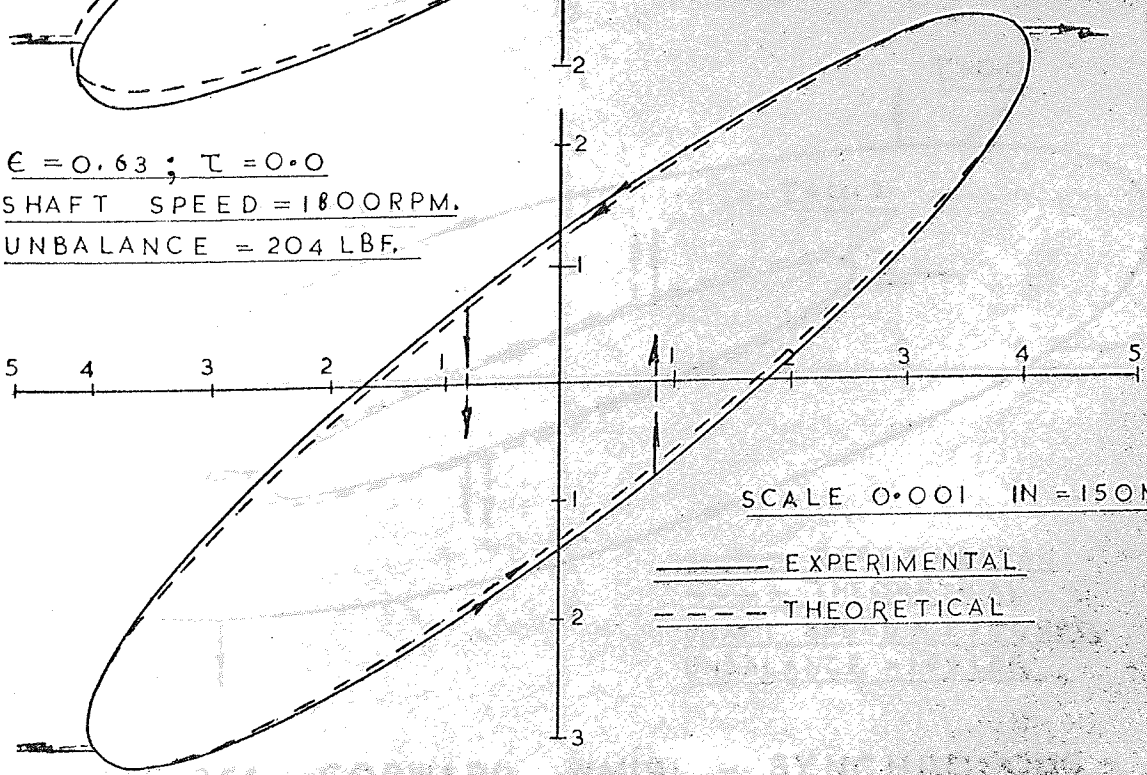

SCALE 0·001 IN = 150 MM

——— EXPERIMENTAL

– – – – THEORETICAL

FIG. 10-24B. REVERSE WHIRL

LOW FREQUENCY IE $\Omega < \omega$

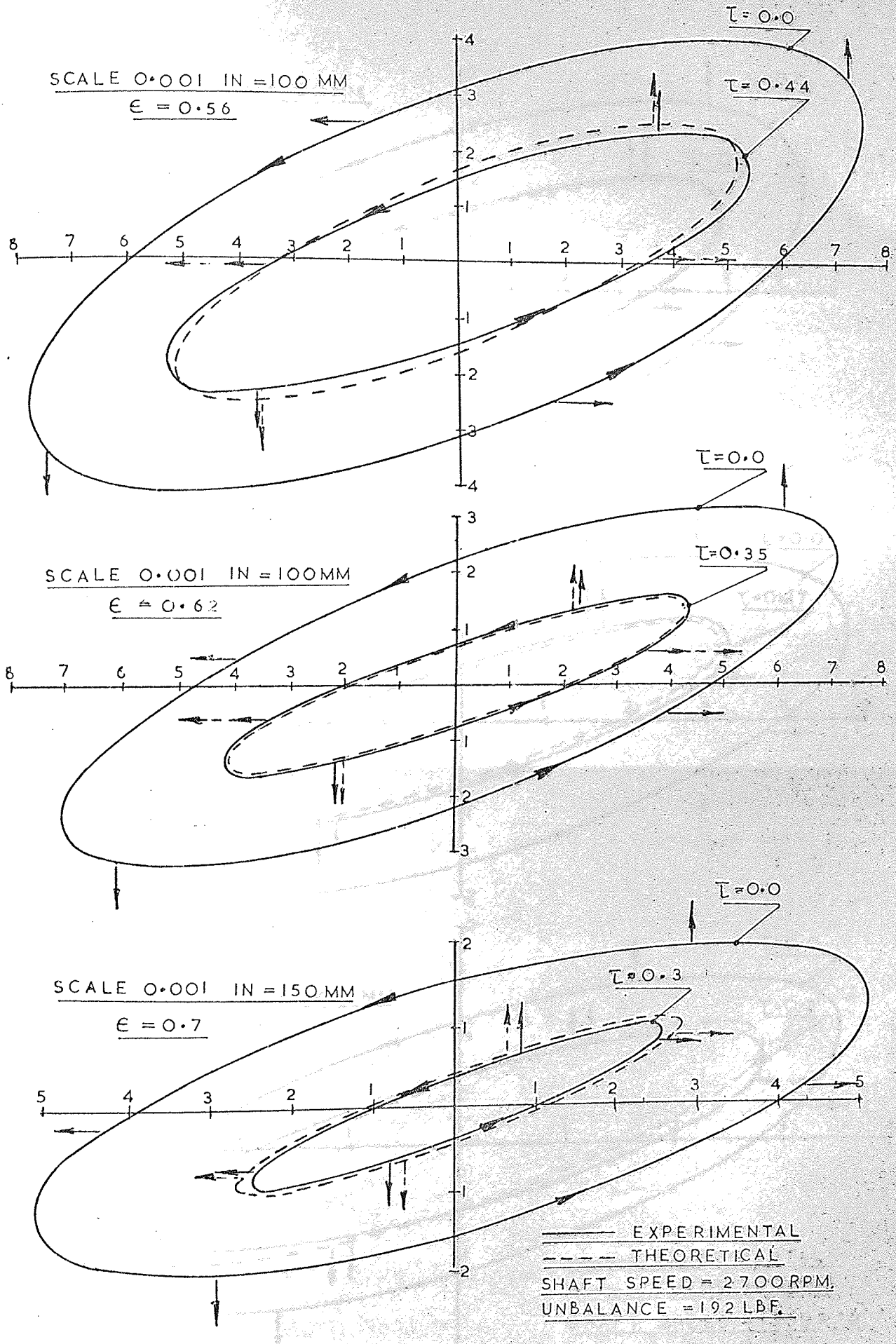

FIG.10-25A. FORWARD WHIRL - SYNCHRONOUS - WITH MISALIGNED JOURNAL

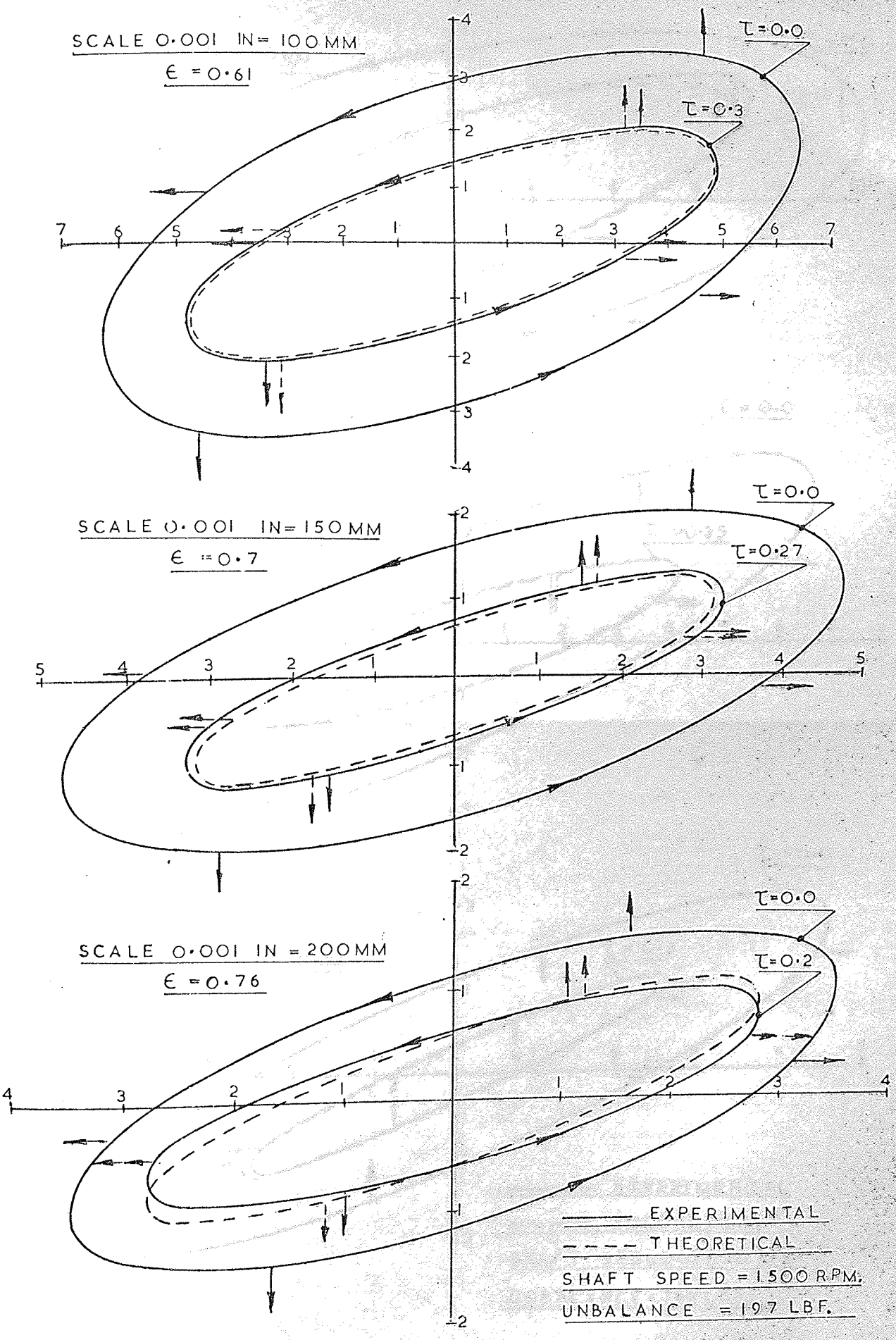

FIG. 10-25B. FORWARD WHIRL - SYNCHRONOUS - WITH MISALIGNED JOURNAL

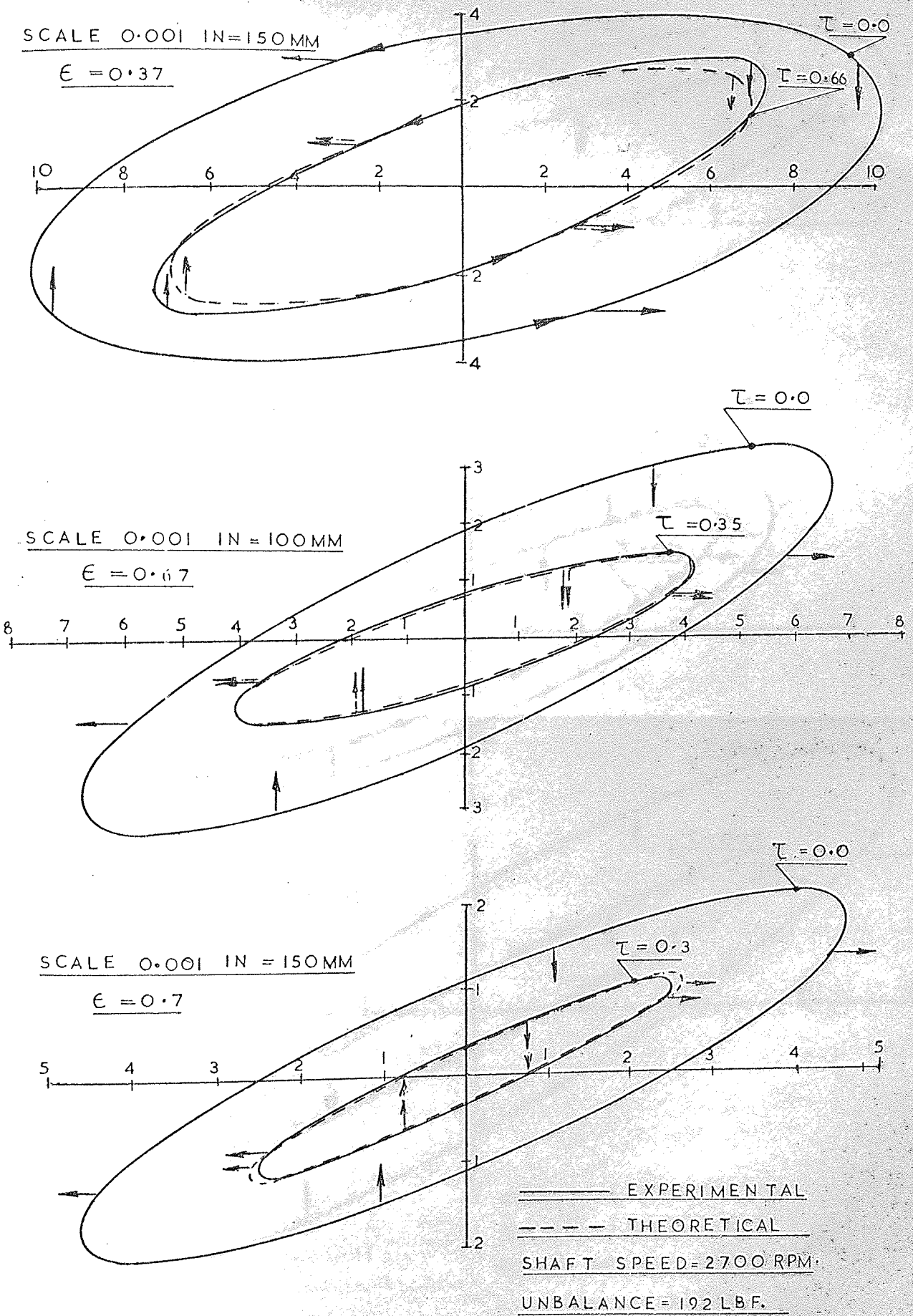

FIG. 10-26A. REVERSE WHIRL - SYNCHRONOUS - WITH MISALIGNED JOURNAL

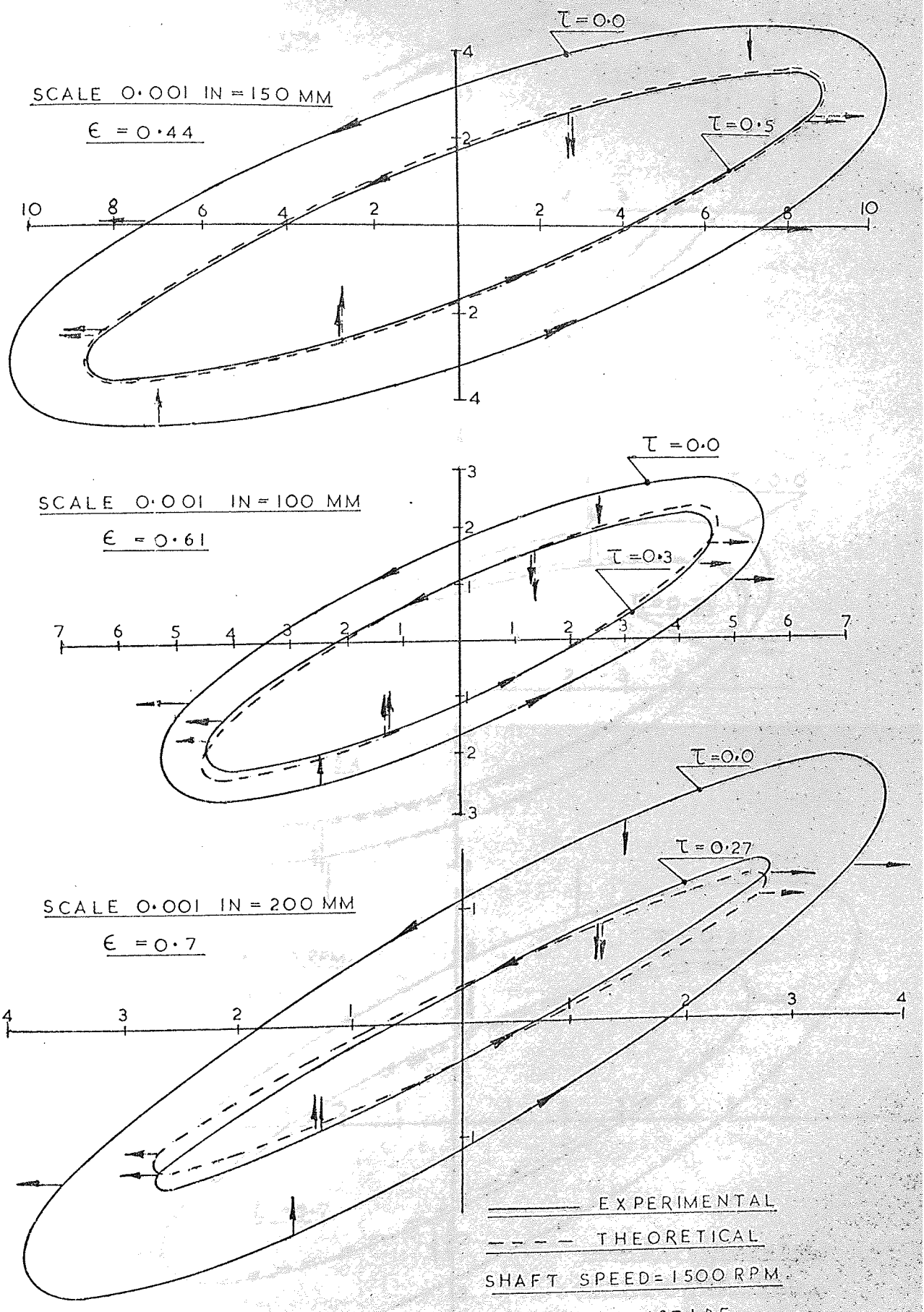

FIG.10-26 B. REVERSE WHIRL - SYNCHRONOUS - WITH MISALIGNED JOURNAL

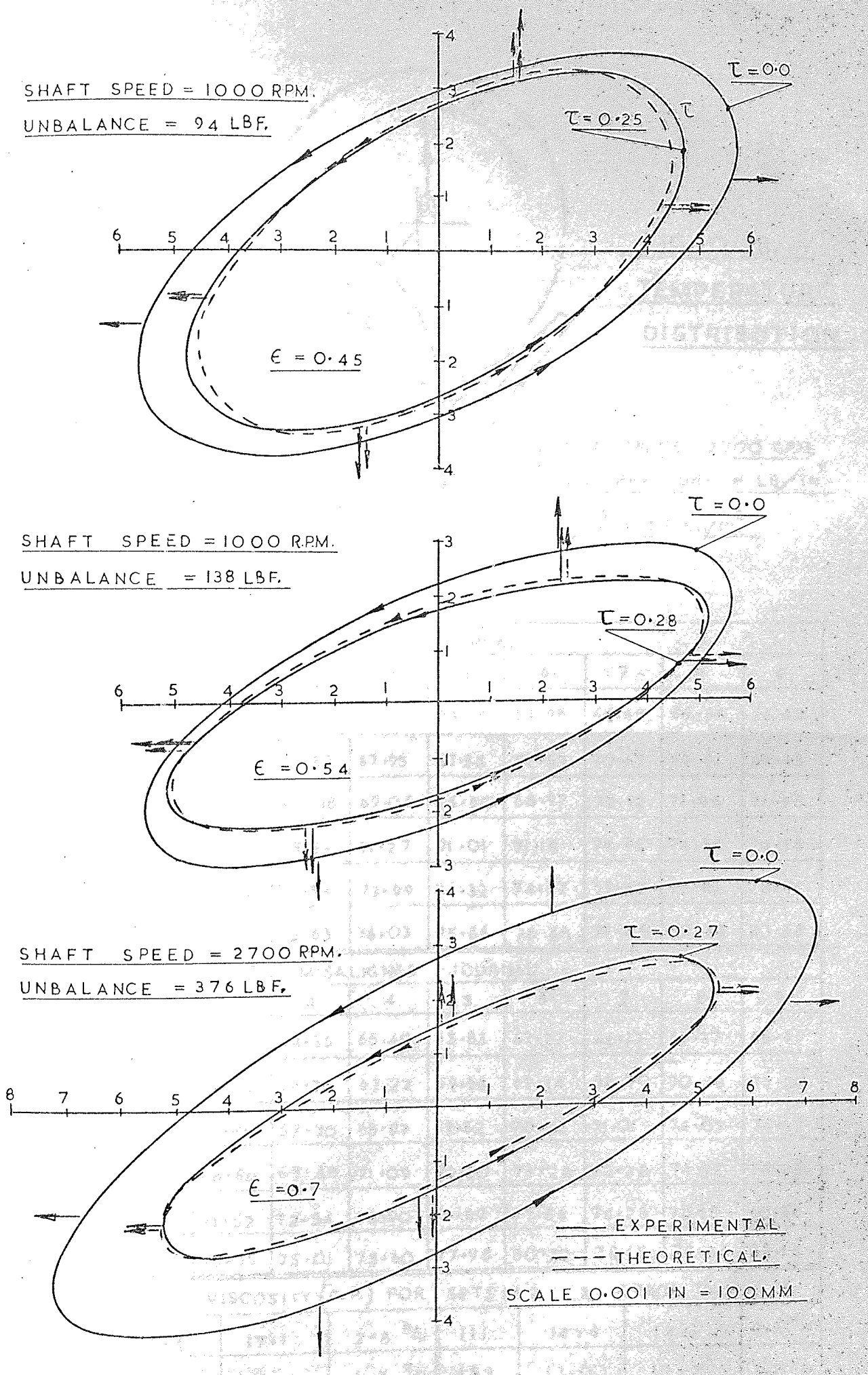

FIG. 10-27. FORWARD WHIRL - LOW FREQUENCY-

ie $\Omega < \omega$ MISALIGNED JOURNAL

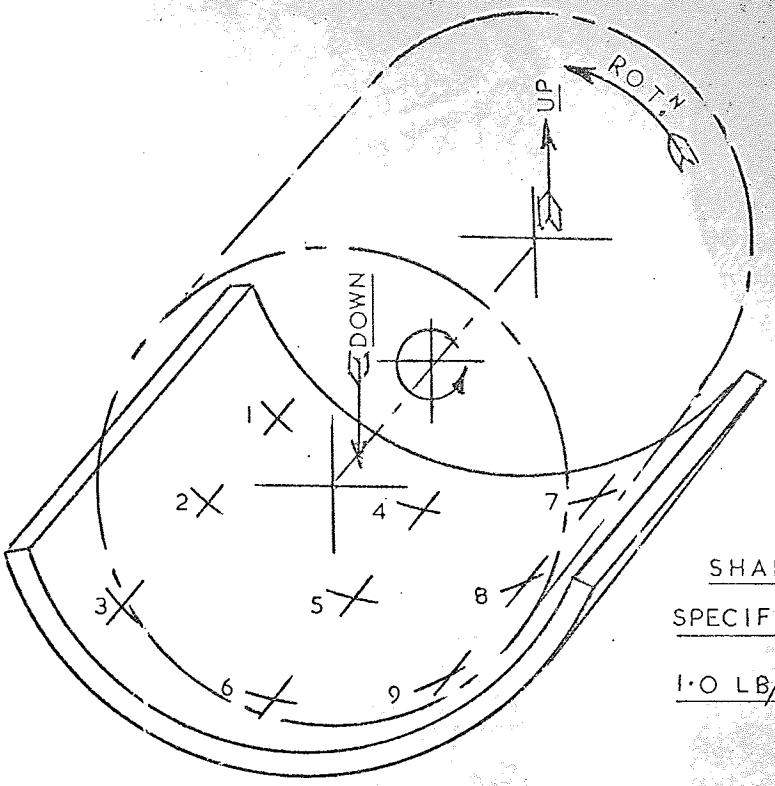

FIG. 10-28.
TEMPERATURE
DISTRIBUTION.

SHAFT SPEED 2700 R.P.M.
SPECIFIC PRESSURE * LB/IN^2
1·0 LB/IN^2 = 69 KN/m^2

PRESS-URE *	SET-1 ALIGNED JOURNAL								
	1	2	3	4	5	6	7	8	9
45	63·53	63·11	63·62	64·89	64·64	64·98	66·68	66·34	66·42
67	65·82	65·57	65·83	67·95	67·53	67·53	70·67	69·91	69·48
89	66·59	66·34	66·68	69·06	66·80	68·97	72·12	71·95	71·95
111	68·21	68·04	68·29	71·27	71·01	71·18	74·75	74·58	74·58
133	70·59	70·59	70·93	73·99	74·33	74·67	77·47	77·81	78·41
155	72·11	72·37	72·63	76·03	75·86	76·88	79·09	79·85	80·28

PRESS-URE *	SET-2 MISALIGNED JOURNAL								
	1	2	3	4	5	6	7	8	9
45	64·55	64·30	64·55	65·40	65·83	67·27	66·17	67·27	69·65
67	66·08	65·83	66·25	67·27	67·95	69·14	68·80	70·33	72·20
89	67·10	67·10	67·70	68·97	69·82	70·23	71·01	74·07	74·49
111	68·80	68·80	69·48	71·09	72·20	73·22	73·22	74·92	76·88
133	71·09	71·52	72·54	73·90	75·69	77·56	76·28	78·15	80·36
155	72·20	73·05	75·01	75·60	77·98	80·70	78·15	79·85	82·15

*	AVE. VISCOSITY (C.P.) FOR SETS 1 & 2		& ERROR %			
45	17·6	17·1	2·8 %	111	14·4	14·1	2·1 %
67	16·0	15·8	1·3 %	133	13·0	12·7	2·3 %
89	15·5	15·1	2·6 %	155	12·5	12·0	4·0 %

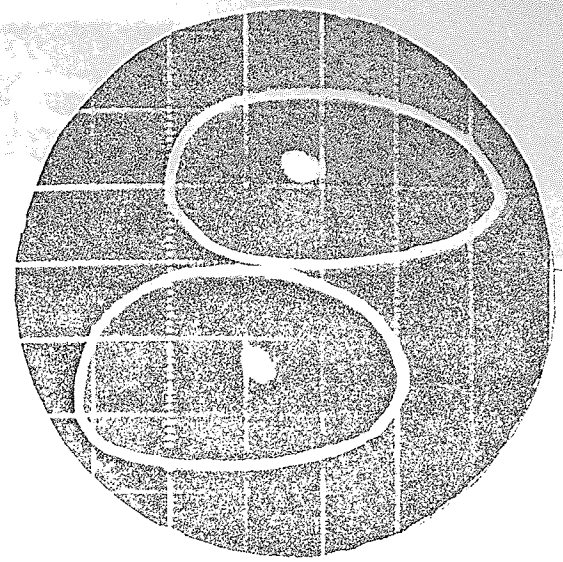

ϵ = 0·37 FORWARD WHIRL

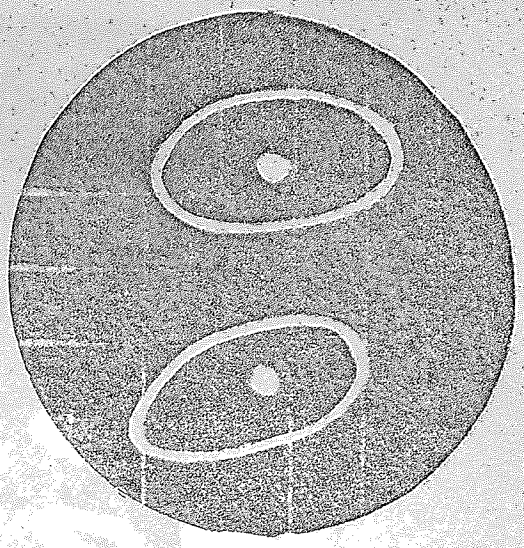

ϵ = 0·49 FORWARD WHIRL

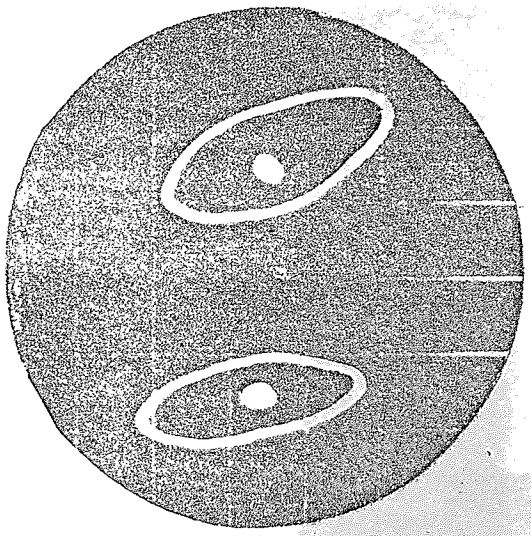

ϵ = 0·63 FORWARD WHIRL

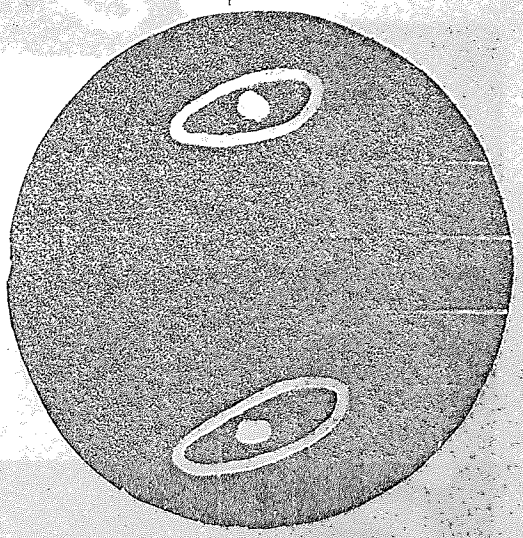

ϵ = 0·70 FORWARD WHIRL

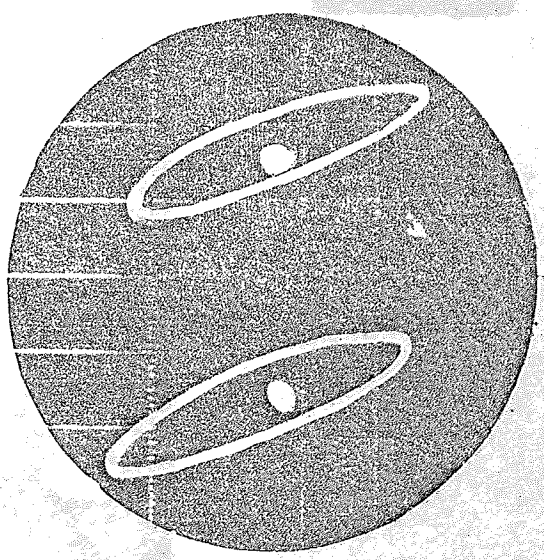

ϵ = 0·37 REVERSE WHIRL

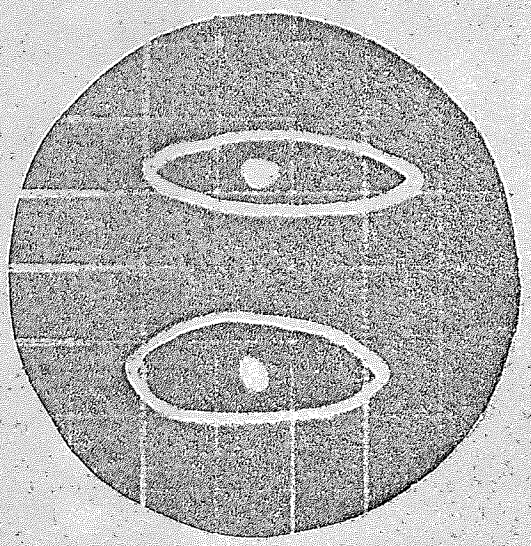

ϵ = 0·49 REVERSE WHIRL

FIG. 10–29. WHIRL TRAJECTORY RELATIVE TO THE STEADY STATE RUNNING POSITION ϵ_o, ϕ_o. FOR A JOURNAL SPEED OF 2700 R.P.M.

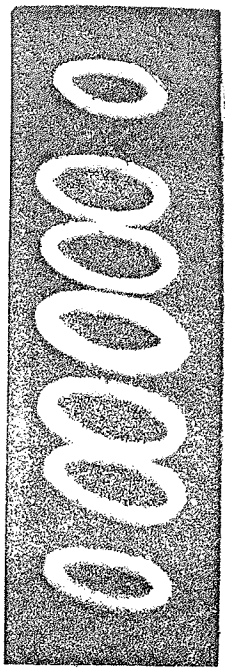

$\epsilon = 0.37$

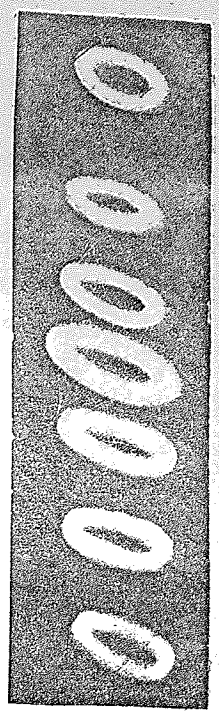

$\epsilon = 0.49$

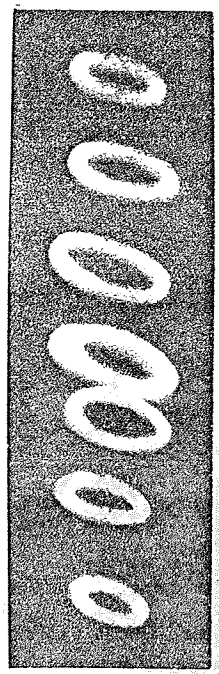

$\epsilon = 0.56$

$\epsilon = 0.63$

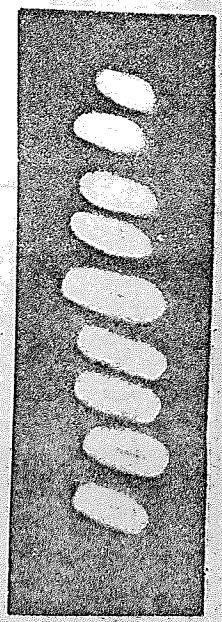

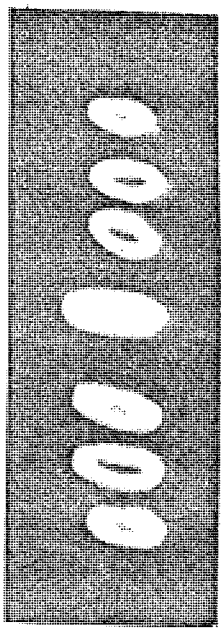

$\epsilon = 0.70$

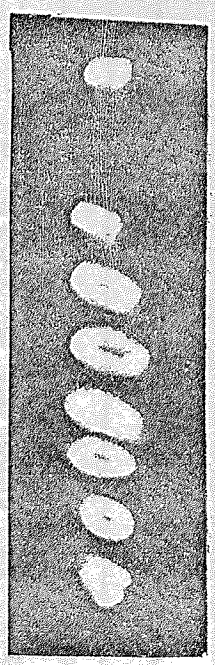

$\epsilon = 0.75$

FIG. 10-30. CHANGE IN WHIRL TRAJECTORY FOR VARYING AMOUNTS OF MISALIGNMENT IN THE VERTICAL PLANE. [2700 R.P.M.]

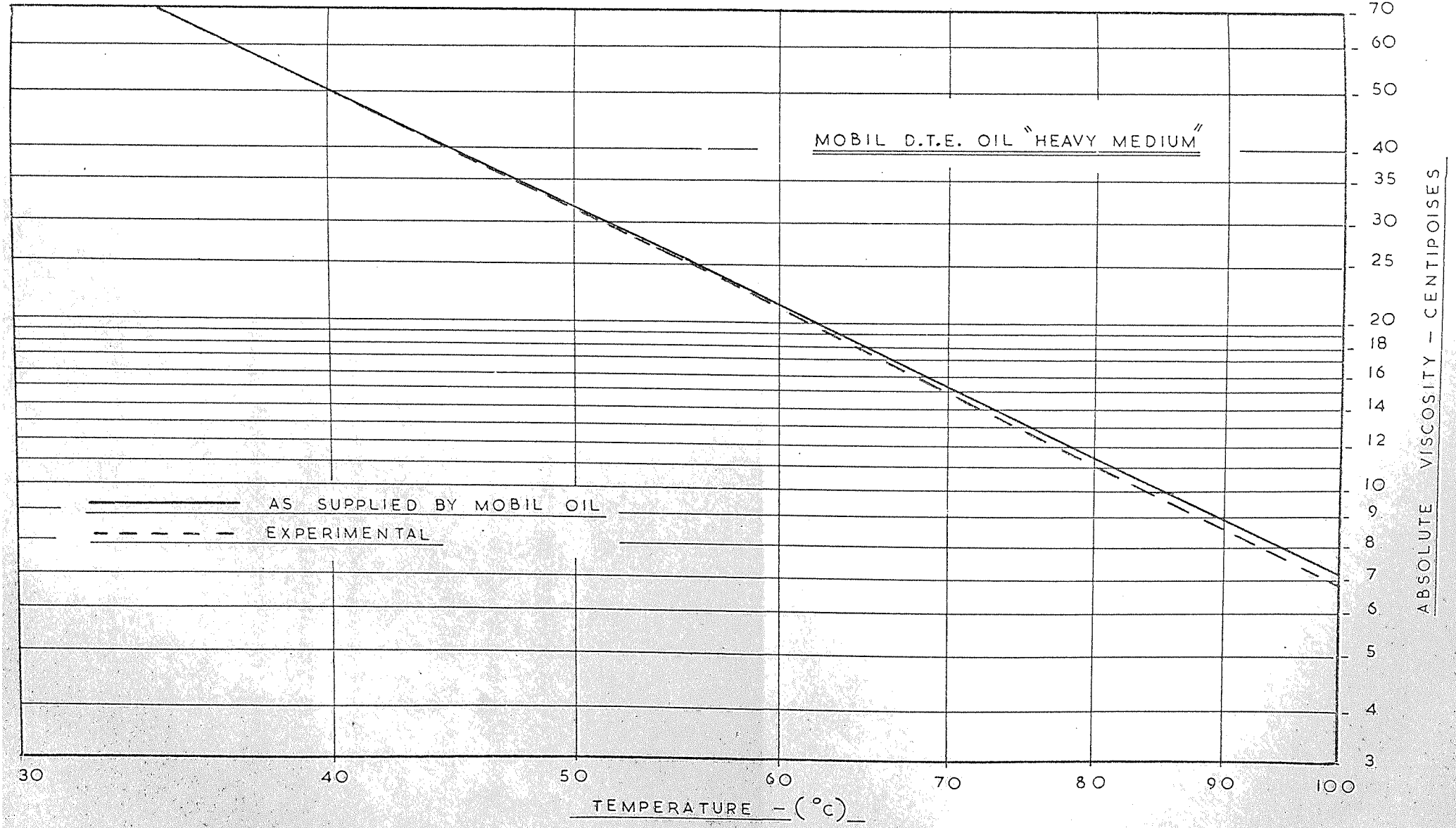

FIG. 10-31. TEMPERATURE — VISCOSITY CHART.

CHAPTER ELEVEN

CHAPTER ELEVEN

ACCURACY OF EXPERIMENTAL RESULTS

11.1 Change in the Sommerfeld duty parameter

One of the fundamental difficulties associated with research on journal bearings is the problems involved when attempting to vary any one of the duty parameters without simultaneously affecting the others. Basically the problem is masked by the change in the shearing action within the oil film wedge inducing a change in the heat balance of the bearing. The Sommerfeld duty parameter has five independent variables as illustrated by the equation

$$S = \frac{\mu N}{P} \left(\frac{R}{C}\right)^2$$

11.1(i) Viscosity μ

The viscosity of an oil is dependent upon temperature and pressure. To obtain the variation of viscosity with temperature for the oil used throughout the tests described in this thesis, charts were obtained from Mobil Co., and in order to check for any discrepancies additional tests were conducted using a Redwood No.1 viscometer. Details of this test equipment will not be discussed here as it is a widely used instrument, and most books on lubrication discuss the viscometer and its use.

Results of these tests are given in figure (10.31) which shows a maximum discrepancy of 0.3 CP at a temperature of 80 degrees C

which could result in a slight error in the Sommerfeld number, therefore averaged values between the manufacturers supplied figures and measured values were used throughout the tests, giving a possible error of in the order of 1.04 per cent.

As described in section (10.6) the oil film temperature of the working face of the bearing was taken to be the averaged reading of the nine thermocouples embedded in the whitemetal of the bush, given by the following equation:-

$$T(^{o}C) = 45.0 + 8.5(v)$$

where v = averaged millivolt reading.

The millivolt meter could be read to within ± 0.02 millivolts, which represented a temperature of ± 0.17 degree C and because the oil viscosity is inversely proportional to the square of the temperature, hence a variation of ± 0.17 degree C gives an error in the viscosity of ± 1.13% at an operating temperature of 60 degree C.

The effect of pressure upon viscosity has little effect for pressures operating below 1000 lb/in^2 (6.9 MN/m^2) therefore it was not essential to investigate the viscosity-pressure relationship. The maximum specific pressure used during tests was 200 lb/in^2 (1.38 MN/m^2) and even allowing for the increase in pressure generated within the oil film wedge, would still have negligible effect upon the viscosity.

At the high speed tests a certain amount of frothing was noticed, however, using results published by the National Engineering Laboratory ref(51) the effect of entrained air upon the viscosity of

oil is shown to obey the following relationship:-

$$\frac{\mu_B}{\mu_o} = 1 + 0.015\beta$$

under the worst conditions β = 1.7 cc in 100 cc it was concluded therefore, that amounts of entrained air experienced during tests had no effect upon the oil viscosity.

11.1(ii) Journal Speed

Speed control of the bearing was considered to offer very little error in controlling the bearing parameter. The Heenan and Froude speed control maintained a speed well within 1.0 R.P.M. over a frequency count of 10 seconds. It was difficult to assess the long term accuracy of the speed controlling system but it was thought to be within 1.0 to 1.5 R.P.M.

11.1(iii) Specific Pressure 'P'

The specific pressure of the journal bearing was made up of the static weight of the test journal plus the pull exerted by the compressed air cylinder. The gauge could be reasonably controlled to within $\pm$ 0.5 lb/in^2 (3450 N/m^2) resulting in an error of 4 per cent for the lightly loaded tests, and 0.9 per cent at the maximum loadings, however, with care these percentage errors could be controlled to give improved accuracy. Balance between the two compressed air cylinders was achieved by monitoring the running position of each end of the test journal.

11.1(iv) Journal radius (R) and radial clearance(C)

The values of R and C describe the geometry of the bearing, they could be a possible source of error by undergoing thermal expansions or elastic distortions, resulting in changing the oil film thickness. An experimental investigation into thermal equilibrium of journal bearings was conducted by Dawson, Hudson, Hunter and March ref.(52). Their published results showed the circumferential and axial variations of journal surface temperature to be negligible, thus allowing the assumption to be made that thermal expansions of the journal will be uniform over the entire surface. The same paper also provided information illustrating the bush isotherms for various lubricant supply temperatures, together with journal operating temperatures. This collection of information allows the determination of the thermal expansion of the bush relative to the journal, indeed, this reference investigated a similar size bearing and when operating at the maximum operating temperatures gave an increase in the radial clearance 'C' of 0.00011 in, thus giving an error in the Sommerfeld number of only 1.5 per cent. When designing a bearing this magnitude of error may be completely neglected, this has always been assumed to be a reasonable assumption by most designers.

In Chapters three and four the analysis presented numerical methods for the solution of Reynolds equation with completely rigid surfaces, and any variations in the oil film thickness as a result of elastic distortion of either the journal or the bearing bush was sufficiently small such that it may be neglected. This assumption was substantiated by experimental work undertaken by Hooke, Brighton and O'Donoghue, ref.(53) who investigated a bearing of the design used in the experimental work contained in this thesis.

The presence of high spots in the babbit may effect the equivalent radial clearance, thus inducing local high intensity of oil pressure, further repeated stopping and starting of the test journal could cause wear to the babbit lining, again affecting the radial clearance. To overcome any ill effects caused by the presence of high spots, a series of rub-tests were conducted and any high spots in the babbit were removed.

The problem of wear was overcome by removing the load off the test journal before starting and again when stopping. An examination of the working face of the test bush was made upon completion of the test programme, and no evidence of wear or damage was present which may prejudice the results.

If the errors described in sections 11.1(i) to 11.1(iv) were accumulative the total error would not exceed 7.67 per cent. Therefore it is reasonable to conclude that the eccentricity ratio determined from the bearing duty parameter should not exceed an error or 0.01 even if the lower values of Sommerfeld number are considered, this being the region where eccentricity is most sensitive to changes in the Sommerfeld number.

11.2 The effect of Turbulence

The remaining source of error effecting the duty parameter and hence the running position of the journal bearing, is if the bearing was operating beyond the laminar flow conditions where vortexes begin to form within the oil film. Under these conditions the hydrodynamic equations governing the behaviour of the journal could no longer be applied without consideration being given to the inertia forces. The

condition where vortexes commence forming can be determined by Taylor's criterion as modified by Wilcock reference (54) and is given as

$$\pi DNC/v = 41.1 \sqrt{\frac{D}{2C}}$$

Using the above equation, for the test bearing to operate under conditions favouring turbulence, would mean having to rotate the journal at a speed of 9500 R.P.M. which would be equivalent to a Reynolds number of 835, which is also very close to that given by Taylor i.e. RE crit = 945. The Reynolds number for the test bearing, operating; at a maximum speed of 2700 R.P.M. would only be 40.0, hence it can be concluded that all tests were conducted well within laminar flow conditions.

11.3 Sensitivity of the Transducers measuring journal movements

Before commencing any experimental work, zero drift of the transducers was investigated with the ambient temperature raised, and it was confirmed that drift was negligibly small over the working range of the bearing, and to ensure that no thermal ratcheting of the transducers occurred, the transducers were re-calibrated every thirty to forty working hours.

The sensitivity of the transducers, as measured from the u.v. recorder, gave for 0.001 inch movement of the journal a corresponding galvonometer displacement of 30 mm. Therefore, as it was reasonable to measure the u.v. trace to within ± 0.5 mm, the orbital displacement measurements could be guaranteed to an accuracy of ± 0.000016 inches. Measurements taken from the millivoltmeter, again for a journal movement of 0.001 inch, gave an averaged reading of 67 mv, and as this

meter could be easily read to within ± 5.0 mv the accuracy to which the journal could be measured, via the millivoltmeter was ± 0.00008 inches giving an error in the radial clearance of 1.33 per cent.

A further error which may have been incurred when measuring the whirl trajectory, could be the machining irregularities of the test journal which are continuously built into the system, these errors could however, only be measured by the transducers giving in the order of 0.00005 inch; this type of error can be seen in figure (10.29) i.e. the centre dot representing the steady state running position, or from the u.v. trace figures (10.19) and (10.20).

Drift of the electrical instruments was kept to a minimum by making a zero check upon completion of a particular test run. Drift measured in this manner was usually found to be very small, and was allowed for in the final calculations for the journal steady running position.

Linearity of the transducers was dependent upon the initial gap between the test journal and the transducer, and for the distance chosen gave a linearity of ± 2.0% over the entire radial clearance of the bearing.

The vibration phase reference transducer, as illustrated in figures (10.19) and (10.20) indicates the instant of time when the vibrating force was acting along the positive x coordinate axis. For the higher frequencies of excitation, the accuracy of the phase angle of the applied out-of-balance force could only be measured to within ± 5 degrees, due to the limiting paper speed of the u.v. recorder. For the very small amplitude of vibration, coupled with the higher

excitation frequencies, phase errors were in the order of ± 10.0 degrees.

11.4 Locus of shaft centre - aligned conditions

Scatter of the results presented in figures (9.1) and (9.2) would seemingly be large, however, it must be remembered that for the radial clearance used on the test bearing an eccentricity ratio of 0.1 corresponds to a displacement of 0.0006 inches. It is awareness of this value that accuracy of results may be judged. Generally the scatter is located to the attitude angle as demonstrated in figure (9.1) having an averaged error of 13.0 per cent compared to an averaged error of 2.5 per cent for the eccentricity ratio. The seriousness of the error for the attitude angle results is confined to the prediction of the minimum oil film thickness, and therefore in no way effects the results of the oil film force coefficients.

11.5 Locus of shaft centre - misaligned conditions

The maximum error between the theory and experimental results was approximately in the order of 6.0 per cent for the larger eccentricity ratio's and considerably less for the smaller eccentricities where the oil film thickness was greatest, thus allowing large amounts of misalignment to be applied to the journal. For the smaller eccentricity ratios the resultant vertical force was completely unchanged due to transferring weights from one side of the test journal to the other. However, for the larger eccentricity ratios, requiring greater applied loads and couples, the error was isolated to the accuracy of reading the air pressure gauges which has already been discussed.

Other errors were probably caused by the amount of trim weights required to ensure that the misalignment was confined to the vertical plane. The test bearing was found to be most sensitive to horizontal components of displacement generated due to the introduction of vertical misalignment, therefore, it was considered unnecessary to investigate the effect of errors due to the presence of horizontal couples, but based upon theoretical reasoning, errors were expected to be in the order of 4 per cent.

CHAPTER TWELVE

CHAPTER TWELVE

DISCUSSION OF THEORETICAL AND EXPERIMENTAL RESULTS

12.1 Oil film pressure distribution

The pressure distribution illustrated in figures (7.1),(7.2) and (7.3) demonstrate that each nodal pressure over the entire grillage is well behaved, even under conditions of misalignment, thus the method of finite differences for values of the required function and its four neighbouring nodes are well conditioned for the selected grillage, having 625 nodes for small eccentricity ratios and up to 1024 nodes for the higher eccentricities experiencing misalignment.

The theoretical predictions for misalignment confined to the vertical plane were very good, indeed even the residual horizontal couple generated by the oil film wedge was detectable by the experimental test journal, and although the magnitude of this couple was only in the order of 4.0 per cent of the applied vertical couple, the journal had to be balanced in order to isolate misalignment in line with the applied load, thus demonstrating the sensitivity of both the computer program and the test rig.

Correlation between theoretical predictions and experimental results presented in figure (7.4) are also considered to be quite good; the maximum error located at point (3) which was in the order of 16 per cent, and zero per cent for the maximum intensity of pressure at the measuring position (6). It must be remembered that these experimental results were conducted on a bearing of only 1.62 inch diameter

having a L/D ratio of unity, therefore to investigate SEVEN pressure sampling positions along the length of such a short bearing, could easily give rise to experimental error. For this reason Du Bois used specific pressures as high as 850 lb/in^2 (5.87 MN/m^2) resulting in certain parts of the bush operating under near boundary lubrication conditions, causing the bush to wear to a bellmouth shape, which of course affects the pressure profile. However, the results obtained are considered to be acceptable thus allowing the experimental investigations to proceed to the testing of the steady running conditions, which again is a measure of the accuracy of the calculated oil film forces.

A pattern emerging from the oil film pressure distribution, is that under operating conditions with an eccentricity ratio of 0.7 and below, for a perfectly aligned journal, the pressure profile is flat and only by increasing the eccentricity ratio above 0.7 does the rate of change of pressure along the axial length become more pronounced, thus demonstrating that side leakage increases with a corresponding increase in the Sommerfeld number. Where the pressure distribution is normally low for a bearing operating under aligned conditions, the film pressure increases severely with only a slight increase in journal tilt, especially so where the Sommerfeld number is small.

Further, by introducing misalignment in the vertical plane the angle of incidence for small values of eccentricity ratio increases in value, this change however diminishes at an eccentricity ratio of 0.5. Above 0.5 the angle of incidence starts to change again but is lowered.

12.2 The effect of the oil pressure distribution upon the critical speed of the shaft system (due to the movement of the centre of pressure)

Where two or more bearings are used in supporting a shaft, the effect of the journal angular displacement on the oil film pressure, can be estimated by calculating the total tilt of the journal, from which it is possible to determine the pressure profile of the oil film wedge. However, it is not readily appreciated that this pressure profile, generated by the introduction of misalignment, introduces a couple trying to resist the induced slope. Therefore, if the shaft system is flexible due allowance should be made by taking into account, in the deflection equations, the equalizing oil film couple. The magnitude of this couple will of course depend upon the amount of induced misalignment, tests undertaken by reference (44) show the couple to be 560 lb.ins (63.0 Nm) for a journal eccentricity ratio of 0.7 and a tilt ratio equal to 0.25, which depending upon the flexural rigidity of the shaft system, will reduce the mid-span deflection and in turn raise the critical speed.

The same problem may be analysed in another way, the natural catenary of the shaft lies towards the centre of the bearing span, therefore the centre of pressure of the hydrodynamic oil film moves towards the centre of the bearing span. To illustrate the amount by which the centre of pressure shifts with misalignment the same reference (44) will be used. For example an eccentricity ratio of 0.7 and tilt ratio of 0.25 moves the centre of pressure along the bearing by 15 per cent of the bush length, thus the shaft system would have its bearing centres reduced by an amount equal to 30 per cent of the

total bearing length. This particular phenomenon has been reported by Downham reference (13). A rough guide of how the critical speed is influenced by a reduction in the bearing span may be given by:-

$$N_c(NEW) = N_c(OLD) \times \left[\frac{L(OLD)}{L(NEW)} \right]^{\frac{3}{2}}$$

12.3 Locus of shaft centre for aligned conditions

No evidence of discontinuity, caused by the boundary condition $dP/d\theta = 0$, could be found between experimental and theoretical results. It was initially feared that under operating conditions the trailing boundary produced cavitation within the oil film wedge, the correlation between theory and practical results would begin to diverge, indeed the running position of the journal bearing was in complete accord with theoretical predictions, with the journal centre tracing a locus within the limits of the radial clearance as follows:- Point A in figure (9.2) was the centre of the journal at standstill and point B would be the same centre if the test bearing would be made to operate at very high speeds with little to no loading, this position is hypothetical as few bearings ever operate under such extreme conditions. During the experimental testing the bearing would operate between points A and B following an arc of the general shape shown. The final position of the test journal for explicit operating conditions was dependent upon the term $\mu N/P$. If μ and N were made large the eccentricity ratio would approach zero, as would be the case if P was made small. If however, μ and N were made small and P large the eccentricity ratio would approach unity and if taken to the limit metal to metal contact would occur.

The experimental results shown in figure (9.2) satisfactorily demonstrates, that the journal bearing performance can be determined with accuracy by making use of the Sommerfeld duty parameter for averaged operating temperatures.

Taking the viewpoint of the design engineer having to compute the force coefficients in order to investigate the dynamical behaviour of a rotor, and further having to design the bearings supporting the rotor, particular attention has to be given to theoretical power losses generated within the oil film, together with the minimum oil film thickness so as not to have oil film rupture. All of these design considerations are dependent upon the successful determination of the journal centre locus as a function of the Sommerfeld duty parameter, based upon the assumption that averaged oil film viscosity would be representative for realistic operating conditions, thus alleviating the need to investigate the effects of varying viscosity. Morton ref.(42) et al have used oil outlet temperatures with reasonable success, but this must be at the expense of accuracy.

12.4 Locus of shaft centre for misaligned conditions

The presentation of the journal running position for various amounts of misalignment is unique. The majority of research work published describing the behaviour of journal bearings under misaligned conditions requires prior knowledge of the externally applied couple, therefore results are usually presented as a function of couple ratio, that is except for reference (46) which although presented the duty parameter as a function of slope did not indicate the position of oil film rupture relative to the degree of misalignment. The results presented in figure (9.3) however, provides a rapid assessment

of the allowable amount of misalignment for various duty parameters and/or eccentricity ratio. The same figure also illustrates the reduction in eccentricity ratio which could be expected for a given misalignment in the vertical plane.

In the majority of cases where misalignment has to be considered at the design stage, it has been the authors experience to be only aware of the slope at which the journal presents itself to the bearing bush, therefore results presented in figure (9.3) are a function of slope and are non-dimensional, thus allowing the resulting graph to act as a design chart for all operating conditions for bearings having the same geometry.

The experimental results presented in figure (9.3) would have perhaps been better presented if changes in duty parameter for a fixed eccentricity ratio had been plotted for varying amounts of misalignment. However, such a task would inevitably have given rise to errors, as changes made to any one of the elements of the duty parameter would effect the heat balance within the oil film, automatically changing the oil film viscosity making it extremely difficult in controlling the bearing as to provide a constant eccentricity ratio. For this reason it was considered better to find changes made to the eccentricity with the introduction of misalignment whilst keeping the Sommerfeld duty parameter constant. The latter method also illustrates the technique to be employed when using these results as a design chart. For example, having decided upon the extent of misalignment, determined from the deflection of the shaft system etc. and having calculated the Sommerfeld duty parameter, the intersection of these coordinates will provide the reduced

eccentricity at which the journal will operate. If, however, the amount of misalignment has to be changed the duty parameter will still remain unchanged, a condition which was shown to be correct from the obtained experimental results illustrated in figure (9.3).

Under misaligned conditions the oil film produces an equal and opposite couple which is analogous to off-setting the line of action of the reactive load away from the centre of the bearing bush. The experimental investigation did not vigorously extend to checking the movement of the centre of pressure of the hydrodynamic oil film along the length of the bearing for varying amounts of misalignment. However several isolated cases did show the theoretical curves presented in figure (9.4) to be within 10 per cent of the applied misaligning couple.

The effects of misalignment upon the oil film may be demonstrated by considering the following:- off-setting the load by 10 per cent of the bearing length away from the bearing centre, reduced the oil film thickness locally at the one end of the bearing by 40 per cent for an eccentricity ratio of 0.9 and 35 per cent for an eccentricity ratio of 0.3. If however, the misalignment is increased such that the load is offset to 37 per cent, would cause metal to metal contact for the majority of eccentricity ratios. The values of the curve illustrated in figure (9.4) would be capable of assessing the changes made to the bearing centres for critical speeds described in Section 12.2.

Introducing misalignment also has the effect of changing the angle of incidence as illustrated in figure (4.5). However, because of the difficulty experienced in measuring these angles, as discussed in section (9.2) it would serve to little value to present small

changes made to the angle of incidence with misalignment. Changes that were measured did follow the general trend as suggested by the theoretical predictions. This point is not investigated to any depth as the attitude angle is not a contributing factor when considering the oil film force coefficients.

A phenomenon of considerable interest to the practising design engineer, is that although the temperature distribution within the oil film wedge changes with the introduction of misalignment, the averaged temperature does in fact remain unchanged, thus the theory of averaged viscosity for the Sommerfeld duty parameter may still be considered. The validity of this statement substantiated by the experimental results, presented in figure (9.3) being a straight line.

12.5 Hagg and Sankey Coefficients

The value of Hagg and Sankey force coefficients for determining the response of rotors are limited, indeed there must be an awareness of their limitations if realistic results are to be expected when investigating rotor dynamics. Because of their simplicity in both their determination and application they have been favoured in the past, however, results presented in figures (10.1) to (10.8) clearly illustrates that for the higher values of $M\omega^2$ Hagg and Sankey coefficients depart substantially from results where the value of $M\omega^2$ is small.

If a qualitative understanding is to be maintained experimental coefficients may only be used where the effect of rotor inertia is identical to the experimental apparatus, and amplitudes of vibration

are also expected to be similar. It is recommended that in order to achieve greater accuracy it would be better to use the eight force coefficients for the rotor system under investigation, and if the Hagg and Sankey type coefficients are required to deduce them from the orbital response characteristics using all eight force coefficients. However it cannot be over emphasized that the amplitudes of vibration must be extremely small, any departure from this will have the effect of suppressing the orbital response.

To present experimental values of the Hagg and Sankey type could be misleading, as they do not include all the contributing factors which influence the orbital response. As described before, for an increase in the value of $M\omega^2$ will reduce the value of K_u and will increase the other coefficients, particularly for the higher speeds of rotation, further any amplitude of vibration having sufficient magnitude to be measurable would introduce non-linearity of the "HARD TYPE", giving the effect of increasing both the oil film stiffness and damping. To separate the above effects from one another would be a formidable task, therefore no attempt was made to present experimental results which would have limited value.

The above discussion is further enhanced by the experimental coefficients published by Duffin and Johnson reference (37). Here Hagg and Sankey type of coefficients were determined as part of an investigation into the performance of a 24 in dia x 18 in long elliptical three-land bearing, however test speeds were not given but it was thought that in order to provide laminar flow conditions the journal speed was in the order of 600 R.P.M. thus the equivalent journal inertia was quite low. The results presented in this reference

display a lowering of the Ku coefficients and an increase in the remaining three, although, in general all the coefficients were larger in magnitude compared with Hagg and Sankey this was most certainly due to the greater stability properties offered by a three-land bearing.

Discrepancies experienced by D. Smith reference (33) are also logically explained by the presence of $M\omega^2$ in the equations of motion. Smith compared the Hagg and Sankey results with those determined analytically, and found that the maximum amplitude obtained by Hagg and Sankey was greater than those determined by Smith at the low eccentricities but improving for the larger eccentricity ratios. This phenomenon is adequately illustrated by equations (5.4), for example the bracketed term $(Axx-m\omega^2)$, at the higher eccentricity ratios, would not be greatly effected by the inertia force as the value of Axx would be large. However, this would not be true for the smaller eccentricities as Axx would be small and $M\omega^2$ would be the predominate term. A general conclusion as to the use of Hagg and Sankey force coefficients, would be to avoid their use if at all possible in view of the fact that there are more sophisticated methods available.

12.6 The use of eight force coefficients for predicting the journal whirl trajectory

The experimental results clearly demonstrate that the frequency of the exciting force plays a most important role when investigating the orbital response of a journal bearing, and in turn illustrates that, depending upon the frequency and amplitude of vibration, methods of deducing the force coefficients from vectors of vibration would

erroneously lead to results which would otherwise pass unnoticed, indeed the results would present averaged stiffness and damping values for each selected amplitude of vibration, whereby different coefficients would be computed for varying displacement amplitudes. This phenomenon has been observed by other research workers in the field, but discounted when proceeding with investigations utilizing small amplitudes of vibration and without presenting evidence of linearity.

The experimental results presented in figures (10.11) and (10.12) show good agreement with the theoretical predictions using only eight force coefficients, suggesting that the influence of non-linearity only becomes noticeable for the higher exciting frequencies, and is most predominant at synchronous vibration. These results also explained the behaviour of those coefficients obtained by Morton, reference(42), the results published in this reference gave force coefficients for low frequencies of vibration, and although this writer cannot agree with the method employed, as discussed in Chapter two, low frequencies of excitation produces force coefficients lower when compared with results obtained for the higher frequencies of vibration.

Using the method described in section (5.3) for obtaining the force coefficients from the experimental vectors of vibration, gave measured values as shown in figures (10.13) and (10.14). The results describing the displacement coefficients are good except for the cross coupling term A(xy), however, a distinct change in sign was observed for this coefficient and because its value is small compared to the remaining three displacement coefficients its influence on the orbital whirl trajectory is obviously less. The results obtained for the

velocity coefficients can only be considered as fair. To determine values of the velocity coefficients requires precise measurement of the angular position of the force vector, together with the angle of inclination of the whirl orbit. Inspection of figures (10.11) and (10.12) show such measurements to be within three to five degrees which have the dramatic effect of producing damping errors as illustrated in figure (10.14). Therefore although the presented values of damping would seemingly be inaccurate they do in fact produce results which would be quite acceptable in practice, as the state of the art at this stage cannot be controlled to within such fine limits.

From the behaviour of the results presented so far, it is clear that for any vibrational frequency and any reasonable amplitude of vibration, investigations would have to proceed with the addition of the non-linear force coefficients, which must be introduced in such a manner that sub or super harmonics do not appear when considering rigid rotor systems.

12.7 The effect of using the second order terms for predicting the journal whirl trajectory - aligned conditions

The results presented in sections (10.3) and (10.4) clearly demonstrates the influence of non-linearity upon the orbital response excited by a periodic disturbing force. Consideration has been given to both the amplitude and frequency of vibration in order to demonstrate the corresponding changes likely to be experienced in both the stiffness and damping coefficients, had only the eight force coefficients been presented, thus illustrating that a knowledge of the

non-linear properties is necessary for the solution of problems related to force oscillations of partial journal bearings of the type used in this research work.

The complexity of the oil film behaviour is demonstrated by the changes experienced in the orbital whirl trajectory resulting from changes made to the vibrational frequency, a condition often found on real rotors. Machines using journal bearings may experience three distinct types of vibration, the first and most common is where the disturbing force is at the fundamental frequency relative to the rotational frequency of the machine, which may be associated with an out-of-balance condition of the rotor or turbine, alternatively the vibration may be caused by misaligning couples or, as is often the case, caused by running on or near to the critical speed of the shaft system. Therefore in order to demonstrate the effects of non-linearity for conditions similar to the above, theoretical and experimental results for K = 1.0 were demonstrated proving that methods adopted for analysing the dynamic behaviour of the rotor must include all the second order force coefficients. The experimental results presented in figures (10.21) and (10.22) also illustrates this type of synchronous vibration, and shows how non-linearity plays a most important role over a wide range of journal amplitudes.

The second type of vibration experienced on many rotors is where the vibrational frequency is greater than the rotational frequency of the journal, for example, in most two pole electrical machines it is not uncommon to experience double frequency vibration, that is a disturbing force having a frequency equal to twice the

running speed of the shaft caused by the gravitational deflection of an unsymmetrical rotor, unsymmetrical due to the rotor slots in which the windings are embedded occupying only part of the rotor circumference, thus giving rise to unequal bending inertias in two mutually perpendicular directions. To demonstrate this type of vibrational frequency theoretical results are presented in figure (10.17) which investigates the condition where K = 2.0 also experimental work, not given here, illustrates non-linearity to be predominant in both phase relationship and vibration amplitudes. Therefore in corditions where the vibrational frequency is greater than the rotational frequency, the second order coefficients should be considered, as the effects of damping caused by the increase in vibrational frequency, is not sufficiently large as to make non-linearity of little value.

The third kind of vibration occurs at frequencies below the rotational speed of the journal, for example, light load instability, half speed whirl or low frequency whirl, where the vibrational frequency is locked to some fractional part of the rotational speed of the shaft. Therefore in order to investigate the effect of subharmonic vibration upon the oil film characteristics both theoretical and practical results have been presented with K = 0.5, demonstrating that non-linearity for vibrational frequencies of 0.5 and below are shown to influence the damping and to a much lesser extent the equivalent film stiffness for the smaller amplitudes of vibration, unless the amplitudes are in excess of 0.0025 in (0.0635 mm), above this amplitude non-linearity is shown to have a considerable effect. These latter results where K = 0.5 having relatively small amplitudes of

vibration are clearly the only conditions where the eight force coefficients could be used without introducing errors of unreasonable proportions. The accuracy of the results for K = 0.5 is further supported by observations made in reference (42); here Morton found that if the perturbations were slow then a reduction in stiffness was found.

Both the computed and experimental results showed the magnitude of damping to be in the same order as the oil film stiffness, thus demonstrating that the damping properties of a hydrodynamic oil film is the controlling influence in suppressing rotor vibrations, also it could be so effective in dissipating energy, that in many machines it is difficult to identify a critical speed without sensitive instrumentation.

The velocity coefficients would also suggest that when a rotor passes slowly through a critical speed, the peak amplitude will be greater for a bearing operating with a low eccentricity ratio, reducing as the eccentricity ratio increases, or for a lowering of the Sommerfeld duty parameter. The situation whereby the lower eccentricity ratio would be present would of course be at the higher rotational speeds, therefore it would be better for this operational condition to ensure that the critical speed was well above the maximum running speed of the machine, further the rotor response for these operating conditions would have a large "Q" factor giving little warning of running into a critical speed which on the larger running speed would give rise to severe vibration. If however, the duty parameter of the bearing is such that the journal has a large eccentricity ratio, the amplitude of vibration would be less, also the response of

the rotor would have a corresponding low Q factor, therefore care should be taken when designing the rotor system to ensure good separation between the critical speed and the running speed so that the running frequency does not lie on the flank of the response curve.

During the experimental investigation with the bearing operating with small eccentricities a certain amount of rocking was observed, this was initially thought to be the friction in the needle roller bearings in the Hardy Spicer Coupling, but it was finally concluded that the greater part was due to the effect of the self pumping action of the top bearing cap. Additional tests were conducted on a 30 Mw exciter, which because of its size, had lightly loaded bearings displaying this same phenomenon and were controlled by adjusting the oil inlet supply pressure. It should be emphasized that this rocking only occurred with no external load applied to the test journal and with a cold inlet oil supply.

The dynamical behaviour of the oil film may be adjusted by changing the radial clearance of the bearing. For example, the Sommerfeld duty parameter is inversely proportional to the square of the bearing radial clearance, therefore a reduction in clearance lowers the eccentricity ratio and also lowers the magnitude of the non-dimensional force coefficient. However, the absolute value of stiffness or damping is inversely proportional to the clearance, thus a reduction in clearance increases the coefficient but the net result would be to lower the stiffness and damping ability of the hydrodynamic oil film. Hence a bearing having a fixed journal diameter for torque requirements, and a fixed length to diameter ratio for the specific

pressure requirements can still be controlled to give a desired stiffness for adjusting the critical speed or conditions of instability. However the design engineer should not be too easily tempted to reduce the bearing clearance too much due to the rapid increase in the losses generated within the oil film, resulting in a very hot bearing together with a reduction in the working efficiency of the machine. Small reductions of the bearing clearance are permissible compared with the recommended values given in Appendix B, further non-linearity being inversely proportional to the square of the radial clearance will have additional stabilising effects upon the oil film.

Pedestal vibration tended to complicate the computation of the oil film force coefficients by introducing another two degrees of freedom in the vertical and horizontal planes, therefore if the journal amplitude of vibration is to be kept larger than pedestal displacements a necessary requirement would be to make the pedestal supporting structure as rigid as possible. Preliminary tests showed the natural frequency of the combined pedestal and supporting structure to be higher than the maximum frequency of the disturbing force, further the phase of the pedestal etc. was within 20 degrees, provided the cast iron support blocks were rigidly bolted down onto the concrete foundations, previous attempts to flexibly mount the pedestal proved to be difficult because of the low frequency requirements of the test programme.

The magnitude of the pedestal vibration at the higher frequencies of vibration, clearly demonstrated that results would be in quantitative error had not the pedestal motion been included when evaluating the resulting inertia force of the test journal, indeed results published by reference (28) et al. could well have low values of

stiffness due to their neglect to consider displacements of the bearing bush supporting structure. The largest movement of the bearing pedestal occurred when the journal was operating with the larger eccentricity ratios. Under these conditions the oil film stiffness was the greatest and in order to generate forces sufficiently large as to produce measurable movements also caused the supporting structure to vibrate. In order to improve the measuring accuracy of the pedestal displacements the pedestal transducers were calibrated upon completion of each test. This was because each running condition of the bearing produced a totally different thermal balance within the bearing, thus the inductance of the bridge network was changed due to the thermal expansion of the bearing pedestal. Further tests were also conducted to ensure that pedestal displacements were equal about the mean position.

The strain gauges measuring vibrations in the vertical load, applied to the test journal under dynamically loaded conditions, gave readings so small that they served no useful purpose, suggesting that the specific pressure remained constant throughout the life of one complete whirl trajectory of the journal. The reason for this was thought to be due to the flexibility of the rubber sealing ring around the piston, this seal was clamped to the piston, but held tightly against the cylinder walls by the air pressure within the cylinder, thus any movement applied to the piston (the peak value being in the order of ± 0.0006 in (0.0152 mm)) was completely taken up by the sealing ring, thus offering very little variation in load to the strain gauges within the load cell.

The presentation of the twenty eight force coefficients would seemingly be incapable of being handled in critical speed calculations, indeed methods such as Mykelstad and Prohl would no longer be used as these methods employ an iterative technique whereby an assumed value for the critical speed has to satisfy the equations of motion, further the resulting modal shape is limited to one plane and relative to some unknown quantity. However, by considering two co-ordinate planes and by using real and imaginary functions to describe the forces, moments, displacements and slope, thus replacing each element of the field matrix by a complex element, it now becomes possible to find the critical frequency by applying a number of different forcing frequencies and analyzing the resulting response. By approaching the problem in this manner the fourteen force co-efficients representing the oil film may be introduced as a function of displacement and velocity. The problem of solving critical speeds and rotor instability now follows the same behaviour as a physical rotor, for example, the critical speed is now replaced by a frequency which gives the maximum amplitude of vibration, further the resulting modal shape would be absolute which would be of considerable value for modal balancing. Although such methods have been published, i.e. reference (55), the writer is not aware of any company or university using the foregoing described method, where the obtained twenty-eight force coefficients could have been used to check the performance of a rotor system.

The only method which could be used utilizing all the twenty-eight force coefficients was to first select the running conditions which were of interest, then by determining the orbital response for

some assumed amount of unbalance, the amount being the degree one could balance a rotor, then from the resulting trajectory determine Hagg and Sankey type of stiffness coefficients for the major and minor axis of vibration which could be used in the conventional methods of critical speed calculations. To demonstrate this method critical speed results are presented in Appendix (B) for the rotor illustrated in figure (1.2). It is not possible to quantify the dynamic characteristics of the hydrodynamic oil film without reference to the rotor which it supports, that is to say that the amount which the oil film stiffness effects the critical speed is also dependant upon the flexural rigidity of the rotor, hence the method of impedance matching has been adopted to illustrate the suppression of rotor critical speeds due to oil film flexibility, taking into account the non-linearity of the oil film.

12.8 The effect of using the second order terms when predicting the journal whirl trajectory, with the bearing operating under misaligned conditions

From the results presented it is quite clear that upon the introduction of misalignment a stabilizing effect was introduced, i.e. an increase in both the stiffness and damping coefficients was experienced. Thus suppression in the journal whirl orbit has often been experienced when balancing and commissioning rotating equipment, particularly turbines and turbo-alternators. These results also show that theoretical coefficients presented in Appendix (B), for conditions of misalignment confined to the vertical plane, to give good results. Errors found in amplitude vary from 2.0 per cent to a maximum of

approximately 9.0 per cent and errors in the angular position of the out-of-balance force vector in the order of zero to 6.0 degrees.

Introducing misalignment to a perfectly aligned bearing, such that the one end of the journal takes up most of the remaining radial clearance has the effect of suppressing the major axis of the whirl trajectory in the order of 55 to 80 per cent and along the minor axis of vibration and in the order of 55 to 60 per cent depending upon the steady state eccentricity ratio. Also the angle of the force vector could change as much as 45 degrees.

In all cases where misalignment was introduced to a dynamically loaded bearing the whirl orbit was shown to be reduced in magnitude, and only on a few occasions did the journal trajectory remain unchanged and this was usually under conditions where the eccentricity ratio was small. A noteworthy point here is that the larger whirl orbits illustrated in figure (10.30), representing the smaller values of eccentricity ratio, demonstrates how the rate of change of the oil film coefficients does not change very drastically for varying amounts of misalignment, which is also suggested by the force coefficients given in Appendix B. Also the smaller whirl orbits given in the same figure, representing the larger eccentricities show how the coefficients must increase quite considerably with the introduction of misalignment, this phenomenon is also illustrated to be correct by the coefficients listed in Appendix B.

The effectiveness of presenting results by this method is demonstrated in the last figure, here excessive misalignment has been introduced causing the one end of the journal to be pivoted about the